Modelling uncertainty in population monitoring data

Vuong Nguyen

A thesis submitted for the Degree of Doctor of Philosophy

School of Biological Sciences

The University of Sydney, Australia

February 2016

Declaration of originality

I hereby declare that the work contained in this thesis is my own and contains the results of an original investigation, except where otherwise referenced or acknowledged. This work was carried out while I was enrolled as a student for the degree of Doctor of Philosophy in the School of Biological Sciences, The University of Sydney. This thesis has not been previously submitted for examination at this, or any other university.

Vuong Nguyen

July 2015

Statement of author contributions (Chapter 2)

Vuong Nguyen and Glenda Wardle conceived the study. Vuong's contribution to this study was substantial, and included conducting the literature search to update the database of population matrix models and identify relevant information to be used in subsequent simulations and writing the scripts to reconstruct models and conduct simulations. The original database of matrix models upon which new models were added was constructed by the Vegetation Function Working Group. Vuong Nguyen wrote the manuscript, with additional comments provided by Yvonne Buckley, Rob Salguero-Gómez and Glenda Wardle.

As co-authors of this manuscript, we concur with the statements above outlining each author's contributions.

G M Wardle
Glenda Wardle

Rob Salguero-Gómez

Yvonne Buckley
Yvonne Buckley

Statement of author contributions (Chapter 3)

Vuong Nguyen and Glenda Wardle conceived the study. It is based on a novel design for analysing the existing long-term datasets to address new questions not already part of previous data collection efforts. Vuong performed considerable work in designing and writing the scripts for the data manipulation, analysis and models. Vuong Nguyen wrote the manuscript, with additional comments provided by Aaron Greenville, Chris Dickman and Glenda Wardle.

Chris Dickman, Glenda Wardle and Aaron Greenville collected the long-term data used in this study, with assistance from members of the Desert Ecology Research Group and volunteers. The original experimental designs for the vegetation surveys were conceived by Glenda Wardle. Funding was provided from grants obtained by Chris Dickman and Glenda Wardle.

As co-authors of this manuscript, we concur with the statements above outlining each author's contributions.

Glenda Wardle

Chris Dickman

Aaron Greenville

Statement of author contributions (Chapter 4)

Vuong Nguyen and Glenda Wardle conceived the study. It is based on a novel design for analysing the existing long-term datasets to address new questions not already part of previous data collection efforts. Vuong performed considerable work in cleaning up the data, writing new scripts to ingest the data into an interogatable database, and designing and writing the scripts for the data analysis and models. Aaron Greenville contributed the data manipulation and modelling for the wide-view dataset. Vuong Nguyen wrote the manuscript, with additional comments provided by Aaron Greenville, Chris Dickman and Glenda Wardle.

Chris Dickman, Glenda Wardle and Aaron Greenville collected the long-term data used in this study, with assistance from members of the Desert Ecology Research Group and volunteers. The original experimental designs for the vegetation surveys were conceived by Chris Dickman (wide view dataset) and Glenda Wardle (high resolution dataset). Funding was provided from grants obtained by Chris Dickman and Glenda Wardle.

As co-authors of this manuscript, we concur with the statements above outlining each author's contributions.

G M Wardle

Glenda Wardle

Chris

Chris Dickman

A. Green

Aaron Greenville

Contents

List of figures

List of tables

Acknowledgements

I am most grateful to my supervisor Glenda Wardle, who I have been working with now for almost five years and got me started on the path of population modelling what seems like an age ago during my undergraduate course that has subsequently led me to where I am today.

Special thanks to the Desert Ecology Research Group and the countless volunteers whose efforts in the field and the lab cannot be understated and without which there would not exist such a valuable dataset to work with. Having been on one of the field trips, I can appreciate the hard work they put in to collect the data. Special thanks to Bobby Tamayo, David Nelson and Chin-Liang Beh. Thanks to Aaron Greenville, Marianna Ferreria and Rob Salguero-Gomez for several helpful discussions on population modelling and population dynamics. Special thanks to Aaron Greenville for involving me in his research and for providing valuable assistance in my own research, and sharing the frustrations of trying to get a script or a model to work. Special thanks to Chris Dickman who provided valuable comments on several chapters of this thesis.

Thanks to my good friends Arunna, Andy, Vu, Danny, Annie, Jacqueline and Christine for helping me retain my sanity for so long. Thanks to my family, particularly my parents, for supporting my decision to pursue a PhD even if it is not the type of “doctor” they were hoping me to be.

Thesis abstract

Uncertainties in ecology are pervasive, and therefore, communicating the level of uncertainty for any inference derived from scientific research is key to sound decision-making and management of species and ecosystems. Characterising uncertainty is part of converting information into knowledge and has the added benefit of identifying fruitful avenues of further investigation. Without such care in accounting for uncertainties, we risk making misleading conclusions and inappropriate management decisions. In this thesis, it is argued strongly that rather than being something to avoid discussing, reducing uncertainty is fundamental to good ecological science. Uncertainty can come from a number of sources. Parameter estimation for demographic studies has inherently high uncertainty due to substantial variation between individuals, years, and spatial locations thus requiring considerable resources to obtain accurate estimates for survival, reproduction and growth. In some cases, certain life stages may be unseen during sampling procedures, such as seeds in the soil seed bank, or if non-breeding components of the population are not present in the selected sampling sites. While the potential sources of uncertainty are diverse, I attempted to cover a range of key areas of uncertainties relevant to ecologists over the course of this thesis. Specific areas of uncertainty were targeted using case studies to provide examples to demonstrate how these uncertainties can be addressed and how they can be used to aid inferences and provide recommendations for future data collection procedures.

First, I highlighted the prevalence of authors excluding a cryptic but important life stage, the dormant seed bank, from their data collection procedures and population models (Chapter 2). The evolution of seed banks acts as a bet hedging strategy, improving the persistence of plant populations in variable environments, thus it is crucial that we are able to address this potential knowledge gap to avoid misleading conclusions. The consequences of this exclusion on model parameters such as population growth rates and extinction risks were explored using a joint empirical and simulation approach, combining information from the published literature with Monte Carlo simulations. These simulations explored a range of assumptions that need to be considered when including a seed bank into the model, such as seed longevity, viability and germination rates. A key result of these simulations is that our perspective regarding the importance of the seed bank can differ, further depending on the species and the type of demographic year. For example, inclusion of the seed bank and demographic uncertainty in seed bank parameters were found to have little effect for stable populations with high post-seedling survival. In such cases, the seed bank can be excluded, however this should be accompanied by appropriate justification either through literature confirmation that dormancy is not existent or demonstrated via simulations that it is of little consequence. Conversely, seed banks had a more demonstrable impact on growth and extinction rates for variable populations, particularly when populations experience poor demographic years. The use of simulations and published literature can thus be an effective means to explore uncertainties resulting from the presence of cryptic life stages.

Second, I explored and demonstrated the use of multivariate auto-regressive state-space (MARSS) models as a versatile framework for capturing and addressing several sources of uncertainty including observation errors, and show how these models can be used to update and improve monitoring design (Chapter 3). MARSS models were constructed for a common, ephemeral plant using a 9 year time series dataset from multiple study sites within the Simpson Desert to explain trends over time and space. Modelling multi-dimensional time series data allowed the identification of spatial sub-population structure with respect to location and fire history, and the incorporation of population structure making use of count data for above ground plants and the seed bank. Model results suggested population dynamics to be driven primarily by geographical location possibly reflecting differences in soil conditions, local competition and local microclimate, overshadowing variation caused by fire history. The seed bank was also found to be characterised by high observation error with low environmental variability, while the converse was true for the above ground population estimates. Knowledge regarding the relative uncertainty of the above and below ground abundance estimates and the spatial distribution of population dynamics can then be used to provide guidelines for future monitoring efforts. For example, it may be more strategic to sample the seed bank less frequently as it less variable over time, and instead focus on obtaining more accurate counts when it is sampled to offset the high observation error. Additionally, the level of spatial heterogeneity in the Simpson Desert provides some justification for expanding spatial replication.

Third, the validity of using visual cover estimates as a means of monitoring vegetation and environmental changes was assessed. Visual cover estimates are particularly susceptible to observation error, and previous studies on the repeatability and reliability of such measurements have raised concerns over their value in ecological monitoring and decision making. I made use of two primary long-term monitoring datasets on spinifex grasslands, each obtained with different motivations, methods of data collection, and varying degrees of spatial and temporal coverage to assess the consistency of spatial and temporal trends between these datasets. Thus it could be determined whether the different sampling strategies and observation errors produced inconsistent and conflicting results. Observation errors were found to be quite large, often exceeding variation due to environmental changes. However, when these errors are accounted for, trends in the spatial dynamics of spinifex cover were consistent between the datasets, with population dynamics being driven primarily by time since last fire. Models also showed similar population traces over time, reflecting the effects of major temporal drivers such as rainfall and fire history. These findings vindicate visual cover estimates as a useful source of information provided that uncertainties in the measurements are appropriately addressed.

Finally, I shift the focus from single species analyses and apply dynamic factor analysis (DFA) to a large, multispecies database of abundances over time, which reduces the temporal dynamics of a large number of species to a small number of common trends. In producing these trends, interpretation of large multispecies data is greatly simplified. Furthermore, the common trends groups species with similar temporal responses, thus revealing where there is potential to borrow strength across species to supplement those that are less well sampled. Five common trends were identified for each site, and crucially, these trends were strongly associated with life form which showed distinctive signatures in the shape of their trends. Forbs and grasses for example demonstrated high levels of synchrony in their responses to rain events, although the signal for shrubs and subshrubs was weaker. These responses were also found to differ over relatively large (>20km) spatial scales. Thus plant life form is a reasonable predictor of changes in abundance over time and offers some justification for borrowing information to supplement data from poorly sampled species, provided the data are within the same locality.

The results of this thesis underpin the value of acknowledging, measuring and managing uncertainties, and that these uncertainties can be used advantageously to guide inferences, extract value from datasets thought to be unreliable, provide justification for sourcing additional sources of information or excluding others, and inform future data collection protocols. Several methods for addressing uncertainty are highlighted, such as the use of simulations when data are unavailable, powerful state-space modelling techniques to account for observation error, and identifying opportunities for supplementing data from the literature, similar sites or species with similar dynamics. There are several more options available for reducing and managing uncertainty, and it is ultimately up to the researcher to first recognise where uncertainties are likely to exist, explore their options, and decide how such uncertainties are to be addressed.

Preface

This thesis is set out as a series of papers, an option available at The University of Sydney. The papers have been submitted or accepted to appropriate peer-reviewed scientific journals in the form presented here or similar. As a consequence, there is some redundancy among chapters and journal-specific formatting.

Chapters that have been published or are currently in review in peer-reviewed journals are indicated at the beginning of each chapter. My co-authors on these papers are Prof. Glenda M. Wardle, Yvonne M. Buckley and others where appropriate. My contribution to these papers was very substantial, including conceptualisation of ideas, data manipulation, construction and analysis of models, and writing and editing drafts of all the chapters.

The data used in Chapters 3, 4 and 5 were obtained by the Desert Ecology Research Group who are based at the University of Sydney, and is currently unpublished. The raw data required extensive cleaning and manipulation to be suitable for analysis. This included identification of errors and typos, ensuring the consistency and integrity of the data, and eventually restructuring the data to be transferred to a database management system for future analyses.

As supervisors of this PhD thesis, we concur with the statements above about Mr Vuong Nguyen's contributions.

G M Wardle
Glenda Wardle

Yvonne Buckley
Yvonne Buckley

Chapter 1 - Overview of common sources of uncertainty in ecological data

Measurements and collection of raw data can be subject to many sources of uncertainty. Photograph by Glenda Wardle.

Introduction

> *"There are known knowns; there are things we know we know. We also know there are known unknowns; that is to say we know there are some things we do not know. But there are also unknown unknowns - the ones we don't know we don't know."*
>
> Donald Rumsfeld, Former United States Secretary of Defence, 2002

Although the context of this statement was in relation to national defence, the idea of "unknown unknowns" is profound in many areas of uncertainty, risk analysis, and indeed understanding ecological systems and making management decisions. This concept can be captured in terms of two axes describing the level of uncertainty (Table 1-1). The first axis of uncertainty can be thought of as describing awareness – are we aware of a problem that requires addressing, a question that needs answering, or an issue that requires investigating. An unknown along this axis for example may include the scenario in which nobody has thought to ask the question in the first place. The second axis of uncertainty then describes the level of information or data that are available to address these questions. Combining these two axes results in the classification presented in Table 1-1, with an additional category, the "unknown knowns" describing opportunities in which two possible scenarios are identified. In the first scenario, data may have been previously collected which would be of interest to a researcher answering a particular question, but may be unaware of its existence or data has not been made publicly available. In the second scenario, the researcher is aware of the data but has not yet realised its full potential, or is simply overwhelmed by the sheer amount of data (termed the 'data smog') and is unable to extract the relevant pieces creating further confusion and uncertainty rather than knowledge (Shenk, 1998).

Table 1-1. Four categories describing the level of uncertainty along two axes: information and awareness.

		INFORMATION	
		Known	**Unknown**
AWARENESS	**Known**	**Knowledge** Information is available and is being used to answer relevant questions e.g. Researchers are certain about the presence/absence of a dormant seed bank, and have data to estimate vital rates	**Gaps** Information is unavailable but the need for such data is acknowledged e.g. Researchers acknowledge the possibility of a dormant seed bank but there is no data available
	Unknown	**Opportunities** Information is available but is inaccessible or its relevance and potential not fully realised e.g. Researchers have not considered the possibility of a dormant seed bank, however there are data available from previous studies/experiments	**Uncertainty and risk** Information is unavailable and there is no acknowledgement that such data are needed or important e.g. Researchers have not considered the possibility of a dormant seed bank and there is no data available

The category describing opportunities is arguably of greatest interest as it captures the largest potential reduction in uncertainty for the least amount of effort. The advent of the information technology age and globalisation has been instrumental in improving data availability, storage, collection, management and analysis in all fields of scientific research. This new age of data availability and accessibility provides many opportunities to make use of pre-existing datasets and infrastructure to produce new knowledge. In the next section, I will discuss some of these improvements in ecological data and the opportunities they provide.

The rise of ecological data

"The coming century is surely the century of data" David Donoho, 2000

Towards open-access data

Over the past few decades, ecologists have collected a wealth of extremely rich datasets that up until recently were difficult to share, resulting in lost opportunities to test general ecological theories and large-scale spatial and temporal patterns (Inchausti and Halley, 2001; Hampton *et al.*, 2013) and many of these valuable datasets would go on to become unavailable. A study investigating the availability of ecology data found several barriers to data availability, particularly for older datasets, including data being stored on now obsolete technologies such as floppy disks, defunct e-mail addresses preventing contact with the authors or simply being misplaced amongst their personal collection (Vines *et al.*, 2014). Key journals such as *The American Naturalist*, *Journal of Ecology* and *PloS One* have recognised the importance of data retention and sharing to scientific progress and now employ strict guidelines requiring that data (and in some cases programming code to reproduce analyses) are archived via public repositories or risk rejection (Whitlock *et al.*, 2010). Online archiving and cloud storage technologies also provide a much safer option for data preservation particularly as storage hardware can quickly become obsolete and are susceptible to failures (Borer *et al.*, 2009). Online storage also has the capacity for storing and extracting relevant information from extremely large datasets that would otherwise be inaccessible from a personal computer (Whitlock, 2011; Marx, 2013). Specialised central repositories such as GenBank (http://www.ncbi.nlm.nih.gov/genbank/) and the Global Population Dynamics Database (http://www3.imperial.ac.uk/cpb/databases/gpdd/) have now made it much simpler for researchers to upload, share and search for data (Whitlock, 2011). The new open-source repository COMPADRE has uploaded thousands of plant matrix population models summarising demographic and life history traits that were previously inaccessible for synthetic analysis with a similar repository for animals to be released (Salguero-Gómez *et al.*, 2015). This push towards data accessibility also benefits authors, allowing researchers to get credit for their data through citations and encouraging its reuse (Whitlock, 2011; Kenall *et al.*, 2014). Indeed, studies have shown that articles connected to a publicly available dataset are associated with an increased citation rate (Piwowar *et al.*, 2007; Piwowar and Vision, 2013). These datasets may then go on to be used to answer novel questions previously not considered by the original authors without the need for additional data collection (Whitlock, 2011), thus bridging the gap between opportunities and knowledge and accelerating the advance of ecological research (Reichman *et al.*, 2011).

Long-term research

There is widespread agreement within the ecological community highlighting the need for long-term ecological research to address important questions about ecosystem, community and population dynamics (Beissinger and Westphal, 1998; Menges, 2000; Lindenmayer *et al.*, 2012; Lindenmayer *et al.*, 2014). However, the acquisition of long-term data remains a significant challenge for ecologists as they exceed the length of government administrations and funding cycles, and growing pressure on researchers to produce publications favouring short-term studies and modelling research (Lindenmayer and Likens, 2011; Lindenmayer *et al.*, 2012). The need to support funding and infrastructure for long-term monitoring and research has driven several international collaborations to establish extensive long-term monitoring networks. The Terrestrial Ecosystem Research Network (TERN) in Australia is a relatively recent data collection, storage and sharing infrastructure network for Australian ecosystem science. One of the core components of TERN is the Long-Term Ecological Research Network (LTERN) built on new and pre-existing long-term terrestrial plot networks with data ranging from several years to decades, in a variety of habitats (Burns *et al.*, 2014). Other national and international networks supporting long-term data collection include the Amazon Forest Inventory Network (RAINFOR; Malhi *et al.*, 2002), the Landsat archives (Wulder *et al.*, 2012), the National Ecological Observatory Network (NEON; Keller *et al.*, 2008), and the International Long Term Ecological Research Network (ILTER) supporting regional networks in Asia/Pacific, Europe, Africa , North America and Central/South America. These programs have extraordinary potential for establishing rich, global datasets for current and future generations (Kim, 2006).

Role of technology

Innovations in computational power and digital advances in technology have allowed researchers to produce and analyse unprecedented amounts of data (Hernandez *et al.*, 2012). Remote sensing technologies can vastly expand data availability with large spatial coverage to investigate changes occurring over regional or global scales that may not be feasible using field-based methods (Booth and Tueller, 2003; Kerr and Ostrovsky, 2003). These sensor networks have allowed ecologists to engage in intensive, convenient and unobtrusive sampling facilitating the collection of high quality, real-time data (Porter *et al.*, 2005; Benson *et al.*, 2009). The Landsat series of satellite missions for example provides an archive of imagery dating back to 1972 and the decision to make this information open access is a promising step towards encouraging international collaboration to address global issues (Wulder *et al.*, 2012). The use of camera traps for studying terrestrial wildlife has become increasingly mainstream in recent times with improvements in camera technology and decreasing costs, providing more opportunities for animal sightings, particularly for elusive species (Rowcliffe and Carbone, 2008; Tobler *et al.*, 2008). The widespread use of smartphones has led to the development of applications linking the process of ecological data collection in the field with online data submission, with the added benefits of providing real time GPS co-ordinates and providing more opportunities for the recruitment of ‘citizen scientists’ to bolster data collection (Aanensen *et al.*, 2009; Kwok, 2009).

At the same time, improved computing and processing power has encouraged the development of more sophisticated tools to store, analyse and perform more rigorous statistical tests on these larger datasets (Brownstone and Valletta, 2001; Marx, 2013). Reduced costs and increased availability in computing power has also permitted the use of sophisticated techniques and models to analyse smaller, but problematic ecological datasets often containing missing values, unbalanced statistical designs, high variability between individuals, sites and time, and high dimensional multivariate data involving several species, interactions and covariates (Andersen *et al.*, 2009; Evans *et al.*, 2012). In addition, these statistical tools are also being made more accessible with the advent of free, open-source programs and packages for statistical analysis (R Core Team, 2014). The provision of programming code for open source software is another important step towards advancement of scientific discoveries, allowing results to be independently verified and reproduced and provides useful examples to follow for researchers wishing to employ these techniques (Gentleman and Lang, 2007).

Current challenges

While advances in ecological data are occurring at an increasingly rapid pace, there are still many challenges to be addressed. International collaborative efforts to address the need for long-term datasets are encouraging, but many have only been proposed or established relatively recently and may take several more years or decades for their full potential to be realised. While the availability of long-term ecological data has also increased, openly accessible long-term datasets are the exceptions and remain quite rare (Lindenmayer *et al.*, 2012). In addition, despite the push towards open-access data, there has yet to be a substantial shift in the culture of ecologists towards data sharing and data transparency, particularly when compared to fields such as genomics and meteorology (Hampton *et al.*, 2013; Kenall *et al.*, 2014; Soranno *et al.*, 2015). Ecologists are collectively producing vast amounts of data, however traditional ecological data tends to come from relatively small projects with high levels of effort and involvement from the direct investigator, resulting in a strong sense of data ownership and concern of having future planned analyses scooped by other researchers (Zimmerman, 2003; Piwowar and Vision, 2013). Furthermore, the lack of any standardised methodology results in large heterogeneity in data characteristics that makes it incredibly difficult to aggregate studies in a meaningful way (Aronova *et al.*, 2010; Borgman, 2012). There is also concern that publicly available data may be misused and that without proper context and specialised knowledge of the study system, ecological data can be difficult to understand (Reichman *et al.*, 2011; Hampton *et al.*, 2013). Optimal use of data produced by remote technologies for example requires field-based methods to provide context and obtain additional measurements that are relevant but cannot be obtained remotely (Lathrop Jr *et al.*, 2014). However, traditional ecological data produced by field-based methods tends to have a large inherent uncertainty due to the challenges of data collection in the field and the difficulty of attempting to estimate certain parameters (Salski, 1992). For the remainder of this chapter, I will briefly discuss the various common sources of uncertainty in ecological data and the methods used to address these issues.

Uncertainty in ecological data

Substantive questions in ecological research often involve uncertainty in central ways, and these uncertainties go on to influence important decisions such as the design of conservation programs, management of populations and risk assessment in the face of human and environmental perturbations (Tuljapurkar, 1989). Uncertainty in data and modelling is pervasive and unavoidable – the central issue therefore is not that uncertainty exists, but in failing to account for uncertainty in the data and models which can lead to misleading conclusions and inappropriate management decisions (Regan *et al.*, 2005). An awareness of the sources of these uncertainties and their potential impact is therefore crucial to avoid these consequences and aid decision making (Regan *et al.*, 2002). I now go through some of the more prevalent sources of uncertainty that can be found in ecological data.

Estimation of demographic parameters and vital rates

Estimates of demographic parameters using field data tends to have an inherently high uncertainty associated with them as they are highly variable between individuals, populations and over time (Ludwig, 1999; McCarthy *et al.*, 2001; McCarthy *et al.*, 2003). Broadly, uncertainty in the estimation of demographic parameters can be thought of as the result of two main sources. Firstly, there is sampling uncertainty arising due to sampling methodology and variation across individuals. Secondly, there is variation across space and time such that demographic parameters are not expected to remain constant at different times or locations. While sampling uncertainty can be addressed statistically, spatial and temporal uncertainty can only be dealt with through long-term and spatially expansive data collection. Obtaining accurate estimates for important vital rates such as survival, reproduction and growth is therefore logistically challenging as it would require intensive demographic sampling tracking individuals over a number of time periods and spatial locations (Beissinger and Westphal, 1998; Bierzychudek, 1999). This is particularly problematic for rare species which are often the target of conservation interest but have unavoidably small sample sizes and limited distributions (Bierzychudek, 1999).

Intensive demographic sampling is unlikely to occur over long time periods, resulting in an overabundance of short-term studies (Menges, 2000; Coulson *et al.*, 2001; Salguero-Gómez *et al.*, 2015). Short-term datasets are inadequate for assessing long-term viability of many populations, failing to account for year-to-year variability in the environment which is likely to influence vital rates, and the potentially devastating impact of rare events such as fire (Bierzychudek, 1999; Ellner *et al.*, 2002). This limits the potential to conduct stochastic analyses that can account for variation in vital rates, instead of asymptotic analyses which naively assume conditions remain constant over time (Tuljapurkar and Lee, 1997; Tuljapurkar *et al.*, 2003). These short-term studies are also unlikely to capture the entire life-cycle of a long-lived species and mortality rates can be difficult to estimate correctly (Elderd *et al.*, 2003).

Resampling procedures such as bootstrapping can do much to alleviate uncertainty in vital rates and subsequent model predictions (Efron and Tibshirani, 1986; McPeek and Kalisz, 1993). Alternative demographic modelling techniques can also provide opportunities to use data more effectively. Currently, matrix models are the dominant method for demographic modelling (Caswell, 2001; Crone *et al.*, 2011), however this approach divides individuals into stage classes (e.g. juveniles, adults) which exacerbates the issue of insufficient sampling as vital rates need to be estimated for each class. Integral projection models on the other hand model vital rates over a continuous variable such as size rather than grouping them by life stages (Easterling *et al.*, 2000; Merow *et al.*, 2014), producing better estimates when sample sizes are small as the regressions make use of all individuals (Ramula *et al.*, 2009b).

However, life stages may not be sufficiently represented depending on the sampling procedures, particularly if some of these life stages are cryptic.

Cryptic life stages

Tracking individuals from all stages in a species' life cycle, including cryptic or less accessible stages, is crucial for estimating vital rates and obtaining an accurate assessment of the size and survival of a population. The seeds of many plant species for example can remain dormant in the soil seed bank for many years before germinating, and in some cases can form the largest component of a plant population (Harper, 1977; Macdonald and Watkinson, 1981). In extreme cases, the observable plant population may disappear for one or several breeding seasons, but still exist in the seed bank. However, estimating abundances and vital rates (germination, viability and seed survival) for the seed bank requires destructive sampling of established plots, or external germination experiments in the laboratory (Kalisz, 1991; Kalisz and McPeek, 1992) which may differ to vital rates obtained from the field (Gross and Mackay, 2014). Other forms of dormancy, such as vegetative dormancy in adult plants, can be equally problematic as they can be easily assumed dead, thus resulting in inflated mortality rates (Lesica and Steele, 1994). Seed and vegetative dormancy form crucial life history strategies to improve the persistence of plant populations in stochastic environments, and ignoring these stages can be detrimental to efforts in conserving rare species or preventing the spread of invasive species (Adams *et al.*, 2005; Regan *et al.*, 2011). Therefore a complete assessment on the viability and demographic implications on plant populations requires relevant data on these life stages (Moriuchi *et al.*, 2000; Doak *et al.*, 2002; Shefferson, 2009; Salguero-Gómez and Casper, 2010).

For animal species, life stages may be cryptic if they are not present in sampled locations, or occupy unknown or inaccessible locations. Population estimates of threatened raptors for example are often based on observations of the breeding sites and ignore the non-breeding component of the population leading to inaccuracies in demographic models (Katzner *et al.*, 2011). Conversely, abundances and population trends from the Breeding Bird Survey, obtained mostly by citizen scientist volunteers, are reported with the caveat that some species counts contain a high proportion of birds away from breeding sites, and monitors nocturnal species poorly (Harris *et al.*, 2014). The study and management of green turtles was hindered as the location of the hatchlings after leaving their nesting beach was unknown, and required the use of stable isotopes to locate the missing juveniles (Reich *et al.*, 2007). In addition, many taxonomic groups undergo metamorphic changes during their lifetime, and often one or more of these stages are cryptic such as insect eggs and larvae, or long-lived cysts of aquatic crustaceans (Lamy *et al.*, 2013).

Collecting data on these life stages will always be the more desirable option when faced with cryptic life stages, although this may not always be possible. In such cases, simulations and statistical models can provide a cost-effective alternative to account for these stages. Multistate occupancy models allow estimation of transition probabilities of patch occupancy between more than two states (MacKenzie *et al.*, 2009), but can also be implemented to model cryptic stages as demonstrated by Lamy *et al.*, (2013) for aestivating freshwater snails. Transition rates for colonisation and extinction rates were estimated by conditioning on environmental variables as cryptic life stages are frequently associated with habitat features such as dry sites for resistant eggs (Lamy *et al.*, 2013). An alternative approach implemented a hidden Markov model to infer parameters for plant populations with a seed bank without the need for environmental variables as seeds need not necessarily emerge when conditions are favourable and can co-exist with above ground life stages (Fréville *et al.*, 2013).

Simulations exploring a range of plausible vital rates as inferred by previous studies can also help reduce uncertainty and determine whether lack of data on a cryptic life stage are only of minor consequence (Garcia *et al.*, 2011). However, many studies have opted to exclude these cryptic life stages owing to the immense difficulty in terms of time, effort and funding to collect relevant data to parameter estimates. Indeed, funding and logistical issues may impede the collection of field data without the added complexity of addressing cryptic life stages, resulting in missing values and uneven sampling intervals.

Missing values and uneven sampling intervals

Ecological time series often contain uneven sampling intervals, arising from missing observations in the data due to financial, logistical and personnel constraints (Humbert *et al.*, 2009). For example, the funding cycle for many research projects can make it difficult to commit to regular long term monitoring resulting in sparse datasets with only occasional sampling opportunities. Furthermore, factors that cannot be controlled such as extreme weather conditions may prevent access to a study site (Ter Braak *et al.*, 1994). Analysis of data from multiple sites can have several missing values at the start of a time series if additional sites were included during the middle of a project that were previously unplanned, and sampling strategies or priorities may change over time to address new research questions (e.g. Dickman *et al.*, 2014). Spreading resources out over several sites also reduces the likelihood that all sites will be sampled during each census.

These missing values can be problematic as many of the traditional time series analysis techniques such as auto-regressive integrated moving average (ARIMA) models can have strict data requirements i.e. relatively long, stationary, evenly spaced, no missing values (Erzini *et al.*, 2005). Numerous statistical methods have been developed to deal with missing values. A common technique involves multiple imputations, in which a statistical model is used to compute multiple estimates for the missing values to produce multiple alternative datasets (Honaker and King, 2010; Nakagawa and Freckleton, 2011). The Expectation-Maximisation algorithm is often used to estimate maximum likelihood estimates for these missing values (Shumway and Stoffer, 1982; Shumway and Stoffer, 2006; Nakagawa and Freckleton, 2011; Holmes *et al.*, 2012). However the uncertainty in any subsequent analysis is necessarily greater than if the data were complete. The two most commonly used methods accommodating unequal sampling intervals are the log-linear regression of counts against time, and the other describes logarithmic abundance by Brownian motion diffusion process with constant drift rate (Dennis *et al.*, 1991; Humbert *et al.*, 2009). Unfortunately, these methods are unable to simultaneously account for and distinguish between variation due to observation error during data collection and variation due to environmental stochasticity.

Observation error

Observation error refers to any deviation from an observed value and its true value (Staples *et al.*, 2004). This includes traditional sampling error obtained from only sampling a portion of the population, and measurement error resulting from sampling methods or incorrect measurements within a chosen sampling unit (Staples *et al.*, 2004; Flesch, 2014). True abundances of populations are rarely known and are often estimated rather than censused, producing variability in observed abundances, which is distinct from variation due to process error that includes all non-observation error such as environmental stochasticity. Observation error arising from imperfect detection is a common issue particularly if a species is rare, small, nocturnal or otherwise elusive. Species with a predisposition towards non-detection may produce observed estimates of zero abundance thereby implying absence from a study site, which may not necessarily be true. Mistakes and disagreement in abundance estimates between field workers are also common and can be exacerbated by factors that cannot be controlled for such as weather conditions, a lack of trained personnel, or simply too many individuals to be counted accurately. These errors can also be present in covariate data including those obtained using technology such as weather machines, and those obtained via human meaurements such as soil readings or trait-based measurements.

Failing to account for observation error can have serious consequences for ecological inferences such as strength of density dependence, population trends, and extinction risks (Shenk *et al.*, 1998; Dennis *et al.*, 2006; Freckleton *et al.*, 2006; Dennis *et al.*, 2010). Statistical models, and their resulting parameter estimates, can be severely biased and environmental variability overestimated if observation error is not properly accounted for (Ludwig, 1999; Dennis *et al.*, 2006; Linden and Knape, 2009). Incorporating observation errors into time series models is not a simple task, generally requiring sufficiently long time series data, and there are many statistical issues to be dealt with (Clark, 2003; Dennis *et al.*, 2010). The diffusion approximation method developed for univariate time series by Holmes, (2001) for example produces estimates of process variation that can be biased high or low with unknown magnitude of direction (Staples *et al.*, 2004). The restricted maximum likelihood (REML)-based method developed by Staples *et al.*, (2004) on the other hand has the strict requirement that data come from even sampling intervals with no missing values. State-space models, prevalent in engineering, economics and more recently the fisheries literature, which partitions the model into one for the observations and another for the unobserved true state have proven a useful tool for modelling both errors (Holmes and Fagan, 2002; De Valpine, 2003; Clark and Bjørnstad, 2004; Humbert *et al.*, 2009). These models and the algorithms implemented to estimate the parameters can become unstable when data are limited, though this can be reduced by taking replicate samples (Dennis *et al.*, 2010).

Additionally, steps can be taken to reduce the size of observer errors during data collection, for example by taking mean values of multiple observations, implementing mark-recapture methods to estimate abundance or increasing sampling time and effort (Klimeš, 2003; Burgman *et al.*, 2011; Herrick and Fox, 2013). Researchers must acknowledge the presence of observation error and while many studies have not accounted for this error (Freckleton *et al.*, 2006), more attention has been paid recently to modelling, measuring and reducing observation error. In recent times, the size and prevalence of observation errors in visual estimates of vegetation cover has led to some major concerns over it use to guide management practices.

Visual cover estimation

Estimation of vegetation cover by visual inspection of fixed plots provides a quick, simple means of carrying out much needed long-term monitoring and is used widespread across a range of study systems including heathlands (Webb, 1990), woodlands (Eckhardt *et al.*, 2000) and grasslands (Henderson *et al.*, 1988). Changes in vegetation cover are strongly linked to important ecological and environmental processes, and effective management of ecosystems therefore requires reliable field estimates of vegetation cover (Eyre *et al.*, 2011). However, such estimates are prone to large observation errors, drawing criticism with regards to the reliability and repeatability of such data (Helm and Mead, 2004; Wintle *et al.*, 2013). As with any other study requiring researchers to take measurements, observer specific biases and errors are present, but visual cover estimates have been demonstrated to be particularly susceptible, with no relationship between experience of the observer and their estimates (Cheal, 2008).

Methods to reduce observation errors such as taking mean values of multiple observers are also applicable to visual estimates. In addition, new technologies such as remote sensing and computer-image analysis can be used to remove observer specific biases associated with field estimates (Bennett *et al.*, 2000; Booth and Tueller, 2003). However, this potentially introduces errors of other kinds, including the choice of post-processing algorithm (Kennedy *et al.*, 2014), and does not eliminate the need for effective field-based measurements (Lathrop Jr *et al.*, 2014). Visual estimates can be improved through a process of active calibration feedback with observers evaluating their own performance but such practices are not commonly afforded to monitoring programs (Wintle *et al.*, 2013). In general, reducing observation errors within the limited funding and personnel constraints may not always be feasible resulting in several trade-offs that must be appropriately balanced.

Monitoring trade-offs

While reduction of observation errors is desirable to ensure high quality data, taking repeated measures for example would necessarily draw resources away from improving spatial and temporal coverage and it is up to the researcher to determine whether the improvement in information is worth the cost. (Dennis *et al.*, 2006). Therefore, in monitoring programs there exists a difficult trade-off between greater accuracy in the data and therefore power to detect small scale changes, and greater spatial and temporal coverage to improve overall understanding of a study system (Morris *et al.*, 1999). Obtaining sufficient spatial and temporal coverage is crucial, as quite often addressing interesting ecological questions requires sufficient data across both these scales.

Space-for-time substitutions can be used to compensate for inadequate temporal data (Pickett, 1989). However, spatial variation between populations can be quite high, sometimes exceeding variation over time, resulting in a mismatch between temporal and spatial variation and renders such substitutions inappropriate (Jongejans and de Kroon, 2005; Ramula *et al.*, 2009a). Information for a particular species may instead be bolstered by using data from another species or population. Phylogenetically related organisms for example show a tendency to resemble each other with regards to their phenotype, however support for the use of phylogenetic signals to explain observed population dynamics is weak (Blomberg *et al.*, 2003; Buckley *et al.*, 2010). Alternatively, life form can be a crude proxy for functional types whereby species within the same life form group often share common ecological properties and have been demonstrated to respond similarly to shared environmental drivers (Lavorel *et al.*, 1997; Pausas and Austin, 2001; Verheyen *et al.*, 2003; Wang *et al.*, 2003; Broennimann *et al.*, 2006). Similarly, while populations are often variable across space, they can also act in synchrony if populations are interconnected or if environmental drivers are large and widespread resulting in shared population dynamics between sites (e.g. Ward *et al.*, 2010). Identifying such spatial structure can reduce the number of parameters needing to be estimated, and allow information from multiple sites to help inform parameter estimation.

Strategic sampling designs and efficient allocation of resources can also prove beneficial. For example, missing values in time series data may be permitted in exchange for improved accuracy for the remaining sampling periods, or extending the time series length (Humbert *et al.*, 2009). Such a strategy places more emphasis on obtaining fewer but higher quality data, in contrast to many monitoring programs which prioritises regular, frequent intervals even if the data are poor (Hauser *et al.*, 2006). Censusing of study sites may also be staggered such that every site need not be visited every field trip, thus more sites can be visited for the duration of the study period (Morris *et al.*, 1999). Some sampling designs may already incorporate a degree of replication but data have inadvertently been aggregated to produce a single estimate – in such cases, it may be desirable to instead disaggregate these observations as independent replicates to improve model performance (Dennis *et al.*, 2010). One can also perform initially intensive demographic sampling (say, over a period of two or three years) which can subsequently inform less intensive monitoring strategies (Morris *et al.*, 1999). For example, it may be sufficient to census a single, informative life history stage to assess population viability and problematic, cryptic life stages may only need to be censused occasionally or not at all. Identifying the extent of spatial heterogeneity is also an important goal that can be examined early on to determine whether populations are independent with differing population dynamics, or are correlated with shared drivers and thus are more susceptible to extinction (Morris *et al.*, 1999; Warton and Wardle, 2003; Ward *et al.*, 2010). Populations with unique, independent dynamics may require more spatial replication to properly manage and understand the dynamics governing each population, whereas a correlated population might need more emphasis on temporal replication since rare, catastrophic events will impact all populations.

Overview of thesis

This chapter (Chapter 1) provides a general introduction to some key concepts regarding ecological data and the uncertainties affecting such datasets. The potential sources of uncertainty listed in this chapter covers a range of issues faced by ecologists but it is by no means exhaustive. Other sources of uncertainty for example may include modelling uncertainty, in both the choice of model and in the modelling of demographic parameters as a function of predictors. The potential sources of uncertainty is extensive - to keep the focus of the thesis tight, the remaining chapters of this thesis will be restricted to discuss and demonstrate techniques only for reducing particular aspects of uncertainty described in this chapter. The results are then related back to the data used to produce them and used to guide future data collection procedures. Chapter 2 will focus on uncertainty related to cryptic life stages. While cryptic life stages emcompass a wide diversity of forms across different taxanomic groups, one of the more common and well studied examples of such a stage is the dormant seed bank. I therefore focus on the seed bank to provide a useful foundation upon which to discuss the impact of uncertainty related tocryptic life stages. First, I give a review of the prevalence of plant population models that fail to take into account this potentially important life stage. Then I demonstrate how this uncertainty in the population models can be quantified and visualised using a combined empirical and simulation based approach, incorporating published demographic models, information on dormancy and germination from the literature and simulations investigating a number of plausible scenarios and assumptions. Chapter 3 will investigate the use of multivariate auto-regressive state space (MARSS) models for time series analysis when data are missing and sampling intervals are uneven. These models are also able to provide estimates for both observation and process error through a combination of the recursive Kalman filter and Expectation-Maximisation (EM) algorithm. Importantly, it is shown how the results from these models can be used to iteratively provide future recommendations for improving long-term monitoring programs. The MARSS framework is demonstrated using a relatively long-term (≈ 9 years) time series of abundances for a highly stochastic plant population from the Simpson Desert, an environment of extreme boom-bust dynamics. This case study is fairly typical of the challenges and difficulties of collecting ecological data whilst attempting to manage limited resources and practical concerns such as safety and access to study sites. Chapter 4 will investigate the validity of visual cover estimates as a legitimate means of assessing environmental changes in the face of heavy criticism with regards to repeatability and reliability of measurements. Making use of two primary independent long-term datasets of visual cover estimates of hummock grasslands, I evaluate whether these datasets produce consistent trends, or whether different sampling strategies and observer errors are driving the results. Chapter 5 demonstrates the use of dynamic factor analysis (DFA) to a large, multispecies dataset of abundances over time to summarise the temporal dynamics of a large number of species to a small number of common trends. This is analogous to a principal component analysis but the common trends (axes) preserve the temporal sequence of the observations. Thus, interpretation of the large multispecies data is greatly simplified and a more meaningful description of the study system is provided compared to a single species analysis. Furthermore, by clustering species with similar temporal dynamics into these common trends, it is possible to identify which species are suitable for borrowing information for species that are not as well sampled. Finally, Chapter 6 will summarise the general conclusions and key findings of the previous chapters.

The specific aims of this thesis and the chapters they are addressed in are as follows:

1. To quantify the amount and effect of uncertainty created by excluding cryptic life stages from demographic models (Chapter 2)
2. To demonstrate the application of multivariate state-space models to account for missing values, uneven sampling intervals, potential spatial heterogeneity and observation error and highlight how addressing these uncertainties can be used advantageously (Chapter 3)
3. To investigate the utility of visual cover estimates for detecting environmental changes and trends despite high errors and low reproducibility (Chapter 4)
4. To identify the potential to borrow information from multiple species by identifying species with similar temporal trends and to provide a holistic description of key temporal dynamics within a study system by taking a multispecies approach to time series analysis (Chapter 5)

These aims are addressed by using a series of case studies, combined with a variety of analytical tools appropriate for estimating uncertainty and accounting for spatial and temporal variation. The material may be read on several levels. First as a roadmap for how typical monitoring data collected in field surveys can be analysed to interpret differences across space and time. Secondly, as a series of vignettes that apply modern analytical tools to real-world data on plant populations and communities, and explicitly account for uncertainty. Finally, the issues addressed in the studies presented here demonstrate the practical advantages of managing uncertainty for decision makers to help guide future protocols for data collection and tracking ecosystem changes.

References

Aanensen, D.M., Huntley, D.M., Feil, E.J., al-Own, F. and Spratt, B.G. (2009) EpiCollect: linking smartphones to web applications for epidemiology, ecology and community data collection. *PloS One,* **4,** e6968.

Adams, V.M., Marsh, D.M. and Knox, J.S. (2005) Importance of the seed bank for population viability and population monitoring in a threatened wetland herb. *Biological Conservation,* **124,** 425-436.

Andersen, T., Carstensen, J., Hernández-García, E. and Duarte, C.M. (2009) Ecological thresholds and regime shifts: approaches to identification. *Trends in Ecology and Evolution,* **24,** 49-57.

Aronova, E., Baker, K.S. and Oreskes, N. (2010) Big science and big data in biology: from the international geophysical year through the international biological program to the long term ecological research (LTER) network, 1957–present. *Historical Studies in the Natural Sciences*, **40**, 183-224.

Beissinger, S.R. and Westphal, M.I. (1998) On the use of demographic models of population viability in endangered species management. *Journal of Wildlife Management,* **62,** 821-841.

Bennett, L.T., Judd, T.S. and Adams, M.A. (2000) Close-range vertical photography for measuring cover changes in perennial grasslands. *Journal of Range Management,* **53,** 634-641.

Benson, B.J., Bond, B.J., Hamilton, M.P., Monson, R.K. and Han, R. (2009) Perspectives on next-generation technology for environmental sensor networks. *Frontiers in Ecology and the Environment,* **8,** 193-200.

Bierzychudek, P. (1999) Looking backwards: assessing the projections of a transition matrix model. *Ecological Applications,* **9,** 1278-1287.

Blomberg, S.P., Garland, T., Jr. and Ives, A.R. (2003) Testing for phylogenetic signal in comparative data: behavioral traits are more labile. *Evolution,* **57,** 717-745.

Booth, D.T. and Tueller, P.T. (2003) Rangeland monitoring using remote sensing. *Arid Land Research and Management,* **17,** 455-467.

Borer, E.T., Seabloom, E.W., Jones, M.B. and Schildhauer, M. (2009) Some simple guidelines for effective data management. *Bulletin of the Ecological Society of America,* **90,** 205-214.

Borgman, C.L. (2012) The conundrum of sharing research data. *Journal of the American Society for Information Science and Technology,* **63,** 1059-1078.

Broennimann, O., Thuiller, W., Hughes, G., Midgley, G.F., Alkemade, J.M.R. and Guisan, A. (2006) Do geographic distribution, niche property and life form explain plants' vulnerability to global change? *Global change biology,* **12,** 1079-1093.

Brownstone, D. and Valletta, R. (2001) The bootstrap and multiple imputations: harnessing increased computing power for improved statistical tests. *The Journal of Economic Perspectives,* **15,** 129-141.

Buckley, Y.M., Ramula, S., Blomberg, S.P., Burns, J.H., Crone, E.E., Ehrlén, J., Knight, T.M., Pichancourt, J.P., Quested, H. and Wardle, G.M. (2010) Causes and consequences of variation in plant population growth rate: a synthesis of matrix population models in a phylogenetic context. *Ecology Letters,* **13,** 1182-1197.

Burgman, M.A., McBride, M., Ashton, R., Speirs-Bridge, A., Flander, L., Wintle, B., Fidler, F., Rumpff, L. and Twardy, C. (2011) Expert status and performance. *PLoS One,* **6,** e22998.

Burns, E., Lindenmayer, D., Tennant, P., Dickman, C.R., Green, P., Hanigan, I., Hoffman, A., Keith, D.A., Metcalfe, D., Nolan, K., Russell-Smith, J., Wardle, G.M., Welsh, A., Williams, R. and Yates, C. (2014) *Making ecological monitoring successful: insights and lessons from the Long Term Ecological Research Network.* LTERN, Australia.

Caswell, H. (2001) *Matrix population models: construction, analysis and interpretation.* Sinauer Associates, Inc., Sunderland, Massachusetts.

Cheal, D. (2008) Repeatability of cover estimates? *Ecological Management & Restoration,* **9,** 67-68.

Clark, J.S. (2003) Uncertainty and variability in demography and population growth: a hierarchical approach. *Ecology,* **84,** 1370-1381.

Clark, J.S. and Bjørnstad, O.N. (2004) Population time series: process variability, observation errors, missing values, lags, and hidden states. *Ecology,* **85,** 3140-3150.

Coulson, T., Mace, G.M., Hudson, E. and Possingham, H. (2001) The use and abuse of population viability analysis. *Trends in Ecology and Evolution,* **16,** 219-221.

Crone, E.E., Menges, E.S., Ellis, M.M., Bell, T., Bierzychudek, P., Ehrlén, J., Kaye, T.N., Knight, T.M., Lesica, P., Morris, W.F., Oostermeijer, G., Quintana-Ascencio, P.F., Stanley, A., Ticktin, T., Valverde, T. and Williams, J.L. (2011) How do plant ecologists use matrix population models? *Ecology Letters,* **14,** 1-8.

De Valpine, P. (2003) Better inferences from population-dynamics experiments using Monte Carlo state-space likelihood methods. *Ecology,* **84,** 3064-3077.

Dennis, B., Munholland, P.L. and Scott, J.M. (1991) Estimation of growth and extinction parameters for endangered species. *Ecological Monographs,* **61,** 115-143.

Dennis, B., Ponciano, J.M., Lele, S.R., Taper, M.L. and Staples, D.F. (2006) Estimating density dependence, process noise, and observation error. *Ecological Monographs,* **76,** 323-341.

Dennis, B., Ponciano, J.M. and Taper, M.L. (2010) Replicated sampling increases efficiency in monitoring biological populations. *Ecology,* **91,** 610-620.

Dickman, C.R., Wardle, G.M., Foulkes, J. and de Preu, N. (2014) Desert complex environments. *In:* Lindenmayer, D., Burns, E., Thurgate, N. & Lowe, A. (eds.) *Biodiversity and environmental change: monitoring, challenges and direction.* Collingwood, Victoria, Australia: CSIRO Publishing.

Doak, D.F., Thomson, D. and Jules, E.S. (2002) Population viability analysis for plants: understanding the demographic consequences of seed banks for population health. *In:* Beissinger, S. R. & McCullough, D. R. (eds.) *Population Viability Analysis.* Chicago, Illinois, USA: The University of Chicago Press.

Donoho, D.L. (2000) Aide-memoire. high-dimensional data analysis: the curses and blessings of dimensionality. *American Math. Society Lecture-Math Challenges of the 21st Century*.

Easterling, M.R., Ellner, S.P. and Dixon, P.M. (2000) Size-specific sensitivity: applying a new structured population model. *Ecology (Washington D C),* **81,** 694-708.

Eckhardt, H., Wilgen, B. and Biggs, H. (2000) Trends in woody vegetation cover in the Kruger National Park, South Africa, between 1940 and 1998. *African Journal of Ecology,* **38,** 108-115.

Efron, B. and Tibshirani, R. (1986) Bootstrap methods for standard errors, confidence intervals, and other measures of statistical accuracy. *Statistical Science,* **1,** 54-75.

Elderd, B., Shahani, P. and Doak, D. 2003. The problems and potential of count-based population viability analyses. *Population Viability in Plants.* Springer.

Ellner, S.P., Fieberg, J., Ludwig, D. and Wilcox, C. (2002) Precision of population viability analysis. *Conservation Biology,* **16,** 258-261.

Erzini, K., Inejih, C.A.O. and Stobberup, K.A. (2005) An application of two techniques for the analysis of short, multivariate non-stationary time-series of Mauritanian trawl survey data. *ICES Journal of Marine Science: Journal du Conseil,* **62,** 353-359.

Evans, M.R., Norris, K.J. and Benton, T.G. (2012) Predictive ecology: systems approaches. *Philosophical Transactions of the Royal Society B: Biological Sciences*, **367,** 163-169.

Eyre, T.J., Fisher, A., Hunt, L.P. and Kutt, A.S. (2011) Measure it to better manage it: a biodiversity monitoring framework for the Australian rangelands. *The Rangeland Journal,* **33,** 239-253.

Flesch, A.D. (2014) Spatiotemporal trends and drivers of population dynamics in a declining Sonoran Desert predator. *Biological Conservation,* **175,** 110-118.

Freckleton, R.P., Watkinson, A.R., Green, R.E. and Sutherland, W.J. (2006) Census error and the detection of density dependence. *Journal of Animal Ecology,* **75,** 837-851.

Fréville, H., Choquet, R., Pradel, R. and Cheptou, P.-O. (2013) Inferring seed bank from hidden Markov models: new insights into metapopulation dynamics in plants. *Journal of Ecology,* **101,** 1572-1580.

Garcia, M.B., Dahlgren, J.P. and Ehrlen, J. (2011) No evidence of senescence in a 300-year-old mountain herb. *Journal of Ecology,* **99,** 1424-1430.

Gentleman, R. and Lang, D.T. (2007) Statistical analyses and reproducible research. *Journal of Computational and Graphical Statistics,* **16**.

Gross, C. and Mackay, D. (2014) Two decades of demography reveals that seed and seedling transitions limit population persistence in a translocated shrub. *Annals of Botany*.

Hampton, S.E., Strasser, C.A., Tewksbury, J.J., Gram, W.K., Budden, A.E., Batcheller, A.L., Duke, C.S. and Porter, J.H. (2013) Big data and the future of ecology. *Frontiers in Ecology and the Environment,* **11,** 156-162.

Harper, J.L. (1977) *Population biology of plants.* Academic Press, London.

Harris, S.J., Risely, K., Massimino, D., Newson, S.E., Eaton, M.A., Musgrove, A.J., Noble, D., Procter, D. and Baillie, S. (2014) *The breeding bird survey 2013*. BTO research report, **658**. British Trust for Ornithology, Thetford.

Hauser, C.E., Pople, A.R. and Possingham, H.P. (2006) Should managed populations be monitored every year? *Ecological Applications,* **16,** 807-819.

Helm, D.J. and Mead, B.R. (2004) Reproducibility of vegetation cover estimates in South-Central Alaska Forests. *Journal of Vegetation Science,* **15,** 33-40.

Henderson, C.B., Petersen, K.E. and Redak, R.A. (1988) Spatial and temporal patterns in the seed bank and vegetation of a desert grassland community. *Journal of Ecology,* **76,** 717-728.

Hernandez, R.R., Mayernik, M.S., Murphy-Mariscal, M.L. and Allen, M.F. (2012) Advanced technologies and data management practices in environmental science: lessons from academia. *Bioscience,* **62,** 1067-1076.

Herrick, G.I. and Fox, G.A. (2013) Sampling stochasticity leads to overestimation of extinction risk in population viability analysis. *Conservation Letters***,** **6**, 238-246.

Holmes, E.E. (2001) Estimating risks in declining populations with poor data. *Proceedings of the National Academy of Sciences,* **98,** 5072-5077.

Holmes, E.E. and Fagan, W.F. (2002) Validating population viability analysis for corrupted data sets. *Ecology,* **83,** 2379-2386.

Holmes, E.E., Ward, E.J. and Wills, K. (2012) MARSS: multivariate autoregressive state-space models for analyzing time series data. *R Journal,* **4,** 11-19.

Honaker, J. and King, G. (2010) What to do about missing values in time-series cross-section data. *American Journal of Political Science,* **54,** 561-581.

Humbert, J.Y., Scott Mills, L., Horne, J.S. and Dennis, B. (2009) A better way to estimate population trends. *Oikos,* **118,** 1940-1946.

Inchausti, P. and Halley, J. (2001) Investigating long-term ecological variability using the global population dynamics database. *Science,* **293,** 655-657.

Jongejans, E. and de Kroon, H. (2005) Space versus time variation in the population dynamics of three co-occurring perennial herbs. *Journal of Ecology,* **93,** 681-692.

Kalisz, S. (1991) Experimental determination of seed bank age structure in the winter annual *Collinsia Verna*. *Ecology,* **72,** 575-585.

Kalisz, S. and McPeek, M.A. (1992) Demography of an age-structured annual: resampled projection matrices, elasticity analyses, and seed bank effects. *Ecology,* **73,** 1082-1093.

Katzner, T.E., Ivy, J.A.R., Bragin, E.A., Milner-Gulland, E. and DeWoody, J.A. (2011) Conservation implications of inaccurate estimation of cryptic population size. *Animal Conservation,* **14,** 328-332.

Keller, M., Schimel, D.S., Hargrove, W.W. and Hoffman, F.M. (2008) A continental strategy for the National Ecological Observatory Network. *Frontiers in Ecology and the Environment,* **6,** 282-284.

Kenall, A., Harold, S. and Foote, C. (2014) An open future for ecological and evolutionary data? *BMC Ecology,* **14,** 10.

Kennedy, R.E., Andréfouët, S., Cohen, W.B., Gómez, C., Griffiths, P., Hais, M., Healey, S.P., Helmer, E.H., Hostert, P. and Lyons, M.B. (2014) Bringing an ecological view of change to Landsat-based remote sensing. *Frontiers in Ecology and the Environment,* **12,** 339-346.

Kerr, J.T. and Ostrovsky, M. (2003) From space to species: ecological applications for remote sensing. *Trends in Ecology and Evolution,* **18,** 299-305.

Kim, E.-S. (2006) Development, potentials, and challenges of the International Long-Term Ecological Research (ILTER) Network. *Ecological Research,* **21,** 788-793.

Klimeš, L. (2003) Scale-dependent variation in visual estimates of grassland plant cover. *Journal of Vegetation Science,* **14,** 815-821.

Kwok, R. (2009) Personal technology: phoning in data. *Nature,* **458,** 959.

Lamy, T., Gimenez, O., Pointier, J.P., Jarne, P. and David, P. (2013) Metapopulation dynamics of species with cryptic life stages. *The American Naturalist,* **181,** 479-491.

Lathrop Jr, R.G., Haag, S.M., Merchant, D., Kennish, M.J. and Fertig, B. (2014) Comparison of remotely-sensed surveys vs. in situ plot-based assessments of sea grass condition in Barnegat Bay-Little Egg Harbor, New Jersey USA. *Journal of Coastal Conservation***,** 1-10.

Lavorel, S., McIntyre, S., Landsberg, J. and Forbes, T.D.A. (1997) Plant functional classifications: from general groups to specific groups based on response to disturbance. *Trends in Ecology and Evolution,* **12,** 474-478.

Lesica, P. and Steele, B.M. (1994) Prolonged dormancy in vascular plants and implications for monitoring studies. *Natural Areas Journal,* **14,** 209-212.

Linden, A. and Knape, J. (2009) Estimating environmental effects on population dynamics: consequences of observation error. *Oikos,* **118,** 675-680.

Lindenmayer, D., Burns, E., Thurgate, N. and Lowe, A.J. (2014) The value of long-term research and how to design effective ecological research and monitoring. *In:* Lindenmayer, D., Burns, E., Thurgate, N. & Lowe, A. J. (eds.) *Biodiversity and Environmental Change.* Collingwood, Victoria, Australia: CSIRO Publishing.

Lindenmayer, D.B. and Likens, G.E. (2011) Losing the culture of ecology. *Bulletin of the Ecological Society of America,* **92,** 245-246.

Lindenmayer, D.B., Likens, G.E., Andersen, A., Bowman, D., Bull, C.M., Burns, E., Dickman, C.R., Hoffmann, A.A., Keith, D.A., Liddell, M.J., Lowe, A.J., Metcalfe, D.J., Phinn, S.R., Russell-Smith, J., Thurgate, N. and Wardle, G.M. (2012) Value of long-term ecological studies. *Austral Ecology,* **37,** 745-757.

Ludwig, D. (1999) Is it meaningful to estimate a probability of extinction? *Ecology,* **80,** 298-310.

Macdonald, N. and Watkinson, A.R. (1981) Models of an annual plant population with a seedbank. *Journal of Theoretical Biology*, **93,** 643-653.

MacKenzie, D.I., Nichols, J.D., Seamans, M.E. and Gutiérrez, R. (2009) Modeling species occurrence dynamics with multiple states and imperfect detection. *Ecology,* **90,** 823-835.

Malhi, Y., Phillips, O., Lloyd, J., Baker, T., Wright, J., Almeida, S., Arroyo, L., Frederiksen, T., Grace, J. and Higuchi, N. (2002) An international network to monitor the structure, composition and dynamics of Amazonian forests (RAINFOR). *Journal of Vegetation Science,* **13,** 439-450.

Marx, V. (2013) Biology: the big challenges of big data. *Nature*, **498,** 255-260.

McCarthy, M.A., Andelman, S.J. and Possingham, H.P. (2003) Reliability of relative predictions in population viability analysis. *Conservation Biology,* **17,** 982-989.

McCarthy, M.A., Possingham, H.P., Day, J.R. and Tyre, A. (2001) Testing the accuracy of population viability analysis. *Conservation Biology,* **15,** 1030-1038.

McPeek, M. and Kalisz, S. (1993) Population sampling and bootstrapping in complex designs: demographic analysis. *Design and analysis of ecological experiments. Chapman & Hall, New York***,** 232-252.

Menges, E.S. (2000) Population viability analyses in plants: challenges and opportunities. *Trends in Ecology and Evolution,* **15,** 51-56.

Merow, C., Dahlgren, J.P., Metcalf, C.J.E., Childs, D.Z., Evans, M.E., Jongejans, E., Record, S., Rees, M., Salguero-Gómez, R. and McMahon, S.M. (2014) Advancing population ecology with integral projection models: a practical guide. *Methods in Ecology and Evolution,* **5,** 99-110.

Moriuchi, K.S., Venable, D.L., Pake, C.E. and Lange, T. (2000) Direct measurement of the seed bank age structure of a Sonoran Desert annual plant. *Ecology,* **81,** 1133-1138.

Morris, W., Doak, D.F., Groom, M., Kareiva, P., Fieberg, J., Gerber, L., Murphy, P. and Thomson, D. (1999) *A practical handbook for population viability analysis.* Nature Conservancy.

Nakagawa, S. and Freckleton, R.P. (2011) Model averaging, missing data and multiple imputation: a case study for behavioural ecology. *Behavioral Ecology and Sociobiology,* **65,** 103-116.

Pausas, J.G. and Austin, M.P. (2001) Patterns of plant species richness in relation to different environments: an appraisal. *Journal of Vegetation Science,* **12,** 153-166.

Pickett, S.T. (1989). Space-for-time substitution as an alternative to long-term studies. *In:* Likens, G. E. (ed.) *Long-term studies in ecology.* New York, New York, USA, Springer.

Piwowar, H.A., Day, R.S. and Fridsma, D.B. (2007) Sharing detailed research data is associated with increased citation rate. *PloS One,* **2,** e308.

Piwowar, H.A. and Vision, T.J. (2013) Data reuse and the open data citation advantage. *PeerJ,* **1,** e175.

Porter, J., Arzberger, P., Braun, H.-W., Bryant, P., Gage, S., Hansen, T., Hanson, P., Lin, C.-C., Lin, F.-P. and Kratz, T. (2005) Wireless sensor networks for ecology. *Bioscience,* **55,** 561-572.

Ramula, S., Dinnetz, P. and Lehtila, K. (2009a) Spatial data replacing temporal data in population viability analyses: an empirical investigation for plants. *Basic and Applied Ecology,* **10,** 401-410.

Ramula, S., Rees, M. and Buckley, Y.M. (2009b) Integral projection models perform better for small demographic data sets than matrix population models: a case study of two perennial herbs. *Journal of Applied Ecology,* **46,** 1048-1053.

Regan, H.M., Ben-Haim, Y., Langford, B., Wilson, W.G., Lundberg, P., Andelman, S.J. and Burgman, M.A. (2005) Robust decision-making under severe uncertainty for conservation management. *Ecological Applications,* **15,** 1471-1477.

Regan, H.M., Colyvan, M. and Burgman, M.A. (2002) A taxonomy and treatment of uncertainty for ecology and conservation biology. *Ecological Applications,* **12,** 618-628.

Regan, T.J., Chades, I. and Possingham, H.P. (2011) Optimally managing under imperfect detection: a method for plant invasions. *Journal of Applied Ecology,* **48,** 76-85.

Reich, K.J., Bjorndal, K.A. and Bolten, A.B. (2007) The ‘lost years’ of green turtles: using stable isotopes to study cryptic lifestages. *Biology Letters,* **3,** 712-714.

Reichman, O., Jones, M.B. and Schildhauer, M.P. (2011) Challenges and opportunities of open data in ecology. *Science,* **331**.

Rowcliffe, J.M. and Carbone, C. (2008) Surveys using camera traps: are we looking to a brighter future? *Animal Conservation,* **11,** 185-186.

Rumsfeld, D.H. (2002). Donald Rumsfeld press conference as US secretary of Defence [Online]. Available: http://www.defense.gov/transcripts/transcript.aspx?transcriptid=2636.

Salguero-Gómez, R. and Casper, B.B. (2010) Keeping plant shrinkage in the demographic loop. *Journal of Ecology,* **98,** 312-323.

Salguero-Gómez, R., Jones, O.R., Archer, C.R., Buckley, Y.M., Che-Castaldo, J., Caswell, H., Hodgson, D., Scheuerlein, A., Conde, D.A., Brinks, E., de Buhr, H., Farack, C., Gottschalk, F., Hartmann, A., Henning, A., Hoppe, G., Römer, G., Runge, J., Ruoff, T., Wille, J., Zeh, S., Davison, R., Vieregg, D., Baudisch, A., Altwegg, R., Colchero, F., Dong, M., de Kroon, H., Lebreton, J.-D., Metcalf, C.J.E., Neel, M.M., Parker, I.M., Takada, T., Valverde, T., Vélez-Espino, L.A., Wardle, G.M., Franco, M. and Vaupel, J.W. (2015) The COMPADRE Plant Matrix Database: an open online repository for plant demography. *Journal of Ecology,* **103,** 202-218.

Salski, A. (1992) Fuzzy knowledge-based models in ecological research. *Ecological Modelling,* **63,** 103-112.

Shefferson, R.P. (2009) The evolutionary ecology of vegetative dormancy in mature herbaceous perennial plants. *Journal of Ecology,* **97,** 1000-1009.

Shenk, D. (1998) *Data smog: surviving the information glut.* Harper San Francisco.

Shenk, T.M., White, G.C. and Burnham, K.P. (1998) Sampling-variance effects on detecting density dependence from temporal trends in natural populations. *Ecological Monographs,* **68,** 445-463.

Shumway, R.H. and Stoffer, D.S. (1982) An approach to time series smoothing and forecasting using the EM algorithm. *Journal of time series analysis,* **3,** 253-264.

Shumway, R.H. and Stoffer, D.S. (2006) *Time series analysis and its applications.* Springer-Verlag, New York, New York, USA.

Soranno, P.A., Cheruvelil, K.S., Elliott, K.C. and Montgomery, G.M. (2015) It's good to share: why environmental scientists’ ethics are out of date. *Bioscience,* **65,** 69-73.

Staples, D.F., Taper, M.L. and Dennis, B. (2004) Estimating population trend and process variation for PVA in the presence of sampling error. *Ecology,* **85,** 923-929.

Ter Braak, C., Van Strien, A., Meijer, R. and Verstrael, T. (1994) Analysis of monitoring data with many missing values: which method. *Bird***,** 663-673.

Tobler, M., Carrillo-Percastegui, S., Leite Pitman, R., Mares, R. and Powell, G. (2008) An evaluation of camera traps for inventorying large-and medium-sized terrestrial rainforest mammals. *Animal Conservation,* **11,** 169-178.

Tuljapurkar, S. (1989) An uncertain life: demography in random environments. *Theoretical Population Biology,* **35,** 227-294.

Tuljapurkar, S., Horvitz, C.C. and Pascarella, J.B. (2003) The many growth rates and elasticities of populations in random environments. *The American Naturalist,* **162,** 489-502.

Tuljapurkar, S. and Lee, R. (1997) Demographic uncertainty and the stable equivalent population. *Mathematical and Computer Modelling,* **26,** 39-56.

Verheyen, K., Honnay, O., Motzkin, G., Hermy, M. and Foster, D.R. (2003) Response of forest plant species to land-use change: a life-history trait-based approach. *Journal of Ecology,* **91,** 563-577.

Vines, Timothy H., Albert, Arianne Y.K., Andrew, Rose L., Débarre, F., Bock, Dan G., Franklin, Michelle T., Gilbert, Kimberly J., Moore, J.-S., Renaut, S. and Rennison, Diana J. (2014) The availability of research data declines rapidly with article age. *Current Biology,* **24,** 94-97.

Wang, G., Zhou, G., Yang, L. and Li, Z. (2003) Distribution, species diversity and life-form spectra of plant communities along an altitudinal gradient in the northern slopes of Qilianshan Mountains, Gansu, China. *Plant Ecology,* **165,** 169-181.

Ward, E.J., Chirakkahl, H., González-Suárez, M., Aurioles-Gamboa, D., Holmes, E.E. and Gerber, L. (2010) Inferring spatial structure from time-series data: using multivariate state-space models to detect metapopulation structure of California sea lions in the Gulf of California, Mexico. *Journal of Applied Ecology,* **47,** 47-56.

Warton, D.I. and Wardle, G.M. (2003) Site-to-site variation in the demography of a fire-affected perennial, Acacia suaveolens, at Ku-ring-gai Chase National Park, New South Wales, Australia. *Austral Ecology,* **28,** 38-47.

Webb, N.R. (1990) Changes on the heathlands of Dorset, England, between 1978 and 1987. *Biological Conservation,* **51,** 273-286.

Whitlock, M.C. (2011) Data archiving in ecology and evolution: best practices. *Trends in Ecology & Evolution,* **26,** 61-65.

Whitlock, M.C., McPeek, M.A., Rausher, M.D., Rieseberg, L. and Moore, A.J. (2010) Data archiving. *The American Naturalist,* **175,** 145-146.

Wintle, B.C., Fidler, F., Vesk, P.A. and L. Moore, J. (2013) Improving visual estimation through active feedback. *Methods in Ecology and Evolution,* **4,** 53-62.

Wulder, M.A., Masek, J.G., Cohen, W.B., Loveland, T.R. and Woodcock, C.E. (2012) Opening the archive: how free data has enabled the science and monitoring promise of Landsat. *Remote Sensing of Environment,* **122,** 2-10.

Zimmerman, A.S. (2003) *Data sharing and secondary use of scientific data: experiences of ecologists.* PhD dissertation, The University of Michigan.

Chapter 2 - Consequences of continuing to exclude cryptic life stages from demographic models

High resolution images of seeds sampled from the Simpson Desert, Australia.
Clockwise from top left: *Trachymene glaucifolia, Crotalaria cunninghamii, Triodia basedowii* and *Acacia dictyophleba.* Photographs by David Nelson.

A version of this chapter has been submitted and is currently under review in Methods in Ecology and Evolution as Nguyen, V., Buckley, Y.M., Salguero-Gómez R. and Wardle, G.M. (2015) Consequences of continuing to exclude cryptic life stages from demographic models. Submitted 4th June 2015.

My contribution was very substantial, including conceptualisation of ideas, reconstruction and analysis of models, conducting simulations, and writing and editing all drafts in consultation with my co-authors.

Summary

1. Estimates of population abundance, viability and invasibility based on population models with incomplete life cycles are likely to be misleading. Thus information on individuals from *all* stages in the life cycle is crucial to explore the ecology, evolution and conservation biology of any organism. However, the life cycles of many species contain cryptic life stages that are difficult to detect and track over time and these individuals are therefore omitted from demographic models. One example is the dormant seed bank, an evolutionary bet hedging mechanism that buffers plant populations in variable environments.

2. To evaluate this methodological oversight, simulations based on plausible values for seed bank vital rates explored the extent and effect of seed bank parameter uncertainties on demographic outputs such as the deterministic population growth rate (λ), stochastic population growth rate (λ_S), and local extinction risk of 12 plant species. The simulations included seed bank parameters from both uninformed and informed priors based on literature estimates, which were used to reconstruct previously published models in which the seed banks were excluded without justification.

3. Inclusion of a seed bank and demographic uncertainty in seed bank parameters had little impact for stable populations ($\lambda \approx 1$) with high post-seedling survival, but it played a greater role in populations with high temporal demographic variation.

4. By exploring underlying assumptions regarding population model structure and seed bank vital rates, I found that our perspective on the importance of the seed bank is context-specific, depending on the species and the type of environmental cues in the period under consideration. While estimates of germination rates obtained from the

literature cannot accurately reflect those obtained in the field, they provide data to evaluate plausible scenarios and thus assess the relative important of a seed bank. The seed bank can be excluded in certain cases, provided that it is justified either through literature confirmation that dormancy is non-existent, greenhouse tests, or through simulations. Overlooking the seed bank stage, or any cryptic stage such as vegetative dormancy, will continue to hinder management efforts of threatened populations and undermines actions to control invasive species.

Introduction

Demographers have long recognised that individuals in a population span across different stages of their life cycle, from propagules up to reproductive adults, and that these stages contribute to its persistence in different ways – failing to account for all these stages can therefore be misleading (Caswell, 2001). However, the life cycles of many species contain cryptic life stages that may be difficult to detect or sample. These cryptic life stages occur over a range of taxonomic groups, and may include hibernating or dormant individuals, clonal individuals, eggs, mobile propagules, or simply stages occupying inaccessible locations (Tanner, 2001; Geiser, 2004; Shefferson, 2009; Katzner *et al.*, 2011). The dormant seed bank is perhaps one of the most common examples of a cryptic life stage whereby seeds enter prolonged dormancy (>1 year) within the soil, and even make up a significant portion of the population (Harper, 1977; Baskin and Baskin, 2014). By spreading germination through time, seed dormancy acts as a bet-hedging mechanism mitigating the effects of unfavourable years in exchange for reduced proliferation during favourable years (Venable, 2007; Gremer *et al.*, 2012). In extreme cases, seed banks can prevent local extinctions when above-ground populations are killed off entirely (Stöcklin and Fischer, 1999). Seed dormancy has also been shown to promote species co-existence in variable environments (Warner and Chesson, 1985) and act as a temporal reservoir for genetic diversity (Vitalis *et al.*, 2004).

With such substantial consequences for population dynamics, it would be a major oversight to exclude the seed bank, or any cryptic life stage, from population estimates and demographic analyses. This argument is indeed not new: the need to incorporate the seed bank into demographic models has been recognised for decades (Harper, 1977; Kalisz and McPeek, 1992). Matrix population models, which divide individuals into their respective stage classes, are currently the most common tool for modelling plant populations – the online database of plant matrix models, COMPADRE, currently contains 5,621 published matrices for 598 species (Salguero-Gómez *et al.*, 2015). These models have a long history in the management of threatened and invasive species (Crone *et al.*, 2011). Yet, a previous review of 70 published matrix population models found almost half (43%) had excluded the seed bank stage without justification (Doak *et al.*, 2002). Shockingly, I have found that this proportion has remained unchanged in the last decade (47%; Table 2-1). It should be acknowledged that including the seed bank is not straightforward as estimation of vital rates such as survival and germination generally rely on additional laboratory experiments (Crone *et al.*, 2011), and even these would inflate actual *in situ* estimates (Gross and Mackay, 2014). Furthermore, unless such experiments are rigorous enough to include age-specific vital rates (Kalisz and McPeek, 1992), the seed bank is generally assumed to be unstructured. Indeed, population data for the seed rain, seed banks, and seedlings tend to be inadequate and are often studied for only a year or less (Clark *et al.*, 1999). Excluding the seed bank may be justified if it is discovered the species, or population, does not possess dormant seeds (see Baskin and Baskin, 2014 for review on the presence of seed dormancy), however, these cases are the minority compared to those that do not provide justification (Doak *et al.*, 2002; Table 2-1). Unjustified exclusion can have real-world consequences if for example the seed bank of an invasive species recolonises after the adult individuals have been eliminated (Regan *et al.*, 2011) or the population size and persistence of threatened species is underestimated (Doak *et al.*, 2002).

The practical issues of including a seed bank and its exclusion from demographic models raise two important questions. Firstly, how can we bridge the gap in our understanding of whether a seed bank is necessary to adequately model the population dynamics in the absence of field data? Secondly, how does uncertainty in the presence of a seed stage and its transition rates translate into uncertainty in the model? Addressing these questions using a simulation based approach can be useful for investigating a range of scenarios and assumptions but may not be biologically meaningful without application to real world examples. An empirical based approach, on the other hand, may be limited in its scope if it were to focus on a single case study, as there are clear difficulties in obtaining individual level records for published models. Using published matrix models that have excluded the seed bank without justification and information on dormancy and germination rates from the literature, I implement a combination of these approaches and perform a comparative analysis across a range of species and life forms (12 species including eight trees, three shrubs and one herb). I conduct Monte Carlo simulations on these published models using uninformed and informed priors (based on literature estimates) for seed bank vital rates to gauge the level of uncertainty when the seed bank presence and parameters are unknown. Although many seed banks are known to respond to triggers such as fire or rainfall, these environmental cues were either not present or would need to be inferred based on the published matrices. Thus, the present

Table 2-1. Comparison of studies from the MPM2008-2011 database with a previous review by (Doak *et al.*, 2002) examining the inclusion of the seed bank in plant population models. Studies were classified as justified exclusion if a valid reason was provided for not including the seed bank (e.g. the authors found no evidence of a seed bank) and unjustified exclusion if the possibility of a seed bank was not explored or mentioned. Studies from COMPADRE were not analysed to determine whether exclusion of the seed bank was justified.

Population models and seed banks	Doak et al. (2002)	MPM2008-2011	COMPADRE v.3.1.0
Included	34 (48.6%)	16 (29.1%)	160 (34.2%)
Justified exclusion	6 (9.6%)	13 (23.6%)	308 (65.8%)
Unjustified exclusion	30 (42.9%)	26 (47.3%)	
Total studies	70	55	468

simulations will only be distinguishing between good and poor demographic years based on the population growth rates.

I make a number of predictions based on the evolutionary advantages of seed dormancy. First, we might expect the relative importance of seed banks to be greater in species where greater environmental variance is observed and variable post-seedling survival compared to stable populations of long-lived species with consistently high adult survival (Venable, 2007). Furthermore, the deterministic growth rate (λ), which assumes vital rates remain constant, should improve population persistence during poor demographic years ($\lambda < 1$) and slow population increases during productive years ($\lambda > 1$) to reflect the function of the seed bank as a bet hedging mechanism against unfavourable years (Kalisz and McPeek, 1992; Gremer *et al.*, 2012). Similarly, elasticities (the relative influence of each demographic process to the population growth rate; de Kroon *et al.*, 2000) for seed bank transition rates should be greater during poor years. There should also be an observed increase in times to local extinction and stochastic growth rates,(λ_s), which incorporate temporal variation in vital rates. Using both an empirical and simulation based approach, I provide more robust projections of the demographic fates of populations and help to motivate the inclusion of the seed bank into demographic models.

Materials and Methods

Database of population matrix models

At the time this study was initially conducted, the COMPADRE Plant Matrix Database had not become open access online (Salguero-Gómez *et al.*, 2015), with the most recent update consisting of 204 terrestrial plant species up to 2007, hereafter referred to as the “MPM2007” database constructed by the Vegetation Function Working Group (see Burns *et al.*, 2010 for further information). I used the ISI Web of Science to identify published plant matrix population models from 2008-2011, hereafter referred to as the “MPM2008-2011” database, which would later go on to be added to COMPADRE. Examples of search terms used include “matrix model*”, “transition matrix”, “demographic model*”, “population model*”, “population viability analysis”, “population growth rate” and “population dynamics”. In total, 55 studies with matrix models for 77 terrestrial plant species were found, including 38 trees, 27 herbs, 8 shrubs and 4 succulents.

Addition and removal of seed bank stages

Using Baskin and Baskin, (2014) and the species name as a search term in ISI Web of Science, I verified whether a seed bank was reported for species in which seed bank exclusion was unjustified (possibility of a seed bank was not mentioned; Table 2-1). While each population may not necessarily possess a seed bank, it is still worth determining the impact of its potential presence on model outcomes. In total, new matrix population models were constructed for 12 plant species for which published germination data on either the species or the genus was available and the original matrices were provided.

Adding, removing or excluding stages without justification alters the dimensionality of the model and this will affect the demographic parameter estimates. Merging or further dividing up stage classes directly alters vital rates for each class being affected and the speed of the life cycle, with lower dimensions reducing the number of stages to progress through the life cycle (Salguero-Gómez and Plotkin, 2010). As the seed bank functions as a bet hedging mechanism, delayed movement through the life cycle is to be expected and this is reflected in the hypotheses outlined in the previous section. Since the seed bank is a separate, discrete stage class that involves no splitting or merging, transition probabilities for the other classes should remain unaffected by its inclusion. However, seedling fecundity would need to be lowered accordingly to account for observed seedlings emerging from the seed bank to avoid overestimating fecundity. Seedling counts were used to estimate for fecundity in all models where the seed bank was excluded without justification. Thus, I assumed the seedlings observed consisted of two components: individuals that germinated immediately between year t and $t + 1$ and individuals that germinated from the unobserved seed bank. This can be described by the following equation:

$$f_{i,j} = F_{j,t}vgs + F_{j,t-1}v(1-g)(1-d)g_{b1} + F_{j,t-2}v(1-g)(1-g_{b1})(1-d)^2g_{b2}\ldots \tag{1}$$

where the first term on the right hand side represents immediate germinants, the second represents germination of seeds from the seed bank produced in the previous time period and the third term represents germination of seeds from the seed bank produced two time periods ago.

$f_{i,j}$ = per-capita fecundity into stage class i by stage class j in one time step

$F_{j,t}$ = total fecundity by stage class j at time t

v = seed viability rate during the period t to $t + 1$

g = probability of germinating during the period t to $t + 1$

g_b = probability of germinating from the seed bank within the period t to $t + 1$

s = probability of seedling survival until the next census

d = seed bank mortality

(See Fig. 2-1 for more information). To simplify the inclusion of the seed bank stage using limited information, the following assumptions were made. First, the probability of a seed surviving to germinate in the period t to $t + 1$ and be alive in the next census $t + 1$ (s), was equal to the probability of surviving in the seed bank ($1 - d$). Second, I conducted simulations focusing on the contribution of the seed bank from $t - 1$. This unstructured model captures the predominant seed bank contribution since the contribution of seeds from previous years will diminish exponentially with each year, assuming vital rates are not seed age dependent.

Fig. 2-1. Life cycle graphs corresponding to **A)** a plant consisting of two life stages: the seedlings, Se, and the adults, Ad, **B)** a plant consisting of seeds that have remained in the seed bank for 1 year, S1, up to n years, Sn (Eq. 1), and **C)** a plant with an unstructured seed bank, SB, (Eq. 2). The transition rate $f_{Se,Ad}$ gives the fecundity into the seedling stage while $f_{S1,Ad}$ and $f_{SB,Ad}$ gives the fecundity into the seed bank. **D)** Details of the derivation of Eq. 1 in which the variables are contained in boxes. Tracking the variables required to reach the seedling stage from the adult stage either directly or via the seed bank demonstrates how each term in Equation 1 was derived.

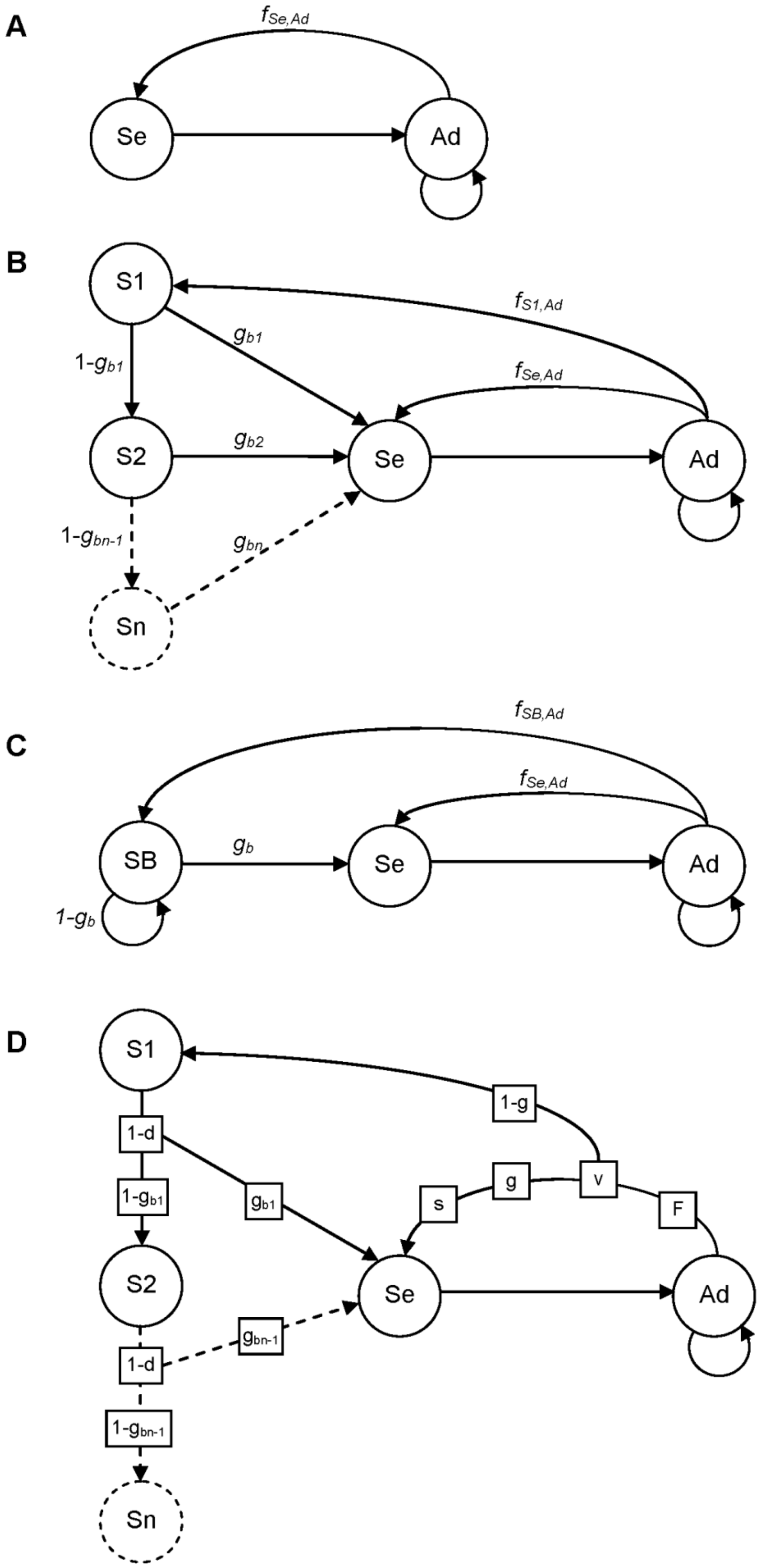
A
$f_{Se,Ad}$
Se
Ad
B
S1
$f_{S1,Ad}$
g_{b1}
$1-g_{b1}$
$f_{Se,Ad}$
S2
g_{b2}
Se
Ad
$1-g_{bn-1}$
g_{bn}
Sn
C
$f_{SB,Ad}$
$f_{Se,Ad}$
SB
g_b
Se
Ad
$1-g_b$
D
S1
1-g
1-d
g
v
s
F
$1-g_{b1}$
g_{b1}
S2
Se
Ad
g_{bn-1}
1-d
$1-g_{bn-1}$
Sn

Alternative age-structured formulations are explored below. Additionally, the fecundity from the previous year was assumed to equal the fecundity in the current year, i.e. $F_{j,t} = F_{j,t-1}$, hereafter denoted by F_j. Finally, the probability of germinating within the census year was equal to the probability of germinating from the seed bank, i.e. $g = g_b$ (Kalisz and McPeek, 1992). Using the published information on germination, eq. 1 is simplified to:

$$f_{i,j} = F_j vgs + F_j v(1-g)(1-d)g \qquad (2)$$

where the first term on the right hand side represents the number of seedlings germinating immediately between t and $t + 1$, and the second term corresponds to the number of seedlings germinating from the seed bank. Seed viability (v), seedling survival (s) and seed survival ($1 - d$) were subject to different values depending on the analysis performed. Taking the observed $f_{i,j}$ from the original matrix, I solved for F_j and calculated the per-capita fertility contributions to seedlings and seed bank (See Appendix 1-1 for an example). Following the same approach, I also explored alternative model formulations and the effect of different assumptions but only performed Monte Carlo simulations for the unstructured scenario, which is the simplest and most common approach to including the seed bank. These alternatives include the addition of an age-structured seed bank distinguishing seeds from t - 2 and t - 3 and more conservative estimates on the effect of the seed bank by further assuming the seeds do not survive beyond the first, second or third year (See Appendix 1-1 and Appendix 1-2 for alternative formulations and population growth rates for all models).

Excluding the seed bank from a model makes the implicit assumption that it is not present in the population, thus the seed bank was intentionally removed from selected models to explore the implications of this assumption. Given the large number of potential models to choose from, I decided to focus on cases in which the seed bank was known to be important (elasticities of λ to seed survival, germination or fecundity > 0.1) to demonstrate the worst case scenario that might be possible when the seed bank is ignored. Six such species were identified from the MPM2007 and MPM2008-2011 databases that fulfilled this criteria whilst retaining ergodicity, the condition that it is possible to transition from each stage to all other stages (Caswell, 2001). Information on seed viability, seedling survival, and seed survival were used if provided, but were otherwise set to 1 and it is no longer assumed that $g = g_b$, since g_b can be obtained from the original matrix. The probability of seeds germinating within the studied period, g, was then estimated based on partitioning the total reproductive output (eqs. 1 and 2) to recalculate only the fecundity into the seedling stage. To further ensure that no artefacts from changes to reproduction or mortality were introduced, the removal protocol was the reverse of the addition protocol and a check of the recovery of the initial matrix after these manipulations was performed (See Appendix 1-3 for an example).

Analyses

Population growth rates (λ), elasticities and stochastic simulations were conducted for case studies involving addition or removal of the seed bank stage. Monte Carlo simulations were conducted only for the addition of the seed stage. All analyses were performed using R (v 3.1.1; The R Foundation for Statistical Computing; see Appendix 1-4 for code to perform Monte Carlo simulations).

Initial Monte Carlo simulations used an uninformed prior for germination, viability, seedling survival and seed survival and thus were drawn from a uniform distribution. Although we might expect covariance among vital rates for the below and above-ground individuals (Morris and Doak, 2002), introducing this structure is complicated particularly when dealing with the seed bank. Models that do include the seed bank for example generally estimate seed bank vital rates through separate germination experiments such that the covariance between the seed bank and the above-ground population is lost in the process. While the impact of this covariance structure on the model outcomes would be of interest, the focus here is on the issue of exclusion of the seed bank from demographic models, leaving investigations regarding correlation structure for future research.

I performed 10,000 simulations, reconstructing the matrix for each set of parameters that was drawn and then calculated the population growth rate. I report the mean growth rates with confidence intervals obtained by the 2.5% and 97.5% quantiles (See Appendix 1-5 for graphs of population growth rates with simulation sizes ranging from 1 to 20000). I then repeated this process using informed priors obtained via literature estimates for germination, and occasionally viability when available, and again, calculated the population growth rate for each set of parameters drawn. Publications on germination often contain multiple treatments and an estimated mean germination rate for each treatment. The prior distributions were specified depending on the type of demographic year to reflect the function of the seed bank as a bet hedging mechanism (the highest germination rate available when $\lambda > 1$ and the lowest when $\lambda < 1$; Kalisz and McPeek, 1992; Gremer *et al.*, 2012). However, if only one germination rate was provided, this value was used for all population matrix models regardless of the demographic year. If only the mean matrix was provided (the element-by-element arithmetic mean matrix across all years and sites), the average germination over all treatments was used. Both germination and viability were modelled using the beta distribution as it is bounded between 0 and 1, with the mode of the distribution equal to the germination rate.

Population growth rates were also calculated using fixed values of germination (0.01-1 by increments of 0.01) and viability (0.1, 0.5, and 1) to capture the complete range of possible values when only these parameters are allowed to vary. The matrices in which the germination rate was set to that obtained from the literature were used to calculate single point estimates of λ, elasticity matrices, λ_S and calculate extinction risks, with viability, seed survival and seedling survival set to 1 if no information was available. The initial population for all stochastic and extinction risk calculations hereafter consisted of 1,000 individuals at stable stage distribution, calculated as the right eigenvector (Caswell, 2001) of the mean matrix. Stochastic growth rates were calculated via matrix selection (Kaye and Pyke, 2003). Briefly, when populations had multiple years of matrices available, at each time step, each matrix had an equal probability of being selected. The initial population was projected over 10,000 time steps with the first 2,000 omitted to remove transient dynamics (Morris and Doak, 2002; Kaye and Pyke, 2003). The mean and variance of the growth rates were used to obtain an estimate for λ_S and 95% confidence intervals.

Extinction risks between models with and without seed banks were also compared. Times to extinction (defined as population size ≤ 100 individuals) were calculated for matrices predicting population decline. An initial population was projected for individual matrices over 100 years and compared the difference in times to extinction with and without the seed bank to quantify the effect of the seed bank on population persistence. Stochastic simulations were conducted to calculate the cumulative probability of quasi-extinction (Morris and Doak, 2002). An initial population was simulated over 100 years with a quasi-extinction threshold set to 100 individuals (i.e. one tenth of the initial population size). I performed 100 runs, with 5000 iterations per run, and calculated the mean fraction of projections that fell below the quasi-extinction threshold during or before year *t* was used to calculate the cumulative probability of quasi-extinction (Morris and Doak, 2002).

Results

Addition of the seed bank and demographic uncertainty

Inclusion of an unstructured seed bank showed fairly small differences in λ for most species regardless of the assumptions made (See Table 2-2 and Fig 2-2 for comparison of growth rates). However, the potential range of growth rates when demographic parameters are uncertain can be large depending on the species and the amount of temporal variation observed. The 8 tree species for example had stable populations ($\lambda \approx 1$), and variation in seed bank parameters had little influence in the overall models with the exception of *Illicium anisatum* (Schisandraceae). Subsequently, using informed priors for these species had little impact on the distribution of possible growth rates. In contrast, the shorter lived shrub species *Atriplex acanthocarpa* (Amaranthaceae) and *Sambucus racemosa* (Adoxaceae) were more sensitive to the introduction of a seed bank and demographic uncertainty in its vital rates. Here, using a high germination prior led to a reduced distribution of possible growth rates for the *A. acanthocarpa* 1996-1997 matrix when the population was extremely productive (Fig. 2-3). Conversely, the use of lower germination rates (or assumed higher levels of dormancy) during the poorer 1997-1999 years appeared to increase the spread of possible growth rates. Despite this, poor years tended to have a smaller distribution of possible growth rates and were therefore less sensitive to changes in demographic parameters compared to good years (Figs. 2-3 and 2-4). Generally, distributions of growth rates were skewed, with peaks being concentrated when germination rates were high and greater variation in λ when germination is low (Figs. 2-3 and 2-4). However, these simulations only investigated the unstructured seed bank scenario. Further uncertainties exist with regards to the longevity and structure of the seed bank, both of which were only briefly explored in this study (Appendix 1-2).

Table 2-2. Comparison of population growth rates (λ) following the addition of a seed bank. *Pop*. refers to populations of the same species in the same study. *Avg*. represents the population growth rate of the mean matrix for each population. *Stoch*. represents the mean stochastic growth rate from populations projected over 10,000 years. SB denotes single point estimates from models with germination and viability equal to that obtained from the literature. Growth rates from Monte Carlo simulations were obtained from the mean of 10,000 simulations with parameters for germination, viability, seed survival and seedling survival drawn from uniform distributions when priors are uninformed, while germination and viability were drawn from beta distributions when priors were informed. 95% confidence intervals for Monte Carlo simulations and stochastic growth rates are displayed in brackets.

Study	**Life Form**	**Pop**	**Period**	**No SB**	**SB**	**Monte Carlo sim. uninformed prior**	**Monte Carlo sim. informed prior**
Single time period							
Chien *et al*., (2008)							
Calocedrus macrolepus	Tree	1	1	0.9683	0.9715	0.9700 (0.9683,0.9785)	0.9699 (0.9683,0.9752)
Parashorea chinensis	Tree	1	1	0.9948	0.9955	0.9963 (0.9948,1.0040)	0.9954 (0.9948,0.9978)
Pinus kwangtungensis	Tree	1	1	0.9776	0.9786	0.9786 (0.9776,0.9834)	0.9782 (0.9776,0.9799)
Kisanuki *et al*., (2008)							
Illicium anisatum	Tree	1	1	1.1271	1.1647	1.1344 (1.1258,1.1765)	1.1408 (1.1263,1.1778)
		2	1	1.1864	1.2276	1.1931 (1.1828,1.2363)	1.2008 (1.1840,1.2416)
Abe *et al*., (2008)							
Sambucus racemosa	Shrub	1	1	1.1696	1.1690	1.1789 (1.1661,1.2355)	1.1951 (1.1674,1.2639)
		2	1	1.0007	1.0012	1.0109 (1.0007,1.0622)	1.0255 (1.0008,1.0963)
		3	1	2.2227	2.2031	2.1588 (2.0468,2.2210)	2.1459 (2.0551,2.2125)
Kouassi *et al*., (2008)							
Eremospatha macrocarpa	Tree	1	1	0.9792	0.9811	0.9806 (0.9792,0.9887)	0.9805 (0.9792,0.9842)
Laccosperma secundiflorum	Tree	1	1	0.9606	0.9661	0.9638 (0.9607,0.9815)	0.9621 (0.9607,0.9658)

Multiple time periods							
Mondragon, (2009)							
Guarianthe aurantiaca	Herb	1	1	0.9851	0.9881	0.9917 (0.9851,1.0253)	0.9872 (0.9851,0.9929)
		1	2	0.9895	0.9908	0.9929 (0.9895,1.0107)	0.9905 (0.9895,0.9931)
			Avg.	0.9869	0.9891	-	-
			Stoch.	0.9869	**0.9891*** (0.9891,0.9892)	-	-
Quitete Portela *et al.*, (2010)							
Astrocaryum aculeatissimum	Tree	1	1	1.0093	1.0106	1.0111 (1.0093,1.0209)	1.0100 (1.0093,1.0112)
		1	2	0.9964	0.9968	0.9971 (0.9964,1.0001)	0.9966 (0.9964,0.9972)
			Avg.	0.9998	1.0085	-	-
Geonoma schottiana			Stoch.	0.9998	**1.0000*** (0.9999,1.0001)	-	-
	Tree	1	1	1.0043	1.0240	1.0114 (1.0050,1.0442)	1.0213 (1.0050,1.0712)
		1	2	0.9823	1.0002	1.0115 (1.0050,1.0453)	1.0216 (1.0050,1.0721)
			Avg.	0.9949	1.0150	-	-
			Stoch.	0.9949	**1.0147*** (1.0142,1.0152)	-	-
Verhulst *et al.*, (2008)							
Atriplex acanthocarpa	Shrub	1	1	2.4526	2.3455	2.3016 (2.0678,2.4476)	2.3541 (2.0759,2.4489)
		1	2	0.7301	0.8305	0.7418 (0.7302,0.8288)	0.7508 (0.7303,0.8362)
		1	3	0.7436	0.8862	0.7712 (0.7438,0.8951)	0.7924 (0.7444,0.9051)
			Avg.	1.3461	1.3351	-	-
			Stoch.	1.1434	**1.1784*** (1.1726,1.1841)	-	-
Atriplex canescens	Shrub	1	1	1.7211	1.7012	1.6883 (1.6184,1.7315)	1.6791 (1.6160,1.7175)
		1	2	0.9451	0.9451	0.9451 (0.9451,0.9453)	0.9451 (0.9451,0.9451)
		1	3	0.8805	0.8835	0.8810 (0.8805,0.8823)	0.8805 (0.8805,0.8807)
			Avg.	1.1346	1.1648	-	-
			Stoch.	1.0776	**1.1168*** (1.1031,1.1308)	-	-

* Population growth rates (λ) between matrix models with and without seed bank were significantly different according to the 95% confidence interval. Statistically different population growth rates are also shown in bold font.

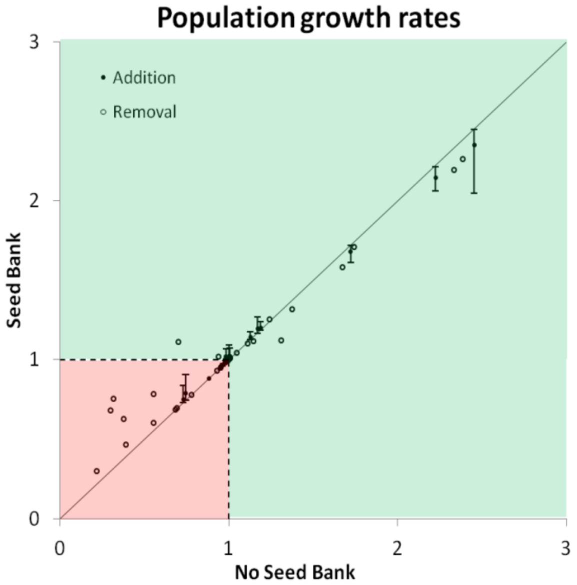

Fig. 2-2. Plot comparing population growth rates between models with and without the seed bank. Growth rates and error bars for models where the seed bank was added were taken from Monte Carlo simulations with germination prior guided by the literature. Points above the one-to-one line indicate the seed bank has a positive effect on λ while points below indicate a negative effect. Points occupying the red section are declining populations (λ < 1) while those occupying the green section are increasing populations (λ > 1).

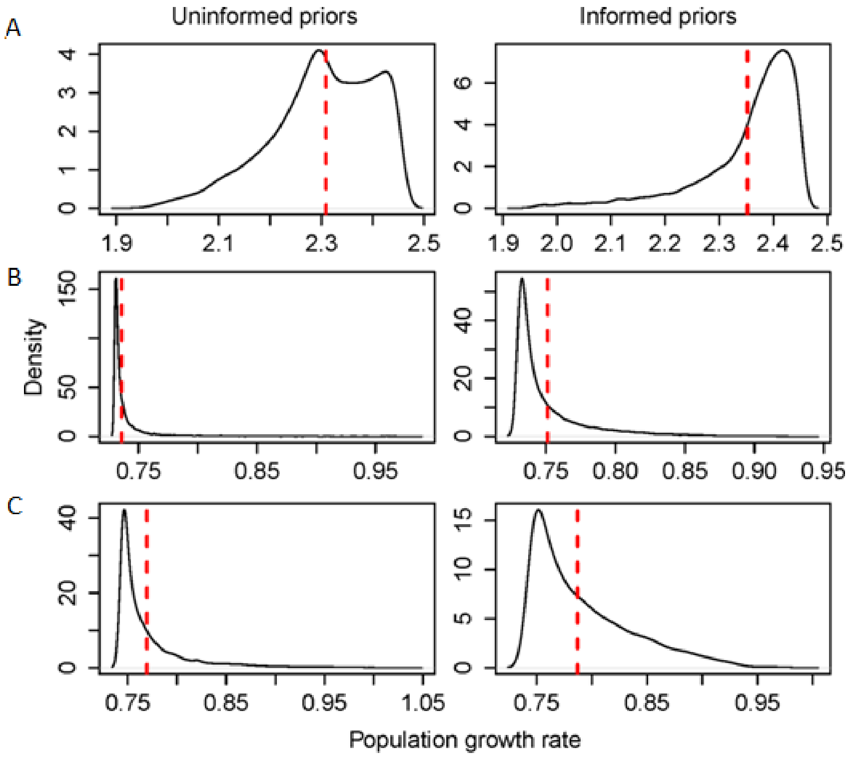

Fig. 2-3. Distribution of population growth rates for *Atriplex acanthocarpa* from **A)** 1996-1997, **B)** 1997-1998 and **C)** 1998-1999 based on 10,000 Monte Carlo simulations when using an uninformed prior on germination (uniform distribution) and an informed prior on germination (beta distribution with mode equal to germination rate obtained from the literature). Red dashed lines indicate the mean growth rate as reported in Table 2-2.

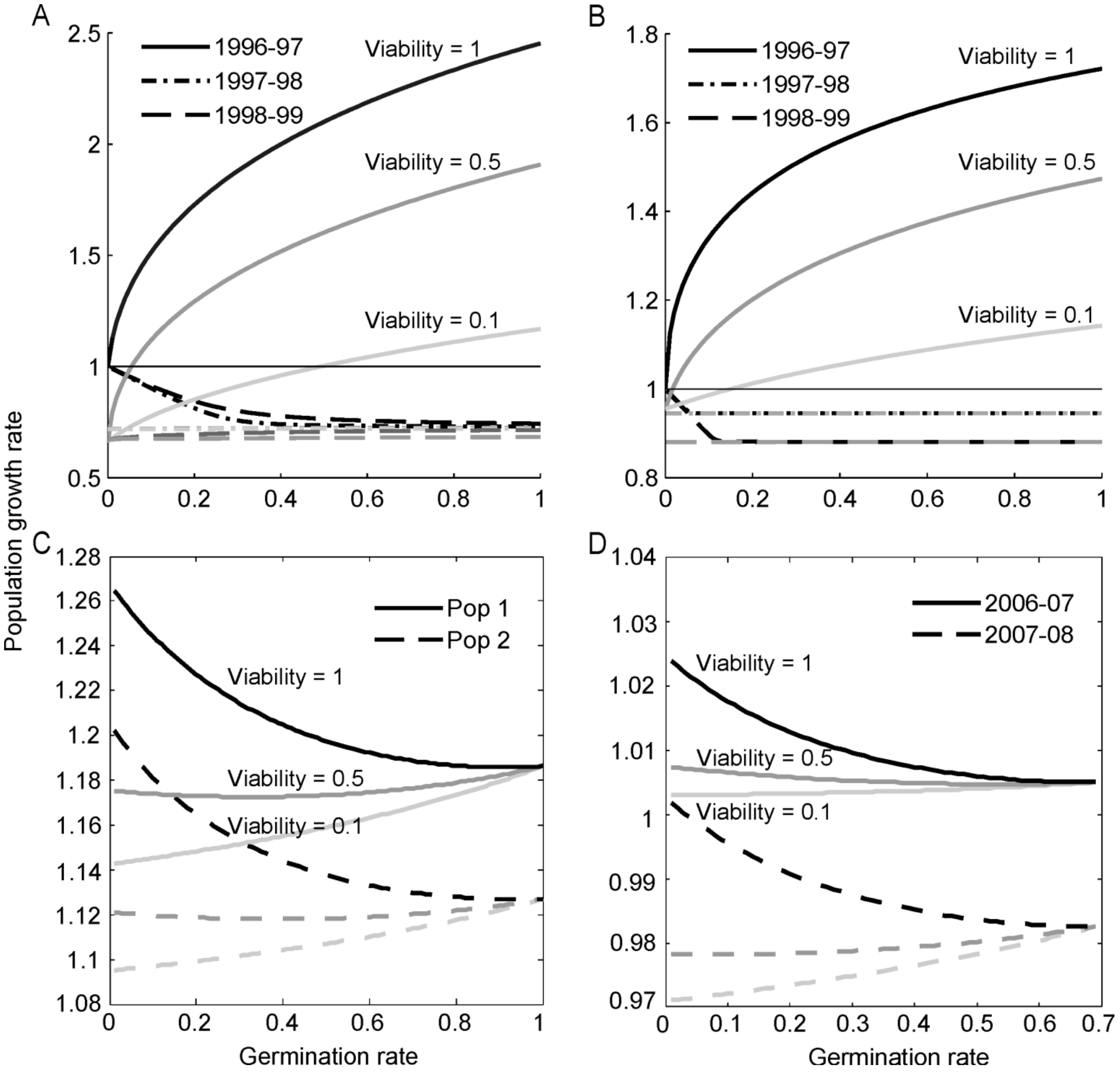

Fig. 2-4. Population growth rate (λ) as a function of germination rate from the seed bank for **A**) *Atriplex acanthocarpa*, **B)** *Atriplex canescens*, **C)** *Illicium anisatum* and **D)** *Geonoma schottiana*. Population growth rates were calculated at seed viability probabilities of 1 (black line), 0.5 (grey line) and 0.1 (light grey line) for germination rates between 0 and 1 at intervals of 0.01. Note that for *G. schottiana*, germination rate was restricted between 0 and 0.69 so as not to exceed the total seed survival estimate obtained from the literature.

Elasticity analyses in most plant species, particularly the trees, revealed survival of the adult or late juvenile stages as the most important demographic process affecting λ. The addition of the seed bank did not change this pattern except in the case of *A. acanthocarpa* during 1997-98 and 1998-99 when the populations were declining (Appendix 1-6). In the 1997-98 period, the elasticity of stasis of the third adult stage was drastically reduced (0.5759 to 0.0647) following inclusion of the seed bank, whereas the elasticity of λ to stasis in the seed bank was high (0.7919). Similarly, elasticity of λ to stasis in the first adult stage during the 1998-99 period, was reduced from 0.3983 to 0.12 after seed bank addition, while elasticity of λ to survival in the seed bank was high (0.5039).

Removal of the seed bank and uncertainty in seed bank presence

Removal of the seed bank led to further population increase when $\lambda > 1$ since germination was no longer delayed, and reduced population persistence when $\lambda < 1$ since the buffering effect was no longer present (Table 2-3). A notable exception was the wetland herb *Helenium virginicum* (Asteraceae), which experienced a comparatively high decrease in λ (1.1145 to 0.6985) when the seed bank was removed even though the population was increasing. This unusual response likely resulted from a combination of extremely high fecundity into the seed bank and probability of stasis within the seed bank (1025 and 0.987 respectively), and the comparatively low fecundity and survival of the smallest stage (0.0075 and 0.199 respectively). Decreases in λ were also particularly substantial for *Carduus nutans* (Asteraceae) and *Digitalis purpurea* (Plantaginaceae), but were much smaller or unchanged for the remaining species when the seed bank was removed during poor years.

Table 2-3. Comparison of population growth rates following removal of the seed bank. Studies are classified on the basis of variability in transition elements that was reported or number of time periods that were provided. Pop. refers to different populations of the same species in the same study. *Avg.* represents the population growth rate of the mean matrix. *Stoch.* gives the mean stochastic growth rate from populations projected over 10,000 years. Confidence intervals for stochastic simulations when the seed bank was removed are shown in brackets.

Study	**Life Form**	**Pop.**	**Period**	**SB**	**No SB**
No variability reported					
Adams *et al.*, (2005)					
Helenium virginicum	Herb	1	1	1.1145	0.6985
de Kroon *et al.*, (1987)					
Hypochaeris radicata	Herb	1	1	0.2973	0.2154
Variability, single time period					
Jongejans *et al.*, (2006)					
Carduus nutans	Herb	1	1	0.4680	0.3894
		2	1	0.6270	0.3771
		3	1	0.6020	0.5524
Multiple time periods					
Angert, (2006)					
Mimulus lewisii	Herb	1	1	0.7778	0.7778
		1	2	0.6863	0.6815
		1	3	0.9959	0.9943
		1	Avg.	0.8541	0.8332
		1	Stoch.	0.8431	**0.8221*** (0.8182, 0.8260)
		2	1	1.0154	1.0053
		2	2	0.6978	0.6917
		2	3	1.3203	1.3746
		2	Avg.	1.0158	1.0410
		2	Stoch.	0.9789	**0.8694*** (0.8592, 0.8797)
		3	1	1.1052	1.1094

		3	2	1.1197	1.1450
		3	3	0.9523	0.9507
		3	Avg.	1.0510	1.0583
		3	Stoch.	1.0482	**1.0539*** (1.0493, 1.0586)
		4	1	1.5841	1.6704
		4	2	1.0459	1.0470
		4	3	1.1227	1.3083
		4	Avg.	1.3112	1.3448
		4	Stoch.	1.2916	**1.3211*** (1.3166, 1.3256)
Parker, (2000)					
Cytisus scoparius	Herb	1	1	2.1963	2.3331
		1	2	2.2629	2.3858
		1	Avg.	2.5019	2.7128
		1	Stoch.	2.4908	**2.6876*** (2.6464, 2.7293)
		2	1	1.7097	1.7407
		2	2	1.2542	1.2406
		2	Avg.	1.5681	1.5552
		2	Stoch.	1.5495	**1.5317*** (1.5260, 1.5374)
		3	1	1.0040	1.0040
		3	2	0.9295	0.9287
		3	Avg.	0.9748	0.9746
		3	Stoch.	0.9739	0.9736 (0.9473, 1.0006)
Sletvold and Rydgren, (2007)					
Digitalis purpurea	Herb	1	1	0.7533	0.3174
		1	2	0.7831	0.5536
		1	Avg.	0.7715	0.5071
		1	Stoch.	0.7711	**0.4738*** (0.4709, 0.4767)
		2	1	0.6831	0.2983
		2	2	1.0198	0.9379
		2	Avg.	0.8565	0.6701
		2	Stoch.	0.8377	**0.5788*** (0.5735, 0.5841)

* Population growth rates between seed bank and no seed bank models are significantly different according to the 95% confidence interval. Statistically different growth rates are also shown in bold font.

Extinction risks

Inclusion of the seed bank using point estimates for germination generally resulted in longer times to local extinction (Appendix 1-7). Extinction times for *A. acanthocarpa* for the 1997-98 and 1998-99 periods received relatively high increases in extinction times (> 25 years). In addition, certain populations of *A. canescens* and the perennial herb *D. purpurea* were no longer predicted to go extinct in the next 100 years. The populations of the short-lived herb *C. nutans* received comparatively smaller increases in extinction times. In one population however, including the seed bank doubled the time to extinction from 8 to 16 years, which is relatively high when compared to its life expectancy ($\eta_E \cong$ 2-3 years, based on the fundamental matrix estimation; Caswell, 2001).

The seed bank improved the outlook of stochastic projections of extinction probability, but patterns varied across species (Appendix 1-8). The cumulative probability of extinction at 100 years decreased drastically for *A. acanthocarpa* from 0.19 to 0.01. The extinction probability for *A. canescens* showed an interesting pattern where the matrix model with the seed bank initially had a higher extinction probability than the original in the first 38 years and ended with a lower extinction probability, but otherwise the seed bank had little effect on the absolute extinction probability. Both populations of *D. purpurea* were predicted to go extinct within 100 years. One population received a modest increase in extinction time (16 to 30 years) while the increase was comparatively smaller for the other (four to nine years).

Discussion

The presence of cryptic life stages and their exclusion from demographic models continues to be an impediment to understand and project population dynamics. These cryptic stages are diverse, ranging from clonality, vegetative dormancy, hibernation, diapause, aestivation, etc., as is their potential impact on population dynamics and model outcomes. Using the seed bank as a well known example of a cryptic life stage, I demonstrate the use of simulations as a means to reduce uncertainty in seed bank dynamics and determining the relative importance of the seed bank and its effect on model outcomes. Ignoring the seed bank in a population increases uncertainty in estimates of population growth rates and extinction risks, and this uncertainty will vary by species and the amount of observed temporal variation in demographic parameters. Furthermore, the potential impact of the seed bank can be influenced by the assumptions being made and the accuracy of the vital rates that are obtained.

Dealing with the seed bank when its presence is unknown or uncertain

Variation in the effects of seed demographic uncertainty across species, populations and time will make it difficult to predict the species for which the seed bank will be an important factor. A protocol outlining the different approaches one can take when conducting a plant population study is provided in Fig. 2-5. Determining the possible presence of a seed bank can be achieved through a literature search (Baskin and Baskin, 2014, is of particular note), but not all populations of a given study species would necessarily have one. If a seed bank in the population is confirmed, the best option would be to obtain field data over the study period to provide estimates for seed bank vital rates. Without this field data, characterising the potential role of the seed bank becomes exceptionally difficult and assumptions regarding fecundity, seed survival, viability and longevity need to be made. Prior knowledge from the literature can narrow down these possibilities, though vital rates in the literature may not reflect those obtained in the field and must be interpreted with caution (Gross and Mackay, 2014). Simulations can be used to complement these literature estimates to efficiently investigate the numerous possible assumptions regarding seed bank vital rates and determine plausible effects of a potential seed bank. Garcia *et al.*, (2010) for example performed simulations covering feasible information obtained in the field or from other publications for the long-lived orchid *Cypripedium calceolus* (Orchidaceae) to justify excluding the seed bank from their models. Likewise, for many of the species in this study, without the benefit of greater observed temporal variation, ignoring the seed bank would appear to have been of minimal consequence for the original study but it is still crucial that an investigation is performed to provide this justification.

Fig. 2-5. Flow chart describing the different approaches for dealing with a potential seed bank when modelling plant population dynamics. Unjustified exclusion results in the highest possible uncertainty whereas justified exclusion by either proving it does not exist or showing it is unimportant via simulations gives the highest level of certainty in the model outcomes. Including the seed bank, either by using the literature or data obtained in the field would unavoidably result in some amount of uncertainty from estimating the vital rates, but is preferable to unjustified exclusion.

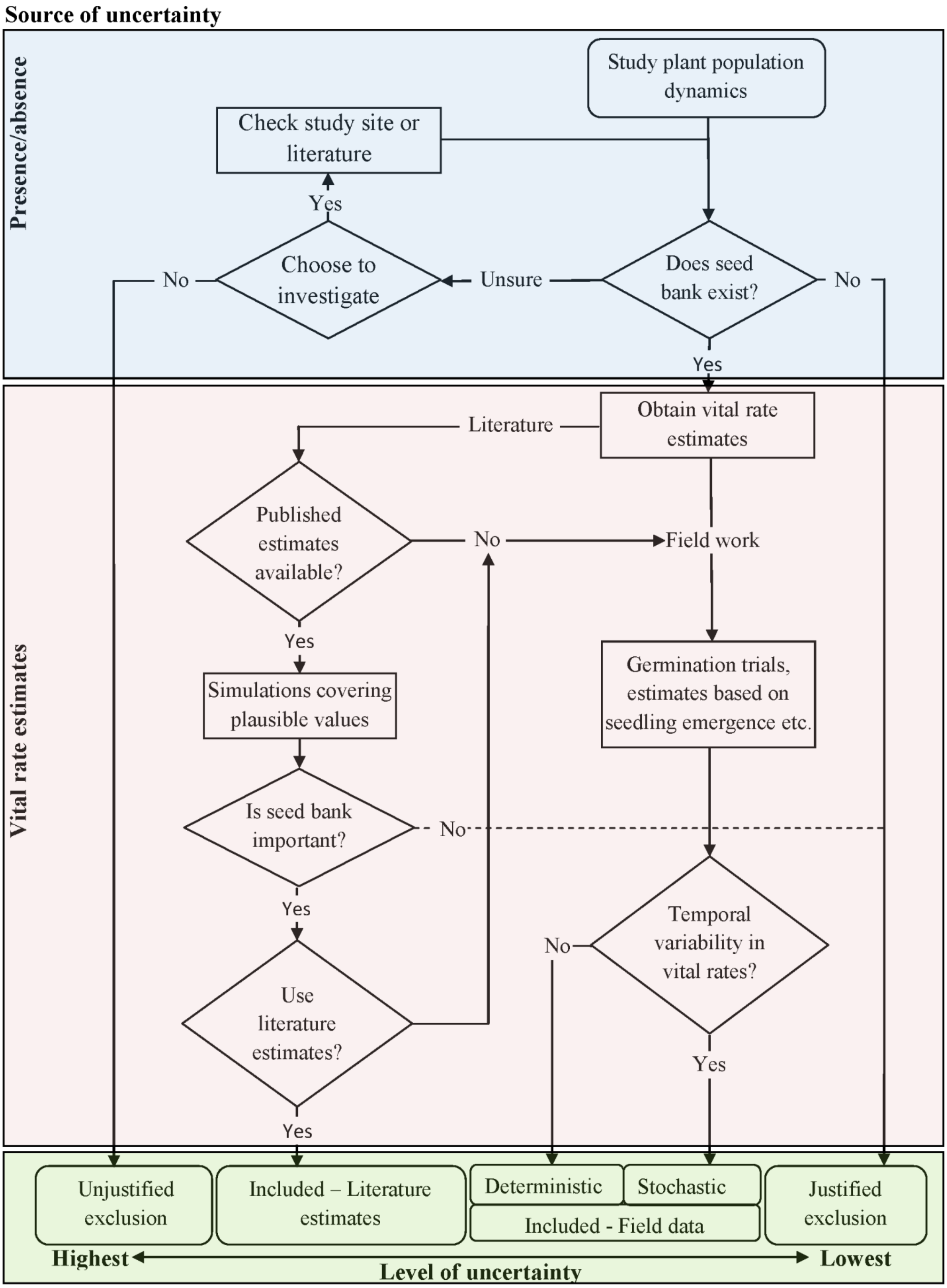
Source of uncertainty
Presence/absence
Study plant population dynamics
Check study site or literature
Yes
Choose to investigate
No
Unsure
Does seed bank exist?
No
Yes
Vital rate estimates
Obtain vital rate estimates
Literature
Published estimates available?
No
Field work
Yes
Simulations covering plausible values
Germination trials, estimates based on seedling emergence etc.
Is seed bank important?
No
Yes
Temporal variability in vital rates?
No
Use literature estimates?
Yes
Yes
Unjustified exclusion
Included – Literature estimates
Deterministic
Stochastic
Included - Field data
Justified exclusion
Highest
Level of uncertainty
Lowest

Uncertainty in the seed bank and its effect on model outcomes

By exploring a range of possible values for seed bank vital rates, and testing underlying assumptions regarding seed longevity and age-structure, it can be shown that conclusions will be dependent on the model structure. Demographic uncertainty in the estimation of vital rates appears to be the major driver in influencing the model predictions but varies by species. The *Atriplex* shrub species for example had much more variation in their growth rates when germination and viability were altered compared to long-lived tree species which were virtually unaffected by both the inclusion of the seed bank, and variation in their demographic parameters. This is not entirely surprising as high adult survival and reduced mortality when environmental conditions are poor can be an alternative strategy to improve long-term fitness (Clauss and Venable, 2000). However, while we might expect the seed bank to have a relatively low impact for species with high post-seedling survival and stable populations, this does not necessarily mean the seed bank will be unimportant if for example the population were to experience a large disturbance. The lack of temporally replicated data can make it difficult to accurately discern the influence of environmental stochasticity and the importance of the seed bank for long-term persistence, a fact occasionally acknowledged by the authors themselves (Quitete Portela *et al.*, 2010). This is also reflected in the miniscule confidence intervals obtained for the stochastic growth rate in many species. Furthermore, the seed bank and seedling stages for long-lived species tend to have much greater variability in their transition rates compared to their adult counterparts (Clark *et al.*, 1999). Thus most comparisons of λ_S were not as useful as they could be, and only hint at the potential importance of the seed bank for λ_S. When sufficient environmental variation is captured, the contribution of the seed bank is more visible as is evident for *A. acanthocarpa* where previously high elasticities for juvenile and adult survival were shifted towards survival in the seed bank during poor demographic years (Appendix 1-6).

Temporal variation and the type of demographic year is also a factor when considering the effect of demographic uncertainty. While altering germination and viability rates for example can have demonstrable effects on λ, this was not the case for the *Atriplex* species during poor demographic years (Fig. 2-4). Large reproductive failures during these years would have resulted in low seed bank and seedling input, reducing the impact of varying seed bank vital rates on λ. However, this only applies when analysing deterministic growth rates, and it would be expected that variations in germination and viability rates during poor years would have a much larger impact when considering long-term persistence. Nonetheless, with the inclusion of prior information from the literature, the distribution of growth rates during these poor demographic years shifts towards one (Fig. 2-3). I note however that this is assuming dormancy is higher (low germination) during poor demographic years and lower during productive years (Kalisz and McPeek, 1992), but seed dormancy need not necessarily be correlated with fitness. Interestingly, contrary to initial predictions, the use of literature did not necessarily reduce uncertainty in the range of possible growth rates and in fact becomes more variable when dormancy is high (Fig. 2-3). Thus, if literature estimates suggest potentially high levels of dormancy, uncertainty in λ resulting from the seed bank may actually increase. This can be particularly concerning if we do indeed expect species to have reduced germination and greater dormancy during poor demographic years and should act as further incentive to collect raw field data.

In addition to variations in demographic parameters, changes to how the seed bank is included can impact the model structure and outcomes. Uncertainty simulations performed in this study investigate only the unstructured scenario with no age structure although this is the most common structure for including a seed stage. Indeed, estimating demographic rates for an age-structured seed bank makes the task of including a seed stage even more difficult and is therefore extremely rare in plant population models (but see Kalizs, 1991; Yates *et al.*, 2007 for examples). Thus, our understanding of the impact of age structure, and variation in seed vital rates in general across time and space, is quite limited. Simulations involving the inclusion of various age-structures found that while single point estimates of λ under the unstructured scenario showed minor increases compared to the original models, this gradually reduces when additional age classes are introduced (See Appendix 1-2 for comparison of growth rates). This is likely because a higher proportion of emergents are now assumed to have germinated from seeds produced in previous years, thus compounding the effect of delayed germination. Similarly, if it is assumed that seeds do not survive beyond the first, second or third year, the effect of the seed bank is almost negligible (See Appendix 1-2). However, such estimates are overly conservative and most models that do include the seed bank do not make this assumption. Another interesting scenario that can be tested is that of no seed bank, and simulations in which the seed bank was removed provides insights into the worst case scenarios when the seed bank is ignored despite being crucial to persistence (as indicated by high elasticities in seed bank transitions). As expected, the implications of ignoring the seed bank in these cases were generally much more evident, with decreases in λ of up to 0.4. The assumption of fecundity being equal to that of the previous year ($F_{j,t} = F_{j,t-1}$) was necessary due to lack of information, however, interannual variation is likely to play an important role for many species. When variance in the fecundity is high, the contribution of the seed bank would be overestimated in good demographic years and underestimated in bad demographic years. This would likely have similar consequences on any changes in λ thus we might expect the benefit of having a seed bank during poor years to also be underestimated.

Analysis of extinction risks over shorter time periods can provide additional insights not considered under asymptotic analyses. Comparing the difference in extinction times and cumulative extinction probabilities between models with and without the seed bank can provide an empirical measure of the uncertainty in population persistence when the seed bank is ignored, which can vary substantially between years and species. Although increases in extinction times can appear trivial, they must also be considered in context of the life expectancy. The seed bank had little effect on the times to extinction for the populations of *C. nutans* for example. However, given the short life expectancy of this species, even a small increase in extinction time may prove crucial.

Conclusions

There is a substantial gap in our knowledge about the role of seed banks in plant population dynamics and this study only scratches the surface of how uncertainty in the seed bank can influence demographic models. It is strongly recommended that plant demographers tackle the seed bank stage and where possible undertake data collection to improve their model structure. In general, potentially important life stages are commonly excluded from demographic analyses if the data are too difficult to obtain, as is often the case in cryptic life stages, or are simply assumed not to matter without the appropriate justification (Clark *et al.,* 1999). Despite the increasingly sophisticated methods available for demographic modelling (e.g. Chandler and Clark, 2014; Robinson *et al.,* 2014) authors must be mindful to consider the entire life cycle of a species when performing demographic research.

In summary, while there is still much progress to be made with regards to the seed bank, it is but one of many cryptic life stages with the potential to create biases in our model outputs. Adult plants, for example, can undergo vegetative dormancy, whereby individuals do not sprout above ground for one or more growing seasons, resulting in overestimated mortality rates and incorrect assignment of false birth events to re-emerging individuals (Shefferson, 2009). Some animal species are also capable of dormancy, characterised by a reduction in metabolic rates and prolonged periods of inactivity, performing a similar function to that of the seed bank (Geiser, 2004). Research by Lamy *et al.*, (2013) on snails found that ignoring individuals remaining dormant in the ground to avoid dry periods can result in the overestimation of extinction and colonisation rates. Demographic studies on animals can be additionally problematic as certain stages of the life cycle may occupy inaccessible locations or be absent from sampling designs. Katzner *et al.*, (2011) found raptor populations to be drastically underestimated as monitoring programs historically focused only on the breeding portion of the population and non-invasive genetic analyses on feather samples were required to estimate the non-breeding component (Schwartz *et al.*, 2007). The extent of exclusion of cryptic life stages in demographic models for animals is not as well characterised as for plants. However, the upcoming release of the COMADRE Animal Matrix Database (Salguero-Gómez *et al.*, in prep.) may provide valuable opportunies for future research into this area.

Acknowledgements

I would like to thank Rob Salguero-Gómez, Elizabeth Crone and Johan Ehrlén for several helpful comments, and Satu Ramula and members of the ARC-NZ Research Network for Vegetation Function Plant Population Syndromes working group.

References

Abe, S., Motai, H., Tanaka, H., Shibata, M., Kominami, Y. and Nakashizuka, T. (2008) Population maintenance of the short-lived shrub *Sambucus* in a deciduous forest. *Ecology,* 89**,** 1155-1167.

Adams, V.M., Marsh, D.M. and Knox, J.S. (2005) Importance of the seed bank for population viability and population monitoring in a threatened wetland herb. *Biological Conservation,* 124**,** 425-436.

Angert, A.L. (2006) Demography of central and marginal populations of monkey flowers (*Mimulus cardinalis* and *M. lewisii*). *Ecology,* 87**,** 2014-2025.

Baskin, C.C. and Baskin, G.M. (2014) *Seeds: Ecology, biogeography, and evolution of dormancy and germination.* Academic Press, San Diego, California.

Burns, J.H., Blomberg, S.P., Crone, E.E., Ehrlén, J., Knight, T.M., Pichancourt, J.P., Ramula, S., Wardle, G.M. and Buckley, Y.M. (2010) Empirical tests of life-history evolution theory using phylogenetic analysis of plant demography. *Journal of Ecology,* 98**,** 334-344.

Caswell, H. (2001) *Matrix population models: construction, analysis and interpretation.* Sinauer Associates, Inc., Sunderland, Massachusetts.

Chandler, R.B. and Clark, J.D. (2014) Spatially explicit integrated population models. *Methods in Ecology and Evolution,* 5**,** 1351-1360.

Chien, P.D., Zuidema, P.A. and Nghia, N.H. (2008) Conservation prospects for threatened Vietnamese tree species: results from a demographic study. *Population Ecology,* 50**,** 227-237.

Clark J, Beckage B, Camill P, Cleveland B, HilleRisLambers J, Lichter J, McLachlan J, Mohan J, Wyckoff P (1999). Interpreting recruitment limitation in forests. *American Journal of Botany,* 86, 1-16.

Clauss, M.J. and Venable, D.L. (2000) Seed germination in desert annuals: an empirical test of adaptive bet hedging. *American Naturalist,* 155**,** 168-186.

Crone, E.E., Menges, E.S., Ellis, M.M., Bell, T., Bierzychudek, P., Ehrlén, J., Kaye, T.N., Knight, T.M., Lesica, P., Morris, W.F., Oostermeijer, G., Quintana-Ascencio, P.F., Stanley, A., Ticktin, T., Valverde, T. and Williams, J.L. (2011) How do plant ecologists use matrix population models? *Ecology Letters,* 14**,** 1-8.

de Kroon, H., Plaisier, A. and J.V., G. (1987) Density dependent simulation of the population dynamics of a perennial grassland species, *Hypochaeris radicata*. *Oikos,* 50**,** 3-12.

de Kroon, H., van Groenendael, J. and Ehrlen, J. (2000) Elasticities: a review of methods and model limitations. *Ecology (Washington DC),* 81**,** 607-618.

Doak, D.F., Thomson, D. and Jules, E.S. 2002. Population viability analysis for plants: understanding the demographic consequences of seed banks for population health. *Population Viability Analysis* (eds. Beissinger, S. R. & McCullough, D. R.), 312-337. Chicago, Illinois, USA, The University of Chicago Press.

Garcia, M.B., Goni, D. and Guzman, D. (2010) Living at the edge: local versus positional factors in the long-term population dynamics of an endangered orchid. *Conservation Biology,* 24**,** 1219-1229.

Geiser, F. (2004) Metabolic rate and body temperature reduction during hibernation and daily torpor. *Annual Review of Physiology,* 66**,** 239-274.

Gremer, J.R., Crone, E.E. and Lesica, P. (2012) Are dormant plants hedging their bets? Demographic consequences of prolonged dormancy in variable environments. *American Naturalist,* 179**,** 315-327.

Gross, C. and Mackay, D. (2014) Two decades of demography reveals that seed and seedling transitions limit population persistence in a translocated shrub. *Annals of Botany*.

Harper, J.L. (1977) *Population biology of plants.* Academic Press, London.

Jongejans, E., Shea, K. and Sheppard, A.W. (2006) What controls the population dynamics of the invasive thistle *Carduus nutans* in its native range? *Journal of Applied Ecology,* 43**,** 877-886.

Kalisz, S. and McPeek, M.A. (1992) Demography of an age-structured annual: resampled projection matrices, elasticity analyses, and seed bank effects. *Ecology,* 73**,** 1082-1093.

Katzner, T.E., Ivy, J.A.R., Bragin, E.A., Milner-Gulland, E. and DeWoody, J.A. (2011) Conservation implications of inaccurate estimation of cryptic population size. *Animal Conservation,* 14**,** 328-332.

Kaye, T.N. and Pyke, D.A. (2003) The effect of stochastic technique on estimates of population viability from transition matrix models. *Ecology,* 84**,** 1464-1476.

Kisanuki, H., Nakasu, M., Nakai, A. and Yurugi, Y. (2008) Predicting the population dynamics of three understory broad-leaved evergreen species under the influence of Sika deer in primary and secondary forests of mid-western Japan. *Journal of Forest Research,* 13**,** 52-58.

Kouassi, K.I., Barot, S., Gignoux, J. and Bi, I.A.Z. (2008) Demography and life history of two rattan species, *Eremospatha macrocarpa* and *Laccosperma secundiflorum,* in Cote d'Ivoire. *Journal of Tropical Ecology,* 24**,** 493-503.

Lamy, T., Gimenez, O., Pointier, J.P., Jarne, P. and David, P. (2013) Metapopulation dynamics of species with cryptic life stages. *The American Naturalist,* 181**,** 479-491.

Mondragon, D. (2009) Population viability analysis for *Guarianthe aurantiaca*, an ornamental epiphytic orchid harvested in Southeast Mexico. *Plant Species Biology,* 24**,** 35-41.

Morris, W.F. and Doak, D.F. (2002) *Quantitative conservation biology: theory and practice of population viability analysis.* Sinauer Associates, Sunderland, Massachusetts.

Parker, I.M. (2000) Invasion dynamics of *Cytisus scoparius*: a matrix model approach. *Ecological Applications,* 10**,** 726-743.

Quitete Portela, R.D.C., Bruna, E.M. and Maes dos Santos, F.A. (2010) Demography of palm species in Brazil's Atlantic forest: a comparison of harvested and unharvested species using matrix models. *Biodiversity and Conservation*, 19**,** 2389-2403.

Regan, T.J., Chades, I. and Possingham, H.P. (2011) Optimally managing under imperfect detection: a method for plant invasions. *Journal of Applied Ecology,* 48**,** 76-85.

Robinson, R.A., Morrison, C.A. and Baillie, S.R. (2014) Integrating demographic data: towards a framework for monitoring wildlife populations at large spatial scales. *Methods in Ecology and Evolution,* 5**,** 1361-1372.

Salguero-Gómez, R., Jones, O.R., Archer, C.R., Buckley, Y.M., Che-Castaldo, J., Caswell, H., Hodgson, D., Scheuerlein, A., Conde, D.A., Brinks, E., de Buhr, H., Farack, C., Gottschalk, F., Hartmann, A., Henning, A., Hoppe, G., Römer, G., Runge, J., Ruoff, T., Wille, J., Zeh, S., Davison, R., Vieregg, D., Baudisch, A., Altwegg, R., Colchero, F., Dong, M., de Kroon, H., Lebreton, J.-D., Metcalf, C.J.E., Neel, M.M., Parker, I.M., Takada, T., Valverde, T., Vélez-Espino, L.A., Wardle, G.M., Franco, M. and Vaupel, J.W. (2015) The COMPADRE Plant Matrix Database: an open online repository for plant demography. *Journal of Ecology,* 103**,** 202-218.

Salguero-Gómez, R. and Plotkin, J.B. (2010) Matrix dimensions bias demographic inferences: implications for comparative plant demography. *American Naturalist,* 176**,** 710-722.

Schwartz, M.K., Luikart, G. and Waples, R.S. (2007) Genetic monitoring as a promising tool for conservation and management. *Trends in Ecology & Evolution,* 22**,** 25-33.

Shefferson, R.P. (2009) The evolutionary ecology of vegetative dormancy in mature herbaceous perennial plants. *Journal of Ecology,* 97**,** 1000-1009.

Sletvold, N. and Rydgren, K. (2007) Population dynamics in *Digitalis purpurea*: the interaction of disturbance and seed bank dynamics. *Journal of Ecology,* 95**,** 1346-1359.

Stöcklin, J. and Fischer, M. (1999) Plants with longer-lived seeds have lower local extinction rates in grassland remnants 1950-1985. *Oecologia,* 120**,** 539-543.

Tanner, J.E. (2001) The influence of clonality on demography: patterns in expected longevity and survivorship. *Ecology,* 82**,** 1971-1981.

Venable, D.L. (2007) Bet hedging in a guild of desert annuals. *Ecology,* 88**,** 1086-1090.

Verhulst, J., Montana, C., Mandujano, M.C. and Franco, M. (2008) Demographic mechanisms in the coexistence of two closely related perennials in a fluctuating environment. *Oecologia (Berlin),* 156**,** 95-105.

Vitalis, R., Glémin, S. and Olivieri, I. (2004) When genes go to sleep: the population genetic consequences of seed dormancy and monocarpic perenniality. *The American Naturalist,* 163**,** 295-311.

Warner, R.R. and Chesson, P.L. (1985) Coexistence mediated by recruitment fluctuations: a field guide to the storage effect. *American Naturalist,* 125**,** 769-787.

Chapter 3 - How to apply multivariate autoregressive state-space models to time series count data to improve population monitoring

Umbel of the ephemeral plant *Trachymene glaucifolia.* Photograph by Glenda Wardle

A version of this chapter has been submitted and is currently under review in Ecological Applications as Nguyen, V., Greenville, A.G., Dickman, C.R. and Wardle, G.M. (2015) How to apply multivariate autoregressive state-space models to time series count data to improve population monitoring. Submitted 16th July 2015.

My contribution was very substantial, including conceptualisation of ideas, data manipulation, construction and analysis of models, and writing and editing all drafts in consultation with my co-authors.

Abstract

Ecological time series data, such as counts of individuals over time, are valuable for scientific research, monitoring and ecosystem management. Effective monitoring programs need to be well-designed to ensure that limited resources are used efficiently to produce high quality, long-term data. However, such data are still subject to inherent uncertainties that arise from observation errors due to sampling and measurement errors, as well as process errors due to the effects of demographic and environmental stochasticity. Here, I apply multivariate autoregressive state space (MARSS) models as a versatile framework to quantify these sources of uncertainty in monitoring data whilst iteratively providing recommendations to improve monitoring design. A common but ephemeral plant in a highly stochastic environment is used as a case study to illustrate how this approach would apply to any plot-based monitoring study, and use site-based environmental data to explain trends over time and space. Modelling multi-dimensional time series data allowed the identification of spatial sub-population structure with respect to location and fire history, and population structure to be accounted for, using above ground and seed bank abundances to improve parameter and true state estimates for both life stages. MARSS models showed plant populations to be highly variable, with local variation determined by wildfire history; however, on a regional scale, this variation was overshadowed by geographical differences that provide justification for spatial replication. Using a hierarchical, state-space approach also allowed us to separate observation and process errors. The seed bank was characterised by lower process than observation errors, while the converse was true for above-ground plants. Thus, the seed bank is more robust to gaps in the time series, making it more strategic to obtain less frequent, but more accurate counts of seeds to offset the higher observational errors. Overall, MARSS models provide a sound framework for assessing spatial and temporal trends in populations, and help to guide updates and improvements in current monitoring programs.

Introduction

Effective monitoring programs provide important insights into ecological processes and are crucial in the management of ecosystems and populations, with time series data of population abundances being particularly useful for managers (Morris et al., 1999; Lindenmayer and Likens, 2009). In contrast to more detailed demographic data on growth, survival and reproduction (e.g. Caswell, 2001), census counts are relatively cheap and easy to collect, thus increasing the scope for monitoring programs to extend over relatively long periods and large spatial scales. However, it is crucial to acknowledge that observed time series of abundances cannot usually be equated with true abundances – indeed, direct inference based on raw observations can be highly misleading, resulting in biased estimates of parameters such as extinction risk and population abundance (Schmidt, 2005; Kéry et al., 2009; Kéry and Schaub, 2012). For example, increases in observed abundances over time may simply be a reflection of changes in the observation process; that is, increased observer experience in identifying species, or changes in visibility and detectability. Thus it is useful to adopt a hierarchical, or state-space framework when analysing such data, as this allows the teasing apart of the true ecological state (true abundances) from the observation process (de Valpine and Hastings, 2002; Clark and Bjørnstad, 2004; Humbert et al., 2009; Kéry and Schaub, 2012). By decoupling these two processes, one can obtain explicit estimates of both the observation error, which includes measurement and sampling error, and process error, which includes variation resulting from demographic and environmental stochasticity (Staples et al., 2004). Estimates of observation errors can then be used adaptively to inform and improve future monitoring strategies to make more efficient use of resources and produce higher quality data.

The state-space modelling framework also has the advantage of being able to model imperfect data sets such as those with missing values or uneven sampling intervals that are common in ecological time series (Clark and Bjørnstad, 2004). This is an important feature as traditional approaches to modelling time series data with missing values, such as log-linear regressions of counts against time and the diffusion approximation, do not explicitly account for both the true ecological and observation processes (Gerrodette, 1987; Dennis et al., 1991; Humbert et al., 2009). The ability to model data with missing values also allows more flexibility in the design of a monitoring program. For example, missing values in the data may be permitted and resources could instead be allocated towards collecting fewer, albeit higher quality data through replicated sampling or extending the duration of monitoring (Morris et al., 1999; Humbert et al., 2009; Dennis et al., 2010). Producing higher quality datasets through replicated sampling and obtaining longer time series can then produce more accurate estimates of trends and reduce computational issues commonly associated with attempting to model both the process and observation errors (Dennis et al., 2006; Humbert et al., 2009; Dennis et al., 2010).

Multivariate autoregressive state-space (MARSS) models based on stochastic Gompertz models for population growth are an extension of state-space models that allow modelling of multi-dimensional time series data (Hinrichsen and Holmes, 2009; Ward et al., 2010; Holmes et al., 2012b). Thus, time series sourced from replicated samples, multiple life stages (e.g. juvenile and adult counts which may be separate time series), and from multiple sites can be modelled concurrently to improve parameter estimates and determine the spatial organisation and environmental drivers that lead to sub-populations (Ward et al., 2010; Holmes et al., 2012a). Identifying the level of spatial heterogeneity and spatial structure of sub-populations is critical from a conservation and management perspective since not all populations can be expected to behave equally (Warton and Wardle, 2003; Buckley et al., 2010). Thus, the

MARSS models provide a versatile framework that can conveniently address several sources of uncertainty that are pervasive in ecological data: the need to decouple true ecological processes and observation processes, missing values or uneven sampling intervals, and identification of spatial sub-population structure.

In this study, an ecological dataset gathered from a plot-based monitoring study is used to demonstrate the use of the MARSS framework in addressing common issues in modelling ecological data, and model results cross-checked by creating MARSS models using two algorithms – the recursive Kalman Filter/Expectation Maximisation algorithms (Shumway and Stoffer, 1982; Shumway and Stoffer, 2006) and Monte Carlo Markov Chains implemented within a traditional Bayesian framework (Plummer, 2003; Plummer, 2015). I further illustrate how these model outputs can be used iteratively to improve monitoring studies. Specifically, it is shown that explicitly estimating the relative contributions of the process and observation errors can be used to help inform future monitoring strategies. The MARSS framework is also used to highlight the advantages and potential reduction in uncertainty that can be achieved by replicating sampling in short-term studies, distinguishing between life history stages and identifying the spatial sub-population structure and the drivers behind these different structures. The case study dataset is typical of ecological time series, containing uneven sampling times and missing values, is relatively long term (≈ 9 years), and has high spatial coverage and replication in an extreme stochastic environment. The consequences of excluding life stages from demographic models, with particular emphasis to the seed bank, were revealed in the previous chapter (Chapter 2). Here, the importance of obtaining data on cryptic life stages is reinforced by constructing population models with time series data on a plant species with two life stages: the dormant seed bank and above-ground plants. These models are used to determine the plant's sub-population structure in relation to fire history, rainfall and spatial location. Finally, I comment on the utility of the

MARSS models in describing the overall biology of the modelled plant species and estimating spatial and temporal trends. Overall, the application of MARSS models in this study makes several original contributions, namely in the use of model output to inform future monitoring strategies, introducing life stage structure, and is one of few applications of this model outside of the fisheries context (but see Flesch, 2014).

Methods

Study species, site and covariates

The case study species for evaluating the multivariate autoregressive state-space (MARSS) approach was the desert herb *Trachymene glaucifolia* (F.Muell.) Benth. (Araliaceae), or wild parsnip (Nicolas and Plunkett, 2009), an erect, ephemeral and typically annual plant of the inland deserts of Australia, often occurring on deep red sand on dunes and plains (Moore, 2005). Stems rise to 70 cm from a taproot, that may sometimes be perennial, and leaves are 2-5 cm long, mostly forming a basal crown with 3-5 lobes (Cunningham et al., 1992; Moore, 2005). Brown semicircular fruits 4.5-5.5 mm long consist of a single papillate mericarp (Hart and Henwood, 2006). Seeds of *T. glaucifolia* have potential for long-term dormancy, building a reserve in the seed bank. While *T. glaucifolia* has the potential to persist beyond a year above-ground, for 17 years of observations it has only exhibited only an annual life cycle in the study site (GM Wardle, pers. obs), and its presence and abundance are more related to the occurrence of rare rainfall events than to a regular growing season. Thus, populations can persist at a site for consecutive seasons only in the seed bank, with above ground plants occurring in sudden and abundant but short-lived population spikes.

Sampling was carried out in the Simpson Desert, central Australia by the Desert Ecology Research Group at the University of Sydney (Wardle and Dickman, unpublished data). The desert is characterised by dunefields, which comprise 73% of the region, with smaller areas of clay pan, rocky outcrop and gibber flat (Shephard, 1999). Vegetation in the interdune swales and dune sides is predominantly hummock grassland dominated by hard spinifex (*Triodia basedowii* E.Pritz.), although vegetation structure can be drastically altered by natural events such as heavy rainfall and wildfire (Dickman et al., 2014). For example, after heavy rain, the build-up of seeds in the soil seed bank allows *T. glaucifolia* and other short-lived plants to respond quickly and dominate the landscape during what is known as a pulse or boom event (Ludwig et al., 1997).

Data were collected from four sites (Main Camp, Field River South, Carlo Shitty and South Site) on Carlo Station and Ethabuka Reserve, covering ~4400 km^2 of the study region (Appendix 3-1). Carlo is grazed by beef cattle, but all cattle were removed from Ethabuka in 2004 (Frank et al., 2013). Two grids were set up at each site (total = 8 grids), with each grid occupying 1 ha and consisting of 15 5 × 5 m plots. Five plots were spaced randomly, but with a minimum separation of 5 m, on 100 m parallel transects along the crest, middle and swale of the dunes, with 100 m separating the crest and the swale transects. Surveys recording counts of individual plants within plots were conducted 4 times a year from 2004-2006 and 1-2 times a year from 2007-2013 in response to available resources. In addition, to quantify the seed bank, soil samples were collected adjacent to each plot using a metal frame 2 cm deep covering a 20 × 20 cm area. Seeds within the samples were later sieved, identified and counted to estimate the size of the seed bank within each plot. Soil samples were not always collected nor all sites sampled on each trip due to time or access constraints, resulting in a mismatch in the time series across sites and life history stages. Note that because the seed bank and the plants were sampled using different methods, the transition rates between seeds and plants in a matrix model would not match up with fecundity, but will be scaled according to the differences in sampling intensities for plants and seeds. Additionally, these different sampling strategies naturally lends itself to producing distinct estimates for observation error for these two life stages. Over the course of the study, across all plots, more than 100,000 above-ground *T. glaucifolia* plants and more than 5000 seeds were counted.

Wildfires in 2001-2002 burnt more than 2500 km^2 of the study region, stripping large areas of spinifex grassland (Greenville et al., 2009). Vegetation assemblages following the fire differed between burnt and unburnt sites, with burnt sites containing mostly annual species with *T. basedowii* the main perennial (Strong et al., 2010). To discern whether populations of *T. glaucifolia* differed between burnt and unburnt habitats, one grid at each site was set up in an area burnt in the 2001-2002 wildfires and another in an unburnt area.

Daily rainfall data were obtained from automated weather stations (Environdata, Warwick, Queensland) located at each site, and monthly aggregates were calculated from May 1995 to September 2012. Weather stations experienced periods of downtime due to malfunctions, resulting in occasional gaps in the data. Unless the weather station was fully operational for the entire month, the data point for that month was discarded – these gaps in the rainfall data for each site did not necessarily coincide.

Model specification

The MARSS model is a stochastic exponential growth model in which there is a model that describes changes in the true abundances in log-space, and a model that describes the observation process which introduces an additional source of variation to account for observation error. Following the notation used by Holmes et al., (2012a), *n* is used to denote the number of discrete survey sites and *m* to denote the number of hypothesised sub-populations. Note that *n* need not necessarily equal *m*. The MARSS model is given by

$$\mathbf{X}_t = \mathbf{B}\mathbf{X}_{t\text{-}1} + \mathbf{u} + \mathbf{C}\mathbf{c}_t + \mathbf{w}_t; \qquad \mathbf{w}_t \sim \text{MVN}(0,\mathbf{Q}) \tag{1}$$

$$\mathbf{Y}_t = \mathbf{Z}\mathbf{X}_t + \mathbf{a} + \mathbf{v}_t; \qquad \mathbf{v}_t \sim \text{MVN}(0, \mathbf{R}) \tag{2}$$

where Eq. (1) represents the model for the true states in log-space, $\mathbf{X}_t$ represents the *m* logarithmic true states at time *t* (usually log-abundance but can be used for other unobserved measurements), **B** is an $m \times m$ matrix in which the diagonal entries represent mean-reversion (the tendency for a fluctuating time series to revert back to a mean value; this may also be interpreted as density-dependence) where $B_{ii} = 1$ indicates no mean-reversion in sub-population *i* and $B_{ii} < 1$ indicates sub-population *i* is mean-reverting, **u** is the trend parameter for the *m* subpopulations, **C** represents covariate effects, $\mathbf{c}_t$ is the value of the covariate at time *t*, and $\mathbf{w}_t$ is the process error assumed to be from a multivariate normal (MVN) distribution with mean zero and variance-covariance matrix **Q** (Holmes et al., 2007). The off-diagonal elements, Q_{ij}, allow for possible correlated dynamics between sub-populations ($Q_{ij} = 0$ indicates sub-populations *i* and *j* are independent). Equation (2) represents the observation model, where $\mathbf{Y}_t$ is the logarithm of the observed states at the *n* surveyed sites at time *t* which may differ from the number of hypothesised sub-populations *m*, **Z** is an $n \times m$ matrix of 0s and 1s denoting population structure, pairing up each of the *n* observations to one of the *m* hypothesised sub-populations, **a** is the mean linear difference between surveyed sites measuring the same sub-population with respect to the first site, and $\mathbf{v}_t$ is the observation error assumed to be MVN with mean zero and variance-covariance matrix **R**. Conceptually, the MARSS model is simply a variation of traditional demographic models (such as population matrix models used in Chapter 2), containing several familiar elements such as the autoregressive abundance component, sampling uncertainty, and covariates.

There are a number of methods in which MARSS models may be constructed. The *MARSS* package (Holmes et al., 2012a; Holmes et al., 2012b) implemented in R (R 2.15.3; The R foundation for Statistical Computing 2004-2008) uses a combination of the Kalman filter and smoothers (Shumway and Stoffer, 2006) and the Expectation-Maximisation (EM) algorithm (Shumway and Stoffer, 1982) to estimate model parameters. Models may also be constructed within a traditional Bayesian framework using Monte Carlo Markov Chain (MCMC) algorithms implemented in JAGS 3.4.0 (Plummer, 2003) via the R2jags 0.05-03 (Su and Yajima, 2015) and rjags 3-14 packages (Plummer, 2015). Models were constructed using both methods to ensure results were valid and robust to the choice of algorithm used. I did not conduct a formal comparison of these two methods as this is outside the scope of this study. Henceforth, MARSS models created using the *MARSS* package will be referred to as MARSS-KFEM, and those created in JAGS as MARSS-MCMC in relation to the algorithms used to estimate parameters and true abundances. The use of JAGS to create MARSS models offers more flexibility, with the option to accommodate alternative observation error structures such as that from a Poisson or negative binomial distribution, which the *MARSS* package currently does not allow. Although an overdispersed Poisson or negative binomial distribution is generally more appropriate for count data (Link and Sauer, 2002; Kéry and Schaub, 2012), these were found to provide an inadequate description of the data and resulted in poor model fits (see Appendix 3-2 for comparison of model parameters and selection criterion for Main Camp). MARSS-MCMC models were fitted with three independent chains for 20 000 iterations after an initial burn-in of 5000 iterations and a thinning rate of 10. Inspection of Gelman-Rubin statistics, in which values close to 1 indicate convergence (Brooks and Gelman, 1998), gave values < 1.1 suggesting model convergence (Gelman and Hill, 2007). Model formulation for the hypotheses described below and example JAGS code are provided in Appendix 3-3.

Covariate model

From equation 1, covariates can be fitted into the model using the **c** matrix; however, this does not allow for missing covariate values using the *MARSS* package. There are two solutions to this problem: incorporate the covariate into the population model as a separate state (i.e. into the **X** matrix) or fit a covariate model separately and add the completed state estimates into the **c** matrix (Holmes et al., 2012a). A separate model was fitted first as this allows spatial hypotheses regarding the spatial extent of rainfall events to also be examined. Additionally, modelling the covariate and the population data simultaneously would result in estimates that are non-independent (i.e. the covariate state estimates would be affected by the population data).

Two rainfall models were constructed to determine the spatial extent of rainfall events in the study region: a **local rainfall model** in which each site has its own unique rainfall trajectories ($m = 4$; Main Camp, Field River South, Carlo Shitty and South Site), and a **regional rainfall model** in which rainfall events are large enough to act over the entire study region ($m = 1$). In the regional model, all sites are independent observations of the same trajectory. Models for the observation and state process follow equations 1 and 2, excluding the mean-reverting matrix **B**, observation bias vector **a**, and covariate effects **C** and $\mathbf{c}_t$.

Wildfire models

To test the effects of wildfire, three separate MARSS models were constructed for each site: a **wildfire model** in which fire history results in distinct sub-populations ($m = 4$; $\mathbf{X}_{1,t}$ and $\mathbf{X}_{2,t}$ are the true states for above-ground plants and the seed bank in burnt grids, $\mathbf{X}_{3,t}$ and $\mathbf{X}_{4,t}$ are the true states in the unburnt grids), a **whole site model** in which fire history has no effect and the burnt and unburnt patches are part of the same sub-population (m = 2; $\mathbf{X}_{1,t}$ are the true states for all above-ground plants using observed abundances from both burnt and unburnt grids. Similarly, $\mathbf{X}_{2,t}$ are the true states for the entire seed bank using observed abundances from both burnt and unburnt grids). An **unstructured life-history model** in which there is no distinction between plants and seed banks (m = 1) was also constructed to confirm that the MARSS approach can distinguish the seed bank and plants as different life stages.

Often, estimated population trends that inform conservation plans are based on averaged (or aggregated) abundances over sites within a region, and methods have been developed to address inconsistencies in sampling times across time series (Johnson and Fritz, 2014). As fire history treatments and spatial hypotheses were tested at the grid level, Counts were not aggregated at the site level, therefore each individual plot (15 plots per grid) was treated as independent replicates of their corresponding hypothesised sub-population, improving both spatial replication (n = 60) and model parameter estimates. Although plots are likely to be spatially correlated, potentially resulting in spuriously high accuracy (Dennis et al., 2010), this is partially accounted for in the observation model through the observation bias, **a**, parameter. In addition, aggregation of abundance estimates can result in considerable loss of information with regards to model parameters, particularly process and observation errors (Dennis et al., 2010). Models for the observation and state process errors follow equations 1 and 2 with 3 months cumulative rainfall added as a covariate as this generally had the highest Pearson correlation with *T. glaucifolia* across sites. In all models, the process error covariance matrix **Q** was modelled as unconstrained with estimates for the off-diagonal elements Q_{ij}. The observation error matrix **R** was modelled as strictly diagonal ($R_{ij} = 0$ for $i \neq j$) with four separate errors (two fire histories × two life stages).

Regional models

To investigate the extent of spatial variation amongst populations, regional models consisting of all sites were constructed: the **independent site model** in which each site represents an independent sub-population ($m = 8$; plants and seed bank in each of the four study sites), the **regional fire model** in which populations that share fire history are similar to each other ($m = 4$; plants and seed bank for both burnt and unburnt areas across the study region), and the **overall regional model** in which sub-populations are not distinguished by space or fire history ($m = 2$). Models for the observation and state processes followed equations 1 and 2, with covariates added once the best fitting model was found. As before, individual plots were treated as independent measurements of their corresponding hypothesised sub-population ($n = 240$). **Q** was modelled as unconstrained with estimates for the off-diagonal elements Q_{ij}, and **R** was modelled as strictly diagonal with 16 separate errors (four sites × two fire histories × two life stages).

Model selection

Akaike's Information Criterion (AIC) is often used to select the best fitting model from a model set, with the modification AIC*c* adjusting for small-sample bias (Hurvich and Tsai, 1989). However, the AIC*c* tends to underestimates the complexity penalty for MARSS models (Cavanaugh and Shumway, 1997; Ward et al., 2010). Thus, for the MARSS-KFEM models, the parametric bootstrapped variant (AIC*b*), which is unbiased for short time series and, unlike its non-parametric counterpart, allows for missing data (Cavanaugh and Shumway, 1997; Holmes et al., 2012a) was used to select the best fitting model. Lower values of AIC*b* indicate greater model support. Models with an AIC*b* value eight points greater than another model are considered weakly supported compared to the competing model (Burnham and Anderson, 2002). For the MARSS-MCMC models, both the deviance information criterion (DIC), the Bayesian analogue of the AIC (Spiegelhalter et al., 2002), and the posterior predictive loss (*D*), a measure of the predictive ability of each model penalised for model complexity (Gelfand and Ghosh, 1998) were used to identify the model with the greatest support. Models with a DIC value between three and seven points of the lowest DIC score are weakly supported, while those seven points greater than the best fitting model are considered substantially inferior (Spiegelhalter et al., 2002).

Results

Covariates

The regional rainfall model had greater support than the local model for both the MARSS-KFEM and MARSS-MCMC models (Table 3-1), suggesting that rainfall events had a similar trajectory across all study sites. State predictions from both algorithms were nearly identical, with the only observable difference at the beginning of the time series in 1995 (Fig. 3-1). As plant population censuses were only conducted from 2004 onwards, for practical purposes, there was no difference between the state predictions, and the MARSS-KFEM values were used in subsequent population models. Trend parameters for both rainfall models in all sites were zero regardless of the algorithm used, indicating no change in rainfall patterns over time (Table 3-1). Observation error for the Field River site was higher than for the other sites, whilst having a lower process error.

Wildfire models

In three of the four sites, the wildfire models had greatest support as given by the AICb's, DIC's and predictive loss values (Table 3-2), suggesting that fire history drives unique sub-population trajectories. However, for South Site, the best fitting model was inconclusive, with the wildfire model being supported by the AICb's and the predictive loss while the whole site model was supported by the DIC. Differences in AICb's and DIC's between the wildfire and whole site model were small (ΔAICb = 4, ΔDIC = 5), suggesting no substantial difference between the two models.

Table 3-1. Model selection criterion and parameter estimates for MARSS-KFEM models (AIC*b*) and MARSS-MCMC models (DIC and predictive loss, *D*) for monthly rainfall from 1995-2012 in the Simpson Desert, central Australia. While the regional rainfall model has only a single state, separate observation errors (*R*) for each of the four sites were still estimated. 95% confidence intervals are shown in brackets. The smallest AIC*b*, DIC or predictive loss score gives the best fit model and is indicated in bold.

	KFEM	**MCMC**	**KFEM**	**MCMC**	**KFEM**	**MCMC**			
Model*	**Q**		**R**		**U**		**AIC*b***	**DIC**	***D***
Local									
MC	2.76 (2.15, 3.32)	2.43 (1.74, 3.22)	0.35 (0.20, 0.50)	0.76 (0.64, 0.89)	0.00 (-0.21, 0.21)	-0.01 (-0.22, 0.20)	2191	6014	1228
FR	1.69 (1.27, 2.06)	1.93 (1.34, 2.67)	0.92 (0.70, 1.21)	0.85 (0.68, 1.01)	0.00 (-0.18, 0.18)	-0.01 (-0.19, 0.17)			
CS	2.35 (1.81, 2.85)	3.19 (2.34, 4.14)	0.60 (0.44, 0.77)	0.47 (0.21, 0.66)	0.00 (-0.23, 0.23)	-0.01 (-0.24, 0.23)			
SS	2.58 (1.98, 3.12)	2.82 (2.07, 3.71)	0.43 (0.28, 0.60)	0.58 (0.43, 0.74)	0.00 (-0.22, 0.22)	-0.01 (-0.23, 0.21)			
Regional									
MC	2.25 (1.72, 2.77)	1.51 (1.33, 1.71)	0.46 (0.31, 0.64)	0.84 (0.72, 0.96)	-0.00 (-0.21, 0.19)	0.00 (-0.20, 0.21)	**2090**	**2326**	**783**
FR			1.19 (0.92, 1.54)	1.11 (0.98, 1.27)					
CS			0.69 (0.51, 0.90)	0.68 (0.55, 0.82)					
SS			0.52 (0.35, 0.70)	0.72 (0.60, 0.86)					

*MC = Main Camp, FR = Field River, CS = Carlo-Shitty, SS = South Site.

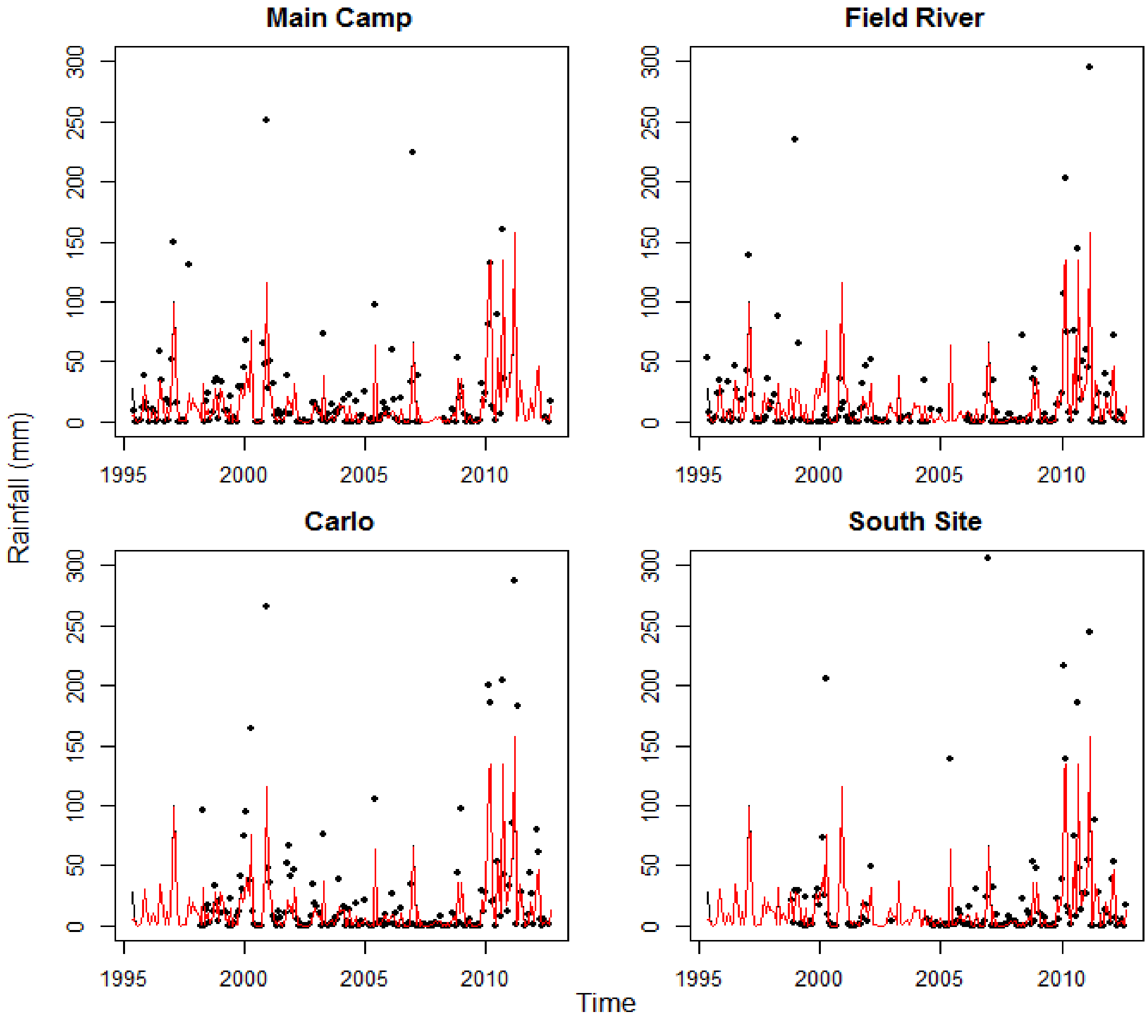

Fig. 3-1. State estimates of monthly rainfall based on regional models from both the MARSS-KFEM (black line) and MARSS-MCMC (red line) models for each study site in the Simpson Desert, central Australia (Main Camp, Field River, Carlo Shitty and South Site). With the exception of the initial period in 1995, state predictions from both algorithms are identical. Black points indicate weather station measurements.

Table 3-2. Model selection criterion for MARSS-KFEM (AIC*b*) and MARSS-MCMC (DIC and predictive loss, *D*) models comparing wildfire hypotheses. Best fit models for each site are given by the lowest AIC*b*, DIC or predictive loss score and are highlighted in bold. MARSS-KFEM models which were unstable and did not converge are left blank.

Model	**States (*m*)**	**AIC*b***	**DIC**	**Predictive Loss (*D*)**
Main Camp				
Wildfire	4	**3299**	**3277**	**24409**
Whole site	2	3327	3324	27382
Unstructured	1	3308	3602	51466
Field River				
Wildfire	4	**2804**	**2673**	**22379**
Whole site	2	3193	3099	27681
Unstructured	1		3164	37929
Carlo Shitty				
Wildfire	4	**2470**	**2937**	**20321**
Whole site	2	2522	3073	24959
Unstructured	1	2562	3185	35534
South Site				
Wildfire	4	**3689**	3650	**25961**
Whole site	2	3693	**3645**	26084
Unstructured	1		3765	34346

Regional models

The independent site model received the greatest support, followed by the regional fire model with the overall regional model performing worst (Table 3-3). Thus, distinct sub-populations of *T. glaucifolia* exist across the four sites. Taken with the wildfire models, which suggested further subdivisions based on fire history, MARSS models found high spatial variation in the population dynamics of *T. glaucifolia*. The regional model results also hinted that spatial location may be a better indicator of population dynamics than fire history as the independent site model performed substantially better than the regional fire model.

Table 3-3. Model selection criterion for MARSS-KFEM models (AIC*b*) and MARSS-MCMC models (DIC and predictive loss, *D*) for *Trachymene glaucifolia* populations over the entire study region in the Simpson Desert, central Australia. The smallest AIC*b*, DIC and predictive loss score gives the best fitting model and is highlighted in bold.

Model	**States (*m*)**	**AIC*b***	**DIC**	**Predictive Loss (*D*)**
Individual site	8	**12067**	**13164**	**106099**
Regional wildfire	4	12590	14079	112291
Overall regional	2	12637	14084	112102

State estimates, life history and parameter comparisons

Differences in parameter estimates between the MARSS-KFEM and the MARSS-MCMC models were potentially quite large, particularly for estimates of the observation errors (Table 3-4). Observation errors for the seed bank, for example, were estimated to be much larger in the MARSS-FKEM models compared to their MARSS-MCMC counterparts and lay outside of the 95% confidence intervals. Regardless of these differences, the relative sizes of the parameters remained consistent and patterns in parameter estimates between life history stages could be identified. For example, in both MARSS-KFEM and MARSS-MCMC models, growth rates for the plant stage class were not significantly different from zero except in the Field River unburnt site, where observations and state predictions showed relatively more pulses in plant abundance. The seed bank showed positive growth rates in all sites except Carlo Shitty, although MARSS-MCMC estimates were more conservative here and were not significantly different from zero. The seed bank was also characterised by higher observation errors relative to their process errors, while the reverse was true for the above-ground plants.

While there were observable patterns between life history stages, this was not true when parameters for fire history were compared across sites. For example, process errors (Q) for Main Camp and Carlo Shitty were higher in burnt sites, but for Field River and South Site the process error was higher in unburnt sites. Similarly, observation errors were higher in unburnt sites for Main Camp, Field River and South Site, but not for Carlo Shitty (Table 3-4).

The state predictions from only the MARSS-KFEM models are presented (Fig. 3-2; see Appendix 3-4 for state predictions from the MARSS-MCMC models). The seed bank generally had greater confidence in its state estimates and fewer fluctuations in its population abundance (Fig. 3-2) despite having fewer data points. As expected, confidence intervals (credible intervals for MARSS-MCMC models) calculated during periods with missing values were wider than for periods with well defined data points, indicating greater uncertainty when data are missing. Interestingly, having data on plant abundance gave greater confidence and reduced uncertainty in the state estimates for the seed bank when it was not measured, particularly in the Field River site.

Table 3-4. Parameter estimates for the process error, **Q**, observation error, **R**, and trend parameter, **U**, from the best fitting models for *Trachymene glaucifolia* populations at each individual site in the Simpson Desert, central Australia, for MARSS-KFEM and MARSS-MCMC models. 95% confidence (or credible) intervals are shown in brackets.

		KFEM	**MCMC**	**KFEM**	**MCMC**	**KFEM**	**MCMC**
Site*	**Stage**	**Q**		**R**		**U**	
MC-B	Seed bank	0.89 (0.00, 2.33)	1.26 (0.30, 3.67)	9.07 (6.93, 10.96)	2.78 (2.45, 3.14)	2.54 (1.91, 3.16)	1.10 (-0.35, 2.49)
	Plants	3.66 (1.08, 5.53)	4.94 (2.31, 10.10)	2.22 (1.80, 2.58)	1.46 (1.33, 1.59)	0.45 (-0.25, 1.15)	0.24 (-1.00, 1.49)
MC-U	Seed bank	0.84 (0.00, 2.30)	1.31 (0.26, 4.33)	12.46 (9.09, 15.06)	3.53 (3.12, 4.03)	2.09 (1.46, 2.71)	0.65 (-0.99, 2.20)
	Plants	2.79 (0.81, 4.25)	3.65 (1.75, 7.51)	0.93 (0.77, 1.09)	0.96 (0.87, 1.05)	0.38 (-0.22, 0.97)	-0.00 (-1.13, 1.11)
FR-B	Seed bank	0.06 (0.01, 0.90)	0.65 (0.13, 2.20)	8.76 (6.51, 10.79)	2.83 (2.50, 3.21)	1.60 (1.29, 1.91)	1.15 (-0.18, 2.39)
	Plants	0.72 (0.23, 1.16)	1.14 (0.52, 2.39)	0.32 (0.26, 0.38)	0.55 (0.50, 0.60)	-0.07 (-0.35, 0.21)	0.10 (-0.64, 0.89)
FR-U	Seed bank	2.16 (0.02, 4.83)	4.30 (1.26, 10.68)	12.79 (9.62, 15.55)	3.46 (3.04, 3.95)	2.84 (2.32, 3.37)	0.97 (-0.54, 2.43)
	Plants	3.87 (1.21, 6.26)	6.46 (3.09, 13.04)	0.87 (0.73, 1.02)	0.90 (0.82, 0.98)	1.14 (0.39, 1.90)	0.78 (-0.60, 2.15)
CS-B	Seed bank	0.02 (0.00, 0.97)	0.77 (0.14, 2.52)	14.06 (10.52, 16.98)	3.22 (2.85, 3.64)	-0.99 (-1.29, -0.70)	0.00 (-1.29, 1.61)
	Plants	3.19 (0.85, 4.89)	3.73 (1.73, 7.85)	0.56 (0.46, 0.65)	0.71 (0.64, 0.78)	0.26 (-0.34, 0.86)	0.00 (-1.09, 1.24)
CS-U	Seed bank	0.01 (0.0, 0.50)	0.43 (0.11, 1.31)	6.12 (4.58, 7.48)	2.71 (2.42, 3.05)	-0.00 (-0.32, 0.31)	-0.21 (-1.19, 0.83)
	Plants	1.73 (0.49, 2.71)	2.11 (0.99, 4.39)	0.33 (0.27, 0.39)	0.57 (0.52, 0.62)	0.24 (-0.20, 0.67)	0.21 (-0.67, 1.08)
SS-B	Seed bank	0.67 (0.00, 3.22)	2.01 (0.47, 5.37)	11.44 (8.95, 13.83)	3.24 (2.90, 3.64)	2.39 (2.04, 2.74)	0.78 (-0.55, 2.14)
	Plants	1.90 (0.55, 2.93)	2.97 (1.36, 6.17)	0.79 (0.64, 0.92)	0.91 (0.83, 1.00)	0.43 (-0.11, 0.97)	0.38 (-0.66, 1.42)
SS-U	Seed bank	0.93 (0.00, 3.22)	1.47 (0.23, 4.67)	12.06 (9.66, 15.05)	3.56 (3.19, 3.97)	4.25 (3.68, 4.81)	0.69 (-0.79, 2.22)
	Plants	2.57 (0.75, 3.85)	3.52 (1.53, 7.42)	1.32 (1.10, 1.57)	1.10 (1.00, 1.22)	0.46 (-0.14, 1.06)	0.54 (-0.61, 1.67)

*MC = Main Camp, FR = Field River, CS = Carlo-Shitty, SS = South Site; B = burnt, U = unburnt.

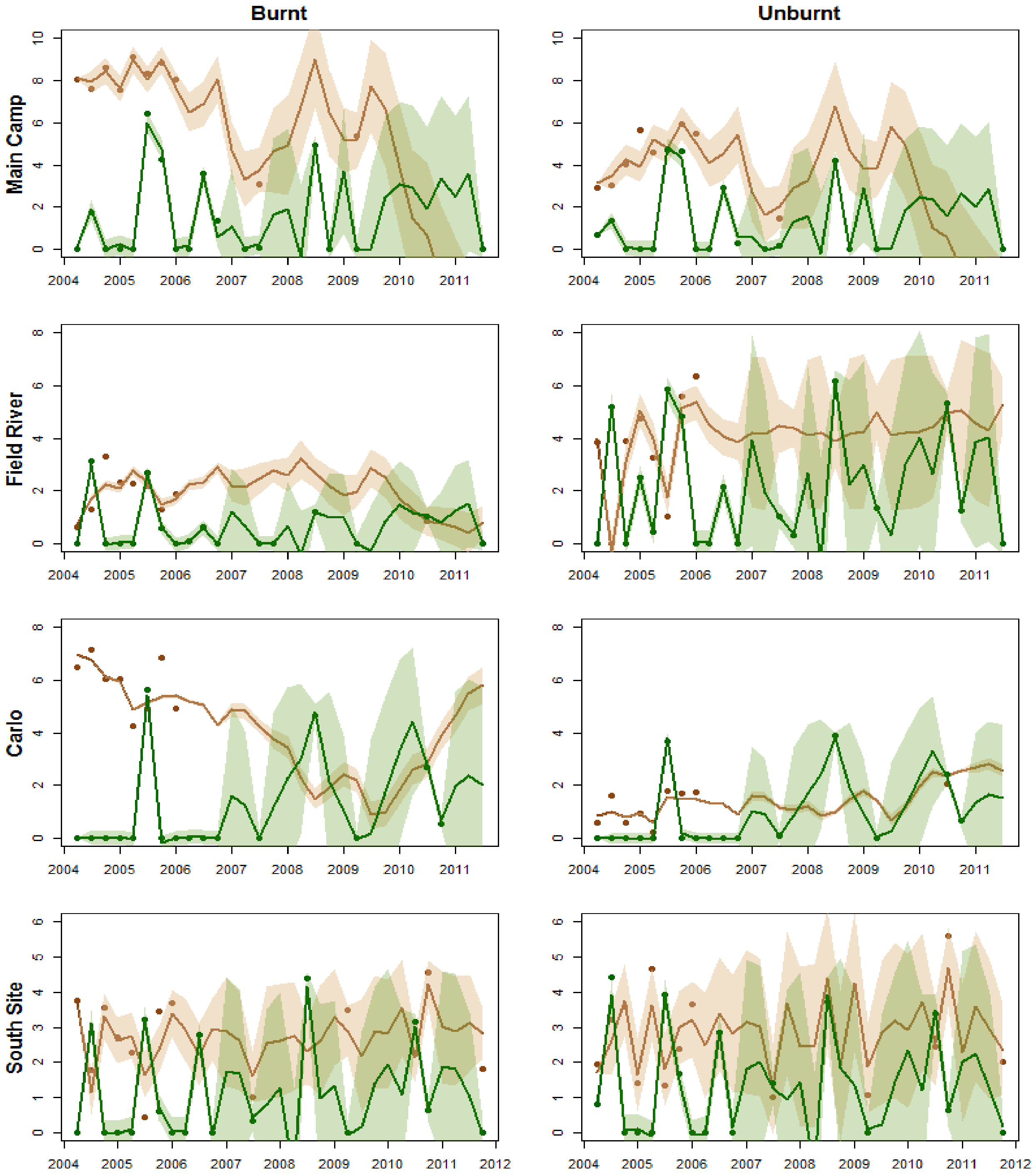

Fig. 3-2. Wildfire models showing predicted log state abundances for *Trachymene glaucifolia* at each of four study sites in the Simpson Desert, central Australia. Points indicate census observations averaged over 15 plots at each site, model-predicted state estimates are given by the solid line, and their 95% confidence intervals by the shaded areas. Seed bank trajectories are brown and above-ground plant trajectories are green.

Discussion

I set out to demonstrate how multivariate autoregressive state-space (MARSS) models can be used to help reduce uncertainties and interpret spatial and temporal trends in time series data, and thus aid in improving data quality and developing more strategic monitoring. These improvements are largely driven by the ability of state-space models to decouple true abundances and the observations used to estimate these abundances, thereby providing a more accurate portrayal of species' true biology rather than reflecting patterns in observation processes (Clark and Bjørnstad, 2004; Kéry and Schaub, 2012). Furthermore, the use of prior information to span missing values allows greater flexibility in the design of monitoring programs and enables ‘gaps’ in surveys to be planned (Morris et al., 1999; Humbert et al., 2009; Dennis et al., 2010). The results from this case study, consisting of abundance estimates for both the dormant seed bank and above-ground individuals of an ephemeral plant, show distinctive patterns that can be used to produce general guidelines for how monitoring could be conducted in future. For example, the seed bank was found to be characterised by higher observation errors and lower process errors, so that observed variation in abundances in the seed bank over time could be attributed mostly to the observation process. Because stochastic fluctuations in seed bank abundance are relatively stable, monitoring should then be more effective if it seeks to obtain fewer, but more accurate counts of the seed bank.

Accounting for all the life stages of a species is another important feature of an effective monitoring design to improve the inferences that it can yield (Chapter 2; Nguyen et al., 2015a in review). A potential weak point of many monitoring studies is the potential presence of cryptic life stages, those that are difficult to sample, or are absent from sampling designs. For example, raptor populations have been drastically underestimated in monitoring programs designed to observe only breeding birds (Katzner et al., 2011). Similarly, estimating the size of the seed bank presents several challenges from a monitoring and demographic perspective as seed-sampling and sorting are time consuming, both in the field and the laboratory, and counts thus are more difficult to make than for adult plants (Kalisz and McPeek, 1992; Adams et al., 2005). Information on cryptic stages can also be gained experimentally, as shown for a related species, *Trachymene incisa* (Wardle, 2003) that exhibited different responses across cohorts. However, the information gained from monitoring and modelling multiple life stages (such as the seed bank and plants) together within the MARSS framework provides valuable information and can be well worth the additional effort. For example, the size of the seed bank can be an indication of the potential size of the above-ground plant population when pulse events occur (Ludwig et al., 1997). Likewise, the difficulty and uncertainty in obtaining estimates for cryptic stages such as the seed bank can be alleviated by using information from more accessible stages. It is encouraging that, at least for this particular case study, the MARSS models suggest the seed bank need not be measured every census period - planned gaps can reduce the burden of resource allocation (Morris et al., 1999), while estimates of the above-ground plants can be used to assist state predictions for the seed bank during the gaps.

One of the key aims of monitoring programs is to detect spatial and temporal trends, with an emphasis on providing guidance for well informed, evidence-based policy management (Yoccoz et al., 2001; Eyre et al., 2011). In this sense, the MARSS framework proved useful for assessing trends on both scales, allowing tests for various spatial sub-population structures, whether driven by environmental or geographical factors, to be carried out (Ward et al., 2010). This case study, for example, reveals wildfire history to be an important driver of population dynamics on the local scale (Greenville et al., 2009). However, when examined on a regional scale, the spatial location appears to be the dominant factor, potentially associated with factors such as soil quality or local competition. Identification of sub-population structure and overall spatial heterogeneity is a worthwhile goal, as populations with shared environmental drivers are more susceptible to extinction (Morris et al., 1999; Warton and Wardle, 2003; Ward et al., 2010). Here, spatial replication may be justified to properly understand and manage the dynamics governing each sub-population (Emery et al., 2015). On the other hand, if sub-populations are found to be spatially homogeneous with shared drivers, more emphasis on temporal replication may be needed since rare, catastrophic events will influence all populations similarly.

Much of the MARSS output appears to be robust to the choice of algorithms used to estimate the parameters and tests for spatial sub-population structure. However, although a formal comparison between the Kalman filter/Expectation-Maximisation algorithms employed in the *MARSS* package (Holmes et al., 2012a; Holmes et al., 2012b) and the Monte Carlo Markov Chain algorithms used in JAGS (Plummer, 2003) was beyond the scope of this study, there were some discrepancies that are worth noting. For example, outputs from the MARSS-MCMC models are generally more conservative in their 95% credible intervals for both the parameters and state predictions (Table 3-4, Appendix 3-4). Another advantage of implementing the MARSS framework within JAGS is that it can accommodate a variety of error structures to the observations, such as the Poisson distribution, although future updates to the *MARSS* package may yet provide this option. Here, the error structure for the observations was assumed to come from a multivariate normal distribution. However, a Poisson error structure with random effects to account for overdispersion or a negative binomial is appropriate for most count data (Kéry and Schaub, 2012); neither distribution was found to produce good model fits (see Appendix 3-2).

Observation error was also assumed to remain constant over time, although the observation process can be subject to temporal change. This can be particularly relevant if the observation process includes detection probabilities, as even standardised field protocols can result in changes in detection probability over time (Schmidt, 2005; Kéry et al., 2009). However, this would not be expected to influence the results as the data come from plot-based sampling for a common species, and the methodology and core observers remained constant throughout the census period. The MARSS framework does allow for time-varying parameters, including observation errors, provided sufficient data are available to estimate these additional parameters (Holmes et al., 2012a). The ability to include time-varying parameters is crucial if long-term monitoring programs are able to capture significant changes in the environmental state (e.g. Chapter 4; Dickman et al., 2014; Nguyen et al., 2015b), or if the monitoring program evolves over time (Lindenmayer and Likens, 2009). Alternatively, factors known to affect the observation process (e.g. change in observer) can be included as a covariate factor, thus breaking down the observation error into its known components (Holmes et al., 2012a).

Conclusions

Monitoring programs are often criticised as being wasteful and unscientific (Lovett et al., 2007). The data produced may be perceived as being coarse or of poor quality and therefore inadequate for identifying and understanding population trends - especially declines - compared to more detailed data on survival and fecundity that are required for demographic models (e.g. Caswell, 2001). However, well designed monitoring programs are essential for the detection of long-term trends, advancement of ecological knowledge and development of effective policies for managing ecosystems at comparatively low cost (Lovett et al., 2007; Lindenmayer and Likens, 2009; Dickman and Wardle, 2012; Lindenmayer et al., 2012). I have demonstrated how such data can be modelled effectively to assess spatial and temporal trends using the MARSS framework, and how adopting a hierarchical view of the data can produce outputs that can be used iteratively to improve monitoring programs and the data they produce. An effective modelling framework can therefore guide the process of sampling and data collection towards designing an increasingly effective, cost-efficient monitoring program. This will produce higher quality data and improve model outputs, and in turn improve the ability of managers to track real trends in populations and to intervene, if needed, to set them on desired trajectories.

Acknowledgements

I would like to thank Chris Dickman and members of the Desert Ecology Research Group, especially Bobby Tamayo, Aaron Greenville, David Nelson, Chin-Liang Beh and the many volunteers, for their dedication to collecting the long-term datasets analysed here. Bush Heritage Australia and the land managers of Carlo Station kindly provided access to their properties for the long-term surveys. Research support was provided by the Australian Research Council and the Long Term Ecological Research Network (www.tern.org.au).

References

Adams, V.M., D.M. Marsh and J.S. Knox. 2005. Importance of the seed bank for population viability and population monitoring in a threatened wetland herb. Biological Conservation, 124:425-436.

Brooks, S.P. and A. Gelman. 1998. General methods for monitoring convergence of iterative simulations. Journal of Computational and Graphical Statistics, 7:434-455.

Buckley, Y.M., S. Ramula, S.P. Blomberg, J.H. Burns, E.E. Crone, J. Ehrlén, T.M. Knight, J.P. Pichancourt, H. Quested and G.M. Wardle. 2010. Causes and consequences of variation in plant population growth rate: a synthesis of matrix population models in a phylogenetic context. Ecology Letters, 13:1182-1197.

Burnham, K.P. and D.R. Anderson 2002 Model selection and multimodel inference. Springer Science and Business Media, Inc., New York, NY.

Caswell, H. 2001 Matrix population models: construction, analysis and interpretation. Sinauer Associates, Inc., Sunderland, Massachusetts.

Cavanaugh, J.E. and R.H. Shumway. 1997. A bootstrap variant of AIC for state-space model selection. Statistica Sinica, 7:473-496.

Clark, J.S. and O.N. Bjørnstad. 2004. Population time series: process variability, observation errors, missing values, lags, and hidden states. Ecology, 85:3140-3150.

Cunningham, G.M., W.E. Mulham, P.L. Milthorpe and J.H. Leigh 1992 Plants of Western New South Wales. CSIRO Publishing: Collingwood, Victoria, Australia.

de Valpine, P. and A. Hastings. 2002. Fitting population models incorporating process noise and observation error. Ecological Monographs, 72:57-76.

Dennis, B., P.L. Munholland and J.M. Scott. 1991. Estimation of growth and extinction parameters for endangered species. Ecological Monographs, 61:115-143.

Dennis, B., J.M. Ponciano, S.R. Lele, M.L. Taper and D.F. Staples. 2006. Estimating density dependence, process noise, and observation error. Ecological Monographs, 76:323-341.

Dennis, B., J.M. Ponciano and M.L. Taper. 2010. Replicated sampling increases efficiency in monitoring biological populations. Ecology, 91:610-620.

Dickman, C.R. and G.M. Wardle 2012. Monitoring for improved biodiversity conservation in arid Australia. 157-164 in D. Lindenmayer and P. Gibbons, editors. Biodiversity monitoring in Australia. CSIRO Publishing, Collingwood, Victoria, Australia.

Dickman, C.R., G.M. Wardle, J. Foulkes and N. de Preu 2014. Desert complex environments. 379-438 in D. Lindenmayer, E. Burns, N. Thurgate and A. Lowe, editors. Biodiversity and environmental change: monitoring, challenges and direction. CSIRO Publishing, Collingwood, Victoria, Australia.

Emery, N.J., M.J. Henwood, C.A. Offord and G.M. Wardle. 2015. *Actinotus helianthi* populations across a wide geographic range exhibit different climatic envelopes and complex relationships with plant traits. International Journal of Plant Sciences, in press accepted 8/5/2015.

Eyre, T.J., A. Fisher, L.P. Hunt and A.S. Kutt. 2011. Measure it to better manage it: a biodiversity monitoring framework for the Australian rangelands. The Rangeland Journal, 33:239-253.

Frank, A.S.K., C.R. Dickman, G.M. Wardle and A.C. Greenville. 2013. Interactions of grazing history, cattle removal and time since rain drive divergent short-term responses by desert biota. PloS One, 8:e68488.

Gelfand, A.E. and S.K. Ghosh. 1998. Model choice: a minimum posterior predictive loss approach. Biometrika, 85:1-11.

Gelman, A. and J. Hill 2007 Data analysis using regression and multilevel/hierarchical models. Cambridge University Press.

Gerrodette, T. 1987. A power analysis for detecting trends. Ecology, 68: 1364-1372.

Greenville, A.C., C.R. Dickman, G.M. Wardle and M. Letnic. 2009. The fire history of an arid grassland: the influence of antecedent rainfall and ENSO. International Journal of Wildland Fire, 18:631-639.

Hart, J.H. and M.J. Henwood. 2006. A revision of Australian *Trachymene* (Apiaceae: Hydrocotyloideae). Australian Systematic Botany, 19:11-57.

Hinrichsen, R. and E.E. Holmes 2009. Using multivariate state-space models to study spatial structure and dynamics. 144-166 in S. Cantrell, C. Cosner and S. Ruan, editors. Spatial Ecology. CRC/Chapman Hall, Boca Raton, FL, USA.

Holmes, E.E., J.L. Sabo, S.V. Viscido and W.F. Fagan. 2007. A statistical approach to quasi-extinction forecasting. Ecology Letters, 10:1182-1198.

Holmes, E.E., E.J. Ward and M.D. Scheuerell. 2012a. Analysis of multivariate time-series using the MARSS package. Version 3.4. http://cran.r-project.org/web/packages/MARSS.

Holmes, E.E., E.J. Ward and K. Wills. 2012b. MARSS: multivariate autoregressive state-space models for analyzing time series data. R Journal, 4:11-19.

Humbert, J.Y., L. Scott Mills, J.S. Horne and B. Dennis. 2009. A better way to estimate population trends. Oikos, 118:1940-1946.

Hurvich, C.M. and C.L. Tsai. 1989. Regression and time series model selection in small samples. Biometrika, 76:297-307.

Johnson, D.S. and L. Fritz. 2014. agTrend: A Bayesian approach for estimating trends of aggregated abundance. Methods in Ecology and Evolution, 5:1110-1115.

Kalisz, S. and M.A. McPeek. 1992. Demography of an age-structured annual: resampled projection matrices, elasticity analyses, and seed bank effects. Ecology, 73:1082-1093.

Katzner, T.E., J.A.R. Ivy, E.A. Bragin, E. Milner-Gulland and J.A. DeWoody. 2011. Conservation implications of inaccurate estimation of cryptic population size. Animal Conservation, 14:328-332.

Kéry, M., R.M. Dorazio, L. Soldaat, A. Van Strien, A. Zuiderwijk and J.A. Royle. 2009. Trend estimation in populations with imperfect detection. Journal of Applied Ecology, 46:1163-1172.

Kéry, M. and M. Schaub 2012 Bayesian population analysis using WinBUGS: a hierarchical perspective. Academic Press.

Lindenmayer, D.B. and G.E. Likens. 2009. Adaptive monitoring: a new paradigm for long-term research and monitoring. Trends in Ecology and Evolution, 24:482-486.

Lindenmayer, D.B., G.E. Likens, A. Andersen, D. Bowman, C.M. Bull, E. Burns, C.R. Dickman, A.A. Hoffmann, D.A. Keith, M.J. Liddell, A.J. Lowe, D.J. Metcalfe, S.R. Phinn, J. Russell-Smith, N. Thurgate and G.M. Wardle. 2012. Value of long-term ecological studies. Austral Ecology, 37:745-757.

Link, W.A. and J.R. Sauer. 2002. A hierarchical analysis of population change with application to Cerulean Warblers. Ecology, 83:2832-2840.

Lovett, G.M., D.A. Burns, C.T. Driscoll, J.C. Jenkins, M.J. Mitchell, L. Rustad, J.B. Shanley, G.E. Likens and R. Haeuber. 2007. Who needs environmental monitoring? Frontiers in Ecology and the Environment, 5:253-260.

Ludwig, J., D. Tongway, D. Freudenberger, J. Noble and K. Hodgkinson 1997 Landscape ecology function and management: principles from Australia's rangelands. CSIRO, Canberra.

Moore, P. 2005 A guide to plants of inland Australia. New Holland Publishers, Sydney, New South Wales, Australia.

Morris, W., D.F. Doak, M. Groom, P. Kareiva, J. Fieberg, L. Gerber, P. Murphy and D. Thomson 1999 A practical handbook for population viability analysis. Nature Conservancy.

Nguyen, V., Y.M. Buckley, R. Salguero-Gomez and G.M. Wardle. 2015a. Consequences of continuing to exclude cryptic life stages from demographic models. Submitted to Methods in Ecology and Evolution, in review.

Nguyen, V., A.C. Greenville, C.R. Dickman and G.M. Wardle. 2015b. On the validity of visual cover estimates for time series analyses: a case study of hummock grasslands. Plant Ecology, 216:975-988.

Nicolas, A.N. and G.M. Plunkett. 2009. The demise of subfamily Hydrocotyloideae (Apiaceae) and the re-alignment of its genera across the entire order Apiales. Molecular Phylogenetics and Evolution, 53:134-151.

Plummer, M. JAGS: A program for analysis of Bayesian graphical models using Gibbs sampling. Proceedings of the 3rd international workshop on distributed statistical computing, 2003. Technische Universit at Wien, 124:125.

Plummer, M. 2015. rjags: bayesian graphical models using MCMC. R package version 3-14.

Schmidt, B.R. 2005. Monitoring the distribution of pond-breeding amphibians when species are detected imperfectly. Aquatic Conservation: Marine and Freshwater Ecosystems, 15:681-692.

Shephard, M. 1999 The Simpson Desert: natural history and human endeavour. Corkwood Press, North Adelaide, South Australia.

Shumway, R.H. and D.S. Stoffer. 1982. An approach to time series smoothing and forecasting using the EM algorithm. Journal of Time Series Analysis, 3:253-264.

Shumway, R.H. and D.S. Stoffer 2006 Time series analysis and its applications. Springer-Verlag, New York, New York, USA.

Spiegelhalter, D.J., N.G. Best, B.P. Carlin and A. Van Der Linde. 2002. Bayesian measures of model complexity and fit. Journal of the Royal Statistical Society: Series B (Statistical Methodology), 64:583-639.

Staples, D.F., M.L. Taper and B. Dennis. 2004. Estimating population trend and process variation for PVA in the presence of sampling error. Ecology, 85:923-929.

Strong, C.L., J.E. Bullard, C. Dubois, G.H. McTainsh and M.C. Baddock. 2010. Impact of wildfire on interdune ecology and sediments: an example from the Simpson Desert, Australia. Journal of Arid Environments, 74:1577-1581.

Su, Y.-S. and M. Yajima. 2015. R2jags: a package for running jags from R. R package version 0.05-03.

Ward, E.J., H. Chirakkahl, M. González-Suárez, D. Aurioles-Gamboa, E.E. Holmes and L. Gerber. 2010. Inferring spatial structure from time-series data: using multivariate state-space models to detect metapopulation structure of California sea lions in the Gulf of California, Mexico. Journal of Applied Ecology, 47:47-56.

Wardle, G.M. 2003. Experimental determination of seed emergence and carry-over in the soil seed bank of the herbaceous perennial, Trachymene incisa (Apiaceae). Austral Ecology, 28:161-172.

Warton, D.I. and G.M. Wardle. 2003. Site-to-site variation in the demography of a fire-affected perennial, Acacia suaveolens, at Ku-ring-gai Chase National Park, New South Wales, Australia. Austral Ecology, 28:38-47.

Yoccoz, N.G., J.D. Nichols and T. Boulinier. 2001. Monitoring of biological diversity in space and time. Trends in Ecology and Evolution, 16:446-453.

THIS PAGE IS INTENTIONALLY LEFT BLANK

Chapter 4 - On the validity of visual cover estimates for time series analyses: a case study of hummock grasslands

Clump of *Triodia basedowii* (spinifex) forming its distinct ring shape with dieback in the centre as it ages. Photograph by Glenda Wardle.

A version of this chapter is published as Nguyen, V., Greenville, A.C., Dickman, C.R. and Wardle, G.M. (2015) On the validity of visual cover estimates for time series analyses: a case study of hummock grasslands. Plant Ecology, **216**, 975-988.

My contribution was very substantial, including conceptualization of ideas, data manipulation, construction and analysis of models, and writing and editing all drafts in consultation with my co-authors.

Abstract

Changes in vegetation cover are strongly linked to important ecological and environmental drivers such as fire, herbivory, temperature, water availability and altered land use. Reliable means of estimating vegetation cover are therefore essential for detecting and effectively managing ecosystem changes, and visual estimation methods are often used to achieve this. However, the repeatability and reliability of such monitoring is uncertain due to biases and errors in the measurements collected by observers. Here, two primary long-term monitoring datasets on spinifex grasslands, each established with different motivations and methods of data collection, are used to assess the validity of visual estimates in detecting meaningful trends. The first dataset is characterised by high spatial and temporal coverage but has limited detail and resolution, while the second is characterised by more intensive sampling but at fewer sites and over a shorter time. Using multivariate auto-regressive state-space models, I assess consistency between these datasets to analyse long-term temporal and spatial trends in spinifex cover whilst accounting for observation error. The relative sizes of these observation errors generally outweighed process, or non-observational errors, which included environmental stochasticity. Despite this, trends in the spatial dynamics of spinifex cover were consistent between the two datasets, with population dynamics being driven primarily by time since last fire rather than spatial location. Models based on these two datasets also showed clear and consistent population traces. Thus, visual cover estimates, in spite of their potential uncertainty, can be reliable provided that observation errors are accounted for.

Introduction

Monitoring programs that measure changes in vegetation cover provide important information needed to assess the status, trends and dynamics of any study system, and are therefore crucial for evidence-based policy management (Eyre *et al.*, 2011; Dickman and Wardle, 2012; Dickman *et al.*, 2014). Vegetation cover has been demonstrated to have strong relationships with global environmental drivers such as atmospheric CO_2 and global temperatures (Braswell *et al.*, 1997; Zeng *et al.*, 1999), water balance and availability (Joffre and Rambal, 1993), changes in land management practices (Vicente-Serrano *et al.*, 2004) and fire return intervals and fire intensity (Eckhardt *et al.*, 2000). Increased vegetation cover in Australian desert systems, for example, provides the necessary ground fuel required for large wildfires to establish and spread (Gill, 1975; Greenville *et al.*, 2009; Nano *et al.*, 2012).

Monitoring of grasslands often relies on visual inspection of fixed plots to estimate cover (i.e. cover as a percentage of the total plot area), and is a quick and non-intensive method to use (e.g. Tischler *et al.*, 2013; Dickman *et al.*, 2014). However, visual methods are highly susceptible to observation error, raising concerns about the reliability and repeatability of visual estimates (Helm and Mead, 2004; Wintle *et al.*, 2013). Observation errors include traditional sampling error resulting from differences between the sampled population and the overall population, and measurement error resulting from differences between observed estimates and true values (Chapter 3; Staples *et al.*, 2004; Flesch, 2014). These errors are less problematic when sampling designs are standardised as differences in sampling across sites or changes in sampling procedures over the duration of the study can result in variable observation errors over space and time. Process error on the other hand encompasses all non-observational error and includes variation resulting from demographic and environmental stochasticity. Observation errors in grasslands monitoring might arise due to the fine texture of grasses and potentially large areas over which cover is estimated, causing difficulty in obtaining accurate visual estimates and creating errors that are large, unknown or observer-specific (Sykes *et al.*, 1983; Bennett *et al.*, 2000). Cover estimates in spinifex grasslands (*Triodia* spp.) may be potentially more robust, as the hummocks of spinifex are discrete and constitute the dominant life-form over large areas so that estimates can focus on this species rather than on overall vegetative cover, although observation error will still be present. Cheal, (2008), for example, found large discrepancies in estimates of spinifex cover from 16 experienced observers, ranging from 20-60% on a 10% point scale, with no relationship between general ecological experience of the observer (rather than task-specific experience) and cover estimates. In addition to the lack of observer agreement in visual estimates, factors contributing to observation errors can include plot size, plant morphology, distribution and incorrect identification (Kennedy and Addison, 1987; Klimeš, 2003).

Addressing observer biases would vastly improve the quality of visual estimates, but may not always be possible when working within the constraints of project costs, and requires careful consideration of the trade-offs involved. Errors may be reduced by taking group averages rather than relying on a single expert (Klimeš, 2003; Burgman *et al.*, 2011), or by making replicated observations (Dennis *et al.*, 2010; Knape *et al.*, 2011), but this can be costly and draw resources away from improving spatial or temporal coverage. Thus, in monitoring, a choice will usually occur between sampling a few sites with high accuracy and therefore gaining statistical power to detect small-scale dynamical changes, and sampling with more extensive temporal and spatial coverage to improve overall knowledge of populations in the study system (Morris *et al.*, 1999). Similarly, trade-offs in sampling can occur when determining appropriate spatial and temporal coverage. Long-term studies are crucial for understanding ecological processes and are necessary to capture rare disturbance events such as fires that drive many ecosystems (Turner *et al.*, 2003; Lindenmayer *et al.*, 2012).

Monitoring populations from multiple sites is also important to identify whether populations are independent, with different population dynamics, or are correlated and have shared environmental drivers and thus are more susceptible to extinction (Chapter 3; Morris *et al.*, 1999; Warton and Wardle, 2003; Ward *et al.*, 2010). Populations that exhibit unique, independent dynamics may require more spatial replication to properly manage and understand the dynamics governing each population, whereas a correlated population might need more emphasis on temporal replication since rare, catastrophic events will impact all populations similarly. A careful balance is therefore required to ensure that adequate replication occurs on both scales to detect meaningful changes in population abundances.

While many studies have investigated the repeatability and reliability of visual cover estimates and quantified observation errors (Sykes *et al.*, 1983; Klimeš, 2003; Helm and Mead, 2004; Gray and Azuma, 2005), I instead wish to comment on the usefulness of such data for discerning real trends and processes. This study makes use of two primary long-term datasets on the coverage of *Triodia basedowii* obtained from the Simpson Desert, central Australia, which were set up with different motivations and methods of data collection, and ran for different lengths of time. The first places greater emphasis on spatial and temporal coverage at the expense of accuracy and detail (Dickman *et al.*, 2014). The other begins with highly intensive sampling and investigates fewer sites over a relatively shorter period, but has greater resolution at each site (Chapter 3; Wardle and Dickman, unpublished data). Using a multivariate auto-regressive state-space (MARSS) approach to account for observation error, I compare and assess the utility of monitoring data for making informed decisions by first analysing long-term trends in spinifex cover and whether the two independent datasets produce similar results. By comparing the changes in cover over time revealed by each dataset, the robustness of visual cover estimates to different sampling strategies can be assessed.

Using the MARSS models, several hypotheses regarding spatial relationships in *T. basedowii* populations are examined. Re-establishment of spinifex cover post-fire will vary depending on the amount of rainfall (Griffin *et al.*, 1983; Nano *et al.*, 2012; Nano and Pavey, 2013); a diverse community of herbs and grasses can emerge during the recovery period, supplying more palatable food sources for livestock grazing compared to persistent stands of long-unburnt spinifex (Dickman *et al.*, 2014). The post-fire recovery period might therefore produce distinct spinifex population dynamics and responses to rainfall depending on the time since last fire. Additionally, this rainfall can be spatially restricted, producing isolated pockets of productivity (Letnic and Dickman, 2005; Letnic and Dickman, 2006), such that population dynamics depend more on the study location rather than fire history. The interaction between the post-fire recovery and rainfall could further distinguish spinifex population dynamics such that study sites impacted by the same fire may have different population dynamics due to spatially variable rainfall regimes. Finally, the relative sizes of observation and process errors as estimated by the MARSS models are compared. By using two independent datasets, I aim to determine whether visual cover estimates are capable of detecting meaningful trends despite concerns regarding their reliability, or whether observation error is sufficiently large to result in misleading and contradictory conclusions.

Methods

Study region

Two long-term datasets (hereafter referred to as the ‘wide view’ dataset, and the ‘high resolution’ dataset; Table 4-1) were obtained by the Desert Ecology Research Group based at the University of Sydney (Wardle and Dickman, unpublished data). Sampling was conducted across four pastoral stations in the Simpson Desert, central Australia: Carlo Station, Tobermorey Station, Cravens Peak and Ethabuka Reserves (Fig. 4-1), covering a combined area of 8000 km^2. The study region is mostly comprised of dune fields, with remaining areas consisting of clay pans, rocky outcrops and gibber flats (Dickman *et al.*, 2014). Vegetation is dominated by lobed spinifex (*T. basedowii*) with occasional small stands of gidgee trees (*Acacia georginae*), other *Acacia* shrubs and mallee eucalypts (Frank *et al.*, 2012; Tischler *et al.*, 2013; Wardle *et al.*, 2015). Long-term annual rainfall for this part of the desert averages ca. 250 mm, with decreasing gradients in annual rainfall occurring from north to south and east to west that partition the study region into three broad geographical areas (Greenville *et al.*, 2012).

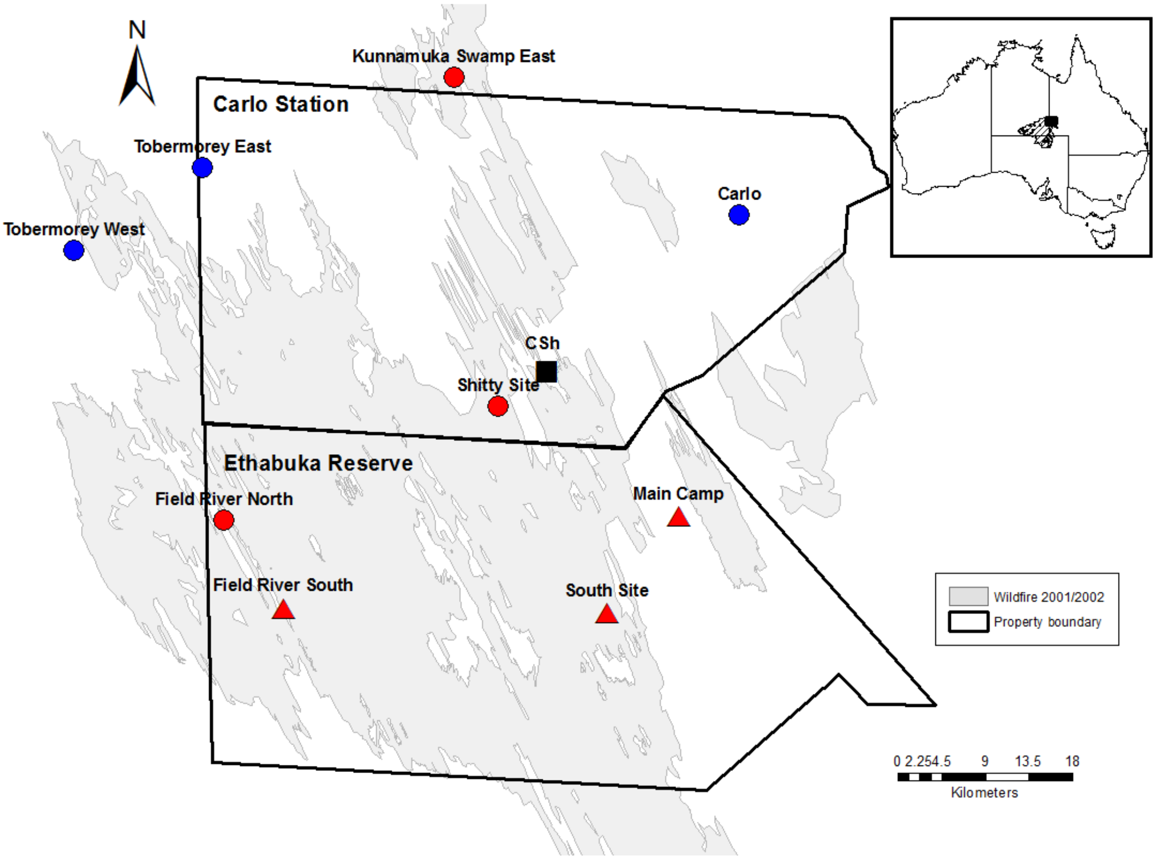

Fig. 4-1. Location of study sites across Carlo Station, Tobermorey Station, Cravens Park and Ethabuka Reserve, Simpson Desert, central Australia. Circles indicate sites that belong to the wide view dataset, the square indicates a site belonging to the high resolution dataset and triangles belong to both. Red fills are sites that were retrospectively labelled as burnt for the wide view dataset and indicate sites that experienced a fire over the summer of 2001-2002 and are designated as burnt sites for the duration of the time series (1995-2013), while blue indicates unburnt sites. Since Carlo Shitty was not part of the wide view dataset, it was not retrospectively labelled as burnt or unburnt.

Wide view dataset

The wide view dataset was initially created to track small mammal and lizard populations with the intention of long-term monitoring to capture important boom-bust dynamics associated with sporadic, heavy rainfall, and responses to major fire events (Dickman *et al.*, 1999; Letnic and Dickman, 2005; Dickman *et al.*, 2010; Dickman *et al.*, 2011; Greenville *et al.*, 2012). Spinifex cover and seeding were estimated visually as additional covariates as they are important components of the habitat and diet of small mammals (Dickman *et al.*, 2011). Live-trapping and wide view data sampling were carried out from 1990-2013 at one site and at eight other sites from 1995-2013 (Fig. 4-1), each site containing 2-12 grids spaced 0.5-2 km apart in randomly chosen positions along access tracks (Table 4-1). Sampling was conducted at irregular intervals from 2-6 times a year and missing values were included in the time series when sites were not sampled. As sampling did not begin at most sites (8 of 9) until 1995, I use data from 1995 onward. Models using data only from 2004 onwards (‘truncated wide view’ dataset) were also constructed to match the temporal scale of the high resolution dataset (see below), allowing comparisons of state predictions and temporal trends in spinifex cover assuming that data collection for both datasets began at the same time. Spinifex cover was measured visually as percentage cover (5% point scale) in a 2.5 m radius around six points on each sampling grid (Table 4-1). Due to the irregularity of sampling intervals and the need to reflect divergent response times, data were aggregated by year to account for the time needed for spinifex growth to respond to rainfall whilst simplifying model construction and subsequent comparisons with the high resolution dataset. Fire treatment allocation was *ad hoc* and done retrospectively, whereby a site was labelled as burnt if most sampling grids experienced a fire during the study period (six of nine sites). In such cases, grids that were unaffected by fire for that site were discarded for analyses. Likewise, for sites labelled as unburnt, grids that did experience a fire were discarded.

Table 4-1. Comparison of the main features of the wide view and high resolution datasets of spinifex cover obtained from sampling at multiple sites in the Simpson Desert, central Australia.

Design Feature	**Wide View Dataset**	**High Resolution Dataset**
Time series length	Long (1995-2013)	Medium (2004-2013)
Spatial coverage	High	Medium
Number of sites	9	4
Blocks/grids	2-12	2
Accuracy/detail	Low	High
Plots	6 per grid, circular 2.5 m radius	15 per grid, square, 5×5 m
Spinifex estimation method	Percentage cover, 5% point scale	Area cover, 0.5 m^2 point scale
Number of observers	High (>10, with varying experience)	Low (four trained personnel)
Data analysis	Aggregated by site and year	Not aggregated
Fire treatment	Site level, ad hoc assignment	Grids within sites

High resolution dataset

The high resolution dataset was created to monitor vegetation abundance and diversity with a particular focus on the effects of a wildfire that spread through the Simpson Desert in 2001-2002 (Greenville *et al.*, 2009). Subsequently, fire treatment was incorporated into a stratified design, whereby each site consisted of two 1-ha grids with one grid positioned in an area burnt during the 2001-2002 wildfire while the other was placed in an unburnt area. Vegetation surveys were carried out from 2004-2013 at four sites (Fig. 4-1). Within each grid, 15 5×5 m plots were placed in a 3×5 arrangement where the five plots on each row were placed on the swale, the middle, and the crest of the linear dunes and spaced randomly with a minimum separation of 5 m along a 100 m transect, giving a total of 120 plots across the eight grids (Table 4-1). Data were not previously aggregated and each plot was treated as a replicate sample of its corresponding grid (Chapter 3; Dennis *et al*., 2010). Intensive sampling was carried out in the first three years of data collection (2004-2006), with surveys being conducted quarterly. However, from 2007 onwards, surveys were only conducted 1-2 times a year at unequal time intervals due to funding and logistical constraints. As with the wide view dataset, missing values were included when sites were not sampled. Spinifex cover was measured in m^2 rather than as a percentage, and models for both datasets are presented as estimates of cover area.

Model description

Data were analysed using multivariate auto-regressive state-space (MARSS) models (Holmes *et al.*, 2012a; Holmes *et al.*, 2012b). These models were used to calculate true state estimates for spinifex cover accounting for process and observation error, estimate missing values, and to investigate various spatial hypotheses. Maximum likelihood parameters and state estimates for these models are achieved via recursive Kalman-Filter and Expectation-Maximisation algorithms until the models reach convergence (Shumway and Stoffer, 2006). Conceptually, the state-space model partitions population models into observed (data) and unobserved (true state) components. Let *n* denote the number of discrete survey sites and *m* denote the number of hypothesised populations. The MARSS model is then denoted by

$$\mathbf{X}_t = \mathbf{X}_{t-1} + \mathbf{u} + \mathbf{C}\mathbf{c}_t + \mathbf{w}_t; \qquad \mathbf{w}_t \sim \mathrm{MVN}(0, \mathbf{Q}) \qquad (1)$$

$$\mathbf{Y}_t = \mathbf{Z}\mathbf{X}_t + \mathbf{a} + \mathbf{v}_t; \qquad \mathbf{v}_t \sim \mathrm{MVN}(0, \mathbf{R}) \qquad (2)$$

where Eq. (1) represents the model for the true states, $\mathbf{X}_t$ is the *m* true states at time *t*, $\mathbf{u}$ is the trend parameter, $\mathbf{C}$ is the covariate effect, $\mathbf{c}_t$ is the covariate value at time *t,* and $\mathbf{w}_t$ is the process error assumed to be from a multivariate normal (MVN) distribution with mean zero and variance-covariance matrix **Q** (Holmes *et al.*, 2007; Hinrichsen and Holmes, 2009). Equation (2) represents the model for the observed states, where $\mathbf{Y}_t$ is the n observed estimates at time t, **Z** is a $n \times m$ matrix of 0's and 1's denoting population structure, pairing up each of the n observations to one of the m hypothesised states, and is used to explore various spatial hypotheses, **a** is the mean linear difference between survey sites measuring the same sub-population with respect to the first site, and $\mathbf{v}_t$ is the observation error assumed to be MVN with mean zero and variance-covariance matrix **R**.

For the wide view dataset, the following hypotheses were tested: 1) *Individual site model (9 states):* Each of the nine sampling sites act as independent, uncorrelated populations (Z is a 9 x 9 diagonal matrix, whereby each site is paired up with its own corresponding state); 2) *Geographical region model (3 states):* Sites can be grouped by geographical area into northern, southern and western populations partitioned by rainfall (Z is a 9 x 3 matrix whereby for each row, a 1 in the first, second or third column pairs that observation with the northern, southern or western population respectively); 3) *Wildfire model (2 states):* Sites can be grouped into burnt and unburnt populations based on their time since last fire, with particular reference to the 2001-2002 wildfires (Z is a 9 x 2 matrix whereby for each row, a 1 in the first or second column pairs that observation with the burnt or unburnt population respectively). The $\mathbf{C}\mathbf{c}_t$ parameters were used to model the immediate effect of the 2001-2002 wildfires, whereby $\mathbf{c}_t$ was set to 1 for 2002 and 0 for the remaining years: 4) *Complete homogeneity (1 state):* Populations from all nine sites act as a single population following the same trajectory with shared model parameters (Z is a 9 x 1 column vector of 1's). For the high resolution dataset, similar hypotheses were set up with slight variations due to the different design: 1) *Complete heterogeneity (8 states)*: Each of the grids acts as independent, uncorrelated populations. This can be likened to an interaction effect between fire history and site; 2) *Individual site model (4 states):* Each of the four sites acts as an independent population with no significant effect of fire history on the trajectory or parameters; 3) *Wildfire model (2 states)*: Populations on burnt grids follow the same trajectory with shared parameters regardless of site and similarly for unburnt grids; *4) Complete homogeneity*: There is no effect of site or fire history, and all grids in the study area follow the same trajectory with shared parameters. For each of the hypotheses, a unique trend parameter u was estimated for each hypothesised state. The variance-covariance matrix $\mathbf{Q}$ for the process errors was modelled as unconstrained (i.e. non-zero covariances) for all hypotheses except the “Individual site model” for the wide view dataset, in which $\mathbf{Q}$ was modelled as a diagonal matrix due to convergence issues. These convergence issues resulted in degenerate variance estimates and is generally caused by a lack of data relative to the number of parameters being estimated (Holmes *et al.*, 2012b). A unique observation error was estimated for each site in the high resolution dataset, while only a single error term was estimated for the wide view dataset due to similar issues. For both datasets, the variance-covariance matrix $\mathbf{R}$ was modelled with zero covariance. The best fitting model was identified as having the lowest Akaike Information Criterion adjusted for small sample sizes (AIC*c*), whereby ΔAIC*c* < 2 points suggests no substantial difference between models, and ΔAIC*c* > 8 points is considered weakly supported (Burnham and Anderson, 2002).

Results

Spatial hypotheses and state predictions

Multivariate autoregressive state-space (MARSS) models for the wide view and truncated wide view datasets show the wildfire model to have the greatest support (ΔAIC*c* > 8 compared to the next lowest AIC*c* values), with the individual site model having the least support (Table 4-2). MARSS models for the high resolution dataset show similar results, with the wildfire model having the greatest support despite a shorter time series which did not include the 2001-2002 wildfires (Table 4-2). Thus, there is agreement between both datasets and *T. basedowii* can be grouped reliably into burnt and unburnt populations, with trends in spinifex population dynamics better explained by time since last fire than by spatial location.

True state estimates produced by the wildfire model for the wide view dataset indicate gradually increasing cover from 1995 onwards across all sites until the 2001-2002 wildfires, creating a distinct division between the burnt and unburnt populations (Fig. 4-2). Following the fire, state estimates for both datasets show similar temporal trends in spinifex cover in which burnt populations remained low throughout the remainder of the monitoring period, with only a slight hint of a recovery by the end of the monitoring period (Figs 4-2 and 4-3). Meanwhile, spinifex cover in unburnt populations decreased gradually, dipping to a minimum in 2008 as a result of an extended drought period, followed by a relatively rapid recovery that followed heavy rains in 2010 and led to an outpacing of growth compared to that in the burnt populations. While truncating the wide view dataset to match the high resolution dataset in terms of time series length still retains the population structure results (Table 4-2), this model was unable to disentangle observation error from the process error, resulting in poor state estimates for the burnt population (Fig. 4-4).

Table 4-2. Comparison of model performance investigating subpopulation structure of spinifex at sites in the Simpson Desert, central Australia, using wide view, truncated wide view (from 2004 onward) and high resolution datasets of spinifex cover (see Methods for description of hypotheses), with the best fitting model given by the lowest AIC*c*.

	States	AIC*c*
Wide view dataset		
Wildfire	2	449.1845
Complete homogeneity	1	487.8002
Geographical region	3	511.8400
Independent site	9	539.2734
Truncated wide view dataset		
Wildfire	2	195.6980
Complete homogeneity	1	206.0595
Geographical region	3	222.0316
Independent site	9	245.1594
High resolution dataset		
Wildfire	2	6672.06
Complete homogeneity	1	6688.90
Independent site	4	6923.79
Complete heterogeneity	8	7171.68

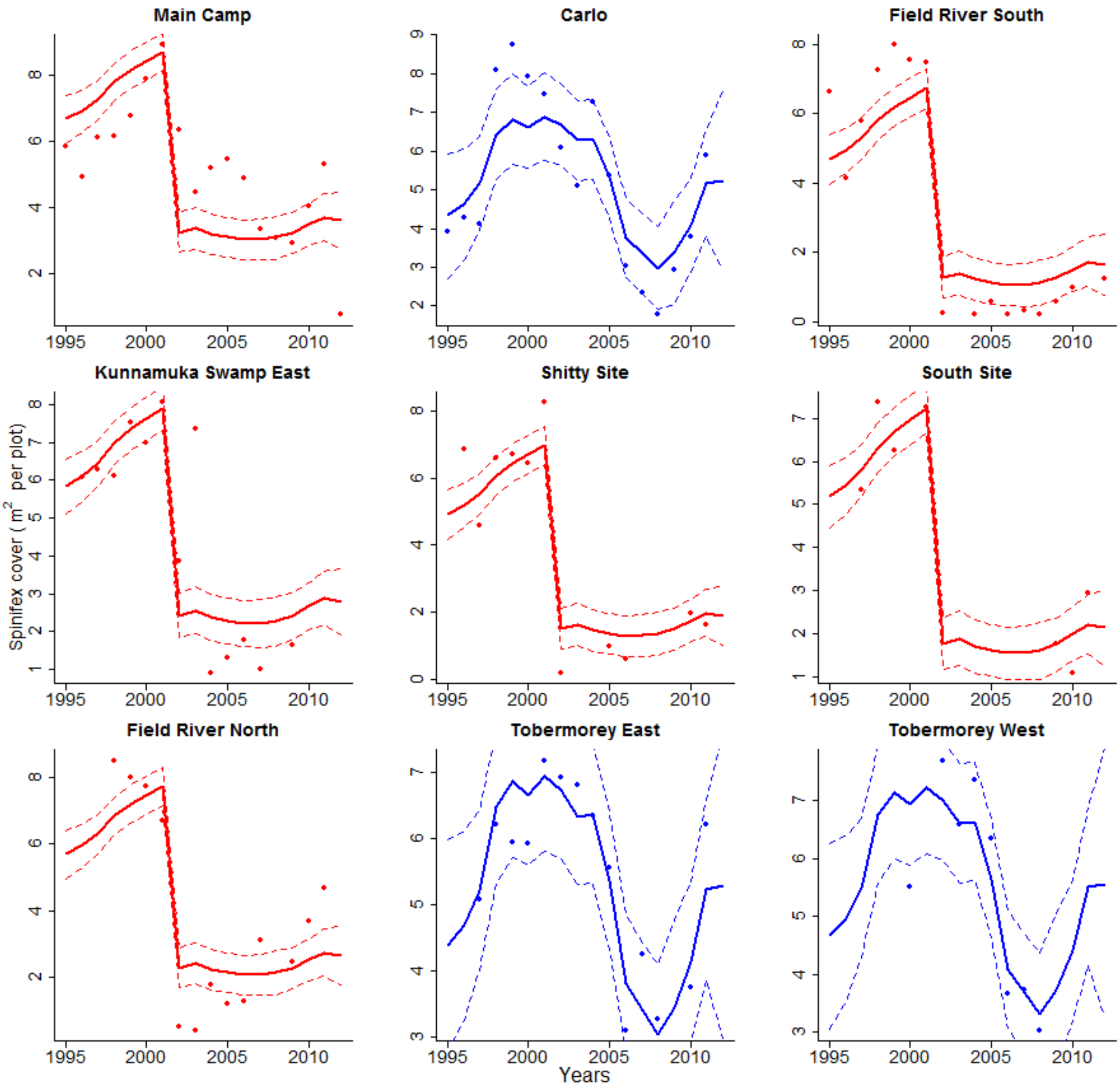

Fig. 4-2. State predictions (solid line) and their 95% confidence intervals (dashed lines) for cover of spinifex from the best fitting model (wildfire) for the wide view dataset obtained from nine sites in the Simpson Desert, central Australia. Filled points indicate actual observations. Red represents state predictions and observations from burnt sites, while blue represents those from unburnt populations.

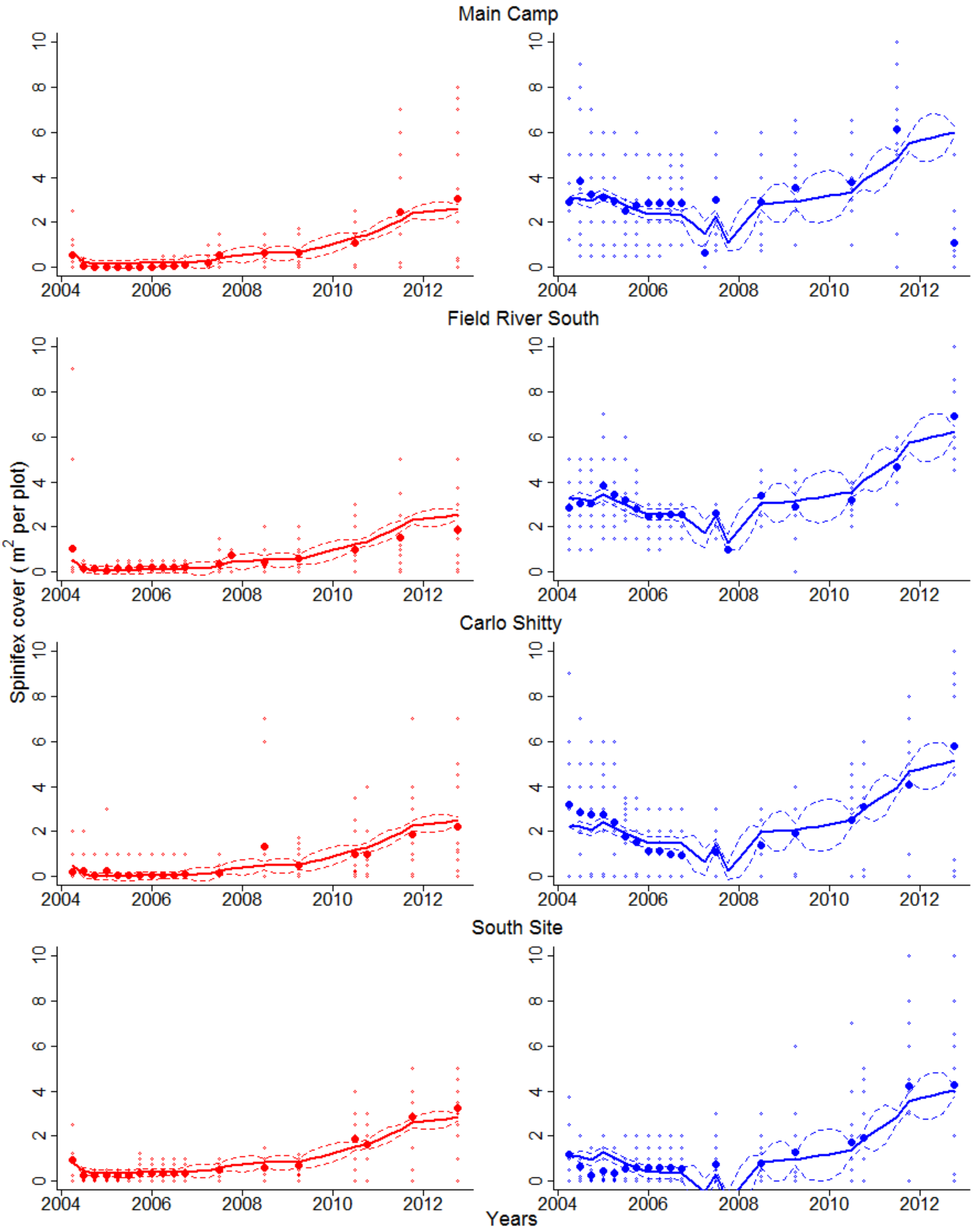

Fig. 4-3. State predictions (solid lines) with their 95% confidence intervals (dashed lines) for cover of spinifex from the best fitting model (wildfire) for the high resolution dataset obtained from four sites in the Simpson Desert, central Australia. Small circles indicate observations from each of 15 replicate plots, while large filled points indicate the means of these plots. Each of the four sites contains state predictions and observations from burnt (red) and unburnt (blue) populations.

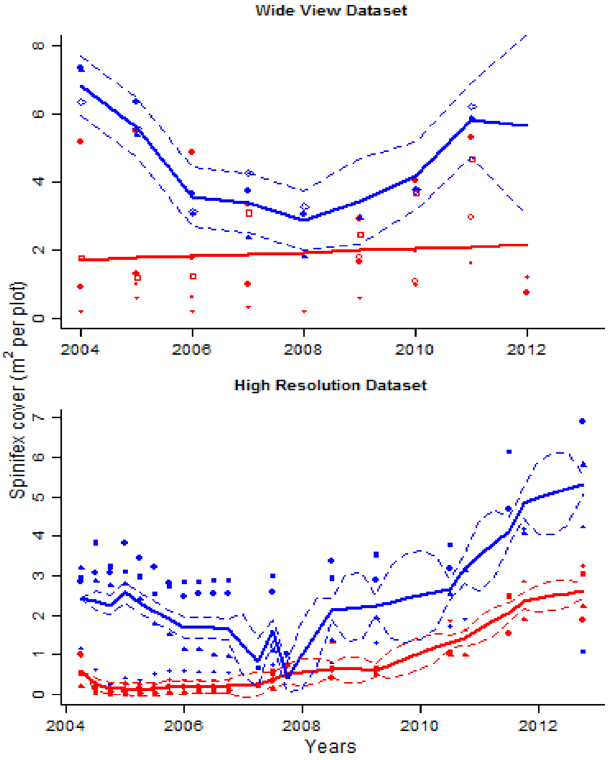

Fig. 4-4. Comparison of state predictions (solid lines) averaged across sites and 95% confidence intervals (dashed lines) for cover of spinifex derived from wildfire models for the wide view dataset and the high resolution dataset obtained from multiple sites in the Simpson Desert, central Australia. The wildfire model for the wide view dataset was constructed using only data from 2004 onward to allow comparison with the high resolution dataset, thus assuming that data collection for both datasets began at the same time. Observations (points) for the high resolution dataset are presented as site means. Red represents mean state predictions and observations for the burnt, while blue represents those from unburnt populations.

Comparison of maximum likelihood parameter estimates

In both the wide view and high resolution datasets, the observation error made up a larger component of the error term compared to process error, *Q* (Table 4-3). Observation errors were also found to be spatially variable, differing across and within sites. For example, the high resolution dataset showed that the Main Camp site had substantially higher observation error terms compared to the other sites. In addition, both datasets suggested that observation error in unburnt sites was larger relative to that in burnt sites. In contrast, while both datasets suggested positive spinifex growth (μ) in burnt and unburnt populations, the relative growth rates differed between burnt and unburnt populations. Spinifex growth in burnt sites was estimated to be substantially higher compared to unburnt sites for the wide view dataset, while the reverse was true for the high resolution dataset. However, confidence intervals in both cases were overlapping zero suggesting that this growth is non-significant. In general, confidence intervals for the wide view dataset were much larger when compared to the high resolution dataset, despite the longer time-series.

Table 4-3. Maximum likelihood parameter estimates from the best fitting models using wide view and high resolution datasets on spinifex cover sampled at multiple sites in the Simpson Desert, central Australia. The effect of a wildfire in 2001-2002 is given by the C parameter and is estimated only for the wide view dataset as it covered the time period in which it occurred. Observation error (R) was estimated for each grid in the high resolution dataset, while only a single, shared observation error term was estimated for the wide view dataset due to convergence issues. Bootstrapped 95% confidence intervals are given in parentheses.

	Wide view		High resolution	
Parameter	Burnt	Unburnt	Burnt	Unburnt
Growth rate (μ)	0.169 (-0.056,0.360)	0.056 (-0.469,0.604)	0.059 (-0.001,0.119)	0.086 (-0.102,0.273)
Effect of fire (C)	-5.645 (-7.267,-4.039)		-	-
Process error (Q)	0.119 (0.000,0.302)	0.907 (0.001,2.063)	0.032 (0.004,0.059)	0.265 (0.035,0.495)
Observation error (R)				
All	1.467 (1.051,1.883)		-	-
Main Camp	-	-	2.635 (2.187,3.083)	2.795 (2.285,3.304)
Field River	-	-	0.570 (0.469,0.670)	0.613 (0.499,0.727)
Carlo Shitty	-	-	0.865 (0.717,1.013)	1.460 (1.204,1.716)
South Site	-	-	0.328 (0.269,0.386)	1.262 (1.040,1.484)

Discussion

Ecological monitoring programs are critical for understanding ecological processes, provision of long-term data, supporting evidence-based decision making, and adaptive conservation management (Spellerberg, 2005; Wintle *et al.*, 2010; Eyre *et al.*, 2011; Lindenmayer *et al.*, 2012; Lindenmayer *et al.*, 2014). Visual cover estimates are cheap, rapid and are prevalent in monitoring programs of vegetation cover. That these cover estimates in forests (Helm and Mead, 2004) have previously been shown to be non-reproducible and highly susceptible to error is therefore a serious issue, and has implications for management decisions based upon such inputs. More positively, the use of feedback and calibration of observer results does improve reliability of visual estimation (Wintle *et al.*, 2013). Despite these widely acknowledged concerns, this study demonstrates through the use of two empirical datasets that monitoring data can still uncover conclusive trends. Although the wide view and high resolution datasets began with different motivations, and subsequently employed varying study designs and collection methods, monitoring data from these datasets were mostly consistent in terms of population structure and temporal trends. Models constructed from both datasets, for example, suggested that population dynamics for spinifex can be grouped by time since last fire into distinct burnt and unburnt populations, and there was generally little support for models suggesting site by site differences in the response to fire. Thus, the impact of the major 2001-2002 wildfire, and the subsequent temporal dynamics driven by rainfall events and periods of drought, were so extreme as to obscure any potential spatial heterogeneity that might have existed, for example, as a result of spatially variable rainfall regimes or pre-fire vegetation composition (Wardle *et al.*, 2013). Trends such as the relatively slow post-fire recovery in the burnt populations following the 2001-2002 wildfires and the impact of the drought on the unburnt populations are also consistent and reasonably identifiable between the two datasets. A comparison of the relative growth rates between burnt and unburnt sites showed conflicting results, however this was likely because estimation for the high resolution dataset only captures the period following the 2001-2002 wildfires in which the population experiences comparatively slow recovery, resulting in lower growth estimate compared to the wide view dataset. Thus, monitoring data in both cases had enough power to detect these large environmental drivers despite the substantial observation errors.

Concerns regarding observer bias and errors when making visual cover estimates are not without good reason as errors can be potentially quite large (Helm and Mead, 2004; Cheal, 2008; Vittoz *et al.*, 2010). These errors can be so large as to exceed actual year to year variation in cover (Klimeš, 2003), and error estimates for spinifex cover seem to confirm this, *albeit* over the period of least change in cover post-fire rather than including the fire itself. While one might expect that such substantial errors would provide unreliable and misleading results (Kennedy and Addison, 1987), these errors did not appear to prevent the models from discerning consistent trends for the two datasets. Having replicate observations in the high resolution dataset vastly improved the model's capacity to disentangle both process and observation error, and additionally allowed estimates of observation error to be calculated for each sampling location (Chapter 3). This was not possible when the high resolution data were aggregated, as the models encountered convergence issues in the algorithms, a common problem when data are insufficient (Dennis *et al.*, 2006; Holmes *et al.*, 2012a). Similar issues occurred with the wide view dataset despite the longer time series, particularly as there were more sites for which observation error needed to be estimated and many missing values for some sites. Consequently, only a single observation error term was calculated for the nine sites. However, the high resolution dataset suggests it may not be appropriate to assume that all sites have equal observation errors as they can differ substantially both between and within sites. For example, observation errors were larger in unburnt sites, likely due to greater variation in cover between plots, higher overall cover and higher process error resulting in bigger changes over time. Combined with the higher frequency of large, mature hummocks of spinifex which vary greatly in shape and distribution in unburnt sites, and increased likelihood of overhanging the plot, these factors all add to the difficulty of providing reliable estimates of cover.

In contrast, spinifex cover at burnt sites remained low throughout the study and consisted mostly of small, re-establishing seedlings post-fire (Rice and Westoby, 1999), resulting in lower estimates for observation error at burnt sites. Kennedy and Addison, (1987) compared observation errors between species and found larger errors for those with low cover, but this result was driven by detection errors where small, infrequently distributed species were seen in one sampling unit but not the next. Conversely, Sykes *et al.*, (1983) suggested that observation errors are less likely to occur at the lower and higher extremities and most likely to occur in between, and the results of this study seem to follow this pattern. Variation in the distribution and amount of cover between sites can therefore lead to some sites being more difficult to estimate cover than others. Thus, observation error can be better accounted for by focusing on fewer sites with greater replication than with the approach taken in the wide view dataset that emphasised greater spatial and temporal coverage (Dennis *et al.*, 2010). In addition, the potential size of observation errors might sometimes be anticipated; for example, if a site is known to have consistently lower cover or species diversity, monitoring resources could be distributed more efficiently. Higher diversity sites can complicate visual estimates as there is more heterogeneity in the possible sources of error, and cover estimates for individual plant species are more susceptible to errors than overall estimates of vegetation cover (Klimeš, 2003). In contrast, study systems dominated by a single species, as is the case in this study, would be less vulnerable to complications associated with estimating cover for multiple, low abundance species, and estimating cover for only the dominant life form can be quite informative of the study system. Thus, visual estimates may be more appropriate for grassland study systems compared to other environments such as woodlands where species diversity may be higher.

Investigating the extent of spatial heterogeneity and determining whether populations exhibit unique population trajectories can be particularly informative (Chapter 3; Ward *et al.*, 2010). Since spinifex population dynamics were shared across sites and driven predominantly by time since last fire, the increased spatial coverage observed in the wide view dataset may not have been necessary if one is purely interested in monitoring spinifex cover. However, the longer time series provided this monitoring program with an *ad hoc* opportunity to observe the impacts of a major wildfire. Wildfires are known to be a major driver of Australian desert ecosystems (Gill, 1975; Griffin *et al.*, 1983), and though fire cannot occur without consecutive seasons of high rainfall that promote plant growth and hence ground fuel, such events remain difficult to anticipate, with fire return intervals ranging from 20 to 50 years (Greenville *et al.*, 2009; Nano *et al.*, 2012). While it cannot be known exactly when wildfire events might occur, identifying potentially important drivers *a priori* is the key to a well designed monitoring program (Wintle *et al.*, 2010). In contrast, while the targeted monitoring approach of the high resolution dataset is expected to have more power to detect meaningful trends relating to time since last fire, the actual event itself may not always be captured, and is a testament to the value of long-term monitoring (Franklin, 1989; Dickman and Wardle, 2012; Lindenmayer *et al.*, 2012). Interestingly, even when the wide view dataset was truncated to be of similar length to the high resolution dataset but without the additional sampling intensity, the fire signal was still strong enough to be detected despite not being incorporated into the study design. However, this shortened time series had insufficient data from each site to properly disentangle process and observation errors, and resulted in poor state estimates for the burnt population. If funding uncertainties result in researchers being unable to commit to long-term monitoring programs, it may therefore be prudent to ensure that short-time series are of high quality, either through achieving sufficient replication over short periods to estimate observation errors, or through use of solutions that reduce impact such as taking mean values (Klimeš, 2003; Wintle *et al.*, 2013).

Visual cover estimates are by no means perfect, but are rapid, cheap, non-destructive, and commonly available, and therefore realistically are more likely to be carried out over long time periods and over large spatial scales than intensive repeat sampling. The use of remote sensing technologies and computer-image analysis provide an attractive alternative for reducing observation error (Bennett *et al.*, 2000; Booth and Tueller, 2003) but will introduce observation errors of other kinds, including the choice of post-process algorithms (Kennedy *et al.*, 2014). Furthermore, this does not reduce the need for field based approaches to assist with image interpretation and obtain other important measurements to provide a complete picture of the study system (Lathrop Jr *et al.*, 2014). While it is important to acknowledge the presence of errors and biases, visual estimates can generally be relied upon to detect meaningful changes (Vanha-Majamaa *et al.*, 2000; Irvine and Rodhouse, 2010), and this study provide some vindication for their continued use in management and monitoring studies. However, this conclusion depends on observer error being accounted for. There are several options for reducing observation error such as taking group averages rather than relying on a single expert (Klimeš, 2003; Burgman *et al.*, 2011), bias correction factors (Sykes *et al.*, 1983), or active calibration feedback to evaluate performance (Wintle *et al.*, 2013), and how one wishes to address this issue should be considered before deciding to implement sampling based on visual cover estimates.

Acknowledgements

I would like to thank Chris Dickman and other members of the Desert Ecology Research Group, especially Bobby Tamayo, Aaron Greenville, David Nelson, Chin-Liang Beh, and the many volunteers, for their dedication to collecting both the wide view and high resolution datasets used in this study. Bush Heritage Australia and the land managers at Carlo and Tobermorey Stations kindly provided access to their properties for the long-term surveys. Research support was provided by the Australian Research Council and the Long Term Ecological Research Network (www.tern.org.au).

References

Bennett, L.T., Judd, T.S. and Adams, M.A. (2000) Close-range vertical photography for measuring cover changes in perennial grasslands. *Journal of Range Management*, **53,** 634-641.

Booth, D.T. and Tueller, P.T. (2003) Rangeland monitoring using remote sensing. *Arid Land Research and Management,* **17,** 455-467.

Braswell, B.H., Schimel, D.S., Linder, E. and Moore, B. (1997) The response of global terrestrial ecosystems to interannual temperature variability. *Science,* **278,** 870-873.

Burgman, M.A., McBride, M., Ashton, R., Speirs-Bridge, A., Flander, L., Wintle, B., Fidler, F., Rumpff, L. and Twardy, C. (2011) Expert status and performance. *PLoS One,* **6,** e22998.

Burnham, K.P. and Anderson, D.R. (2002) *Model selection and multimodel inference.* Springer Science and Business Media, Inc., New York, NY.

Cheal, D. (2008) Repeatability of cover estimates? *Ecological Management and Restoration,* **9,** 67-68.

Dennis, B., Ponciano, J.M., Lele, S.R., Taper, M.L. and Staples, D.F. (2006) Estimating density dependence, process noise, and observation error. *Ecological Monographs,* **76,** 323-341.

Dennis, B., Ponciano, J.M. and Taper, M.L. (2010) Replicated sampling increases efficiency in monitoring biological populations. *Ecology,* **91,** 610-620.

Dickman, C.R., Greenville, A.C., Beh, C.-L., Tamayo, B. and Wardle, G.M. (2010) Social organization and movements of desert rodents during population “booms” and “busts” in central Australia. *Journal of Mammalogy,* **91,** 798-810.

Dickman, C.R., Greenville, A.C., Tamayo, B. and Wardle, G.M. (2011) Spatial dynamics of small mammals in central Australian desert habitats: the role of drought refugia. *Journal of Mammalogy,* **92,** 1193-1209.

Dickman, C.R., Letnic, M. and Mahon, P.S. (1999) Population dynamics of two species of dragon lizards in arid Australia: the effects of rainfall. *Oecologia,* **119,** 357-366.

Dickman, C.R. and Wardle, G.M. (2012) Monitoring for improved biodiversity conservation in arid Australia. *In:* Lindenmayer, D. & Gibbons, P. (eds.) *Biodiversity monitoring in Australia.* Collingwood, Victoria, Australia: CSIRO Publishing.

Dickman, C.R., Wardle, G.M., Foulkes, J. and de Preu, N. (2014) Desert complex environments. *In:* Lindenmayer, D., Burns, E., Thurgate, N. & Lowe, A. (eds.)

Biodiversity and environmental change: monitoring, challenges and direction. Collingwood, Victoria, Australia: CSIRO Publishing.

Eckhardt, H., Wilgen, B. and Biggs, H. (2000) Trends in woody vegetation cover in the Kruger National Park, South Africa, between 1940 and 1998. *African Journal of Ecology,* **38,** 108-115.

Eyre, T.J., Fisher, A., Hunt, L.P. and Kutt, A.S. (2011) Measure it to better manage it: a biodiversity monitoring framework for the Australian rangelands. *The Rangeland Journal,* **33,** 239-253.

Flesch, A.D. (2014) Spatiotemporal trends and drivers of population dynamics in a declining Sonoran Desert predator. *Biological Conservation,* **175,** 110-118.

Frank, A.S.K., Dickman, C.R. and Wardle, G.M. (2012) Habitat use and behaviour of cattle in a heterogeneous desert environment in central Australia. *The Rangeland Journal,* **34,** 319-328.

Franklin, J.F. 1989. Importance and justification of long-term studies in ecology. *In:* Likens, G. E. (ed.) *Long-term studies in ecology.* New York, New York, USA: Springer-Verlag.

Gill, A.M. (1975) Fire and the Australian flora: a review. *Australian forestry,* **38,** 4-25.

Gray, A.N. and Azuma, D.L. (2005) Repeatability and implementation of a forest vegetation indicator. *Ecological Indicators,* **5,** 57-71.

Greenville, A.C., Dickman, C.R., Wardle, G.M. and Letnic, M. (2009) The fire history of an arid grassland: the influence of antecedent rainfall and ENSO. *International Journal of Wildland Fire,* **18,** 631-639.

Greenville, A.C., Wardle, G.M. and Dickman, C.R. (2012) Extreme climatic events drive mammal irruptions: regression analysis of 100-year trends in desert rainfall and temperature. *Ecology and Evolution,* **2,** 2645-2658.

Griffin, G., Price, N. and Portlock, H. (1983) Wildfires in the central Australian rangelands. *Journal of Environmental Management,* **17,** 311-323.

Helm, D.J. and Mead, B.R. (2004) Reproducibility of vegetation cover estimates in South-Central Alaska Forests. *Journal of Vegetation Science,* **15,** 33-40.

Hinrichsen, R. and Holmes, E.E. 2009. Using multivariate state-space models to study spatial structure and dynamics. *In:* Cantrell, S., Cosner, C. & Ruan, S. (eds.) *Spatial Ecology.* Boca Raton, FL, USA: CRC/Chapman Hall.

Holmes, E.E., Sabo, J.L., Viscido, S.V. and Fagan, W.F. (2007) A statistical approach to quasi-extinction forecasting. *Ecology Letters,* **10,** 1182-1198.

Holmes, E.E., Ward, E.J. and Scheuerell, M.D. (2012a) Analysis of multivariate time-series using the MARSS package. Version 3.4. http://cran.r-project.org/web/packages/MARSS.

Holmes, E.E., Ward, E.J. and Wills, K. (2012b) MARSS: multivariate autoregressive state-space models for analyzing time series data. *R Journal,* **4,** 11-19.

Irvine, K.M. and Rodhouse, T.J. (2010) Power analysis for trend in ordinal cover classes: implications for long-term vegetation monitoring. *Journal of Vegetation Science,* **21,** 1152-1161.

Joffre, R. and Rambal, S. (1993) How tree cover influences the water balance of Mediterranean rangelands. *Ecology,* **74,** 570-582.

Kennedy, K. and Addison, P. (1987) Some considerations for the use of visual estimates of plant cover in biomonitoring. *Journal of Ecology***,** **75**, 151-157.

Kennedy, R.E., Andréfouët, S., Cohen, W.B., Gómez, C., Griffiths, P., Hais, M., Healey, S.P., Helmer, E.H., Hostert, P. and Lyons, M.B. (2014) Bringing an ecological view of change to Landsat-based remote sensing. *Frontiers in Ecology and the Environment,* **12,** 339-346.

Klimeš, L. (2003) Scale-dependent variation in visual estimates of grassland plant cover. *Journal of Vegetation Science,* **14,** 815-821.

Knape, J., Jonzén, N. and Sköld, M. (2011) On observation distributions for state space models of population survey data. *Journal of Animal Ecology,* **80,** 1269-1277.

Lathrop Jr, R.G., Haag, S.M., Merchant, D., Kennish, M.J. and Fertig, B. (2014) Comparison of remotely-sensed surveys vs. in situ plot-based assessments of sea grass condition in Barnegat Bay-Little Egg Harbor, New Jersey USA. *Journal of Coastal Conservation***,** 1-10.

Letnic, M. and Dickman, C.R. (2005) The responses of small mammals to patches regenerating after fire and rainfall in the Simpson Desert, central Australia. *Austral Ecology,* **30,** 24-39.

Letnic, M. and Dickman, C.R. (2006) Boom means bust: interactions between the El Niño/Southern Oscillation (ENSO), rainfall and the processes threatening mammal species in arid Australia. *Biodiversity and Conservation,* **15,** 3847-3880.

Lindenmayer, D., Burns, E., Thurgate, N. and Lowe, A.J. (2014) The value of long-term research and how to design effective ecological research and monitoring. *In:* Lindenmayer, D., Burns, E., Thurgate, N. & Lowe, A. J. (eds.) *Biodiversity and Environmental Change.* Collingwood, Victoria, Australia: CSIRO Publishing.

Lindenmayer, D.B., Likens, G.E., Andersen, A., Bowman, D., Bull, C.M., Burns, E., Dickman, C.R., Hoffmann, A.A., Keith, D.A., Liddell, M.J., Lowe, A.J., Metcalfe, D.J., Phinn, S.R., Russell-Smith, J., Thurgate, N. and Wardle, G.M. (2012) Value of long-term ecological studies. *Austral Ecology,* **37,** 745-757.

Morris, W., Doak, D.F., Groom, M., Kareiva, P., Fieberg, J., Gerber, L., Murphy, P. and Thomson, D. (1999) *A practical handbook for population viability analysis.* Nature Conservancy.

Nano, C.E. and Pavey, C.R. (2013) Refining the 'pulse-reserve'model for arid central Australia: seasonal rainfall, soil moisture and plant productivity in sand ridge and stony plain habitats of the Simpson Desert. *Austral Ecology,* **38,** 741-753.

Nano, C.E.M., Clarke, P.J. and Pavey, C.R. 2012. Fire regimes in arid hummock grasslands and Acacia shrublands. *In:* Bradstock, R. A., Williams, J. E. & Gill, A. M. (eds.) *Flammable Australia: fire regimes, biodiversity and ecosystems in a changing world.* Collingwood, Victoria, Australia: CSIRO Publishing.

Rice, B. and Westoby, M. (1999) Regeneration after fire in *Triodia* R. Br. *Australian Journal of Ecology,* **24,** 563-572.

Shumway, R.H. and Stoffer, D.S. (2006) *Time series analysis and its applications.* Springer-Verlag, New York, New York, USA.

Spellerberg, I.F. (2005) *Monitoring ecological change.* Cambridge University Press, Cambridge, England.

Staples, D.F., Taper, M.L. and Dennis, B. (2004) Estimating population trend and process variation for PVA in the presence of sampling error. *Ecology,* **85,** 923-929.

Sykes, J.M., Horrill, A.D. and Mountford, M.D. (1983) Use of visual cover assessments as quantitative estimators of some British woodland taxa. *Journal of Ecology,* **71,** 437-450.

Tischler, M., Dickman, C.R. and Wardle, G.M. (2013) Avian functional group responses to rainfall across four vegetation types in the Simpson Desert, central Australia. *Austral Ecology,* **38,** 809-819.

Turner, M.G., Collins, S.L., Lugo, A.L., Magnuson, J.J., Rupp, T.S. and Swanson, F.J. (2003) Disturbance dynamics and ecological response: the contribution of long-term ecological research. *BioScience,* **53,** 46-56.

Vanha-Majamaa, I., Salemaa, M., Tuominen, S. and Mikkola, K. (2000) Digitized photographs in vegetation analysis-a comparison of cover estimates. *Applied Vegetation Science,* **3,** 89-94.

Vicente-Serrano, S.M., Lasanta, T. and Romo, A. (2004) Analysis of spatial and temporal evolution of vegetation cover in the Spanish central Pyrenees: role of human management. *Environmental Management,* **34,** 802-818.

Vittoz, P., Bayfield, N., Brooker, R., Elston, D.A., Duff, E.I., Theurillat, J.P. and Guisan, A. (2010) Reproducibility of species lists, visual cover estimates and frequency methods for recording high-mountain vegetation. *Journal of Vegetation Science,* **21,** 1035-1047.

Ward, E.J., Chirakkahl, H., González-Suárez, M., Aurioles-Gamboa, D., Holmes, E.E. and Gerber, L. (2010) Inferring spatial structure from time-series data: using multivariate state-space models to detect metapopulation structure of California sea lions in the Gulf of California, Mexico. *Journal of Applied Ecology,* **47,** 47-56.

Wardle, G.M., Greenville, A.C., Frank, A.S.K., Tischler, M.K., Emery, N.J. and Dickman, C.R. (2015) Ecosystem risk assessment of Georgina gidgee woodlands in central Australia (Qld, NT, SA). *Austral Ecology in press*.

Wardle, G.M., Pavey, C.R. and Dickman, C.R. (2013) Greening of arid Australia: new insights from extreme years. *Austral Ecology,* **38,** 731-740.

Warton, D.I. and Wardle, G.M. (2003) Site-to-site variation in the demography of a fire-affected perennial, Acacia suaveolens, at Ku-ring-gai Chase National Park, New South Wales, Australia. *Austral Ecology,* **28,** 38-47.

Wintle, B.A., Runge, M.C. and Bekessy, S.A. (2010) Allocating monitoring effort in the face of unknown unknowns. *Ecology Letters,* **13,** 1325-1337.

Wintle, B.C., Fidler, F., Vesk, P.A. and L. Moore, J. (2013) Improving visual estimation through active feedback. *Methods in Ecology and Evolution,* **4,** 53-62.

Zeng, N., Neelin, J.D., Lau, K.-M. and Tucker, C.J. (1999) Enhancement of interdecadal climate variability in the Sahel by vegetation interaction. *Science,* **286,** 1537-1540.

Chapter 5 - Life form explains consistent temporal trends across species: the application of dynamic factor analysis

Four main life forms were identified in study sites within the Simpson Desert. Clockwise from top left: *Trachymene glaucifolia* (forb), *Eriachne aristidea* (grass), *Grevillea stenobotrya* (shrub) and *Newcastelia spodiotricha* (subshrub).

Abstract

Long-term survey data are important for detecting trends and guiding management decisions, however in practice, such data are scarce. Thus, to improve ecological inferences an appealing option is to borrow information about population trends and parameters from multiple data sources, including other species. If species respond similarly across space or time, then it is possible to understand trajectories at the aggregate level and manage accordingly. However, it is crucial to first establish the extent of heterogeneity in these responses across temporal and spatial scales to determine if such aggregations are indeed appropriate. Dynamic factor analysis (DFA) is a multivariate time series technique well suited for identifying such similarities as it reduces the temporal dynamics of a large number of species to a small number of common trends whilst retaining the temporal order of the observations. Thus, interpretation of large multispecies data is simplified, and these common trends can be used to reveal where there is potential to share information across species that are less well sampled. Here I apply DFA to a multispecies (27-30) time series dataset (9 years) obtained from multiple sites (3) in arid central Australia and search for the existence of common trends, and any patterns in how species are clustered. Five common trends were identified for each site, and they were strongly associated with life form. Forbs and grasses in particular showed high levels of synchrony in their responses to rain events with life-form distinctive signatures in the shape of their trends, although this was less pronounced for shrubs and subshrubs. However, these responses differed over relatively large (>20km) spatial scales. I conclude that plant life form reasonably predicts changes in abundance over time, albeit only for local scales, offering some justification for borrowing strength to supplement data for poorly sampled species.

Introduction

The availability of long-term ecological data is an essential ingredient for quantifying ecological responses to environmental stochasticity, detecting trends such as population decline, and for supporting evidence-based policies for management (Coulson *et al.*, 2001; Ellner *et al.*, 2002; Eyre *et al.*, 2011; Lindenmayer *et al.*, 2012). However, funding uncertainty, limited resources and a lack of recognition for monitoring programs amongst funding bodies has made it difficult to obtain this data (Lovett *et al.*, 2007; Lindenmayer *et al.*, 2012). Furthermore, monitoring programs may struggle to sample sufficient individuals for rare species that occur at low densities over large spatial scales, or are locally abundant but not widely distributed (Rabinowitz, 1981; Thompson, 2004) making it difficult to estimate population parameters and extinction risks. In practice, long-term datasets are quite rare (Magurran and Henderson, 2010) and analyses based on insufficient information can result in misleading conclusions and flawed conservation strategies (Coulson *et al.*, 2001). Thus an attractive option for improving ecological inferences is to borrow or aggregate information about population parameters from multiple data sources (MacKenzie *et al.*, 2005; Hui *et al.*, 2013).

Monitoring data are often obtained from multiple sites (e.g. Dickman *et al.*, 2014), however before such data can be aggregated, it is necessary to first identify the extent of spatial heterogeneity to determine which sites can be aggregated whilst estimating the smallest number of parameters possible (Burnham and Anderson, 2002; MacKenzie *et al.*, 2005). When spatial heterogeneity is sufficiently large, separate trends and parameter estimates may be required for each sampled location (Warton and Wardle, 2003; Jongejans and de Kroon, 2005; Peek and Forseth, 2009). Alternatively, population dynamics in sampled locations may be similar enough such that a single trend and set of parameter estimates can sufficiently describe the dynamics of multiple sites (Chapters 3 and 4; Ward *et al.*, 2010; Nguyen *et al.*, 2015). Shared trends and parameter estimates within a species over space may result naturally if populations display congruent dependence on an exogenous factor such as temperature or rainfall (Liebhold *et al.*, 2004).

Ecological monitoring programs focused on ecosystem and biodiversity management generally obtain information for multiple species (Nichols and Williams, 2006; Watson *et al.*, 2007), thus presenting opportunities for borrowing strength across species (MacKenzie *et al.*, 2005). The use of data from multiple species obtained from monitoring programs is appealing – analysis of multispecies data within a multivariate framework (in contrast to separate analysis of individual species) can provide greater insights into the ecology of a system and recognises that species can show covariation in their responses (Dunstan *et al.*, 2013; McGarigal *et al.*, 2013). I have previously used multivariate methods focusing on a single species, taking advantage of multiple life stages, replicates and sites to help parameterise models and identify important spatial and temporal trends (Chapters 3 and 4; Nguyen *et al.*, 2015). For large multi-species datasets however, it is inefficient to analyse each species separately and any similarities or covariation between species in their responses is not exploited (Dunstan *et al.*, 2013; Hui *et al.*, 2013). While the multivariate autoregressive state-space (MARSS) models (Chapters 3 and 4) can theoretically produce high level analysis for multiple species, high dimensionality and parameter estimates can become an issue for large numbers of species.

There are many alternative methods for modelling high dimensional multivariate data involving several species. These techniques have previously focused on measuring changes in biodiversity metrics such as α and β diversity (e.g. Magurran and Henderson, 2010; Legendre and De Cáceres, 2013; Dornelas *et al.*, 2014), or testing for changes in community structure over time or space as demonstrated via time lag analysis (Collins *et al.*, 2000) and the *mvabund* R package (Wang *et al.*, 2012). However, measures of biodiversity and community structure do not maintain species' identity and are not suited for assessing and utilising the strength of similarities in species' responses as demonstrated by Hui *et al.*, (2013) for species distribution modelling. Traditional dimension reduction techniques for multivariate data such as ordination and principal component analysis (PCA) can be useful for identifying such similarities (McCune *et al.*, 2002; McGarigal *et al.*, 2013). However, these techniques do not explicitly account for time and are therefore inappropriate for identifying shared temporal responses in time series data (Zuur *et al.*, 2003a). Dynamic factor analysis (DFA) on the other hand is ideal as it retains the temporal order of the observations, and produces similar output analogous to the principal components in PCA in the form of common trends (Zuur *et al.*, 2003a; Zuur *et al.*, 2003b). Thus the temporal dynamics of a large number of species is reduced to a smaller number of easily interpretable trends. By clustering species with similar temporal dynamics into these common trends, we can also identify which species are suitable for borrowing strength.

Here, I demonstrate the use of DFA on a multispecies time series dataset across multiple sites (9 years, 3 sites) to assess the suitability of borrowing strength across species and sites for estimating trends. The study system is an arid hummock grassland that is well-suited for the purpose as it experiences strong environmental drivers that might be expected to influence species in similar ways (Wardle *et al.*, 2013; Dickman *et al.*, 2014). In addition, by examining the trends of multiple species simultaneously rather, than a single species (Chapters 3 and 4), a broader description of the study system is provided. First, DFA will be used to determine whether any common trends exist, and if so, how many of these common trends are required to describe the temporal dynamics for the pool of species. If no such trends exist, then each species is acting idiosyncratically in response to environmental drivers and borrowing strength across species is unfeasible. If trends do exist however, then similarities between species can be exploited and patterns may be identified as to which species have shared temporal dynamics and why. Species that share common ecological properties such as those within the same life form group have been demonstrated to respond similarly to a shared environmental driver (Lavorel *et al.*, 1997; Lavorel and Garnier, 2002; Verheyen *et al.*, 2003; Broennimann *et al.*, 2006) and might therefore provide an explanation for the presence of common trends. DFA will also be used to assess the extent of spatial heterogeneity in species' responses on both a local (within sites) and regional (across sites) scales. Species' responses can differ by site (Warton and Wardle, 2003) or have similar dynamics due to shared external drivers such as environmental factors or geography (Hinrichsen and Holmes, 2009; Ward *et al.*, 2010). By identifying patterns across species and space, recommendations are provided regarding the suitability of borrowing strength across species and sites.

Methods

Study site

The study was conducted across Ethabuka Reserve and Carlo Station covering ~4400 km^2 within the Simpson Desert, central Australia (Fig. 5-1). The study region is mostly comprised of dune fields, with remaining areas consisting of clay pans, rocky outcrops and gibber flats (Dickman *et al.*, 2014). The climate is hot and dry, with daily temperatures regularly exceeding 40°C in the summer and falling below 5°C during the winter. Average annual rainfall is about 150mm with large rainfall pulses falling disproportionately in the summer however they can occur throughout the year (Nano and Pavey, 2013). Vegetation is dominated by lobed spinifex (*Triodia basedowii* E.Pritz.) with occasional small stands of gidgee trees (*Acacia georginae*; Wardle *et al.*, 2015), other woody *Acacia* shrubs and mallee eucalypts (Frank *et al.*, 2012; Tischler *et al.*, 2013). Short-lived grasses and forbs are diverse and abundant following rainfall and persist in the dormant seed bank during dry periods.

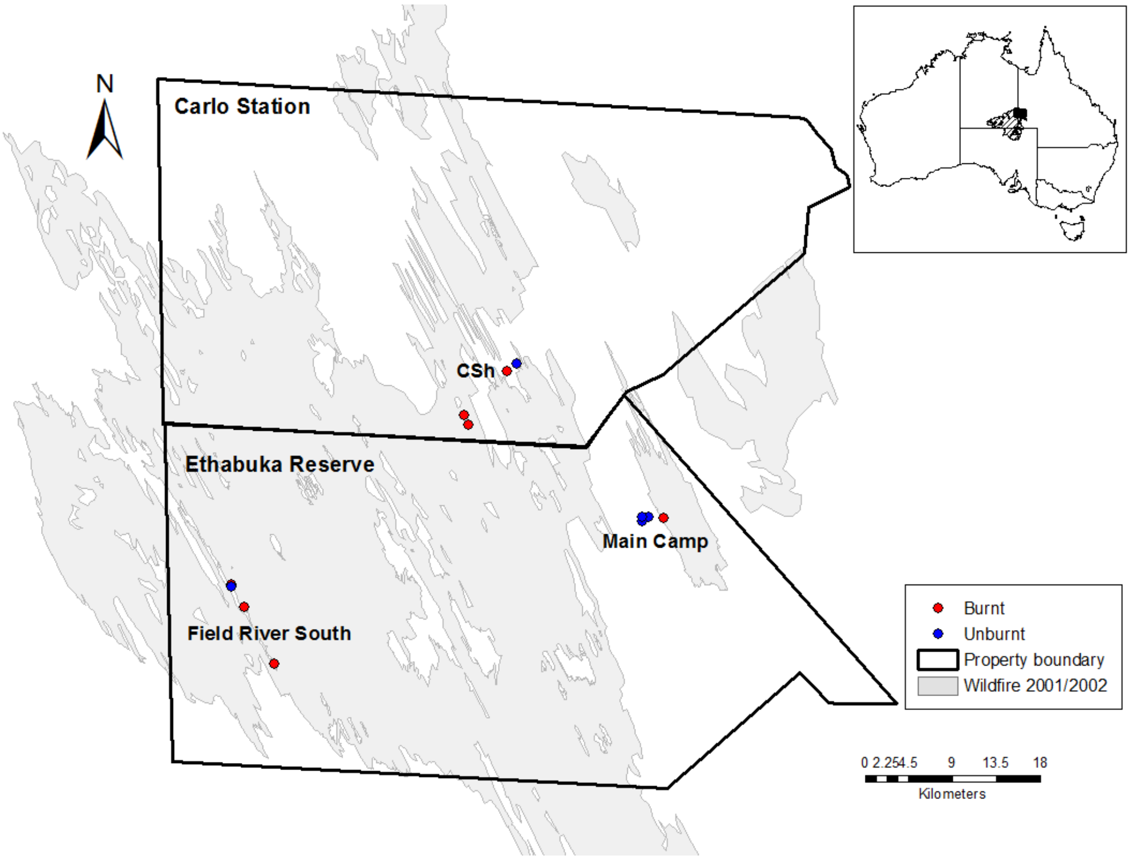

Fig. 5-1. Location of the three study sites (Main Camp, Field River and Carlo Shitty) across Ethabuka Reserve and Carlo Station.

Data collection

Vegetation surveys recording plant species' abundances were conducted from 2004-2013 by the Desert Ecology Research Group at the University of Sydney (Wardle and Dickman unpublished data). Each site consisted of four 1-ha grids made up of 15 5 × 5 m plots placed in a 3 × 5 arrangement in which five plots on each row were placed along the swale, the middle and the crest of the dunes. Plots were spaced randomly with a minimum of 5m along a

100m transect. It should also be noted that the relatively small size of these plots is generally more suited for sampling grasses and other small species rather than large woody species such as the *Acacias* and *Grevilleas* (Gregoire and Valentine, 2007), thus capturing changes in abundances for woody species would be difficult. Sampling was conducted four times a year from 2004-2006 to ensure the entire life cycle for the ephemeral species was captured. However, due to funding and logistical constraints, sampling could only be conducted 1-2 times a year from 2007 onwards at unequal time intervals. Additionally, not all grids were sampled every trip resulting in missing values in the time series.

The placement of the grids was originally intended to focus on the effects of a wildfire that spread through the Simpson Desert in 2001-2002, incorporating both a local, stratified design where a site contained both a burnt and unburnt grid, and a regional design in which both grids were burnt or unburnt (Chapters 3 and 4; Greenville *et al.*, 2009). Three study sites were incorporated into both the local and regional designs and therefore had four grids instead of two, with at least one burnt grid: Main Camp and Field River located on Ethabuka Reserve, and Carlo Shitty located on Carlo Station (Fig. 5-1). For the current analysis, I use data only for these three sites (total 12 grids and 180 plots) as those with two grids are unlikely to be sufficient to determine the extent of within-site spatial heterogeneity in species' abundances. Fire history is likely to be an important factor in determining species abundances (Wright and Clarke, 2009; Dickman *et al.*, 2014) and a potential cause of spatial heterogeneity on a local scale (Chapter 3). I do not conduct any formal examination of the effects of fire history in this analysis, however burnt and unburnt grids are distinguished when presenting the results of the DFA below.

Daily rainfall data were obtained from automated weather stations (Environdata, Warwick, Queensland) located at each site and 3 month seasonal aggregates (Dec-Feb, Mar-May, Jun-

Aug, Sep-Nov) were calculated and lined up with the census dates were calculated from May 1995 onwards.

Dynamic factor analysis

Dynamic factor analysis (DFA) is a dimension reduction technique that models multivariate time-series data as a linear combination of common trends representing the dominant common temporal patterns, explanatory variables and noise (Zuur *et al.*, 2003a; Zuur *et al.*, 2003b; Zuur and Pierce, 2004). Structurally, these models are very similar to the state-space models used in Chapters 3 and 4, albeit the different states are now species rather than spatial locations. The goal of these models is to find the smallest number of common trends, *m*, required to sufficiently describe the data (Zuur *et al.*, 2003a). The DFA is distinguished from factor analysis in that the dynamic factor model assumes the common trends (axes) are correlated through time, whereas factor analysis does not (Zuur *et al.*, 2003b). These models have been applied to a wide range of fields including psychology (Molenaar, 1985; Ferrer and Nesselroade, 2003), economics (Stock and Watson, 2012), health sciences (Hasson and Heffernan, 2011), hydrology (Muñoz-Carpena *et al.*, 2005), but its application to ecology is mostly focused on marine ecology and fisheries literature (Erzini, 2005; Erzini *et al.*, 2005; Andrews *et al.*, 2014; Baudron *et al.*, 2014). Following the notation of Holmes *et al.*, (2012a), the mathematical formulation for the DFA model is:

$$\mathbf{x}_t = \mathbf{x}_{t-1} + \mathbf{w}_t \text{ where } \mathbf{w}_t \sim MVN(0, \mathbf{Q}) \quad (1)$$

$$\mathbf{y}_t = \mathbf{Z}\mathbf{x}_t + \mathbf{D}\mathbf{d}_t + \mathbf{v}_t \text{ where } \mathbf{v}_t \sim MVN(0, \mathbf{R}) \quad (2)$$

Equation 1 models the trends, whereby the $m \times 1$ column vector $\mathbf{x}_t$ represents the values of the *m* common trends at time *t* and **Q** is a diagonal error covariance matrix set equal to the identity matrix (Zuur *et al.*, 2003b). Equation 2 relates the *n* observed time series to the *m* common trends, whereby the $n \times m$ matrix **Z** consists of factor loadings indicating the strength of the relationship between an observed time series and each of the common trends, **D** indicates effects of explanatory variables, $\mathbf{d}_t$ contains the value of the explanatory variable at time t, and the covariance matrix **R** represents the noise component. The error structure for both equations are assumed to come from a multivariate normal distribution. While a Poisson or negative binomial distribution may be more appropriate for count data, implementing these distributions would require extensive modifications to the estimation procedure used in Zuur *et al*, 2003b, and is outside the scope of this study.

Separate DFA models were constructed for each site on the standardised abundances for species that were included and the resulting common trends used to describe the different types of responses and life-history strategies present in the plant community. Factor loadings obtained from the DFA were used to link species with the common trends and compare loadings across species to determine whether plant species exhibit any patterns in their groupings based on their life form. Four life form groups were identified from the data: forbs, grasses, subshrubs and shrubs. Subshrubs are defined here as short shrubs that are typically only woody at the base, while shrubs consist of woody species that are typically over 1m in height. Species sharing high, positive factor loadings for a particular trend are highly associated and can be described as acting in synchrony. In contrast, species with negative factor loadings for that same trend would suggest a negative correlation, and thus can be considered to act antagonistically to species with positive loadings. In addition, factor loadings were compared across grids to assess whether species behaviour and groupings are consistent within sites. Given the high number of factor loading parameters estimated for each species, grid, and trend, factor loadings are presented as a colour coded table instead of traditional factor loadings plots such as those in Zuur *et al.*, (2003a) to facilitate identification of patterns across species. Finally, models including rainfall were used to identify relationships between species groups or common trends and patterns relating to rainfall. For each site, species that were spatially or temporally sparse (i.e. only observed in a single census, plot or grid) and therefore had insufficient observations for estimation of spatial and temporal trends were not considered for this analysis (See Appendix 4-1 for full list of species for each site). For Main Camp, the total species pool was reduced from 70 to 27 species (14 forbs, 5 grasses, 5 subshrubs and 2 shrubs), 65 to 28 species for Field River (15 forbs, 5 grasses, 5 subshrubs and 3 shrubs), and 52 to 30 species for Carlo Shitty (16 forbs, 5 grasses, 5 subshrubs and 4 shrubs).

Dynamic factor models containing 1-5 common trends were constructed for each site with and without rainfall. The error covariance matrix, **R**, was modelled as diagonal. While a symmetric positive-definite matrix with non-zero off-diagonal elements can be used, the number of parameters increases drastically, particularly given the dimensionality of the covariance matrix (Zuur *et al.*, 2003a). Models were compared using Akaike's information criterion corrected for small sample sizes (AIC*c*) in which the model with the lowest score provides the best fit (Burnham and Anderson, 2002). Estimated state predictions were also checked to determine appropriateness of the model. To ease comparisons of factor loadings, covariate coefficients and trends in abundance estimates between species (which can range from <10 to >1000 individuals for a single census), all data including rainfall were standardised by deducting the mean and dividing by the standard deviation (Zuur *et al.*, 2003a; Zuur *et al.*, 2003b). Dynamic factor models were constructed via the Kalman Filter and Expectation-Maximisation algorithms implemented by the MARSS package (Holmes *et al.*, 2012a; Holmes *et al.*, 2012b) in R (R 3.1.2; The R foundation for Statistical Computing; see Appendix 4-2 for custom functions used in DFA models). Following construction of the dynamic factor models, factor loadings were transformed using the varimax rotation, which produces an equivalent solution for Eqs. 1 and 2, but creates larger differences in loadings between trends thereby reducing ambiguity and simplifying interpretations of factor loadings (Holmes *et al.*, 2012a; Thorson *et al.*, 2015).

Results

The presence/absence and relative abundances over time of species for one grid in Main Camp are shown in Fig. 5-2 (see Appendix 4-3 for remaining grids). A number of species experienced peak abundance concurrently during the winter/spring seasons of 2005, but were present in comparatively lower abundances throughout the rest of the census period. The unpredictability in occurrence for the shorter lived species, namely the forbs and grasses, highlighted the difficulty in attempting to extrapolate species persistence from one season to the next where missing values are present.

The results of dynamic factor analysis suggested that for each of the three sites, the model with five common trends provided the best fit; although the inclusion of the rainfall covariate did not necessarily provide the best model for all sites. (Table 5-1). The best model for Main Camp included rainfall whereas the best models for Field River and Carlo Shitty did not. However, the state predictions for Carlo Shitty without rainfall were a poor fit and thus the model with rainfall included is presented instead (see Appendix 4-4 for details).

Fig. 5-2. Plot of **A)** presence/absence and **B)** relative frequency of species present for a single grid in Main Camp divided by life form. Species in black are forbs, red are grasses, blue are shrubs and green are subshrubs. Red cells indicate presence, white indicates absence while gray indicates a missing value when a census was not conducted.

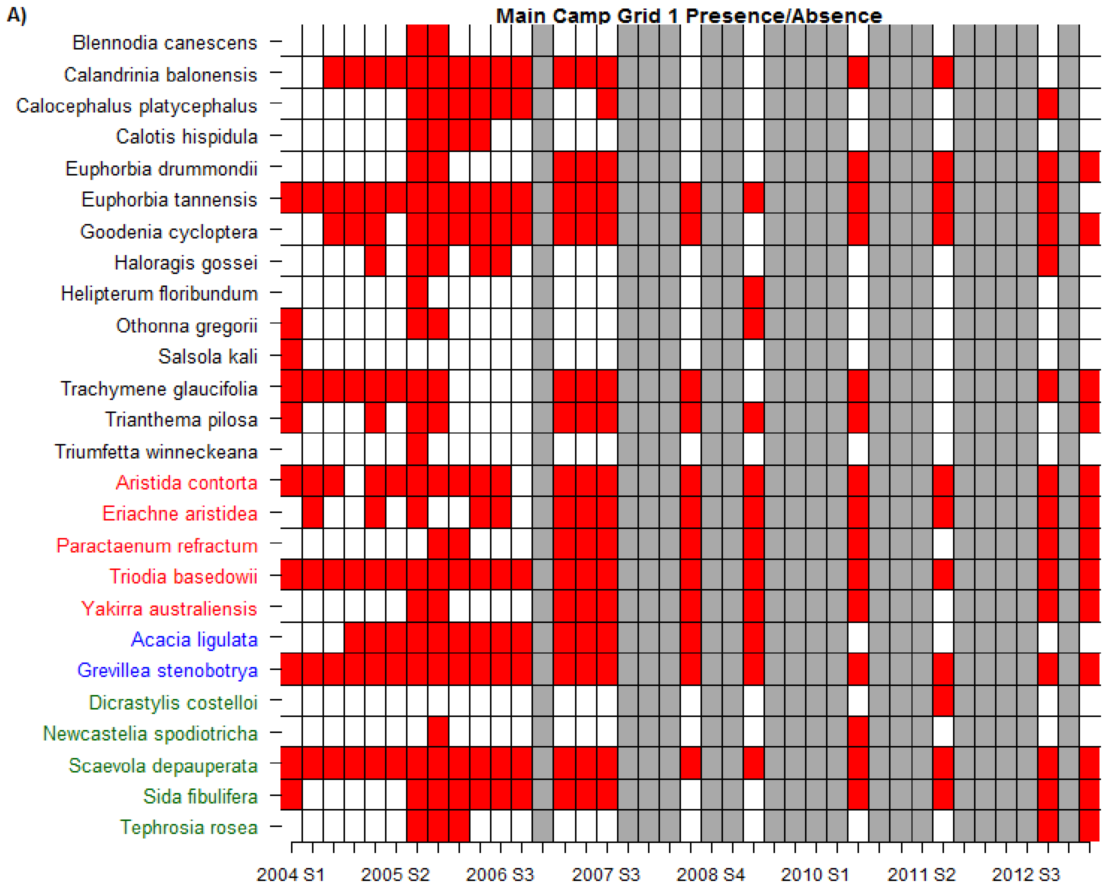

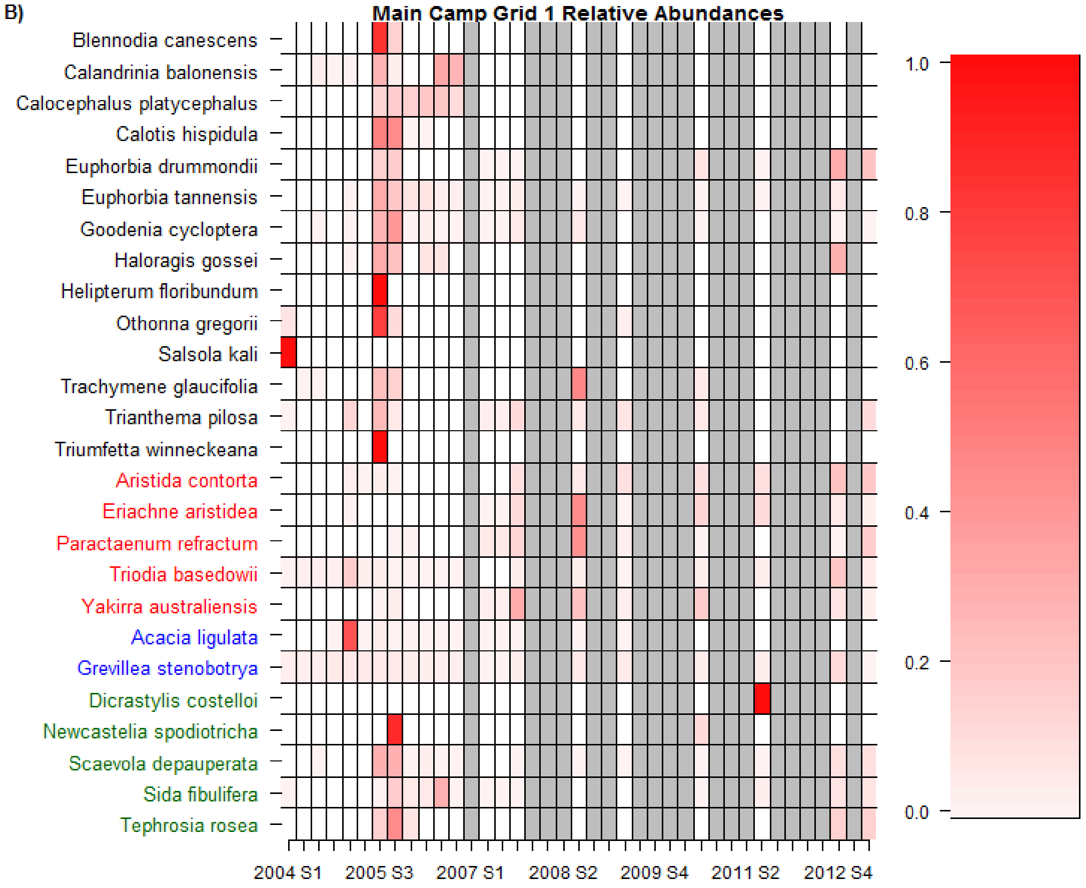
B)
Main Camp Grid 1 Relative Abundances
Blennodia canescens
Calandrinia balonensis
Calocephalus platycephalus
Calotis hispidula
Euphorbia drummondii
Euphorbia tannensis
Goodenia cycloptera
Haloragis gossei
Helipterum floribundum
Othonna gregorii
Salsola kali
Trachymene glaucifolia
Trianthema pilosa
Triumfetta winneckeana
Aristida contorta
Eriachne aristidea
Paractaenum refractum
Triodia basedowii
Yakirra australiensis
Acacia ligulata
Grevillea stenobotrya
Dicrastylis costelloi
Newcastelia spodiotricha
Scaevola depauperata
Sida fibulifera
Tephrosia rosea
2004 S1
2005 S3
2007 S1
2008 S2
2009 S4
2011 S2
2012 S4
1.0
0.8
0.6
0.4
0.2
0.0

Table 5-1. Comparison of model selection criteria for dynamic factor analysis models of temporal trends in plant abundance for each of three sites. Each model included up to five common trends, and for each of these model types, separate models were run with or without rainfall. Best fitting models with the lowest AICc values are highlighted in bold. I note that while the model with five trends and no rainfall covariate was the best fit for Carlo Shitty, state predictions were extremely poor thus the five trend model with rainfall was used instead (see Appendix 4-1 for more details).

		AIC*c* values for each model	
		Inclusion of covariate	
Site	Number of common trends	No Rainfall	Rainfall
Main Camp	1	5421.708	5310.029
	2	5338.202	5252.031
	3	5295.429	5255.762
	4	5229.903	5195.189
	5	**5222.686**	**5125.651**
Field River	1	5820.614	5711.964
	2	5217.596	**5130.007**
	3	5184.068	5154.563
	4	5154.660	5180.860
	5	**5082.698**	5188.875
Carlo Shitty	1	5864.093	5685.216
	2	5424.609	5344.75
	3	5320.715	5327.155
	4	5199.496	5276.44
	5	**5124.69**	**5162.35**

The estimated common trends and standardised rainfall data for all sites are presented in Fig. 5-3. The DFA does not order the common trends by their relative importance (Zuur *et al.*, 2003b). Thus to simplify comparisons, rather than present common trends in the default order provided by DFA, trends were re-arranged to be sequential in time with respect to their maximum value. The first common trend for all sites was characterised by a short-term maximum in abundance in winter 2005, with a dip through 2009-2011 in Main Camp and Carlo Shitty, likely to account for species associated with this trend that did not respond to the heavy rainfall that fell during this period. Since the trends for Field River did not contain rainfall, this decline was not observed. The second trend showed a brief peak in abundance in spring 2005 for all sites, with an additional increase in abundance through 2010-2012 for Main Camp. The third trend for Main Camp and Field River was characterised by a brief peak in abundance in winter 2006, while the third trend for Carlo Shitty showed a steady increase in abundance until autumn 2008 at which point it drops and levels off. Together, the first and second trends for all sites and the third for Main Camp and Field River appeared to reflect behaviour of an opportunistic, ephemeral species albeit appearing at different times. The fourth trend for Main Camp described a sudden increase in abundance from winter 2007 through to spring 2008, followed by a second peak in abundance in winter 2010. In Field River and Carlo Shitty, trend four showed an increase in abundance beginning in winter 2009 reaching a maximum in winter 2010 and dropping off quickly thereafter. This trend suggested a more sustained increase in abundance over the course of at least a year in contrast to the short-lived seasonal increases in abundances of the previous trends. The final trend indicated steady increase in abundance, likely resembling the life history of a perennial species rather than a short-lived annual. These steady increases in abundance begin in winter 2008 for Main Camp and Field River, and autumn 2006 for Carlo Shitty.

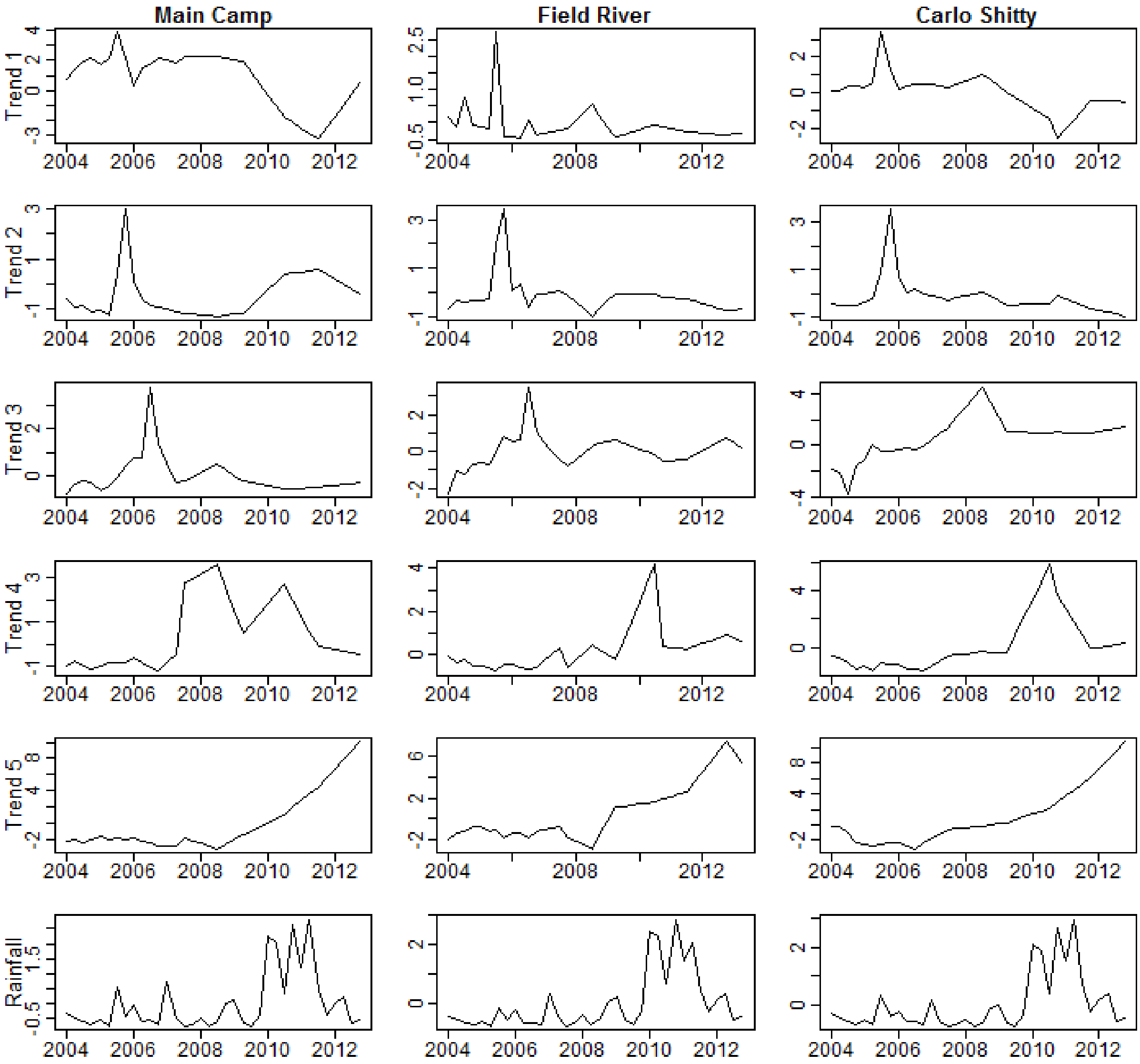

Fig. 5-3. Plots of common trends and rainfall (both standardised) from the best fitting model for Main Camp, Field River and Carlo Shitty. Trends have been re-arranged to be sequential with respect to their maximum value.

Comparison of factor loadings across life forms indicated the forbs were highly associated with the first common trend in most grids for Main Camp, Field River and to a lesser extent Carlo Shitty (Table 5-2). This suggested a collective response by the forbs across sites in winter 2005, likely in response to the relatively minor rainfall event during this time. The grasses, with the exception of the perennial hard spinifex *Triodia basedowii,* showed strong associations with trend four in all grids for each site across a majority of the grids suggesting high levels of synchrony in species responses amongst the grasses. Subshrubs were somewhat synchronous in their response, although the shape and timing of their responses differed by site. In Main Camp, subshrubs were associated with trends one and two, responding in tandem with the forbs in winter and spring of 2005. Subshrubs in Field River were mostly associated with trend four along with the grasses and many forb species, while the responses of subshrubs in Carlo Shitty were diverse, being spread across trends one, two, four and five. Shrubs in general did not appear to have any consistent associations with any of the trends within their life form or across grids, although *Grevillea stenobotrya* was weakly associated with trend five across grids and sites. None of the common trends or their corresponding factor loadings suggested any long term decline for any of the species present.

Table 5-2. Strength of factor loadings as indicated by colour* for the best fitting model for **A)** Main Camp, **B)** Field River and **C)** Carlo Shitty for each species divided by life form. Each trend is sub-divided into four columns to indicate factor loadings for the four grids. Grids affected by the 2001-2002 wildfire appear to the right of the dashed line (Main Camp: grid 4, Field River: grids 3 and 4, Carlo Shitty: grids 2,3 and 4).

A)

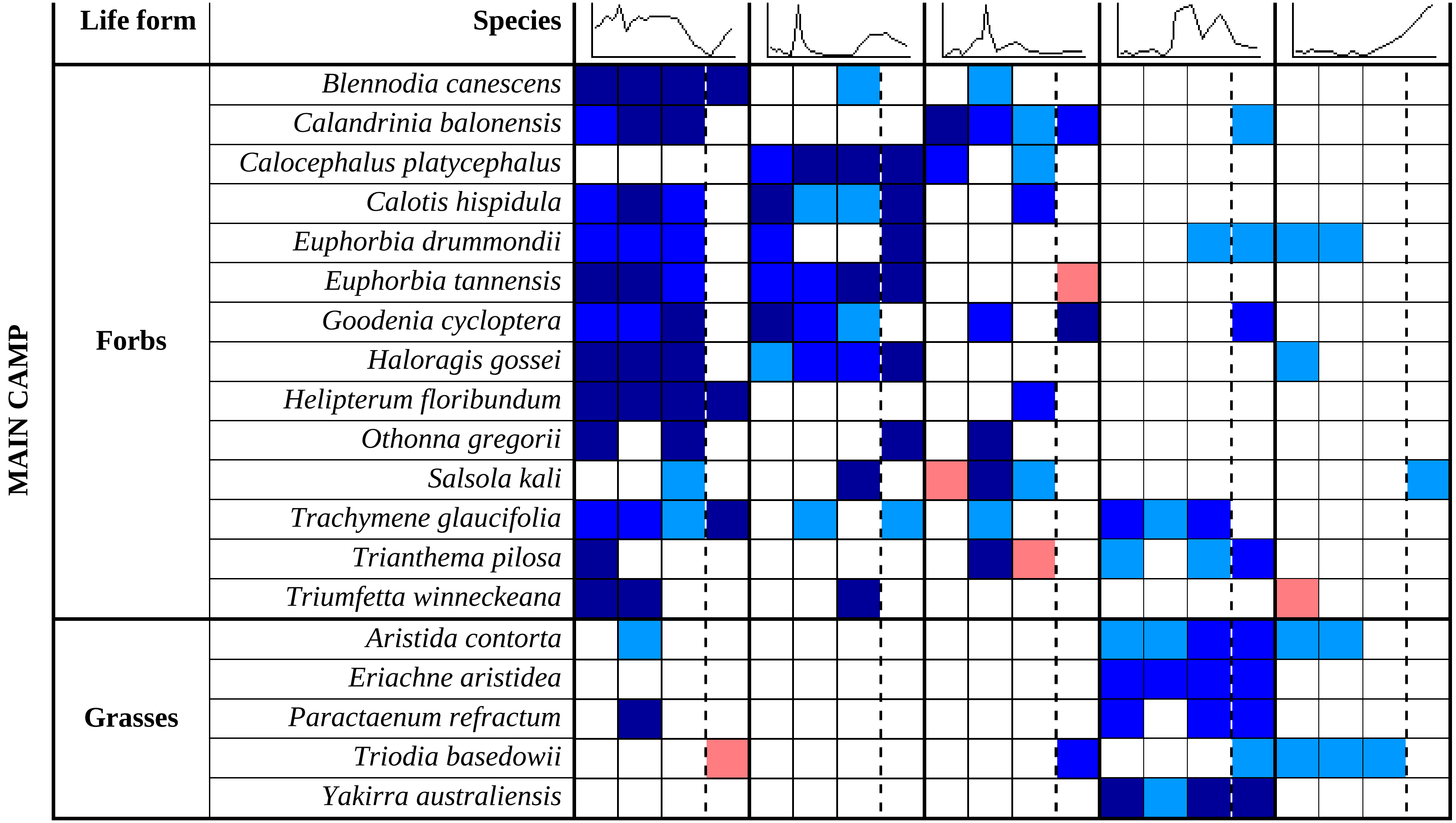

	Life form	Species																				
MAIN CAMP	Forbs	*Blennodia canescens*	▓	▓	▓	▓			░			░										
		Calandrinia balonensis	▒	▓	▓						▓	▒	░	▒				░				
		Calocephalus platycephalus					▒	▓	▓	▓	▒		░									
		Calotis hispidula	▒	▓	▒		▓	░	░	▓			▒									
		Euphorbia drummondii	▒	▒	▒		▒			▓							░	░	░	░		
		Euphorbia tannensis	▓	▓	▒		▒	▒	▓	▓				🟥								
		Goodenia cycloptera	▒	▒	▓		▓	▒	░			▒		▓				▒				
		Haloragis gossei	▓	▓	▓		░	▒	▒	▓									░			
		Helipterum floribundum	▓	▓	▓	▓							▒									
		Othonna gregorii	▓		▓					▓		▓										
		Salsola kali			░				▓		🟥	▓	░									░
		Trachymene glaucifolia	▒	▒	░	▓		░		░		░			▒	░	▒					
		Trianthema pilosa	▓									▓	🟥		░		░	▒				
		Triumfetta winneckeana	▓	▓					▓										🟥			
	Grasses	*Aristida contorta*		░											░	░	▒	▒	░	░		
		Eriachne aristidea													▒	▒	▒	▒				
		Paractaenum refractum		▓											▒		▒	▒				
		Triodia basedowii				🟥								▒				░	░	░	░	
		Yakirra australiensis													▓	░	▓	▓				

Subshrubs	*Dicrastylis costelloi*		▤						▣		▣		▣			▧					
	Newcastelia spodiotricha		■	▣		■	▣	■													
	Scaevola depauperata	■	▣	▣		■	▣	▣					■						▧		
	Sida fibulifera		▣	▣		▣		■	▧	■	■		▣		▧		▣				
	Tephrosia rosea	▧		▤		■						▤			▧						
Shrubs	*Acacia ligulata*															▣					▧
	Grevillia stenobotrya	▧									▧					▧		▧	▧		▧

B)

FIELD RIVER

Life form	**Species**	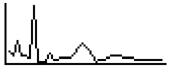				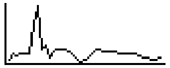								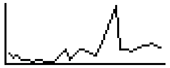				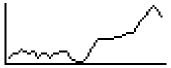			
Forbs	*Brunonia australis*			▤	🟥										▣	■	■				
	Calandrinia balonensis	■	■	■	■					▣	▣		▧								
	Calotis hispidula	■	■	■	■																
	Euphorbia drummondii	▣	▣	■	■									▣	▣						
	Goodenia cycloptera	▣	▣	▣	■					▣	▣	▣	▣	▣	▣	■	▧				
	Halgania cyanea		▧			▤					▣	▧	▧								
	Haloragis gossei		▣	▣	■					▧					▣	■					
	Helipterum muelli		▣	▣	▣																
	Lepidium phlebopetalum	■	▣	■	■																
	Oldenlandia pterospora													■	■	■	■				
	Othonna gregorii	■	■	■	▣					▧	▣	■	■								
	Salsola kali	▧	▧	▤			▧			■	▧	▣	■		■	▧					
	Swainsona microphylla	■	▧	▤						■			▧	▣	▧	▧	■				
	Trachymene glaucifolia	■	■	■	■										▧	▣					
	Trianthema pilosa				■									■	■	■	■				

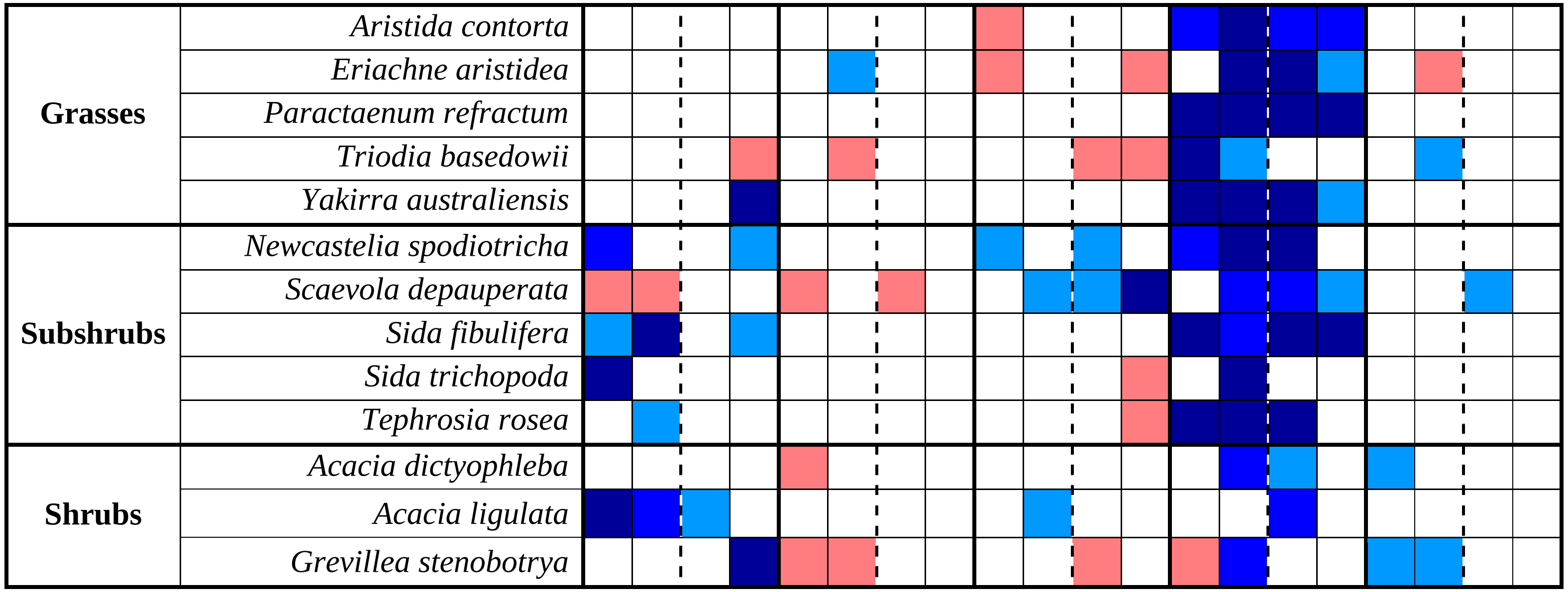
Grasses
Aristida contorta
Eriachne aristidea
Paractaenum refractum
Triodia basedowii
Yakirra australiensis
Subshrubs
Newcastelia spodiotricha
Scaevola depauperata
Sida fibulifera
Sida trichopoda
Tephrosia rosea
Shrubs
Acacia dictyophleba
Acacia ligulata
Grevillea stenobotrya

C)

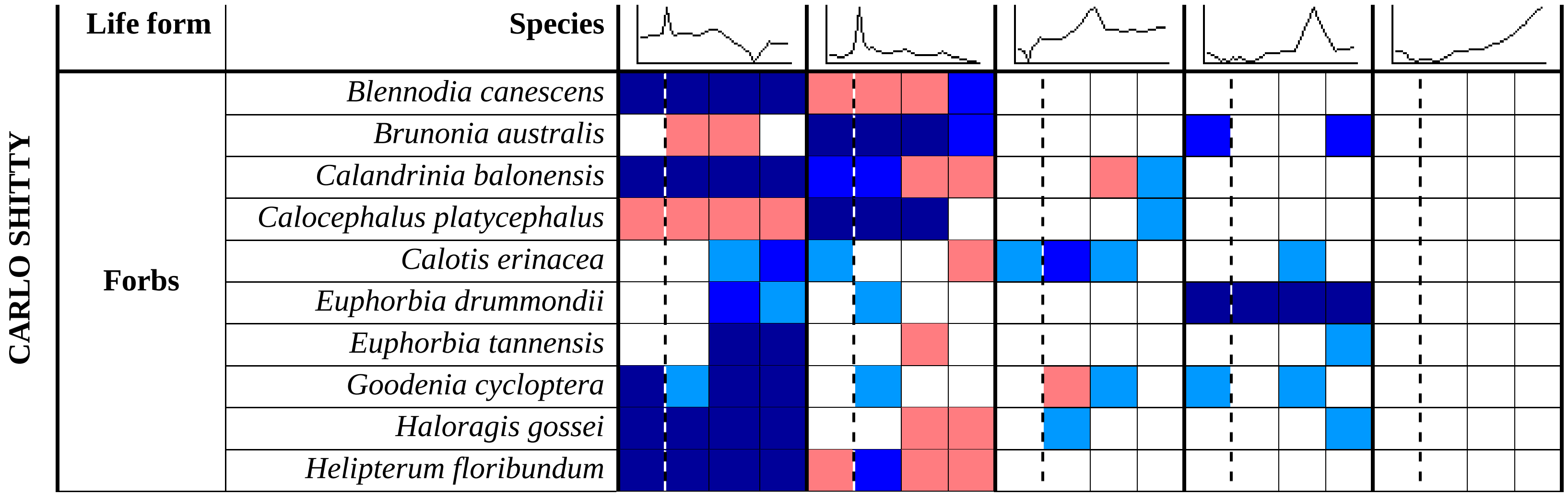
CARLO SHITTY
Life form
Species
Forbs
Blennodia canescens
Brunonia australis
Calandrinia balonensis
Calocephalus platycephalus
Calotis erinacea
Euphorbia drummondii
Euphorbia tannensis
Goodenia cycloptera
Haloragis gossei
Helipterum floribundum

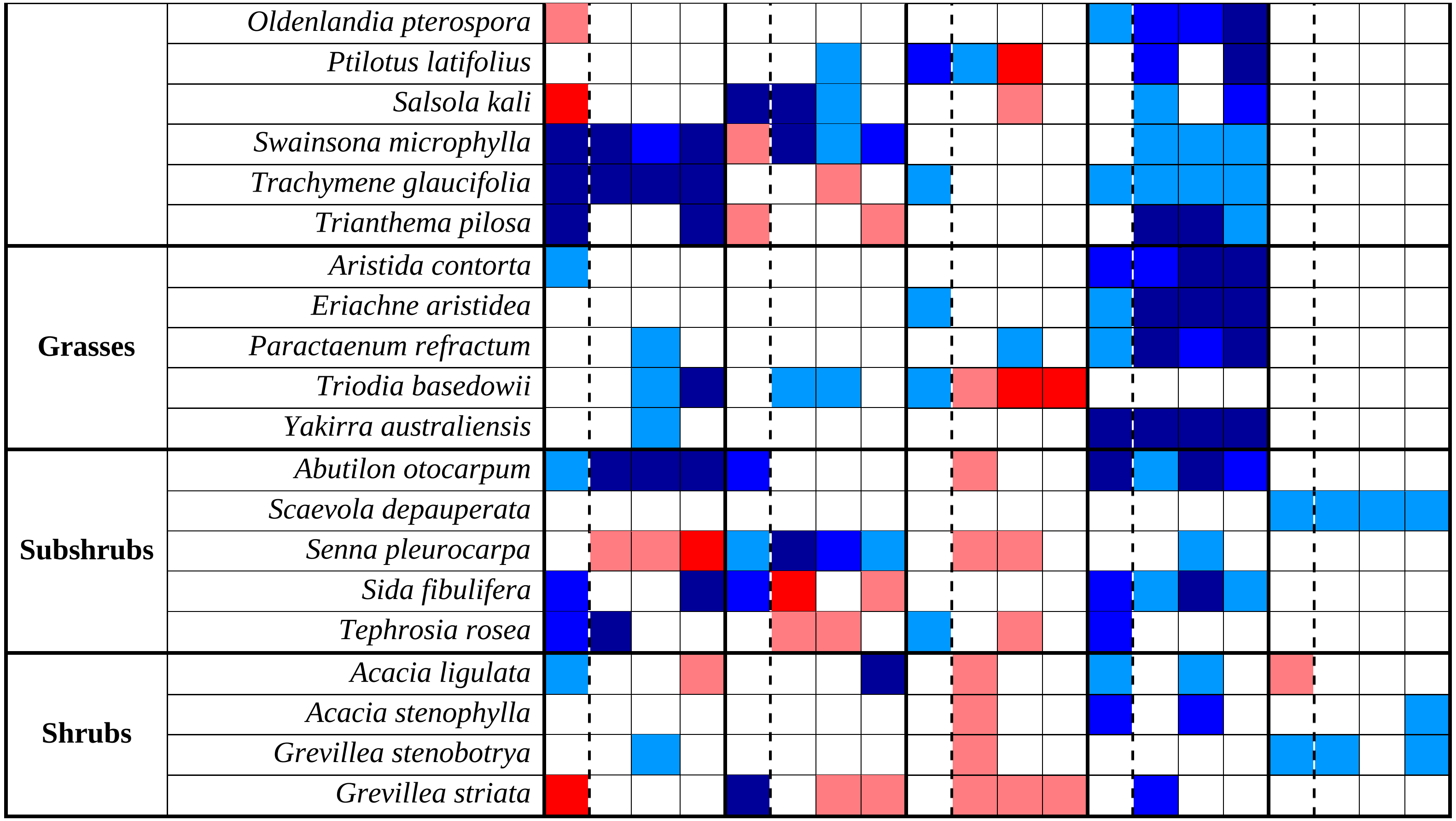

*** Trend key**

Dark blue	Strong positive	$Z > 0.6$
Blue	Moderate positive	$0.4 < Z < 0.6$
Light blue	Weak positive	$0.2 < Z < 0.4$
White	Neutral	$-0.2 < Z < 0.2$
Light red	Weak negative	$-0.4 < Z < -0.2$
Red	Moderate negative	$-0.6 < Z < -0.4$

Examination of state predictions averaged within sites highlighted clear patterns in time series abundance across life forms and reinforced the results of the factor loadings (Table 5-3). State predictions for individual species' generally conformed to that of their life form with some exceptions. For example, the forb species *Brunonia australis, Euphorbia drummondii, Oldenlandia pterospora, Swainsona microphylla* and *Trianthema pilosa* showed trajectories either resembling that of the grasses or a combination of the forbs and grasses. The shrubs (with the exception of *Acacia ligulata*) and the perennial grass *T. basedowii* followed a trajectory resembling persistent growth despite weak factor loadings for trend five. While life form categories exhibited consistent trends within sites, comparisons between sites revealed variable responses, particularly for the subshrubs. For example, the subshrubs at the Main Camp site had multiple peaks in abundance throughout the census period, but peaks appeared only intermittently in Field River and Carlo Shitty. Similarly, the grasses at the Main Camp site increased in abundance much sooner than at the Field River or Carlo Shitty sites, despite similar rainfall patterns across the three sites.

Figure 5-4. Mean state predictions for the best fitting models from 2004-2013 across grids for each species and site. State predictions are calculated as a linear function of their factor loadings multiplied by the corresponding common trends. Since data were standardised prior to model construction, all state predictions are unitless.

Life form	Species	Main Camp	Field River	Carlo Shitty
Forbs	*Blennodia canescens*	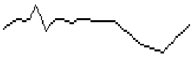		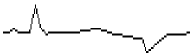
	Brunonia australis			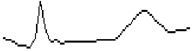
	Calandrinia balonensis			
	Calocephalus platycephalus			
	Calotis erinacea			
	Calotis hispidula	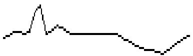		
	Euphorbia drummondii			
	Euphorbia tannensis			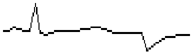
	Goodenia cycloptera			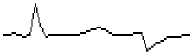
	Halganea cyanea			
	Haloragis gossei	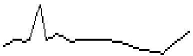		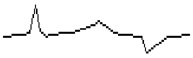
	Helipterum floribundum	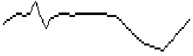		
	Helipterum muelli			
	Lepidium phlebopetalum		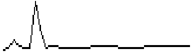	
	Oldenlandia pterospora			
	Othonna gregorii			
	Ptilotus latifolius			
	Salsola kali	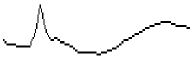		
	Swainsona microphylla		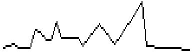	
	Trachymene glaucifolia			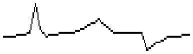
	Trianthema pilosa			
	Triumfetta winneckeana			
Grasses	*Aristida contorta*			
	Eriachne aristidea			
	Paractaenum refractum			
	Triodia basedowii			
	Yakirra australiensis			
Subshrubs	*Abutilon otocarpum*			
	Dicrastylis costelloi			
	Newcastelia spodiotricha			
	Scaevola depauperata			
	Senna pleurocarpa			
	Sida fibulifera			
	Sida trichopoda			
	Tephrosia rosea			

Shrubs	*Acacia dictyophleba* *Acacia ligulata* *Acacia stenophylla* *Grevillea stenobotrya* *Grevillea striata*	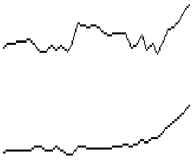	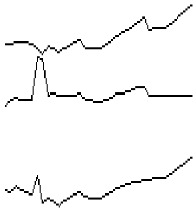	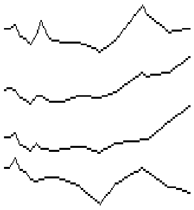

Discussion

In this study, dynamic factor analysis was applied to multivariate time series abundance data to identify possibilities for borrowing strength across species with similar temporal trends. Achieving this would help to improve ecological inferences as the common trends could then be applied to species with scarce data. While many multivariate techniques measure changes in overall community structure (Collins *et al.*, 2000; Wang *et al.*, 2012) or biodiversity metrics (Magurran and Henderson, 2010; Legendre and De Cáceres, 2013; Dornelas *et al.*, 2014), DFA focuses on temporal changes at the species level making it particularly well suited for this task. By linking the temporal dynamics of a large number of species into a small set of common trends, species with similar responses over time are clustered, demonstrating the species and spatial locations, for which borrowing strength across species is possible. Another advantage of DFA is that the common trends provide a neat visualisation of the dynamics for a large number of species that might otherwise by difficult to interpret or analyse if species were studied individually (Zuur *et al.*, 2003a; Zuur *et al.*, 2003b). Finding ways to identify patterns in large multivariate datasets produced by monitoring programs is important. Simple techniques such as graphing the raw data are an informative, albeit an under-used tool for analysing multivariate abundance data (Warton, 2008). Here, combined tabulation of presence-absence information and relative abundance time series plots (Fig. 5-2) revealed important patterns of response and also exposed the loss of information when large gaps are present in the data. Patterns emerged in the timing of pulse events where numerous species were suddenly in abundance producing concurrent peaks indicating similar responses to environmental drivers. While factor loadings are usually presented as a plot with vertical lines indicating the strength of the factor loading (e.g. Zuur and Pierce, 2004; Erzini, 2005), here they are presented as a colour coded gridded table to help identify within site heterogeneity (Table 5-2). This visualisation, combined with plots of the state predictions for each species (Table 5-3), revealed important spatial and temporal patterns across species.

A key result of this study was that life form is a strong predictor of temporal responses across species. Forbs and grasses in particular showed high levels of synchrony in response of rain events, but this was less pronounced for shrubs and subshrubs. Life form can be a crude proxy for functional types, often sharing key functional and life-history traits that affect plant responses to biotic and abiotic factors (Lavorel *et al.*, 1997; Lavorel and Garnier, 2002). Previous research has demonstrated similar responses to shared environmental drivers amongst species within the same life form group (e.g. Pausas and Austin, 2001; Verheyen *et al.*, 2003; Wang *et al.*, 2003; Broennimann *et al.*, 2006), and the results of this study affirm this shared response. This has several implications for management - life form can be viewed as a reasonable criterion for selecting species to borrow strength from to supplement data for poorly sampled species (MacKenzie *et al.*, 2005). However, the unique responses of each life form highlight the need for a diversity of sampling across each life form. Monitoring of arid zones for example is often focused only on perennial or woody vegetation (Watson *et al.*, 2007) and is therefore unlikely to be representative of the full range of responses to environmental drivers. Shorter lived species with rapid life-cycles and high environmental stochasticity may require more frequent sampling and smaller gaps between censuses (Chapter 3), however large woody long-lived species may be sampled less frequently provided the time scales are long enough to capture any changes. The current dataset used in this study was only of moderate length and the relatively small plot sizes meant shrubs were not as well represented (Gregoire and Valentine, 2007). Furthermore, shrubs are not likely to show much change in abundance over time in the absence of major environmental drivers such as wildfires. Despite this setback, DFA was still able to detect a common trend describing these species (Fig 5-3, Trend 5) although factor loadings for shrubs were quite low.

While life form was found to be an important predictor of temporal trends in this study, there are several limitations that need to be considered. Firstly, the temporal and spatial scale across which these shared responses needs to be taken into account. For example, the spatial heterogeneity in species' responses was found to be quite large such that borrowing strength may only be applicable at local spatial scales. This spatial heterogeneity may be driven by a number of factors including soil properties (Peek and Forseth, 2009), distribution of rainfall (Greenville *et al.*, 2012), and wildfire history (Greenville *et al.*, 2009; Peek and Forseth, 2009; Greenville *et al.*, 2012). I had previously shown that for the ephemeral plant *Trachymene glaucifolia*, differences between sites were large enough to require separate trends and parameter estimates (Chapter 3). In contrast, population dynamics for the perennial grass *Triodia basedowii* were driven primarily by fire history rather than study site (e.g. Chapter 4; Nguyen *et al.*, 2015). Indeed, some species appear to show more spatial variation in their dynamics than others. It is therefore plausible that short-lived plants may be more sensitive to differences in resources across space, while long-lived perennials only show substantial differences in dynamics when impacted by sufficiently large disturbances such as wildfire. Furthermore, while species can respond similarly in the short term to major stochastic events such as heavy rainfall and wildfires, population dynamics across species would be less likely to be synchronous over longer temporal scales. This is consistent with the need to account for scale in tracking changes over space or time (Peters and Havstad, 2006; Wardle *et al.*, 2013).

The common trends produced by the DFA models also provided a useful description of the overall study system. The five trends produced in this case study for example suggest no long-term decline over the duration of the census period. The trends also described well-recognised population dynamics characteristic of arid zone ecosystems. Several of the common trends showed brief surges in abundance, indicating pulse events whereby heavy rain and the build-up of seeds in the soil seed bank permitted short-lived plants to quickly dominate the landscape (Ludwig *et al.*, 1997). However, not all species were responding to every pulse event suggesting variation in the timing and ability of species to respond to rainfall events (Nano and Pavey, 2013). The remaining common trends reflect species that responded with more sustained increases in abundance over time likely requiring more continuous rainfall, and or those that experienced gradual increases in abundance, such as the woody shrubs and perennial grass *T. basedowii*.

A more accurate description of the study system, common trends and factor loadings would have been possible had the covariance matrix **R** been modelled as symmetric rather than strictly diagonal (Zuur *et al.*, 2003a). However, the burden of estimating additional parameters, could potentially cause instabilities in the algorithm if the number of time series were too large, and would greatly increase computing time (Zuur *et al.*, 2003a). Such an error structure might also be expected to favour fewer trends during the model selection process as the number of parameter estimates can increase substantially with every additional time series added. Furthermore, to prevent instabilities in the algorithm and facilitate estimation of trends, species with insufficient observations to discern any temporal and spatial dynamics were removed from this analysis (see Appendix 4-1 for full list of species). The appropriateness of borrowing strength based on life form for these insufficiently sampled species may differ based on the type of rarity being displayed. For example, there may be potential to borrow strength species that are locally abundant but not widely distributed, as life form patterns seem to hold at a local scale. On the other hand, if a species is rare because it consistently occurs at low densities even though it is widely distributed (Rabinowitz, 1981), then borrowing strength may be limited as it is not as responsive to environmental drivers. Although beyond the scope of this study, in future work, modelled predictions based on borrowing strength for species with varying patterns of rarity could by tested with new field data by intensifying the surveys to ensure that adequate information is available for each species.

Finally, DFA results would be more informative if the model were extended to include non-normal distributions for the error structure such as Poisson or negative binomial distributions which are more suited to count data (Kéry and Schaub, 2012). However, implementation of these distributions would require extensive modifications to the parameter estimation procedure used in (Zuur *et al.*, 2003b), and to date incorporation of a non-normal error structure has yet to be applied to DFA. While I am confident the results and patterns of the current study are robust, it would be well worth further developing the DFA models and conducting simulations studies on data with known error structures to examine the impact of the normality assumption on trend estimation.

Final thoughts

While the availability of long-term ecological data is on the rise, high quality data continue to be a scarce commodity (Chapter 1; Lindenmayer *et al.*, 2012), thus any opportunities to supplement deficient datasets by sourcing information from multiple sources can be valuable (MacKenzie *et al.*, 2005). Based on the results of the DFA models, it is proposed to managers that life form is a reasonably strong predictor of temporal responses but with the necessary caution that extending inferences across species applies only to local spatial scales. Furthermore, if monitoring programs are able to produce multispecies abundance data, analysis of such data within a multivariate framework will provide several advantages over single species analysis (Dunstan *et al.*, 2013; Hui *et al.*, 2013), and DFA is a useful addition to the numerous multivariate techniques currently available. Currently, DFA has been applied mostly in the context of fisheries and marine biology (e.g. Erzini, 2005; Tulp *et al.*, 2008; Nye *et al.*, 2010; Maurer *et al.*, 2014), however this study has demonstrated this technique to be just as applicable to terrestrial ecological data, particularly those obtained from long-term monitoring programs.

Acknowledgements

I would like to thank Chris Dickman and other members of the Desert Ecology Research Group, especially Bobby Tamayo, Aaron Greenville, David Nelson, Chin-Liang Beh and the many volunteers, for their dedication to collecting the long-term datasets analysed here. Bush Heritage Australia and the land managers of Carlo Station kindly provided access to their properties for the long-term surveys. Research support was provided by the Australian Research Council and the Long Term Ecological Research Network (www.tern.org.au).

References

Andrews, K.S., Williams, G.D., Samhouri, J.F., Marshall, K.N., Gertseva, V. and Levin, P.S. (2014) The legacy of a crowded ocean: indicators, status, and trends of anthropogenic pressures in the California Current ecosystem. *Environmental Conservation,* **42,** 139-151.

Baudron, A.R., Needle, C.L., Rijnsdorp, A.D. and Tara Marshall, C. (2014) Warming temperatures and smaller body sizes: synchronous changes in growth of North Sea fishes. *Global Change Biology,* **20,** 1023-1031.

Broennimann, O., Thuiller, W., Hughes, G., Midgley, G.F., Alkemade, J.M.R. and Guisan, A. (2006) Do geographic distribution, niche property and life form explain plants' vulnerability to global change? *Global Change Biology,* **12,** 1079-1093.

Burnham, K.P. and Anderson, D.R. (2002) *Model selection and multimodel inference.* Springer Science and Business Media, Inc., New York, NY.

Collins, S.L., Micheli, F. and Hartt, L. (2000) A method to determine rates and patterns of variability in ecological communities. *Oikos,* **91,** 285-293.

Coulson, T., Mace, G.M., Hudson, E. and Possingham, H. (2001) The use and abuse of population viability analysis. *Trends in Ecology and Evolution,* **16,** 219-221.

Dickman, C.R., Wardle, G.M., Foulkes, J. and de Preu, N. 2014. Desert complex environments. *In:* Lindenmayer, D., Burns, E., Thurgate, N. & Lowe, A. (eds.) *Biodiversity and environmental change: monitoring, challenges and direction.* Collingwood, Victoria, Australia: CSIRO Publishing.

Dornelas, M., Gotelli, N.J., McGill, B., Shimadzu, H., Moyes, F., Sievers, C. and Magurran, A.E. (2014) Assemblage time series reveal biodiversity change but not systematic loss. *Science,* **344,** 296-299.

Dunstan, P.K., Foster, S.D., Hui, F.K. and Warton, D.I. (2013) Finite mixture of regression modeling for high-dimensional count and biomass data in ecology. *Journal of Agricultural, Biological, and Environmental Statistics,* **18,** 357-375.

Ellner, S.P., Fieberg, J., Ludwig, D. and Wilcox, C. (2002) Precision of population viability analysis. *Conservation Biology,* **16,** 258-261.

Erzini, K. (2005) Trends in NE Atlantic landings (southern Portugal): identifying the relative importance of fisheries and environmental variables. *Fisheries Oceanography,* **14,** 195-209.

Erzini, K., Inejih, C.A.O. and Stobberup, K.A. (2005) An application of two techniques for the analysis of short, multivariate non-stationary time-series of Mauritanian trawl survey data. *ICES Journal of Marine Science: Journal du Conseil,* **62,** 353-359.

Eyre, T.J., Fisher, A., Hunt, L.P. and Kutt, A.S. (2011) Measure it to better manage it: a biodiversity monitoring framework for the Australian rangelands. *The Rangeland Journal,* **33,** 239-253.

Ferrer, E. and Nesselroade, J.R. (2003) Modeling affective processes in dyadic relations via dynamic factor analysis. *Emotion,* **3,** 344.

Frank, A.S.K., Dickman, C.R. and Wardle, G.M. (2012) Habitat use and behaviour of cattle in a heterogeneous desert environment in central Australia. *The Rangeland Journal,* **34,** 319-328.

Greenville, A.C., Dickman, C.R., Wardle, G.M. and Letnic, M. (2009) The fire history of an arid grassland: the influence of antecedent rainfall and ENSO. *International Journal of Wildland Fire,* **18,** 631-639.

Greenville, A.C., Wardle, G.M. and Dickman, C.R. (2012) Extreme climatic events drive mammal irruptions: regression analysis of 100-year trends in desert rainfall and temperature. *Ecology and Evolution,* **2,** 2645-2658.

Gregoire, T.G. and Valentine, H.T. (2007) *Sampling strategies for natural resources and the environment.* CRC Press.

Hasson, C.J. and Heffernan, K.S. (2011) Dynamic factor analysis and the exercise sciences. *Pediatric Exercise Science,* **23,** 17-22.

Hinrichsen, R. and Holmes, E.E. 2009. Using multivariate state-space models to study spatial structure and dynamics. *In:* Cantrell, S., Cosner, C. & Ruan, S. (eds.) *Spatial Ecology.* Boca Raton, FL, USA: CRC/Chapman Hall.

Holmes, E.E., Ward, E.J. and Scheuerell, M.D. (2012a) Analysis of multivariate time-series using the MARSS package. Version 3.4. http://cran.r-project.org/web/packages/MARSS.

Holmes, E.E., Ward, E.J. and Wills, K. (2012b) MARSS: multivariate autoregressive state-space models for analyzing time series data. *R Journal,* **4,** 11-19.

Hui, F.K., Warton, D.I., Foster, S.D. and Dunstan, P.K. (2013) To mix or not to mix: comparing the predictive performance of mixture models vs. separate species distribution models. *Ecology,* **94,** 1913-1919.

Jongejans, E. and de Kroon, H. (2005) Space versus time variation in the population dynamics of three co-occurring perennial herbs. *Journal of Ecology,* **93,** 681-692.

Kéry, M. and Schaub, M. (2012) *Bayesian population analysis using WinBUGS: a hierarchical perspective.* Academic Press.

Lavorel, S. and Garnier, E. (2002) Predicting changes in community composition and ecosystem functioning from plant traits: revisiting the Holy Grail. *Functional Ecology,* **16,** 545-556.

Lavorel, S., McIntyre, S., Landsberg, J. and Forbes, T.D.A. (1997) Plant functional classifications: from general groups to specific groups based on response to disturbance. *Trends in Ecology and Evolution,* **12,** 474-478.

Legendre, P. and De Cáceres, M. (2013) Beta diversity as the variance of community data: dissimilarity coefficients and partitioning. *Ecology Letters,* **16,** 951-963.

Liebhold, A., Koenig, W.D. and Bjørnstad, O.N. (2004) Spatial synchrony in population dynamics. *Annual Review of Ecology, Evolution, and Systematics,* **35,** 467-490.

Lindenmayer, D.B., Likens, G.E., Andersen, A., Bowman, D., Bull, C.M., Burns, E., Dickman, C.R., Hoffmann, A.A., Keith, D.A., Liddell, M.J., Lowe, A.J., Metcalfe, D.J., Phinn, S.R., Russell-Smith, J., Thurgate, N. and Wardle, G.M. (2012) Value of long-term ecological studies. *Austral Ecology,* **37,** 745-757.

Lovett, G.M., Burns, D.A., Driscoll, C.T., Jenkins, J.C., Mitchell, M.J., Rustad, L., Shanley, J.B., Likens, G.E. and Haeuber, R. (2007) Who needs environmental monitoring? *Frontiers in Ecology and the Environment,* **5,** 253-260.

Ludwig, J., Tongway, D., Freudenberger, D., Noble, J. and Hodgkinson, K. (1997) *Landscape ecology function and management: principles from Australia's rangelands.* CSIRO, Canberra.

MacKenzie, D.I., Nichols, J.D., Sutton, N., Kawanishi, K. and Bailey, L.L. (2005) Improving inferences in population studies of rare species that are detected imperfectly. *Ecology,* **86,** 1101-1113.

Magurran, A.E. and Henderson, P.A. (2010) Temporal turnover and the maintenance of diversity in ecological assemblages. *Philosophical Transactions of the Royal Society B: Biological Sciences,* **365,** 3611-3620.

Maurer, B.A., Bence, J.R. and Brenden, T.O. (2014) *Assessing dynamics of Lake Huron fish communities using dynamic factor analysis* (QFC Technical Report No. T2014-01). Quantitative Fisheries Center, Michigan State University, East Lansing, MI.

McCune, B., Grace, J.B. and Urban, D.L. (2002) *Analysis of ecological communities.* MjM software design Gleneden Beach, OR.

McGarigal, K., Landguth, E. and Stafford, S. (2013) *Multivariate statistics for wildlife and ecology research.* Springer Science and Business Media.

Molenaar, P.M. (1985) A dynamic factor model for the analysis of multivariate time series. *Psychometrika,* **50,** 181-202.

Muñoz-Carpena, R., Ritter, A. and Li, Y. (2005) Dynamic factor analysis of groundwater quality trends in an agricultural area adjacent to Everglades National Park. *Journal of Contaminant Hydrology,* **80,** 49-70.

Nano, C.E. and Pavey, C.R. (2013) Refining the 'pulse-reserve'model for arid central Australia: seasonal rainfall, soil moisture and plant productivity in sand ridge and stony plain habitats of the Simpson Desert. *Austral Ecology,* **38,** 741-753.

Nguyen, V., Greenville, A.C., Dickman, C.R. and Wardle, G.M. (2015) On the validity of visual cover estimates for time series analyses: a case study of hummock grasslands. *Plant Ecology,* **216,** 975-988.

Nichols, J.D. and Williams, B.K. (2006) Monitoring for conservation. *Trends in Ecology and Evolution,* **21,** 668-673.

Nye, J.A., Bundy, A., Shackell, N., Friedland, K.D. and Link, J.S. (2010) Coherent trends in contiguous survey time-series of major ecological and commercial fish species in the Gulf of Maine ecosystem. *ICES Journal of Marine Science,* **67,** 26-40.

Pausas, J.G. and Austin, M.P. (2001) Patterns of plant species richness in relation to different environments: an appraisal. *Journal of Vegetation Science,* **12,** 153-166.

Peek, M.S. and Forseth, I.N. (2009) Positive effects of soil nitrogen pulses on individuals can have negative consequences for population growth during drought in a herbaceous desert perennial. *Journal of Ecology,* **97,** 440-449.

Peters, D.P.C. and Havstad, K.M. (2006) Nonlinear dynamics in arid and semi-arid systems: interactions among drivers and processes across scales. *Journal of Arid Environments,* **65,** 196-206.

Rabinowitz, D. 1981. Seven forms of rarity. *In:* Synge, H. (ed.) *The biological aspects of rare plant conservation.* New York: Wiley.

Stock, J.H. and Watson, M.W. (2012) *Disentangling the channels of the 2007-2009 recession*. National Bureau of Economic Research.

Thompson, W. (2004) *Sampling rare or elusive species: concepts, designs, and techniques for estimating population parameters.* Island Press.

Thorson, J.T., Scheuerell, M.D., Shelton, A.O., See, K.E., Skaug, H.J. and Kristensen, K. (2015) Spatial factor analysis: a new tool for estimating joint species distributions and correlations in species range. *Methods in Ecology and Evolution*, **6**, 627-637.

Tischler, M., Dickman, C.R. and Wardle, G.M. (2013) Avian functional group responses to rainfall across four vegetation types in the Simpson Desert, central Australia. *Austral Ecology,* **38,** 809-819.

Tulp, I., Bolle, L.J. and Rijnsdorp, A.D. (2008) Signals from the shallows: in search of common patterns in long-term trends in Dutch estuarine and coastal fish. *Journal of Sea Research,* **60,** 54-73.

Verheyen, K., Honnay, O., Motzkin, G., Hermy, M. and Foster, D.R. (2003) Response of forest plant species to land-use change: a life-history trait-based approach. *Journal of Ecology,* **91,** 563-577.

Wang, G., Zhou, G., Yang, L. and Li, Z. (2003) Distribution, species diversity and life-form spectra of plant communities along an altitudinal gradient in the northern slopes of Qilianshan Mountains, Gansu, China. *Plant Ecology,* **165,** 169-181.

Wang, Y., Naumann, U., Wright, S.T. and Warton, D.I. (2012) mvabund– an R package for model-based analysis of multivariate abundance data. *Methods in Ecology and Evolution,* **3,** 471-474.

Ward, E.J., Chirakkahl, H., González-Suárez, M., Aurioles-Gamboa, D., Holmes, E.E. and Gerber, L. (2010) Inferring spatial structure from time-series data: using multivariate state-space models to detect metapopulation structure of California sea lions in the Gulf of California, Mexico. *Journal of Applied Ecology,* **47,** 47-56.

Wardle, G.M., Greenville, A.C., Frank, A.S.K., Tischler, M.K., Emery, N.J. and Dickman, C.R. (2015) Ecosystem risk assessment of Georgina gidgee woodlands in central Australia (Qld, NT, SA). *Austral Ecology in press*.

Wardle, G.M., Pavey, C.R. and Dickman, C.R. (2013) Greening of arid Australia: new insights from extreme years. *Austral Ecology,* **38,** 731-740.

Warton, D.I. (2008) Raw data graphing: an informative but under-utilized tool for the analysis of multivariate abundances. *Austral Ecology,* **33,** 290-300.

Warton, D.I. and Wardle, G.M. (2003) Site-to-site variation in the demography of a fire-affected perennial, Acacia suaveolens, at Ku-ring-gai Chase National Park, New South Wales, Australia. *Austral Ecology,* **28,** 38-47.

Watson, I.W., Thomas, P.W.E. and Fletcher, W.J. (2007) The first assessment, using a rangeland monitoring system, of change in shrub and tree populations across the arid shrublands of Western Australia. *The Rangeland Journal,* **29,** 25-37.

Wright, B.R. and Clarke, P.J. (2009) Fire, aridity and seed banks. What does seed bank composition reveal about community processes in fire-prone desert? *Journal of Vegetation Science,* **20,** 663-674.

Zuur, A. and Pierce, G. (2004) Common trends in northeast Atlantic squid time series. *Journal of Sea Research,* **52,** 57-72.

Zuur, A., Tuck, I. and Bailey, N. (2003a) Dynamic factor analysis to estimate common trends in fisheries time series. *Canadian journal of fisheries and aquatic sciences,* **60,** 542-552.

Zuur, A.F., Fryer, R., Jolliffe, I., Dekker, R. and Beukema, J. (2003b) Estimating common trends in multivariate time series using dynamic factor analysis. *Environmetrics,* **14,** 665-685.

THIS PAGE IS INTENTIONALLY LEFT BLANK

Chapter 6 - Summary and conclusions

Raw data measurements, while containing many uncertainties, form the backbone of ecological research. Photograph by Glenda Wardle.

Overview

"It is in the admission of ignorance and the admission of uncertainty that there is hope for the continuous motion of human beings in some direction that doesn't get confined, permanently blocked, as it has so many times before in various periods in the history of man"

Richard Feynman, 1999

Uncertainty is a pervasive concept; complete certainty can be an illusion, potentially more damaging and misleading than recognising that every data set, conclusion or inference will exhibit some uncertainty (Tukey, 1969). Importantly, uncertainty can be measured and by doing so, the current state of knowledge is clearer and new directions for progress illuminated. In chapter 1, I introduced a table (Table 1-1) producing four broad categories describing different levels of uncertainty (knowledge, gaps, opportunities, and uncertainty and risk) along two axes. The first axis described the level of information available (known or unknown) and the second axis categorised the awareness of the need or availability of such information, also known or unknown. The most interesting category, arguably, is the one referred to as "opportunities", in which a simple shift in awareness from unknown to known can produce the most knowledge for the least amount of effort. Indeed, successful companies are those that are well prepared to deal with future uncertainties by investing in preparation and innovation, and viewing uncertainty as an opportunity to gain an advantage over their competitors (von Oetinger, 2004). Reducing uncertainty is a noble goal, however successfully addressing ecological uncertainty also requires that we acknowledge it cannot be eliminated entirely. By embracing this simple reality we will be more prepared for managing uncertainties and thus avoid drawing inappropriate conclusions. On the practical side moving towards methodologies that incorporate measures of uncertainty directly will help guide directions for profitable future research and inspire new data collection protocols.

The research outlined in this thesis was designed around a framework of structured population models and multi-species models to illustrate these points. A number of sources of uncertainty have been explored using a series of case studies to demonstrate the impact of common sources of uncertainties, in detecting individuals, measuring observations, or identifying the underlying causal processes for differences from place-to-place or over time. To bring this all together, Table 6-1 summarises the links between the ideas and how they are addressed in each of the thesis chapters. I compare the areas of uncertainty covered, the type of data in the case study, the analytical techniques used and the key findings. Following that, I discuss the key findings of this thesis in relation to the key areas of uncertainty, any limitations in what can be inferred from the current analyses and how that highlights areas for future research.

Table 6-1. Summary of the sources of uncertainty addressed in this thesis and the key findings

Chapter	Areas of uncertainty	Case study	Techniques used	Key findings
2	Demographic parameters Cryptic life stages	Addition of seed bank for 12 species and removal for 6 species	Monte Carlo simulations External literature	Quantification of uncertainty in demographic models resulting from exclusion of seed bank stage
3	Cryptic life stages Observation error Missing values	Ephemeral plant and seed bank across four sites	Multivariate state-space modelling	Contrasting patterns in error terms between seed bank and plants
4	Observation error Visual cover estimates	Two long term monitoring datasets covering nine sites	Multivariate state-space modelling	Justified validity of visual cover estimates
5	Monitoring trade-offs	Plant communities of up to 30 species in three sites	Dynamic factor analysis	Species responses strongly associated with life form but not over space

Key findings

A key message of this thesis is that it confirms the importance of acknowledging and incorporating uncertainty into our modelling, statistical design and data collection procedures. Before data collection can even begin, one must make a careful evaluation of the potential sources of uncertainty and plan strategically to either reduce these errors or assess how they can be accounted for. It is of some concern that many authors (approximately 47%; Appendix 1-1) had not even considered the possibility of a seed bank stage despite it being an important life history strategy in stochastic environments (Chapter 2; Evans *et al.*, 2007; Venable, 2007). It is contingent on researchers to be aware of the full life cycle of their study organisms, and whether cryptic life stages, such as a seed bank or vegetative dormancy, are likely to exist. Once the life cycle has been established, it is then up to the researcher to determine how they wish to address potentially cryptic life stages and uncertainty in their demographic parameters. Using a combination of the pre-existing literature and computer simulations can be a cost-effective method to reduce and quantify uncertainty in demographic output, particularly if obtaining field estimates is unfeasible, and in some cases justify the exclusion of the seed bank altogether (Chapter 2; Fig 2-5; Garcia *et al.*, 2010). Field estimates of vital rates and abundance will always be preferable, however, as literature estimates from germination experiments may not necessarily reflect those in the field (Torang *et al.*, 2010; Gross and Mackay, 2014). Indeed, obtaining information on the seed bank or other cryptic life stages, even if this information is crude, may also help inform and reduce uncertainty of estimates for other life stages and the overall population (Chapter 3).

Researchers allocating resources in monitoring programs may wish to consider the sources and likely sizes of observation and process errors, relative to each other and across sites, as these are influenced by a number of factors that can be predetermined such as life history (long or short-lived, abundant or rare), level of vegetation cover (high or sparse) and biodiversity (many species or single dominate species; Chapters 3 and 4). Some data such as visual cover estimates will be more susceptible to errors and uncertainty (Helm and Mead, 2004), emphasising the need to account for such errors prior to, or during, analysis (Wintle *et al.*, 2013). Importantly, if statistical models are able to incorporate and quantify observation errors, even datasets with substantial observation errors such as those obtained via visual estimation methods can still produce conclusive and meaningful trends (Chapter 4). Adopting a hierarchical modelling framework when analysing ecological data is therefore highly beneficial, as this explicitly separates the observation and the true ecological processes (Chapter 3; Kéry and Schaub, 2012). Parameter estimation for observation and process errors can also be drastically improved through taking replicated samples, particularly when temporal coverage is limited (Chapters 3 and 4; Dennis *et al.*, 2010). Once these errors are quantified, this knowledge can be further applied to develop better strategies and prioritisation for data collection, for example if it is discovered that a population or study site is more susceptible to observation error whilst having little intrinsic variation (Chapter 3). In such cases, it may be strategic to allow for missing values by omitting surveys and instead focus on obtaining more accurate measurements to reduce observation errors, or expand sampling to more sites.

Throughout the thesis, I also highlighted the advantages of modelling times series abundance data within a multivariate framework such that both spatial data, and data across species, are modelled in a joint manner to extract all relevant information and exploit any similarities in dynamics that may exist (Dunstan *et al.*, 2013; Hui *et al.*, 2013). This is particularly important where data are scarce or limited, as information from other sites or species can provide valuable opportunities for borrowing strength to improve ecological inferences (MacKenzie *et al.*, 2005). If population dynamics and trends in abundance between study sites are similar and act in synchrony in response to a shared environmental driver, data across multiple sites can be aggregated and fewer trends and parameters will need to be estimated (MacKenzie *et al.*, 2005; Ward *et al.*, 2010). Using a novel statistical technique, multivariate auto-regressive state-space (MARSS) modelling (Holmes *et al.*, 2012a; Holmes *et al.*, 2012b), I was able to assess the spatial structure for select species whilst simultaneously accounting for missing values and observation error. The results from these models suggested that the trends in abundance for the short lived ephemeral herb *Trachymene glaucifolia* were site-specific (Chapter 3) while for the perennial grass *Triodia basedowii* population dynamics were driven primarily by time-since-last fire, regardless of study site (Chapter 4). Another useful multivariate time series technique, dynamic factor analysis (Zuur *et al.*, 2003a; Zuur *et al.*, 2003b), was able to further explore these spatial and temporal trends but for multiple species simultaneously. By taking a more holistic, multispecies approach, I found some species to show more spatial variation in their dynamics than others. Short-lived plants for example may be more sensitive to geographical differences while populations of long-lived perennials may only show substantial differences in dynamics when impacted by sufficiently large disturbances such as wildfire (Chapter 5). Thus, for short-lived species in particular, quantifying the level of spatial heterogeneity is crucial in order to justify aggregating data across sites.

Another key result produced by DFA was the identification of life form as a powerful predictor of temporal responses across species (Chapter 5). While this is not entirely new, given the long tradition of using life form in plant ecology, the division of species by life form group such as forbs, grasses and shrubs, can be particularly useful as they often share ecological properties and therefore have similar responses to shared responses over time (Pausas and Austin, 2001; Verheyen *et al.*, 2003; Wang *et al.*, 2003; Broennimann *et al.*, 2006). This thesis provides some justification for these shared temporal responses within life form groups to borrow strength across species where data is scarce. Thus, just as information from multiple life stages (Chapters 2 and 3), sites (Chapters 3 and 4) or datasets (Chapter 4) can improve inferences for a species of interest, so too, aggregated information from multiple species can inform the dynamics across species (Chapter 5).

Limitations and future research

It is crucial to consider the entire life cycle of a study species to provide more accurate estimates of population abundance, viability and invasibility. This thesis focused specifically on the seed bank (Chapters 2 and 3), although there exists many other examples of cryptic life stages for both plants and animals that are likewise neglected during data collection. Dormancy can also be found in adult plants, in which individuals do not sprout above ground for one or more growing seasons (Shefferson, 2009). Similarly, some animal species undergo periods of dormancy, performing a similar function to that of the seed bank (Geiser, 2004). Capturing the entire life cycle for animal species can be additionally problematic as certain individuals may occupy inaccessible locations, or be absent from sampling designs. Monitoring of raptor populations for example failed to take into account the non-breeding component of the population resulting in severely underestimated population sizes (Katzner *et al.*, 2011). A systematic approach towards investigating the prevalence and impact of models that exclude other cryptic life stages is difficult given the diversity of life forms and life history strategies that potentially involve individuals that are difficult to detect. While there is a breadth of resources available to investigate dormancy and germination rates in relation to the seed bank (e.g. Baskin and Baskin, 1998), this may not be the case for other cryptic life stages. However, the upcoming release of the COMADRE Animal Matrix Database (Salguero-Gómez *et al.*, in prep.) may provide a useful starting point for future research into this area. In the absence of direct observations of cryptic life stages, multistate occupancy models and the recently developed hidden Markov models are able to use time series of presence-absence data to infer the presence or absence of a species below ground, or indeed any unobservable or cryptic stage class (MacKenzie *et al.*, 2009; Fréville *et al.*, 2013). These techniques are promising in their application however their prevalence in modelling cryptic life stages using real data is as yet quite limited (but see Lamy *et al.*, 2013).

The MARSS framework is quite powerful for modelling multivariate time series data and accounting for observation error, although the models can be data intensive given the difficulty in partitioning observation and process variance (Dennis *et al.*, 2010; Holmes *et al.*, 2012b; Appendix 3). Estimating both observation and process error becomes increasingly problematic in general when sampling intervals are uneven or there are missing values in the data, as this restricts the usage of more simpler and perhaps less data intensive modelling techniques and necessarily complicates parameter estimation (Dennis *et al.*, 2010; Dennis and Ponciano, 2014). The state-space model based on the Ornstein-Uhlenbeck process (OUSS), a continuous time model of a stochastic process at equilibrium, provides a simple alternative using maximum likelihood methods that still accounts for uneven intervals, process and observation errors, and the option to include density dependence (Dennis and Ponciano, 2014). This method is less data intensive than the MARSS framework, but there is the additional restriction having no zeroes in the time series which is quite rare in ecological count data (Damgaard, 2009).

Implementation of the MARSS models within R (R 2.15.3; The R foundation for Statistical Computing 2004-2008) via the *MARSS* package (Holmes *et al.*, 2012a; Holmes *et al.*, 2012b) assume the error structure for the observations come from multivariate normal distributions, however an overdispersed Poisson or negative binomial distribution may be more appropriate for count data (Link and Sauer, 2002; Kéry and Schaub, 2012). Implementing the state-space models within a Bayesian framework which makes use of Markov chain Monte Carlo (MCMC) simulations (e.g. Clark and Bjørnstad, 2004; Chaloupka and Balazs, 2007; Lele *et al.*, 2007; Shelton *et al.*, 2013) provides more flexibility and can accommodate complex model structures when parameters come from non-normal distributions. In this thesis, the overdispersed Poisson and negative binomial distributions produced poor model fits compared to the multivariate normal (Chapter 3; Appendix 3-2). Furthermore, while constructing MARSS models via MCMC algorithms can accommodate non-normal error structures (compared to the Kalman-Filter/Expectation Maximisation algorithms used in the *MARSS* package), the results of this thesis did not suggest any reason to favour one algorithm over the other (Chapter 3). However, there were some discrepancies in the results worth taking note of, and although a formal comparison between these two methods was beyond the scope of this thesis, this may be an interesting avenue for future research. One advantage of using the *MARSS* package is its ease of implementation, whereas MCMC calculations are more computationally demanding and requires considerable expertise in statistical theory and programming (Dennis and Ponciano, 2014) involving third party software such as JAGS or WINBUGS, and can become particularly complicated when dealing with large multivariate time series with alternative spatial hypotheses and error structures. Ideally, multivariate time series techniques that account for missing values and observation errors should be accessible for the layman ecologist (*MARSS* package and OUSS), but flexible enough to incorporate data from non-normal distributions (MCMC algorithms). As the availability of high quality long-term time series data become more prominent, it is expected data requirements will become less of an issue, opening up the possibility of the MARSS framework to be used more prominently in the terrestrial ecological literature.

The incorporation of alternative error structures also presents an interesting challenge when conducting DFA. To date, implementation of non-normal error structures has yet to be applied to DFA, but would require substantial modifications to the parameter estimation procedure currently employed (Zuur *et al.*, 2003b). As before, an overdispersed Poisson or negative binomial distributions may yield more accurate results, and a simulation study investigating data with known error structures to examine the impact of assuming normality can be an important and fruitful area for future research.

Concluding remarks

Ecological research has experienced an enormous surge in the availability, quantity and quality of data (Chapter 1). The push towards open-access data and establishment of international long-term research programs will provide exciting opportunities for ecological research in the years to come (Kim, 2006; Whitlock, 2011). Regardless, the one constant that remains in this new age of data is the presence of uncertainty. Throughout this thesis, I have attempted to link together several key aspects of uncertainty affecting ecological data and demonstrate how these uncertainties can be managed and used advantageously to guide inferences and future data collection protocols. It is imperative that we not only acknowledge and accept uncertainty, but that we learn from it. Thus, rather than view uncertainty in a negative light, I stress that there is much opportunity and knowledge to be gained in addressing this uncertainty.

Acknowledgements

Research funds were provided by the Australian Research Council, an Australian Postgraduate Award, and the Terrestrial Ecological Research Network (www.tern.org.au)

References

Baskin, C.C. and Baskin, G.M. (1998) *Seeds: Ecology, biogeography, and evolution of dormancy and germination.* Academic Press, San Diego, California.

Broennimann, O., Thuiller, W., Hughes, G., Midgley, G.F., Alkemade, J.M.R. and Guisan, A. (2006) Do geographic distribution, niche property and life form explain plants' vulnerability to global change? *Global Change Biology,* **12,** 1079-1093.

Chaloupka, M. and Balazs, G. (2007) Using Bayesian state-space modelling to assess the recovery and harvest potential of the Hawaiian green sea turtle stock. *Ecological Modelling,* **205,** 93-109.

Clark, J.S. and Bjørnstad, O.N. (2004) Population time series: process variability, observation errors, missing values, lags, and hidden states. *Ecology,* **85,** 3140-3150.

Damgaard, C. (2009) On the distribution of plant abundance data. *Ecological Informatics,* **4,** 76-82.

Dennis, B. and Ponciano, J.M. (2014) Density dependent state-space model for population abundance data with unequal time intervals. *Ecology*.

Dennis, B., Ponciano, J.M. and Taper, M.L. (2010) Replicated sampling increases efficiency in monitoring biological populations. *Ecology,* **91,** 610-620.

Dunstan, P.K., Foster, S.D., Hui, F.K. and Warton, D.I. (2013) Finite mixture of regression modeling for high-dimensional count and biomass data in ecology. *Journal of Agricultural, Biological, and Environmental Statistics,* **18,** 357-375.

Evans, M.E.K., Ferriere, R., Kane, M.J. and Venable, D.L. (2007) Bet hedging via seed banking in desert evening primroses (*Oenothera*, Onagraceae): demographic evidence from natural populations. *American Naturalist*, **169,** 184-194.

Feynman, R.P. (1998) *The meaning of it all: thoughts of a citizen scientist.* Da Capo Press.

Fréville, H., Choquet, R., Pradel, R. and Cheptou, P.-O. (2013) Inferring seed bank from hidden Markov models: new insights into metapopulation dynamics in plants. *Journal of Ecology,* **101,** 1572-1580.

Garcia, M.B., Goni, D. and Guzman, D. (2010) Living at the edge: local versus positional factors in the long-term population dynamics of an endangered orchid. *Conservation Biology,* **24,** 1219-1229.

Geiser, F. (2004) Metabolic rate and body temperature reduction during hibernation and daily torpor. *Annual Review of Physiology,* **66,** 239-274.

Gross, C. and Mackay, D. (2014) Two decades of demography reveals that seed and seedling transitions limit population persistence in a translocated shrub. *Annals of Botany*.

Helm, D.J. and Mead, B.R. (2004) Reproducibility of vegetation cover estimates in South-Central Alaska Forests. *Journal of Vegetation Science,* **15,** 33-40.

Holmes, E.E., Ward, E.J. and Scheuerell, M.D. (2012a) Analysis of multivariate time-series using the MARSS package. Version 3.4. http://cran.r-project.org/web/packages/MARSS.

Holmes, E.E., Ward, E.J. and Wills, K. (2012b) MARSS: multivariate autoregressive state-space models for analyzing time series data. *R Journal,* **4,** 11-19.

Hui, F.K., Warton, D.I., Foster, S.D. and Dunstan, P.K. (2013) To mix or not to mix: comparing the predictive performance of mixture models vs. separate species distribution models. *Ecology,* **94,** 1913-1919.

Katzner, T.E., Ivy, J.A.R., Bragin, E.A., Milner-Gulland, E. and DeWoody, J.A. (2011) Conservation implications of inaccurate estimation of cryptic population size. *Animal Conservation,* **14,** 328-332.

Kéry, M. and Schaub, M. (2012) *Bayesian population analysis using WinBUGS: a hierarchical perspective.* Academic Press.

Kim, E.-S. (2006) Development, potentials, and challenges of the International Long-Term Ecological Research (ILTER) Network. *Ecological Research,* **21,** 788-793.

Lamy, T., Gimenez, O., Pointier, J.P., Jarne, P. and David, P. (2013) Metapopulation dynamics of species with cryptic life stages. *The American Naturalist,* **181,** 479-491.

Lele, S.R., Dennis, B. and Lutscher, F. (2007) Data cloning: easy maximum likelihood estimation for complex ecological models using Bayesian Markov chain Monte Carlo methods. *Ecology Letters,* **10,** 551-563.

Link, W.A. and Sauer, J.R. (2002) A hierarchical analysis of population change with application to Cerulean Warblers. *Ecology,* **83,** 2832-2840.

MacKenzie, D.I., Nichols, J.D., Seamans, M.E. and Gutiérrez, R. (2009) Modeling species occurrence dynamics with multiple states and imperfect detection. *Ecology,* **90,** 823-835.

MacKenzie, D.I., Nichols, J.D., Sutton, N., Kawanishi, K. and Bailey, L.L. (2005) Improving inferences in population studies of rare species that are detected imperfectly. *Ecology,* **86,** 1101-1113.

Pausas, J.G. and Austin, M.P. (2001) Patterns of plant species richness in relation to different environments: an appraisal. *Journal of Vegetation Science,* **12,** 153-166.

Shefferson, R.P. (2009) The evolutionary ecology of vegetative dormancy in mature herbaceous perennial plants. *Journal of Ecology,* **97,** 1000-1009.

Shelton, A.O., Satterthwaite, W.H., Beakes, M.P., Munch, S.B., Sogard, S.M. and Mangel, M. (2013) Separating intrinsic and environmental contributions to growth and their population consequences. *The American Naturalist,* **181,** 799-814.

Torang, P., Ehrlen, J. and Agren, J. (2010) Linking environmental and demographic data to predict future population viability of a perennial herb. *Oecologia,* **163,** 99-109.

Tukey, J.W. (1969) Analyzing data: sanctification or detective work? *American Psychologist,* **24,** 83.

Venable, D.L. (2007) Bet hedging in a guild of desert annuals. *Ecology,* **88,** 1086-1090.

Verheyen, K., Honnay, O., Motzkin, G., Hermy, M. and Foster, D.R. (2003) Response of forest plant species to land-use change: a life-history trait-based approach. *Journal of Ecology,* **91,** 563-577.

von Oetinger, B. (2004) A plea for uncertainty: everybody complains about uncertainty, but it might be a good thing to have. *Journal of Business strategy,* **25,** 57-59.

Wang, G., Zhou, G., Yang, L. and Li, Z. (2003) Distribution, species diversity and life-form spectra of plant communities along an altitudinal gradient in the northern slopes of Qilianshan Mountains, Gansu, China. *Plant Ecology,* **165,** 169-181.

Ward, E.J., Chirakkahl, H., González-Suárez, M., Aurioles-Gamboa, D., Holmes, E.E. and Gerber, L. (2010) Inferring spatial structure from time-series data: using multivariate state-space models to detect metapopulation structure of California sea lions in the Gulf of California, Mexico. *Journal of Applied Ecology,* **47,** 47-56.

Whitlock, M.C. (2011) Data archiving in ecology and evolution: best practices. *Trends in Ecology & Evolution,* **26,** 61-65.

Wintle, B.C., Fidler, F., Vesk, P.A. and L. Moore, J. (2013) Improving visual estimation through active feedback. *Methods in Ecology and Evolution,* **4,** 53-62.

Zuur, A., Tuck, I. and Bailey, N. (2003a) Dynamic factor analysis to estimate common trends in fisheries time series. *Canadian journal of fisheries and aquatic sciences,* **60,** 542-552.

Zuur, A.F., Fryer, R., Jolliffe, I., Dekker, R. and Beukema, J. (2003b) Estimating common trends in multivariate time series using dynamic factor analysis. *Environmetrics,* **14,** 665-685.

Appendices

Appendix 1

Consequences of continuing to exclude cryptic life stages from demographic models

Appendix 1-1: Methods for alternative formulations that include the seed bank

Model with unstructured seed bank

The inclusion of the seed bank using estimates for germination from the literature to inform the prior distribution is demonstrated. For the uninformed case, germination rates were taken from a uniform distribution.

The following transition matrix was taken from Verhulst et al. (2008) for a population of *Atriplex acanthocarpa* in 1996:

	J1	J2	A1	A2	A3
J1	0.045	0.002	**0.86**	**4.468**	**17.82**
J2	0.093	0.041	0	0	0
A1	0.16	0.102	0.119	0.062	0.012
A2	0.14	0.204	0.309	0.175	0.093
A3	0.142	0.347	0.257	0.5	0.538

where J1 and J2 represent juvenile stages, A1, A2 and A3 are reproductive adult stages and values in bold indicate fecundity.

Germination trials were performed by Gaylord and Egan (2006). This is an increasing population ($\lambda > 1$), thus the treatment with the highest mean germination rate was used to narrow our distribution. This yielded a germination rate, $g = 0.86$ and the probability of remaining in the seed bank was 1-g = 0.14. For our simulations, germination rates were drawn from a beta distribution with mode equal to g, and parameters α and β calculated by:

$$\alpha = mode \times (n - 2) + 1$$

$$\beta = (1 - mode) \times (n - 2) + 1$$

where n is the sample size for the treatment from which the germination study derived its estimates. In this case, $n = 40$, so we have $g \sim \text{beta}(33.68, 6.32)$ which gives the following distribution:

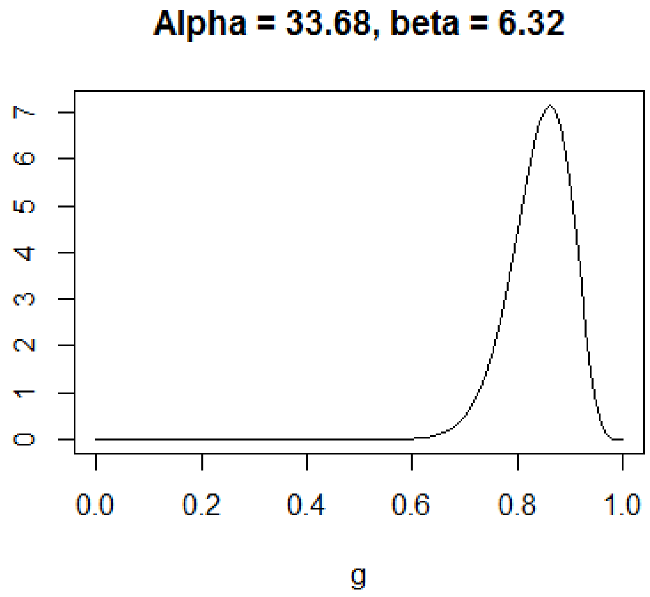

When the sample size is small, the spread of the distribution increases allowing for greater uncertainty in our priors. For example, if $n = 10$, then we have $g \sim \text{beta}(7.88, 2.12)$:

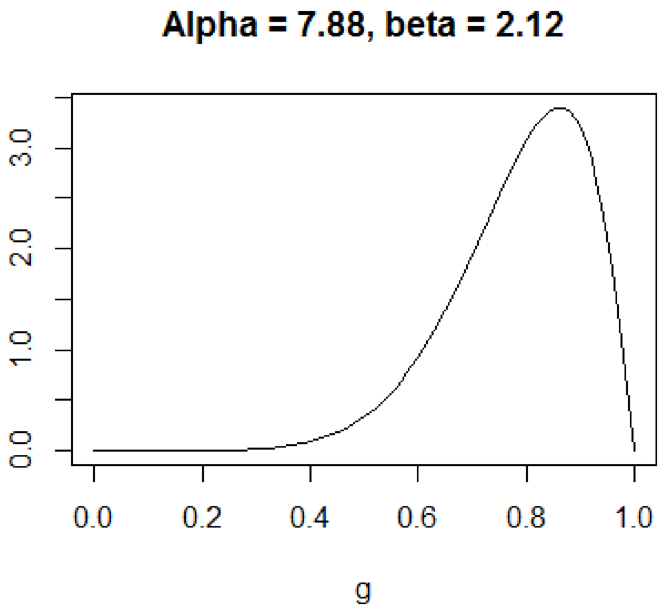

Drawing from this distribution, the seed bank is added to the original matrix. The germination rates obtained from the literature will be used in this example, giving the following matrix:

	SB	J1	J2	A1	A2	A3
SB	0.3	0	0	**?**	**?**	**?**
J1	0.7	0.045	0.002	**0.86**	**4.468**	**17.82**
J2	0	0.093	0.041	0	0	0
A1	0	0.16	0.102	0.119	0.062	0.012
A2	0	0.14	0.204	0.309	0.175	0.093
A3	0	0.142	0.347	0.257	0.5	0.538

Fecundity into the J1 stage was originally calculated by dividing the number of new seedlings observed by the proportional contribution of the adult life stages (Verhulst et al. 2008). All new seedlings observed were assumed to result from a combination of individuals that germinated within the census year and individuals that germinated from the persistent seed bank. Thus the fecundity of the adult stages into the juvenile stages should be lowered by some unknown amount representing germination from the seedbank. The following formula derived in the methods is used to solve for F_j, the total fecundity of stage class j:

$$f_{i,j} = F_j vgs + F_j v(1-g)(1-d)g$$

$$F_j = f_{i,j} \div [vg(\mathrm{s}+(1-g)(1-d)] \tag{1}$$

For example, the number of new seedlings produced by the A3 stage, $f_{1,6}$ as observed by the author is 17.82. Occasionally, viability (v) was also estimated in the study from which the germination rate was obtained, and was subsequently treated the same i.e. drawn from a beta distribution with mode equal to v. The unknown parameters seedling survival (s) or seed survival ($1-d$) and sometimes viability were drawn from uniform distributions. For simplicity, we set these equal to 1 in this example. Then, substituting $f_{1,6}$ and the estimates for germination obtained from the literature into equation 1, we solve for F_6.

$$17.82 = [F_6 \times 1 \times 0.7 \times 1] + [F_6 \times 1 \times 0.3 \times 1 \times 0.7]$$

$$F_6 = 17.82 \div (0.7+0.21) = 19.58$$

Now we allocate this fecundity into the J1 and SB stages:

Fecundity into J1 $f_{2,6} = F_j vgs = 19.58 \times 1 \times 0.7 \times 1 = 13.71$

Fecundity into SB $f_{1,6} = F_j v(1-g)(1-d) = 19.58 \times 1 \times 0.3 \times 1 = 5.87$

This conserves the number of seedlings as observed by the authors.

Germinants from previous year’s seed bank = $F_j v(1-g)(1-d)g = 19.58 \times 1 \times 0.3 \times 1 \times 0.7 =$ 4.11

Number of observed seedlings = immediate germinants + germinants from seed bank

= 13.71 + 4.11

= 17.82

This process is repeated for the other reproductive stages to obtain the new transition matrix:

	SB	J1	J2	A1	A2	A3
SB	0.3	0	0	**0.28**	**1.47**	**5.87**
J1	0.7	0.045	0.002	**0.66**	**3.44**	**13.71**
J2	0	0.093	0.041	0	0	0
A1	0	0.16	0.102	0.119	0.062	0.012

A2	0	0.14	0.204	0.309	0.175	0.093
A3	0	0.142	0.347	0.257	0.5	0.538

Model with age structured seed bank up to 2 years

I start again with the original model for *Atriplex acanthocarpa* in 1996:

	J1	J2	A1	A2	A3
J1	0.045	0.002	**0.86**	**4.468**	**17.82**
J2	0.093	0.041	0	0	0
A1	0.16	0.102	0.119	0.062	0.012
A2	0.14	0.204	0.309	0.175	0.093
A3	0.142	0.347	0.257	0.5	0.538

As before, germination experiments from Gaylord and Egan (2006) yielded a germination rate, g = 0.7 and the probability of remaining in the seed bank was 1-g = 0.3. This time, we incorporate age structure into our seed bank. I make an additional assumption that the probability of remaining in the seed bank and germinating in the seed bank remains constant in time.

	SB 1 Year	SB 2+ Years	J1	J2	A1	A2	A3
SB 1 Year	0	0	0	0	**?**	**?**	**?**
SB 2+ Years	0.3	0.3	0	0	**0**	**0**	**0**
J1	0.7	0.7	0.045	0.002	**0.86**	**4.468**	**17.82**
J2	0	0	0.093	0.041	0	0	0
A1	0	0	0.16	0.102	0.119	0.062	0.012
A2	0	0	0.14	0.204	0.309	0.175	0.093
A3	0	0	0.142	0.347	0.257	0.5	0.538

The formula used to solve for F_j, the total fecundity of stage class j taking into account seed bank contributions from t-1 and t-2 is:

$$f_{i,j} = F_j vgs + F_j v(1\text{-}g)(1\text{-}d)g + F_j v(1\text{-}g)^2(1\text{-}d)^2 g$$

$$F_j = f_{i,j} \div \{vg[\mathrm{s}+(1\text{-}g)(1\text{-}d) + (1\text{-}g)^2(1\text{-}d)^2]\} \tag{3}$$

For example, the number of new seedlings produced by the A3 stage, $f_{1,6}$ as observed by the author is 17.82. Again we set viability (v), seedling survival (s) or seed survival (1-d) equal to 1. Then, substituting $f_{1,6}$ and the estimates for germination obtained from the literature into equation 1, I solve for $F_{6.}$

$$17.82 = [F_6\times1\times0.7\times1] + [F_6\times1\times0.3\times1\times0.7] + [F_6\times1\times(0.3)^2\times(1)^2\times0.7]$$

$$F_6 = 17.82 \div (0.7+0.21+0.063) = 18.3145$$

Now this fecundity is allocated into the J1 and SB stages:

Fecundity into J1 $f_{6,2} = F_j vgs = 18.3145 \times 1 \times 0.7 \times 1 = 12.8201$

Fecundity into SB $f_{6,1} = F_j v(1\text{-}g)(1\text{-}d) = 18.3145 \times 1 \times 0.3 \times 1 = 5.4943$

This conserves the number of seedlings as observed by the authors.

Germinants from seed bank from t-1 and t-2 = $F_j v(1\text{-}g)(1\text{-}d)g + F_j v(1\text{-}g)^2(1\text{-}d)^2 g$

$$= [18.3145 \times 1 \times 0.3 \times 1 \times 0.7] + [18.3145 \times 1 \times (0.3)^2 \times (1)^2 \times 0.7] = 4.9999$$

Number of observed seedlings = immediate germinants + germinants from seed bank

= 12.8201 + 4.9999

= 17.82

This process is repeated for the other reproductive stages to obtain the new transition matrix:

	SB 1 Year	SB 2+ Years	J1	J2	A1	A2	A3
SB 1 Year	0	0	0	0	**0.2652**	**1.3776**	**5.4943**
SB 2+ Years	0.3	0.3	0	0	0	0	0
J1	0.7	0.7	0.045	0.002	**0.6187**	**3.2144**	**12.8201**

J2	0	0	0.093	0.041	0	0	0
A1	0	0	0.16	0.102	0.119	0.062	0.012
A2	0	0	0.14	0.204	0.309	0.175	0.093
A3	0	0	0.142	0.347	0.257	0.5	0.538

Model with seed bank lasting no longer than 1 year

I start with the unstructured model obtained previously.

	SB	J1	J2	A1	A2	A3
SB	0.3	0	0	**0.28**	**1.47**	**5.87**
J1	0.7	0.045	0.002	**0.66**	**3.44**	**13.71**
J2	0	0.093	0.041	0	0	0
A1	0	0.16	0.102	0.119	0.062	0.012
A2	0	0.14	0.204	0.309	0.175	0.093
A3	0	0.142	0.347	0.257	0.5	0.538

Now it is assumed that if seeds do not germinate within the first year, they die, thus their survival is set to 0. The new model is then given by the following with the altered transition rate coloured in red:

	SB	J1	J2	A1	A2	A3
SB	0	0	0	**0.28**	**1.47**	**5.87**
J1	0.7	0.045	0.002	**0.66**	**3.44**	**13.71**
J2	0	0.093	0.041	0	0	0
A1	0	0.16	0.102	0.119	0.062	0.012
A2	0	0.14	0.204	0.309	0.175	0.093
A3	0	0.142	0.347	0.257	0.5	0.538

The same procedure is then used for the models with age structure. For example, the following shows seeds that do not survive beyond the second year:

	SB 1 Year	SB 2 Years	J1	J2	A1	A2	A3
SB 1 Year	0	0	0	0	**0.2652**	**1.3776**	**5.4943**
SB 2 Years	0.3	0	0	0	0	0	0
J1	0.7	0.7	0.045	0.002	**0.6187**	**3.2144**	**12.8201**
J2	0	0	0.093	0.041	0	0	0
A1	0	0	0.16	0.102	0.119	0.062	0.012
A2	0	0	0.14	0.204	0.309	0.175	0.093
A3	0	0	0.142	0.347	0.257	0.5	0.538

Appendix 1-2: Comparison of population growth rates using alternative model formulations that include the seed bank. SB denotes point estimates from models with an unstructured seed bank and germination rate equal to that obtained from the literature. SB MC Uniform represents the mean of 10,000 simulations with parameters for germination, viability, seed survival and seedling survival drawn from uniform distributions, while SB MC Beta has germination rates drawn from a beta distribution with α and β generated from the mode and sample size as determined by the external literature. SB2 and SB3 represent models with an age structured seed bank distinguishing seeds from *t* – 2 and *t* – 3 respectively. SB1, 2 and 3 Max represent models in which the seeds do not survive beyond the first, second and third years respectively. Studies were divided depending whether multiple time periods were provided. *Avg.* represents the population growth rate of the mean matrix. *Stoch.* gives the mean stochastic growth rate from populations projected over 10,000 years.

Study	**Pop**	**Period**	**No SB**	**SB**	**SB MC Uniform**	**SB MC Beta**	**SB1 Max**	**SB2**	**SB2 Max**	**SB3**	**SB3 Max**
Single time period											
Chien et al. 2008											
Calocedrus macrolepus	1	1	0.9683	0.9715	0.9700	0.9699	0.9684	0.9701	0.9684	0.9694	0.9685
Parashorea chinensis	1	1	0.9948	0.9955	0.9963	0.9954	0.9948	0.9955	0.9948	0.9950	0.9948
Pinus kwangtungensis	1	1	0.9776	0.9786	0.9786	0.9782	0.9776	0.9780	0.9776	0.9778	0.9776
Kisanuki et al. 2008											
Illicium anisatum	1	1	1.1271	1.1647	1.1344	1.1408	1.1241	1.1462	1.1216	1.1354	1.1195
	2	1	1.1864	1.2276	1.1931	1.2008	1.1807	1.2032	1.1761	1.1892	1.1723
Abe et al. 2008											
Sambucus racemosa	1	1	1.1696	1.1690	1.1789	1.1955	1.1683	1.1681	1.1680	1.1680	1.1680
	2	1	1.0007	1.0012	1.0109	**1.0249***	1.0007	1.0008	1.0007	1.0007	1.0007
	3	1	2.2227	2.2031	**2.1588***	**2.1480***	2.2023	2.1996	2.1996	2.1992	2.1992
Kouassi et al. 2008											
Eremospatha macrocarpa	1	1	0.9792	0.9811	0.9806	0.9805	0.9792	0.9802	0.9793	0.9797	0.9793
Laccosperma secundiflorum	1	1	0.9606	0.9661	**0.9638***	**0.9621***	0.9608	0.9637	0.9609	0.9625	0.9680
Multiple time periods											
Mondragon 2009											

Guarianthe aurantiaca	1	1	0.9851	0.9881	0.9881	0.9872	0.9851	0.9861	0.9852	0.9855	0.9852
	1	2	0.9895	0.9908	0.9908	0.9904	0.9895	0.9900	0.9896	0.9897	0.9896
		Avg.	0.9869	0.9891	-	-	0.9869	0.9877	0.9870	0.9872	0.9870
		Stoch.	0.9869	**0.9891***	-	-	0.9869	**0.9877***	0.9870	**0.9872***	0.9870
Quitete Portela et al. 2010											
Astrocaryum aculeatissimum	1	1	1.0093	1.0106	1.0111	1.0100	1.0093	1.0095	1.0091	1.0009	1.0089
	1	2	0.9964	0.9968	0.9971	0.9966	0.9964	0.9965	0.9964	0.9965	0.9965
		Avg.	0.9998	1.0085	-	-	0.9998	0.9999	0.9997	0.9965	0.9997
		Stoch.	0.9998	**1.0000***	-	-	0.9998	0.9999	0.9998	0.9999	0.9998
Geonoma schottiana	1	1	1.0043	1.0240	**1.0114***	**1.0220***	1.0050	1.0157	1.0049	1.0114	1.0049
	1	2	0.9823	1.0002	**1.0115***	**1.0217***	0.9827	0.9942	0.9829	0.9901	0.9830
		Avg.	0.9949	1.0150	-	-	0.9950	1.0006	0.9950	1.0002	0.9950
		Stoch.	0.9949	**1.0147***	-	-	0.9950	**1.0064***	0.9950	**1.0019***	0.9950
Verhulst et al. 2008											
Atriplex acanthocarpa	1	1	2.4526	2.3455	**2.3016***	**2.3522***	2.3367	2.3735	2.3733	2.3714	2.3714
	1	2	0.7301	0.8305	**0.7418***	**0.7509***	0.7318	0.8242	0.7337	0.8208	0.7357
	1	3	0.7436	0.8862	**0.7712***	**0.7914***	0.7506	0.8722	0.7580	0.8637	0.7647
		Avg.	1.3461	1.3351	-	-	1.2977	1.3280	1.3217	1.3258	1.3232
		Stoch.	1.1434	**1.1784***	-	-	1.1284	**1.1583***	1.1305	1.1481	1.1337
Atriplex canescens	1	1	1.7211	1.7012	1.6883	**1.6790***	1.6423	1.6381	1.6247	1.6093	1.6047
	1	2	0.9451	0.9451	0.9451	0.9451	0.9451	0.9451	0.9451	0.9451	0.9451
	1	3	0.8805	0.8835	0.8810	0.8805	0.8805	0.8805	0.8805	0.8805	0.8805
		Avg.	1.1346	1.1648	-	-	1.1273	1.1406	1.1418	1.1319	1.1338
		Stoch.	1.0776	**1.1168***	-	-	**1.1128***	**1.0938***	1.0843	1.0858	1.0821

* Population growth rates compared to the no seed bank models are significantly different according to the 95% confidence interval. Statistically different growth rates are also shown in bold font.

Appendix 1-3: Example of removing the seed bank stage from a matrix model

The following transition matrix was taken from Sletvold and Rydgren (2007) for a population of *Digitalis purpurea* in a disturbed habitat

	Seed bank	Tiny rosettes	Small rosettes	Medium rosettes	Large rosettes	Flowering rosettes
Seed bank	0.67	0	0	0	0	**30.5**
Tiny rosettes	0.0871	0.00424	0.0385	0.00911	0	**3.41**
Small rosettes	0.0165	0.0127	0.0315	0.0478	0	**0.646**
Medium rosettes	0.00261	0.00847	0.0175	0.164	0.0313	**0.102**
Large rosettes	0	0	0	0.0387	0.121	0
Flowering rosettes	0	0	0	0.00911	0.383	0

To simplify the estimation for the seedling fecundity, we first collapse the matrix so fecundity only goes into the seed bank and one merged seedling stage. Once an estimate for seedling fecundity is obtained, we can redistribute this proportionally amongst the tiny, small and medium rosette classes.

	Seed bank	Seedlings	Large rosettes	Flowering rosettes
Seed bank	0.67	0	0	**30.5**
Seedlings	0.10621	0.33382	0.0313	**4.158**
Large rosettes	0	0.0387	0.121	0
Flowering rosettes	0	0.00911	0.383	0

Since we no longer assume germinating within the census year is equal to germination from the seed bank, the formula for estimating seedling fecundity is

$$f_{i,j} = F_j vgs + F_j v(1\text{-}g)(1\text{-}d)g_b \qquad (2)$$

Sletvold and Rydgren (2007) also provide a value for seed survival in the seed bank, (1-d) = 0.75 We furthermore assume that the probability of surviving in the seed bank is equal to the probability of seedling survival s (see Methods).We have the following information available:

F_i = 30.5+4.158 = 34.66

g_b = 0.10621

1-d = 0.75

s = 0.75

v = 1 (no mention of viability probability in original paper)

g = ?

$f_{i,j}$ = ?

To estimate g, the proportion of seedlings germinating during the study period t to t + 1, we know F_jvgs = # of seedlings germinating within the census year and surviving = 4.158. Solving for g gives

g = 4.158 ÷ (34.66 × 0.75) = 0.15995

Now we have all the necessary parameters to estimate $f_{i,j}$ from equation 3.

Fecundity into seedling stage = 4.158 + 34.66 × 1 × (1-0.15995) × 0.75 × 0.10621

= 6.4773

Note that this is higher than the original seedling fecundity of 4.158 since individuals that actually germinated from the seed bank are perceived to have germinated immediately instead. Using 6.4773 as our new estimate for the fecundity into the seedling stage and removing the seed bank stage gives the following matrix

	seedlings	large rosettes	flowering rosettes
seedling	0.33382	0.0313	**6.4773**
large rosettes	0.0387	0.121	0
flowering rosettes	0.0091	0.383	0

This is not the final matrix as we still need to redistribute the seedling fecundity proportionally amongst the tiny, small and medium rosette stage classes.

Fecundity into tiny rosette = (3.41 ÷ 4.158) × 6.4773 = 5.31209

Fecundity into small rosette = (0.646 ÷ 4.158) × 6.5876 = 1.00633

Fecundity into medium rosette = (0.102 ÷ 4.158) × 6.5876 = 0.15890

The final matrix with the seed bank removed used to calculated new growth rates is now

	tiny rosettes	small rosettes	medium rosettes	large rosettes	flowering rosettes
tiny rosettes	0.00424	0.0385	0.00911	0	**5.31209**
small rosettes	0.0127	0.0315	0.0478	0	**1.00633**
medium rosettes	0.00847	0.0175	0.164	0.0313	**0.15890**
large rosettes	0	0	0.0387	0.121	0
flowering rosettes	0	0	0.00911	0.383	0

Appendix 1-4: R script for reading matrices and conducting Monte Carlo simulations to include the seed bank.

Part I: Helper functions
Part II: Monte Carlo simulations

```
# PART I: HELPER FUNCTIONS

######################################
####  MATRICES
######################################

# See Appendix 1-4 for list of references

all.matrices = function() {

  #--------------------------
  # 1) Astrocaryum

  Astrocaryum.2006 = matrix(c(0.6939,  0.0085,  0.0000,         0.0000,   0.4340,
                         0.1360, 0.9700,   0.0304,   0.0000,   0.0000,
                         0.0034, 0.0112,   0.9325,   0.0000,   0.0000,
                         0.0000, 0.0000,   0.0180,   0.9053,   0.0000,
                         0.0000, 0.0000,   0.0010,   0.0888,   0.9937),
                       nrow = 5, byrow = T)

  Astrocaryum.2007 = matrix(c(0.7131,  0.0075,  0.0000,         0.0000,   0.3123,
                         0.1562, 0.9419,   0.4128,   0.0000,   0.0000,
                         0.0028, 0.0176,   0.5696,   0.0000,   0.0000,
                         0.0000, 0.0000,   0.0114,   0.8538,   0.0000,
                         0.0000, 0.0000,   0.0000,   0.1345,   0.9940),
                       nrow = 5, byrow = T)

  #--------------------------
  # 2) Atriplex acanthocarpa

  Acanthocarpa.1996 = matrix(c(0.045,  0.002,  0.86,  4.468,     17.82,
                          0.093,  0.041,     0,           0,          0,
                          0.16,    0.102,    0.119,    0.062,    0.012,
                          0.14,    0.204,    0.309,    0.175,    0.093,
                          0.142,  0.347,    0.257,    0.5,        0.538),
                        nrow = 5, byrow = T)

  Acanthocarpa.1997 = matrix(c(0.321,  0,  0.002,        0.011,    0.035,
                          0.147,  0.05,      0,           0,          0,
                          0.042,  0.177,    0.245,    0.112,    0.033,
                          0.011,  0.311,    0.196, 0.266,       0.124,
                          0.006,  0.21,      0.082,    0.319,    0.599),
                        nrow = 5, byrow = T)

  Acanthocarpa.1998 = matrix(c(0.461, 0.045,            0.028,    0.088,    0.223,
                          0.042,  0.061,    0,           0,          0,
                          0.226,  0.595,    0.566,    0.204,    0.071,
                          0.002,  0.156,    0.131,    0.298,    0.155,
                          0,         0.034,    0.021,    0.123,    0.353),
```

```
                    nrow = 5, byrow = T)

#--------------------------
# 3) Atriplex Canescens

Canescens.1996 = matrix(c(0.361,  0.056,   0.15,      0.477,    5.489,
                 0.177,     0.191,    0,         0,         0,
                 0.13,      0.145,    0.481,     0.163,     0.013,
                 0.044,     0.193,    0.342,     0.418,     0.044,
                 0.109,     0.344,    0.051,     0.397,     0.9),
                nrow = 5, byrow = T)

Canescens.1997 = matrix(c(0.546,  0.043,   0,         0,         0.001,
                 0.027,     0.362,    0,         0,         0,
                 0.005,     0.052,    0.469,     0.132,     0.011,
                 0.003,     0.147,    0.259,     0.395,     0.066,
                 0.002,     0.267,    0.074,     0.38,      0.883),
                nrow = 5, byrow = T)

Canescens.1998 = matrix(c(0.02,  0.01,     0.001,     0.002,     0.007,
                 0.043,     0.361,    0,         0,         0,
                 0.012,     0.103,    0.556,     0.222,     0.049,
                 0.004,     0.124,    0.099,     0.403,     0.088,
                 0.001,     0.237,    0.062,     0.255,     0.796),
                nrow = 5, byrow = T)

#--------------------------
# 4) Calocedrus

Calocedrus = matrix(c(0.683,  0,    0,         0,         0,         0,         1.38,      2.7,       3.78,      4.3,
        4.53,     4.53,     4.51,     4.51,
              0.091,        0.691,    0,         0,         0,         0,         0,         0,         0,         0,         0,
        0,        0,        0,
              0,  0.11,     0.768,    0,         0,         0,         0,         0,         0,         0,         0,         0,
        0,        0,
              0,  0,        0.07,     0.808,     0,         0,         0,         0,         0,         0,         0,         0,
        0,        0,
              0,  0,        0,        0.0742,    0.898,     0,         0,         0,         0,         0,         0,         0,
        0,        0,
              0,  0,        0,        0,         0.015,     0.93,      0,         0,         0,         0,         0,         0,
        0,        0,
              0,  0,        0,        0,         0,         0.028,     0.917,     0,         0,         0,         0,         0,
        0,        0,
              0,  0,        0,        0,         0,         0,         0.042,     0.906,     0,         0,         0,         0,
        0,        0,
              0,  0,        0,        0,         0,         0,         0,         0.052,     0.898,     0,         0,         0,
        0,        0,
              0,  0,        0,        0,         0,         0,         0,         0,         0.06,      0.8929,    0,         0,
        0,        0,
              0,  0,        0,        0,         0,         0,         0,         0,         0,         0.0654,    0.924,     0,
        0,        0,
              0,  0,        0,        0,         0,         0,         0,         0,         0,         0,         0.034,
        0.925,    0,        0,
              0,  0,        0,        0,         0,         0,         0,         0,         0,         0,         0,
        0.033,    0.923,    0,
              0,  0,        0,        0,         0,         0,         0,         0,         0,         0,         0,         0,
        0.03,     0.953),
            nrow = 14, byrow = T)

#--------------------------
```

```
# 5) Eremospatha

Eremospatha = matrix(c(0.866,  0.062,       0,          0.096,
                       0.057,       0.804,    0,          0.011,
                       0, 0.017,    0.587,    0.09,
                       0, 0,        0.397,    0.881),
                     nrow = 4, byrow = T)

#--------------------------
# 6) Geonoma

Geonoma.2006 = matrix(c(0.26843796,  0.012032048,          0,          0,          4.5344,
                        0.017029285,         0.643425,          0.072044286,      0.002362243,      0,
                        0,           0.136727813,      0.696018464,      0.011808379,      0,
                        0.001621188,         0.077747188,      0.15943725,       0.768736678,      0,
                        0.000811567,         0,          0,          0.1263927,         0.9683),
                      nrow = 5, byrow = T)

Geonoma.2007 = matrix(c(0.26843796,  0.012032048,          0,          0,          4.5344,
                        0.017029285,         0.643425,          0.072044286,      0.002362243,      0,
                        0,           0.136727813,      0.696018464,      0.011808379,      0,
                        0.001621188,         0.077747188,      0.15943725,       0.768736678,      0,
                        0.000811567,         0,          0,          0.1263927,         0.9683),
                      nrow = 5, byrow = T)

#--------------------------
# 7) Guarianthe

Guarianthe.2005 = matrix(c(0.512,  0,        0,          0.007,    0.121,
                           0.381,    0.326,    0.05,     0,          0,
                           0,          0.512,    0.669,    0.016,    0,
                           0,          0,          0.187,    0.629,    0.1,
                           0,          0,          0,          0.306,    0.85),
                         nrow = 5, byrow = T)

Guarianthe.2006 = matrix(c(0.6,  0,           0,          0.009,    0.096,
                           0.233,    0.188,    0.024,    0,          0,
                           0,          0.688,    0.78,     0.21,     0,
                           0,          0, 0.159,0.645,    0.123,
                           0,          0,          0,          0.129,    0.86),
                         nrow = 5, byrow = T)

#--------------------------
# 8) Illicium

Illicium.pop1 = matrix(c(0.898,  0,            1.61,
                         0.087,      0.942,    0,
                         0,            0.043,    0.985),
                       nrow = 3, byrow = T)

Illicium.pop2 = matrix(c(0.898,  0,            3.67,
                         0.084,      0.925,    0,
                         0,            0.048,    0.99),
                       nrow = 3, byrow = T)

#--------------------------
# 9) Laccosperma

Laccosperma = matrix(c(0.863,  0.031,       0,          2.139,
                       0.064,       0.919,    0.19,     0,
```

```
                 0, 0.011,    0.619,    0,
                 0, 0,        0.071,    0.75),
               nrow = 4, byrow = T)

#--------------------------
# 10) Parashorea

Parashorea = matrix(c(0.7,  0,       0,        0,        0,        0,        0.78,     1.17,     1.64,     2.13,
        2.58,    2.94,    3.28,    3.5,     3.57,
              0.101,      0.704,   0,        0,        0,        0,        0,        0,        0,        0,        0,
        0,        0,        0,        0,
              0,  0.136,   0.793,   0,        0,        0,        0,        0,        0,        0,        0,        0,
        0,        0,        0,
              0,  0,        0.096,   0.819,   0,        0,        0,        0,        0,        0,        0,        0,
        0,        0,        0,
              0,  0,        0,        0.118,   0.901,   0,        0,        0,        0,        0,        0,        0,
        0,        0,        0,
              0,  0,        0,        0,        0.019,   0.922,   0,        0,        0,        0,        0,        0,
        0,        0,        0,
              0,  0,        0,        0,        0,        0.039,   0.946,   0,        0,        0,        0,        0,
        0,        0,        0,
              0,  0,        0,        0,        0,        0,        0.037,   0.93,    0,        0,        0,        0,
        0,        0,        0,
              0,  0,        0,        0,        0,        0,        0,        0.0527,  0.9238,  0,        0,        0,
        0,        0,        0,
              0,  0,        0,        0,        0,        0,        0,        0,        0.0594,  0.924,   0,        0,
        0,        0,        0,
              0,  0,        0,        0,        0,        0,        0,        0,        0,        0.059,   0.929,   0,
        0,        0,        0,
              0,  0,        0,        0,        0,        0,        0,        0,        0,        0,        0.055,
        0.935,   0,        0,        0,
              0,  0,        0,        0,        0,        0,        0,        0,        0,        0,        0,
        0.048,   0.964,   0,        0,
              0,  0,        0,        0,        0,        0,        0,        0,        0,        0,        0,        0,
        0.019,   0.97,    0,
              0,  0,        0,        0,        0,        0,        0,        0,        0,        0,        0,        0,
        0,        0.014,   0.983),
              nrow = 15, byrow = T)

#--------------------------
# 11) Pinus

Pinus = matrix(c(0.54,  0,0,        0,        0,        0,        0,        0.21,     0.28,     0.33,     0.37,
        0.39,    0.4,     0.41,    0.41,    0.41,    0.4,
           0.106,          0.636,   0,        0,        0,        0,        0,        0,        0,        0,        0,
        0,        0,        0,        0,        0,        0,
           0,     0.171,   0.787,   0,        0,        0,        0,        0,        0,        0,        0,        0,
        0,        0,        0,        0,        0,
           0,     0,        0.123,   0.801,   0,        0,        0,        0,        0,        0,        0,        0,
        0,        0,        0,        0,        0,
           0,     0,        0,        0.119,   0.911,   0,        0,        0,        0,        0,        0,        0,
        0,        0,        0,        0,        0,
           0,     0,        0,        0,        0.009,   0.935,   0,        0,        0,        0,        0,        0,
        0,        0,        0,        0,        0,
           0,     0,        0,        0,        0,        0.025,   0.935,   0,        0,        0,        0,        0,
        0,        0,        0,        0,        0,
           0,     0,        0,        0,        0,        0,        0.045,   0.925,   0,        0,        0,        0,
        0,        0,        0,        0,        0,
           0,     0,        0,        0,        0,        0,        0,        0.062,   0.915,   0,        0,        0,
        0,        0,        0,        0,        0,
```

```
    0,   0,      0,      0,      0,      0,      0,      0,      0.073,  0.91,   0,      0,
0,      0,      0,      0,      0,
    0,   0,      0,      0,      0,      0,      0,      0,      0,      0.077,  0.911,  0,
0,      0,      0,      0,      0,
    0,   0,      0,      0,      0,      0,      0,      0,      0,      0,      0.076,
0.916,  0,      0,      0,      0,      0,
    0,   0,      0,      0,      0,      0,      0,      0,      0,      0,      0,
0.071,  0.9227, 0,      0,      0,      0,
    0,   0,      0,      0,      0,      0,      0,      0,      0,      0,      0,      0,
0.0647, 0.93,   0,      0,      0,
    0,   0,      0,      0,      0,      0,      0,      0,      0,      0,      0,      0,
0,      0.0574, 0.937,  0,      0,
    0,   0,      0,      0,      0,      0,      0,      0,      0,      0,      0,      0,
0,      0,      0.05,   0.937,  0,
    0,   0,      0,      0,      0,      0,      0,      0,      0,      0,      0,      0,
0,      0,      0,      0.043,  0.96),
  nrow = 17, byrow = T)

#--------------------------
# 12) Sambucus

Sambucus.pop1 = matrix(c(0,  0,   0,      398,
                0.088,  0.716,  0.355,  0,
                0,      0.228,  0.579,  0.125,
                0,      0,      0.008,  0.875),
              nrow = 4, byrow = T)

Sambucus.pop2 = matrix(c(0,  0,   0,      102,
                0.088,  0.694,  0.373,  0,
                0,      0.239,  0.567,  0.321,
                0,      0,      0.007,  0.643),
              nrow = 4, byrow = T)

Sambucus.pop3 = matrix(c(0,  0,   0,      528,
                0.416,  0.52,   0.104,  0,
                0,      0.28,   0.729,  0.167,
                0,      0,      0.125,  0.833),
              nrow = 4, byrow = T)

#--------------------------
# List of matrices
#--------------------------

num.matrices = c(2,3,3,1,1,2,2,2,1,1,1,3)

all_matrices = list("Astrocaryum.2006" = Astrocaryum.2006, "Astrocaryum.2007" = Astrocaryum.2007,
            "Acanthocarpa.1996" = Acanthocarpa.1996, "Acanthocarpa.1997" = Acanthocarpa.1997,
"Acanthocarpa.1998" = Acanthocarpa.1998,
            "Canescens.1996" = Canescens.1996, "Canescens.1997" = Canescens.1997, "Canescens.1998" =
Canescens.1998,
            "Calocedrus" = Calocedrus, "Eremospatha" = Eremospatha,
            "Geonoma.2006" = Geonoma.2006, "Geonoma.2007" = Geonoma.2007,
            "Guarianthe.2005" = Guarianthe.2005, "Guarianthe.2006" = Guarianthe.2006,
            "Illicium.pop1" = Illicium.pop1, "Illicium.pop2" = Illicium.pop2,
            "Laccosperma" = Laccosperma, "Parashorea" = Parashorea, "Pinus" = Pinus,
            "Sambucus.pop1" = Sambucus.pop1, "Sambucus.pop2" = Sambucus.pop2, "Sambucus.pop3" =
Sambucus.pop3)


#--------------------------
```

```
# Fecundity entries
#--------------------------

Astrocaryum.fecundity = matrix(c(1,5), ncol = 2)
Acanthocarpa.fecundity = matrix(c(1,1,1,1,2,3,4,5), ncol = 2)
Canescens.fecundity = matrix(c(1,1,1,1,2,3,4,5), ncol = 2)
Calocedrus.fecundity = matrix(c(1,1,1,1,1,1,1,1,7,8,9,10,11,12,13,14), ncol = 2)
Eremospatha.fecundity = matrix(c(1,4), ncol = 2)
Geonoma.fecundity = matrix(c(1,5), ncol = 2)
Guarianthe.fecundity = matrix(c(1,1,4,5), ncol = 2)
Illicium.fecundity = matrix(c(1,3), ncol = 2)
Laccosperma.fecundity = matrix(c(1,4), ncol = 2)
Parashorea.fecundity = matrix(c(1,1,1,1,1,1,1,1,1,7,8,9,10,11,12,13,14,15), ncol = 2)
Pinus.fecundity = matrix(c(1,1,1,1,1,1,1,1,1,1,8,9,10,11,12,13,14,15,16,17), ncol = 2)
Sambucus.fecundity = matrix(c(1,4), ncol = 2)

# List of fecundity entries

fecundity_entries = c(lapply(seq_len(num.matrices[1]), function(X) Astrocaryum.fecundity),
                      lapply(seq_len(num.matrices[2]), function(X) Acanthocarpa.fecundity),
                      lapply(seq_len(num.matrices[3]), function(X) Canescens.fecundity),
                      lapply(seq_len(num.matrices[4]), function(X) Calocedrus.fecundity),
                      lapply(seq_len(num.matrices[5]), function(X) Eremospatha.fecundity),
                      lapply(seq_len(num.matrices[6]), function(X) Geonoma.fecundity),
                      lapply(seq_len(num.matrices[7]), function(X) Guarianthe.fecundity),
                      lapply(seq_len(num.matrices[8]), function(X) Illicium.fecundity),
                      lapply(seq_len(num.matrices[9]), function(X) Laccosperma.fecundity),
                      lapply(seq_len(num.matrices[10]), function(X) Parashorea.fecundity),
                      lapply(seq_len(num.matrices[11]), function(X) Pinus.fecundity),
                      lapply(seq_len(num.matrices[12]), function(X) Sambucus.fecundity))

names(fecundity_entries) = names(all_matrices)

# ------------------------------------------------
# List of germination rate priors and sample sizes
#-------------------------------------------------

Astrocaryum.germ = matrix(c(0.64, 100), ncol = 2)
Acanthocarpa.1996.germ = matrix(c(0.86, 40), ncol = 2)
Acanthocarpa.1997.germ = matrix(c(0.2, 40), ncol = 2)
Canescens.germ = matrix(c(0.55, 100), ncol = 2)
Calocedrus.germ = matrix(c(0.41, 10), ncol = 2)
Eremospatha.germ = matrix(c(0.36, 75), ncol = 2)
Geonoma.germ = matrix(c(0.01, 10), ncol = 2)
Guarianthe.germ = matrix(c(0.68, 300), ncol = 2)
Illicium.germ = matrix(c(0.2, 40), ncol = 2)
Laccosperma.germ = matrix(c(0.58, 150), ncol = 2)
Parashorea.germ = matrix(c(0.689, 10), ncol = 2)
Pinus.germ = matrix(c(0.556, 24), ncol = 2)
Sambucus.germ = matrix(c(0.019, 10), ncol = 2)

germ_par = c(lapply(seq_len(num.matrices[1]), function(X) Astrocaryum.germ),
             lapply(1, function(X) Acanthocarpa.1996.germ),
             lapply(1:2, function(X) Acanthocarpa.1997.germ),
             lapply(seq_len(num.matrices[3]), function(X) Canescens.germ),
             lapply(seq_len(num.matrices[4]), function(X) Calocedrus.germ),
             lapply(seq_len(num.matrices[5]), function(X) Eremospatha.germ),
             lapply(seq_len(num.matrices[6]), function(X) Geonoma.germ),
             lapply(seq_len(num.matrices[7]), function(X) Guarianthe.germ),
             lapply(seq_len(num.matrices[8]), function(X) Illicium.germ),
```

```
              lapply(seq_len(num.matrices[9]), function(X) Laccosperma.germ),
              lapply(seq_len(num.matrices[10]), function(X) Parashorea.germ),
              lapply(seq_len(num.matrices[11]), function(X) Pinus.germ),
              lapply(seq_len(num.matrices[12]), function(X) Sambucus.germ))

  names(germ_par) = names(all_matrices)
  return(list(all_matrices, fecundity_entries, germ_par))
}

####################################
####  ESTIMATE BETA PARAMETERS
####################################

beta.par = function(sample_mode_mean = 0.5, n_var = 2, type = "mode") {
  # sample_mode_mean    -  sample mode (type = mode) or mean (type = mean)
  # n_var               -  sample size (type = mode) or variance (type = mean)
  # type                -  select from c("mode", "mean") to determine parameters

  if(type == "mode") {
    alpha = sample_mode_mean * (n_var-2) +  1
    beta = (1-sample_mode_mean) * (n_var-2) + 1
    return(c(alpha, beta))
  } else if(type == "mean") {
    alpha = ((1 - sample_mode_mean) / n_var - 1 / sample_mode_mean) * sample_mode_mean ^ 2
    beta = alpha * ((1/sample_mode_mean)-1)
    return(c(alpha, beta))
  }
}

####################################
####  ADD SEED BANK TO MATRIX
####################################

create.seed.matrix = function(pop.matrix, fecundity.entries, germ, viability, seedling.surv, seed.surv) {

  Seedling.fec = Seed.fec = numeric(nrow(fecundity.entries))
  Seed.matrix = pop.matrix
  Seed.row = numeric(nrow(pop.matrix))
  Seed.col = numeric(nrow(pop.matrix)+1)

  for (j in 1:nrow(fecundity.entries)) {
    # Calculate total seed fecundity for class j
    f.ij = pop.matrix[ fecundity.entries[j,1], fecundity.entries[j,2] ]
    Total.fec.j = f.ij / (viability * germ * seedling.surv + viability*germ*(1-germ)*seed.surv)

    # Calculate seedling fecundity for class j
    Seedling.fec[j] = Total.fec.j * viability * germ * seedling.surv

    # Calculate seed bank fecundity for class j
    Seed.fec[j] = Total.fec.j * viability * (1-germ) * seed.surv

    # Create new row/column for seed bank
    Seed.matrix[ fecundity.entries[j,1], fecundity.entries[j,2]] = Seedling.fec[j]
    Seed.row[fecundity.entries[j,2]] = Seed.fec[j]
  }
  # Create new seed bank matrix
  Seed.col[1] = (1-germ)*seed.surv; Seed.col[2] = germ

  Seed.matrix = rbind(Seed.row, Seed.matrix)
  Seed.matrix = cbind(Seed.col, Seed.matrix)
```

```
  return(Seed.matrix)
}

####################################
####  MONTE CARLO FUNCTION
####################################

seed.monte.carlo = function(pop.matrix, fecundity.entries, germ.par = c(germ_mode = 0.5, sample_size = 2),
viab.par = c(1,1), n = 1000, elasticity = F, density.pop = FALSE, density.germ = FALSE) {

  # pop.matrix        -   original nxn matrix of transition rates without seed bank
  # fecundity.entries -   matrix coordinates of fecundity entries: 1st col = row, 2nd col = col
  # germ.par          -   sample germination rates from beta distribution: germ.par = c(alpha, beta)
  # viab.par          -   sample viability rates from beta distribution: viab.par = c(alpha, beta)
  # n                 -   number of matrices/iterations
  # density.pop       -   plot densities of growth rates if TRUE
  # density.germ      -   plot densities of germination rates if TRUE

  # Sample germination rates from beta distribution
  alpha.beta = beta.par(germ.par[1], germ.par[2])
  germ = rbeta(n, alpha.beta[1], alpha.beta[2])

  # Sample viability from beta distribution
  viability = rbeta(n, viab.par[1], viab.par[2])

  # Sample Seedling survival from uniform distribution
  seedling.surv = runif(n)

  # Sample Seed survival from uniform distribution
  seed.surv = runif(n)

  # Vector for storing growth rates
  pop.growth = numeric(n)

  for (i in 1:n) {
    Seed.matrix = create.seed.matrix(pop.matrix, fecundity.entries, germ[i],
                                     viability[i], seedling.surv[i], seed.surv[i])

    # Calculate population growth rates
    pop.growth[i] = Re(eigen(Seed.matrix)$values[1])
  }

  # Mean and 95% CI's of growth rates
  pop.mean = mean(pop.growth)
  CI = c(sort(pop.growth)[0.025*n], sort(pop.growth)[0.975*n])

  if (density.germ) {
    plot(density(germ), xlab = "Germination rate", main = "Density of germination rates")
  }

  if (density.pop) {
    plot(density(pop.growth), xlab = "Population growth rate", main = "Density of growth rates")
    abline(v = pop.mean, lty = 2, col = 2, lwd = 2)
  }

  return(list("Lambda" = pop.mean, "CI" = CI))
}
```

```
# PART II: MONTE CARLO SIMULATIONS

source("Helper functions.R")

# Read matrices/fecundity/germination priors
all_matrices = all.matrices()[[1]]
fecundity_entries = all.matrices()[[2]]
germ_par = all.matrices()[[3]]

# -------------------------------------------------
# Uninformed priors on germination/viability
# -------------------------------------------------
set.seed(length(all_matrices))

Results = rep(list(0), length(all_matrices))

for (i in 1:length(all_matrices)) {
    Results[[i]] = seed.monte.carlo(all_matrices[[i]], fecundity_entries[[i]], n = 10000)
}

names(Results) = names(all_matrices)
Results

# --------------------------------------------------
# Informed priors on germination
# --------------------------------------------------
set.seed(length(all_matrices))

Informed.Results = rep(list(0), length(all_matrices))

for (i in 1:length(all_matrices)) {
  Informed.Results[[i]] = seed.monte.carlo(all_matrices[[i]], fecundity_entries[[i]], germ_par[[i]], n = 10000)
}

names(Informed.Results) = names(all_matrices)
Informed.Results

# --------------------------------------------------
# Plot density of growth rates
# --------------------------------------------------

Acanthocarpa.matrices = all_matrices[3:5]
Acanthocarpa.fecundity = fecundity_entries[3:5]
Acanthocarpa.germ = germ_par[3:5]

par(mfrow = c(3,2), mar = c(4.1, 4.1, 3.1, 2.1))
set.seed(length(all_matrices))
for (i in 1:3) {
  seed.monte.carlo(Acanthocarpa.matrices[[i]], Acanthocarpa.fecundity[[i]], density.pop = T, n = 10000)
  seed.monte.carlo(Acanthocarpa.matrices[[i]], Acanthocarpa.fecundity[[i]], Acanthocarpa.germ[[i]],
density.pop = T, n = 10000)
}
```

Appendix 1-5. Graph showing the mean growth rates resulting from Monte Carlo simulations for sample sizes ranging from 1 to 20000 for *Atriplex acanthocarpa* for 1996.

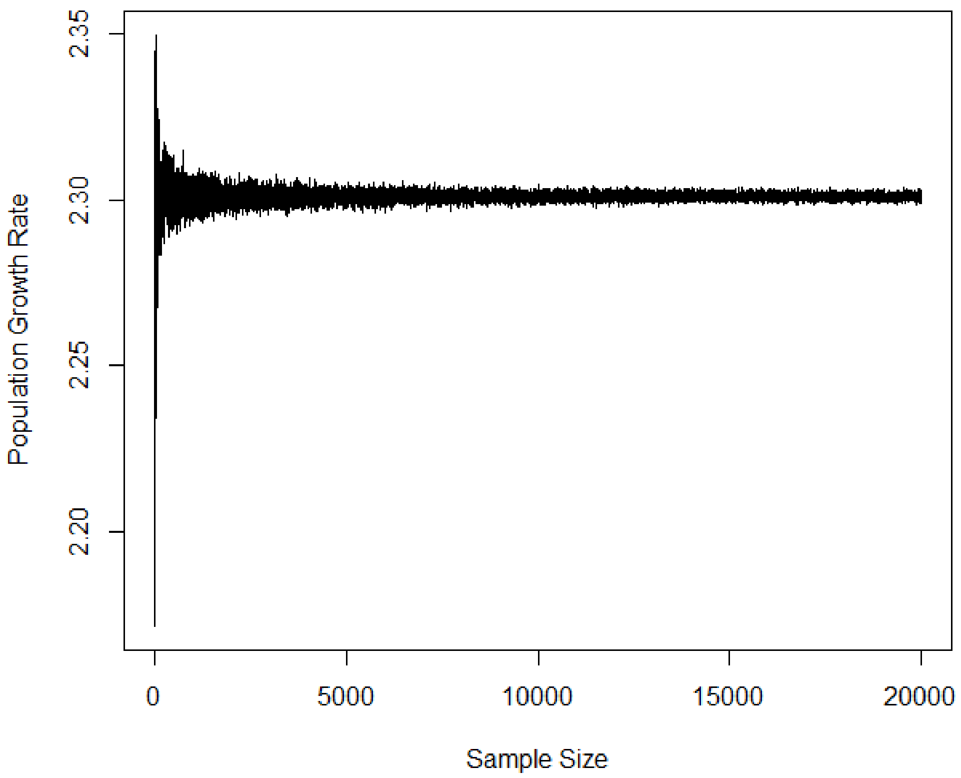

Appendix 1-5. Elasticity matrices for the 1997 and 1998 the desert shrub *Atriplex acanthocarpa* populations (Verhulst *et al.*, 2008) without (left) and with (right) the seed bank (SB). Values in bold indicate elasticities > 0.1. The original matrices consist of 2 non-reproductive juvenile stages (J1 and J2) and 3 reproductive adult stages (A1, A2 and A3).

Elasticities of original model (no seed bank)						
1997						
		J1	J2	A1	A2	A3
	J1	0.0112	0	0.0001	0.0014	0.012
	J2	0.0110	0.0008	0	0	0
	A1	0.0019	0.0018	0.0195	0.0190	0.0159
	A2	0.0008	0.0051	0.0255	0.0255	0.0974
	A3	0.0006	0.0042	0.0130	0.0130	**0.5759**
1998						
		J1	J2	A1	A2	A3
	J1	**0.1118**	0.0007	0.0194	0.0221	0.0263
	J2	0.0125	0.0011	0	0	0
	A1	0.0555	0.0090	**0.3983**	0.0520	0.0085
	A2	0.0005	0.0023	0.0889	0.0732	0.0178
	A3	0	0.0006	0.0167	0.0353	0.0475

Elasticities of model with seed bank						
	SB	J1	J2	A1	A2	A3
SB	**0.7919**	0	0	0.0003	0.0028	0.0173
J1	0.0204	0.0125	0	0	0.0001	0.0004
J2	0	0.0158	0.001	0	0	0
A1	0	0.0028	0.0021	0.0033	0.0023	0.0013
A2	0	0.0014	0.0069	0.005	0.0101	0.0093
A3	0	0.0011	0.0068	0.003	0.0175	0.0647
	SB	J1	J2	A1	A2	A3
SB	**0.5039**	0	0	0.0218	0.0178	0.0174
J1	0.057	0.0655	0.0003	0.002	0.0016	0.0016
J2	0	0.0104	0.0008	0	0	0
A1	0	0.0516	0.0068	**0.12**	0.0113	0.0015
A2	0	0.0006	0.0024	0.0378	0.0224	0.0045
A3	0	0	0.0008	0.0096	0.0146	0.016

Appendix 1-6: Log population size projections for **A)** *Atriplex acanthocarpa*, **B)** *Atriplex canescens*, **C)** *Carduus nutans* and **D)** *Digitalis purpurea* with an initial population of 1000 individuals at stable stage distribution. Populations crossing the horizontal black line indicate it has gone extinct.

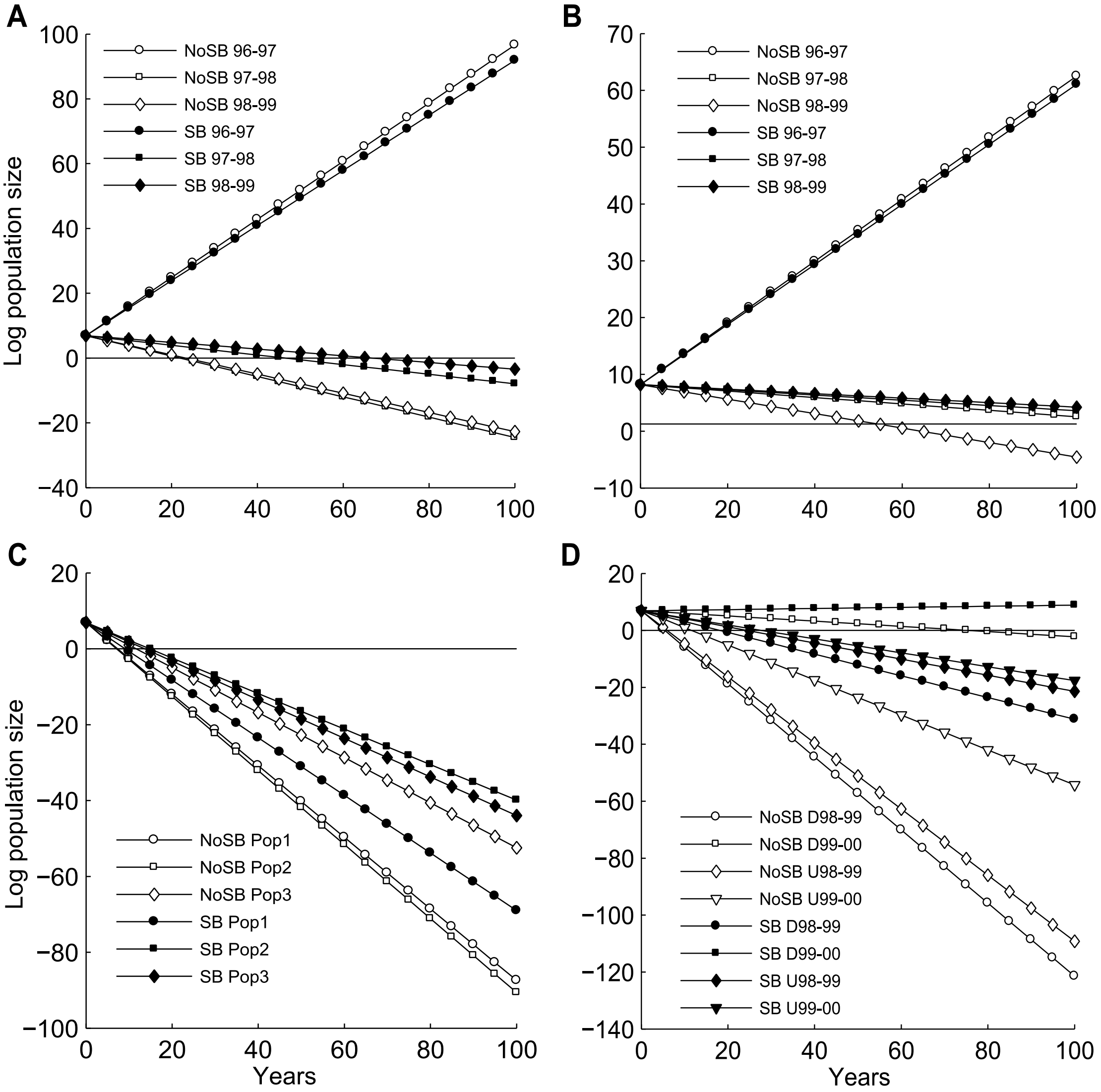

Appendix 1-7: Cumulative extinction probability of quasi-extinction for **A)** *Atriplex acanthocarpa*, **B)** *Atriplex canescens*, **C)** *Digitalis purpurea* population 1 and **D)** *Digitalis purpurea* population 2 with an initial population of 1000 individuals at stable stage distribution. Solid lines indicate models without the seed bank and dotted lines indicate models with the seed bank. Quasi-extinction threshold was set to 100 individuals.

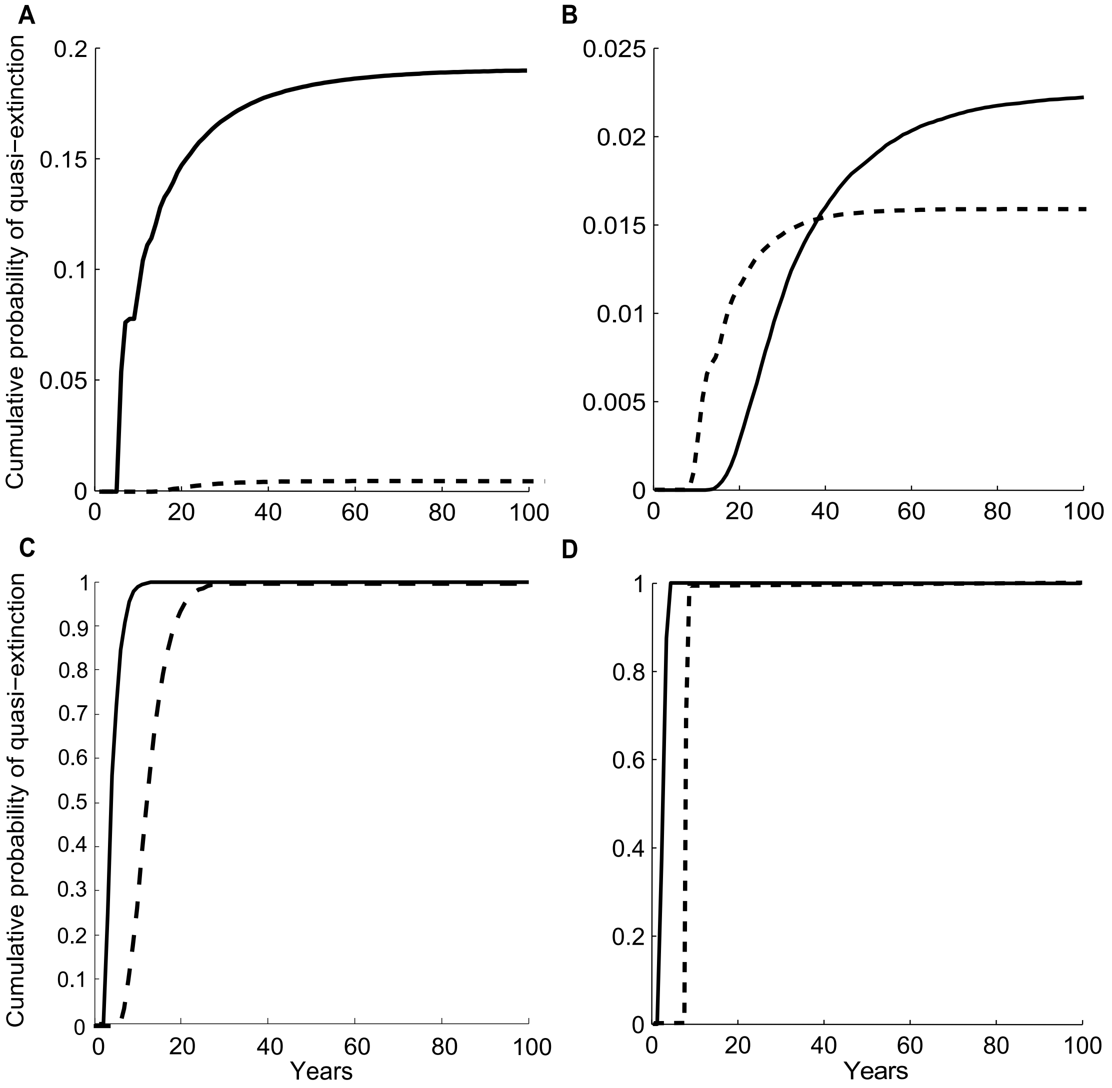

Appendix 2

Exploratory MARSS models

Appendix 2-1: Exploratory models investigating the frequency of zero values and missing values on model convergence

Zeroes

Sample parameter estimates for R, Q, U and B were obtained from MARSS models for *Trachymene glaucifolia* abundances from the unburnt grid MCA, Main Camp. This model yielded the following values; R = 4.489685, Q = 0.3579777, μ = 1.177214 and B = 0.3472462. Using these values, 100 sample datasets of length $t = 200$ were created simulating the univariate state-space model:

$$X_t = BX_{t-1} + \mu + w_t; \quad w \sim N(0, Q)$$

$$Y_t = X_t + v_t; \quad v \sim N(0, R)$$

The initial state value, X_1, was set to equal the initial observed value of grid MCA from which the parameters were estimated from. Years were then randomly sampled and their values set to 0 to investigate the impact of the frequency of zero values on model convergence. Datasets with no zeroes, 25% zeroes, 50% zeroes, and 75% zeroes were created. First, for each dataset, 25% (50 years) of the time steps were randomly sampled ($t = 1$ and $t = 200$ were excluded from sampling to ensure time series length remains the same), and the values at these time steps set to 0. Then a further 25% of the remaining time steps were randomly sampled, and these values set to 0, resulting in a dataset with 50% zeroes. Finally, an additional 25% of the remaining time steps were randomly sampled and set to 0, giving a dataset with 75% zeroes and resulting in a total of 400 datasets for which models were constructed. An example dataset produced by this process is given below (only up to *t* = 50 to ease visualisation):

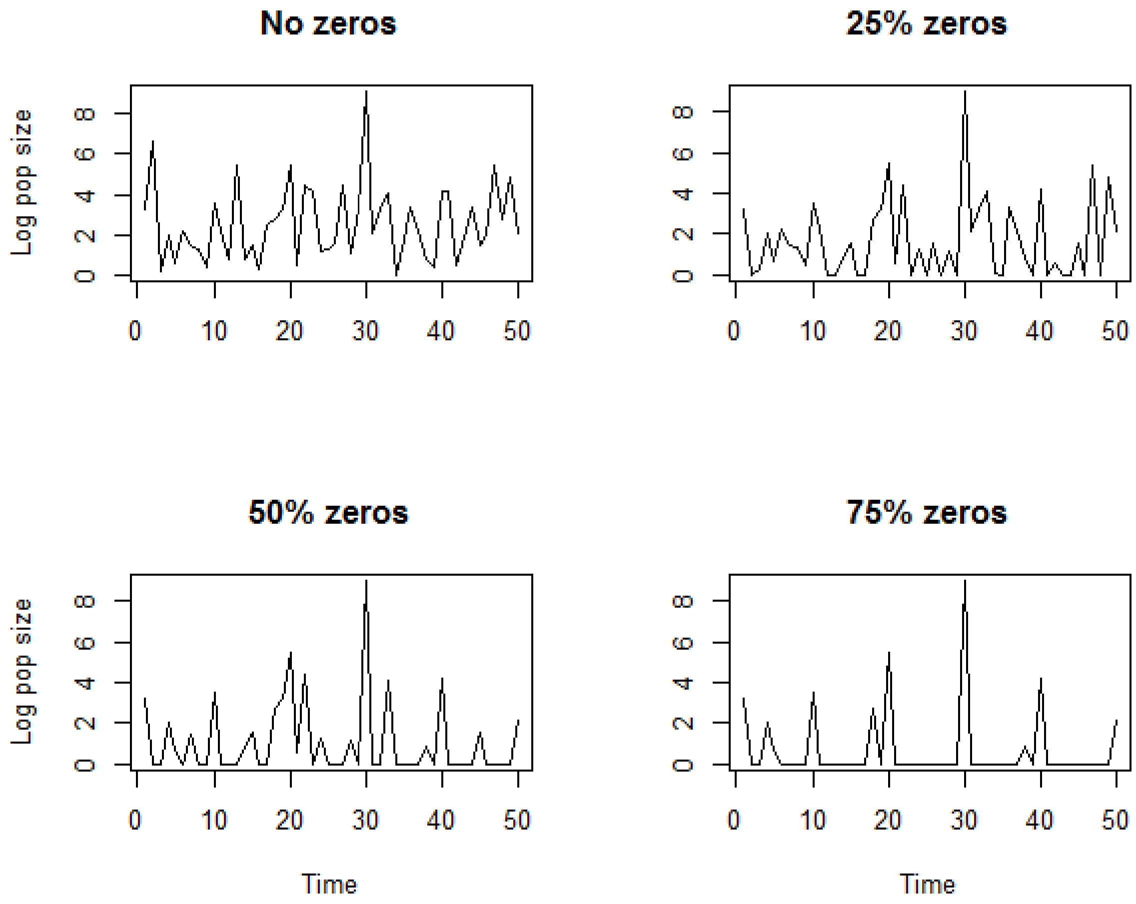

Separate MARSS models were created for each dataset with the maximum number of iterations set to 2000 and then examined for convergence. The table below provides a summary of the convergence results (1 indicates successful convergence, red 0's indicate failure to converge and * indicates critical errors in convergence).

Dataset	No zeros	25% zeros	50% zeros	75% zeros	Dataset	No zeros	25% zeros	50% zeros	75% zeros
1	1	**0**	1	1	51	**0**	1	1	1
2	1	1	1	1	52	1	**0**	1	**0***
3	1	**0***	**0***	**0**	53	1	**0**	**0**	**0**
4	**0**	**0**	1	1	54	1	**0**	1	**0**
5	**0***	1	1	**0***	55	1	1	1	1
6	1	1	**0**	1	56	1	1	**0**	1
7	1	**0**	1	**0***	57	**0**	**0**	**0**	**0**

8	1	1	**0**	**0***	58	**0***	1	**0**	**0***
9	1	1	1	1	59	**0**	1	1	**0***
10	1	1	1	**0***	60	**0**	**0**	1	**0**
11	1	1	**0**	1	61	1	**0**	**0**	**0***
12	1	1	**0**	**0**	62	1	1	1	1
13	1	1	1	1	63	1	**0**	**0**	**0**
14	**0**	1	1	**0***	64	**0***	**0**	**0**	1
15	**0**	**0**	**0**	1	65	**0**	1	1	1
16	**0**	1	1	1	66	**0***	**0***	1	1
17	1	1	**0***	**0**	67	1	**0**	1	**0**
18	1	1	**0**	1	68	1	**0**	**0**	1
19	**0**	1	**0**	**0**	69	**0**	**0**	**0**	1
20	1	**0**	1	**0***	70	**0**	1	1	**0**
21	1	1	1	**0***	71	**0**	**0**	1	**0***
22	1	1	**0**	**0**	72	1	**0**	**0**	1
23	1	1	1	1	73	**0**	**0**	1	1
24	1	**0**	1	1	74	**0**	**0**	**0**	**0**
25	1	1	1	1	75	1	1	1	**0***
26	1	1	1	**0***	76	**0**	1	1	**0**
27	**0**	1	1	**0**	77	1	**0**	1	**0**
28	1	1	1	1	78	**0***	1	**0**	**0***
29	**0**	1	1	**0**	79	1	1	**0**	**0***
30	1	1	**0**	1	80	**0**	**0**	1	1
31	**0**	**0**	1	1	81	1	**0**	**0**	**0**
32	1	1	**0**	**0**	82	**0**	1	1	1
33	**0**	1	1	1	83	1	**0**	1	**0**
34	1	**0**	1	1	84	**0***	**0**	1	1
35	1	**0**	1	1	85	1	1	**0**	1
36	1	1	**0**	**0***	86	1	1	1	**0**
37	**0**	1	1	1	87	**0**	**0**	1	1
38	**0**	**0**	1	1	88	**0**	**0**	1	**0***
39	1	1	1	1	89	1	1	**0**	**0**
40	1	1	**0***	1	90	1	1	1	**0***
41	1	1	**0**	1	91	1	1	1	1
42	1	1	1	1	92	1	1	1	1
43	**0**	**0**	**0**	**0**	93	**0***	1	1	1
44	**0**	1	**0**	1	94	1	**0**	**0**	**0**
45	1	1	**0**	**0***	95	1	1	1	**0**
46	**0**	**0**	**0**	**0**	96	**0**	1	1	1
47	**0**	**0**	1	1	97	1	**0***	1	1
48	1	**0**	**0**	1	98	1	1	**0**	1
49	1	1	**0**	**0***	99	**0**	1	1	**0***
50	**0**	**0**	1	**0***	100	**0**	**0**	1	1
					Total not converging	59	58	61	51
					Total critical errors	7	3	3	23

The total number of models not converging generally remains constant up until the data has more than 50% zeroes, at which point convergence drops off and the number of critical errors in particular increases substantially. A critical error can occur in the model when the solution becomes unstable and the log-likelihood drops, which may be a result of data being unintentionally scrambled during transformation, attempting to fit an illogical model, incorrect specification of the **B** matrix or in the worst case scenario, the Expectation-Maximisation (EM) algorithm has not worked (Holmes *et al*., 2012). Since model specification and data simulation methodology was kept constant for all the datasets, the most likely reason for these errors is the failure of the EM algorithm. Additionally, there appears to be no systematic pattern in failure to converge resulting from the sequential addition of zeroes from 0-75% for each dataset; i.e. failure to converge at 25% zeroes does not imply failure to converge with the addition of further zeroes to the data.

Missing values

Data was simulated using the same methods as the previous section to investigate the impact of the frequency of missing values on MARSS model convergence but instead of zeroes, NAs were used to indicate a missing value. Similarly, maximum iterations were set to 2000 and the models examined for convergence. A summary table of the results is provided below (1 indicates successful convergence, red 0's indicate failure to converge and * indicates critical errors in convergence).

Dataset	No missing	25% missing	50% missing	75% missing	Dataset	No missing	25% missing	50% missing	75% missing
1	1	1	**0**	1	51	**0**	1	**0**	1
2	**0**	1	**0**	**0**	52	1	1	**0**	**0***
3	**0***	**0**	**0**	1	53	1	**0**	1	1
4	**0**	**0**	1	1	54	1	**0**	**0**	**0**
5	**0**	**0**	1	1	55	**0**	1	**0**	1
6	1	1	1	1	56	1	**0**	1	**0**
7	1	**0**	**0**	1	57	1	**0**	1	1

8	1	1	1	**0***	58	1	1	1	1
9	1	**0***	**0***	**0***	59	1	1	1	**0***
10	**0**	1	1	**0***	60	**0**	1	1	**0**
11	**0**	**0**	1	1	61	**0***	**0**	1	1
12	1	**0**	1	1	62	1	**0**	**0**	**0***
13	**0**	1	1	1	63	**0**	**0**	**0**	**0**
14	1	**0**	1	**0**	64	1	**0**	**0**	1
15	1	**0**	1	**0**	65	**0***	1	**0***	1
16	1	**0**	**0**	1	66	**0**	**0**	1	0
17	**0**	1	**0**	**0**	67	0	1	1	**0***
18	**0**	1	**0**	1	68	1	1	1	1
19	1	**0**	**0**	1	69	1	1	1	1
20	**0**	**0**	**0**	1	70	1	1	1	1
21	1	1	1	**0***	71	1	**0**	1	**0**
22	**0**	1	1	1	72	**0***	**0**	1	1
23	1	1	**0**	1	73	1	**0**	1	1
24	1	1	1	1	74	**0**	1	1	1
25	1	1	1	**0***	75	1	1	**0**	1
26	1	1	1	1	76	**0**	**0**	1	**0**
27	1	1	1	1	77	1	1	1	1
28	**0**	**0**	1	**0***	78	1	1	**0**	**0***
29	1	1	1	1	79	1	**0**	**0**	**0***
30	1	**0**	**0**	**0**	80	1	1	**0**	1
31	1	1	1	1	81	**0**	1	**0**	**0***
32	**0**	**0**	**0**	1	82	1	1	1	1
33	**0**	**0**	**0**	1	83	1	1	1	**0***
34	**0**	1	1	1	84	**0**	1	**0**	1
35	1	1	0	**0**	85	1	1	**0**	**0**
36	1	1	1	**0***	86	**0**	1	1	1
37	**0***	**0**	**0**	**0***	87	**0**	1	1	**0***
38	1	**0**	**0**	**0**	88	1	1	**0**	**0**
39	1	**0**	1	**0**	89	1	1	1	**0**
40	**0**	**0**	1	1	90	1	**0***	1	1
41	1	1	1	**0**	91	**0**	1	**0**	**0***
42	1	**0***	1	1	92	**0**	1	**0**	1
43	1	**0**	1	1	93	1	**0**	1	1
44	1	1	1	1	94	1	1	1	**0**
45	**0**	1	1	1	95	1	1	1	1
46	**0**	1	1	1	96	**0**	**0**	1	1
47	**0**	1	**0**	1	97	1	1	1	1
48	1	**0**	1	1	98	1	1	**0**	**0**
49	1	1	**0**	**0**	99	1	**0**	**0**	**0***
50	1	1	1	**0**	100	**0**	**0**	1	**0**
Total not converging						61	58	61	57
Total critical errors						5	3	2	19

The number of overall models converging generally remains constant despite the number of missing values; however as with the previous result, the number of critical errors increases substantially with more than 50% missing values and there is no systematic increase in the failure to converge with increasing the frequency of missing values.

It is important to note that the simulated data produced using pre-specified parameters (atypically large observation error R and mean-reversion B) was intended to resemble abundances for *T. glaucifolia* rather than explore a variety of different parameters and data simulations, and this result may not apply to all time series traces. In addition, it is plausible for models to achieve convergence at iterations well beyond 2000, but given the number of datasets and time constraints, convergence beyond 2000 iterations was not investigated. In terms of critical errors, it would appear in this case that 50% or fewer zeroes or missing values has no substantial or consistent impact on the convergence properties or the failure of the EM algorithm. A more systematic, in-depth, stand-alone investigation may wish to establish a formal relationship between convergence properties and frequency of zeroes or missing values for a number of different parameter combinations but this is outside the scope of the current study.

References

Holmes, E.E., Ward, E.J. and Scheuerell, M.D. (2012) Analysis of multivariate time-series using the MARSS package. Version 3.4. http://cran.r-project.org/web/packages/MARSS.

Appendix 3

How to apply multivariate autoregressive state-space models to time series count data to improve population monitoring

Appendix 3-1: Location of the four study sites at Main Camp, Field River South, South Site, and Carlo Shitty (CSh) on Carlo Station and Ethabuka Reserve, Simpson Desert, Australia. Inset shows location of study region in Australia.

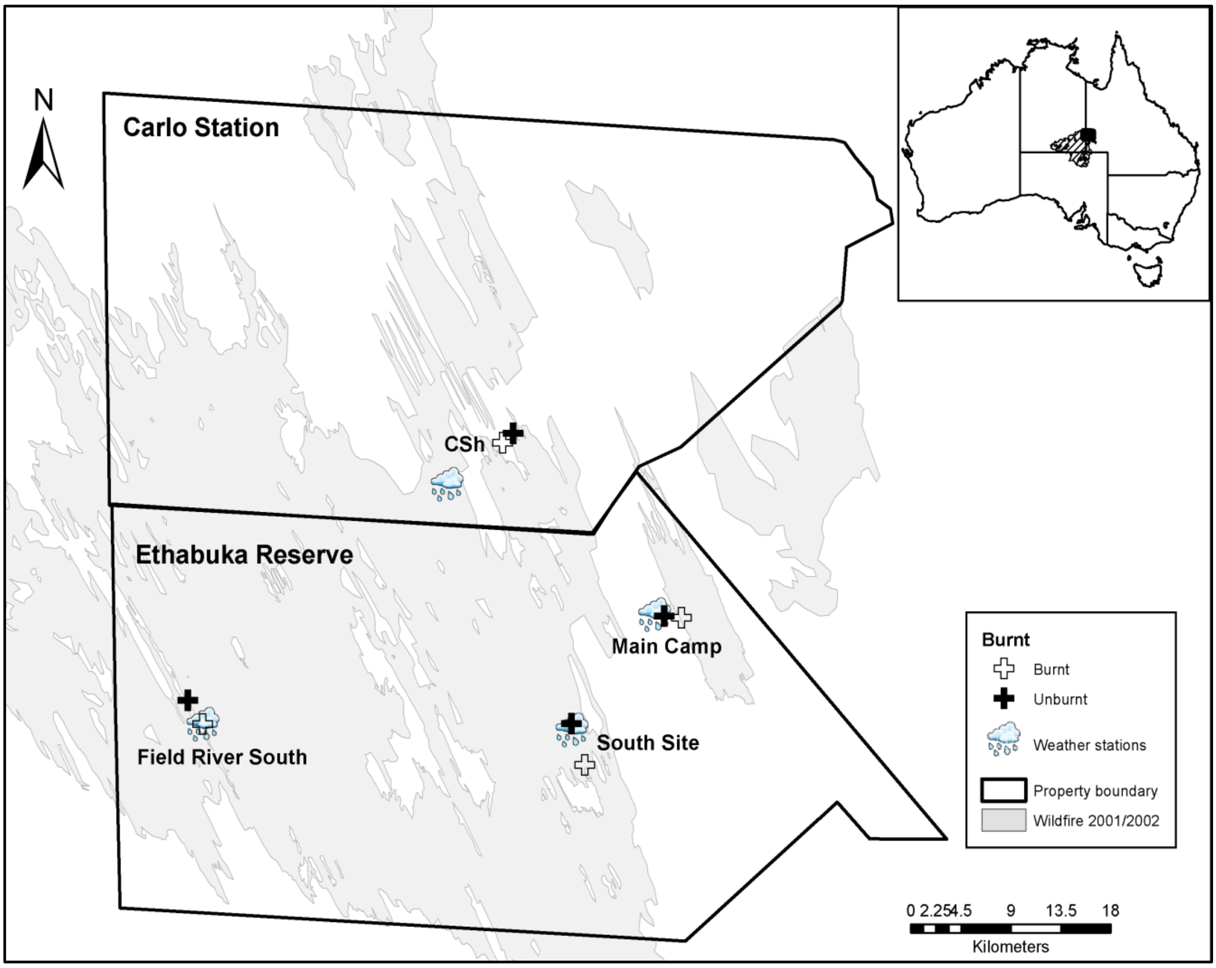

Appendix 3-2: Model selection criterion (DIC only) and parameter estimates for models with observation process drawn from overdispersed Poisson and negative binomial distributions for Main Camp.

Model	States (m)	Normal	Poisson	Negative Bin
Wildfire	4	**3277**	3851	6469
Whole site	2	3324	3832	6391
Unstructured	1	3602	3833	7405

		Normal	Poisson	Negative Bin	Normal	Poisson	Negative Bin
Site	**Stage**		**Q**			**U**	
MC-B	Seed bank	1.26 (0.30, 3.67)	2.03 (0.43, 6.45)	0.72 (0.21, 2.09)	1.10 (-0.35, 2.49)	0.68 (-0.92, 2.30)	0.57 (-0.88, 2.24)
	Plants	4.94 (2.31, 10.10)	121.26 (33.55, 369.05)	71.33 (24.16, 179.63)	0.24 (-1.00, 1.49)	-0.19 (-1.87, 1.42)	0.45 (-1.24, 2.49)
MC-U	Seed bank	1.31 (0.26, 4.33)	3.34 (0.40, 11.86)	1.12 (0.16, 4.20)	0.65 (-0.99, 2.20)	-0.17 (-1.83, 1.66)	0.62 (-1.16, 2.06)
	Plants	3.65 (1.75, 7.51)	99.54 (26.02, 309.31)	58.02 (18.20, 151.94)	-0.00 (-1.13, 1.11)	-0.51 (-2.07, 1.01)	-0.94 (-2.51, 0.60)

Appendix 3-3: Full MARSS model formulations for rainfall models, local wildfire models, and regional models, and JAGS code.

Rainfall

Local rainfall model (*m* = 4)

State model:

$$\begin{bmatrix} X_{Main,t} \\ X_{Field,t} \\ X_{Carlo,t} \\ X_{South,t} \end{bmatrix} = \begin{bmatrix} X_{Main,t-1} \\ X_{Field,t-1} \\ X_{Carlo,t-1} \\ X_{South,t-1} \end{bmatrix} + \begin{bmatrix} \mu_{Main} \\ \mu_{Field} \\ \mu_{Carlo} \\ \mu_{South} \end{bmatrix} + \begin{bmatrix} w_{Main,t} \\ w_{Field,t} \\ w_{Carlo,t} \\ w_{South,t} \end{bmatrix}; \quad \mathbf{w}_t \sim MVN(\mathbf{0}, \mathbf{Q})$$

$$\mathbf{Q} = \begin{bmatrix} q^2_{Main} & q_{Main,Field} & q_{Main,Carlo} & q_{Main,South} \\ q_{Main,Field} & q^2_{Field} & q_{Field,Carlo} & q_{Field,South} \\ q_{Main,Carlo} & q_{Field,Carlo} & q^2_{Carlo} & q_{Carlo,South} \\ q_{Main,South} & q_{Field,South} & q_{Carlo,South} & q^2_{South} \end{bmatrix}$$

Observation model:

$$\begin{bmatrix} Y_{Main,t} \\ Y_{Field,t} \\ Y_{Carlo,t} \\ Y_{South,t} \end{bmatrix} = \begin{bmatrix} 1 & 0 & 0 & 0 \\ 0 & 1 & 0 & 0 \\ 0 & 0 & 1 & 0 \\ 0 & 0 & 0 & 1 \end{bmatrix} \begin{bmatrix} X_{Main,t} \\ X_{Field,t} \\ X_{Carlo,t} \\ X_{South,t} \end{bmatrix} + \begin{bmatrix} v_{Main,t} \\ v_{Field,t} \\ v_{Carlo,t} \\ v_{South,t} \end{bmatrix}; \quad \mathbf{v}_t \sim MVN(\mathbf{0}, \mathbf{R})$$

$$\mathbf{R} = \begin{bmatrix} r^2_{Main} & 0 & 0 & 0 \\ 0 & r^2_{Field} & 0 & 0 \\ 0 & 0 & r^2_{Carlo} & 0 \\ 0 & 0 & 0 & r^2_{South} \end{bmatrix}$$

Regional rainfall model (*m* = 1)

State model:

$$X_{Region,t} = X_{Region,t-1} + \mu_{Region,t} + w_{Region,t}\,; \quad w_{Region,t} \sim N(0, Q)$$

Observation model:

$$\begin{bmatrix} Y_{Main,t} \\ Y_{Field,t} \\ Y_{Carlo,t} \\ Y_{South,t} \end{bmatrix} = \begin{bmatrix} 1 \\ 1 \\ 1 \\ 1 \end{bmatrix} \begin{bmatrix} X_{Region,t} \end{bmatrix} + \begin{bmatrix} v_{Main,t} \\ v_{Field,t} \\ v_{Carlo,t} \\ v_{South,t} \end{bmatrix}; \quad \mathbf{v}_t \sim MVN(\mathbf{0}, \mathbf{R})$$

$$\mathbf{R} = \begin{bmatrix} r_{Main}^2 & 0 & 0 & 0 \\ 0 & r_{Field}^2 & 0 & 0 \\ 0 & 0 & r_{Carlo}^2 & 0 \\ 0 & 0 & 0 & r_{South}^2 \end{bmatrix}$$

Local wildfire models – Main Camp example

Wildfire model (*m* = 4)

B = Burnt U = Unburnt

SB = Seed bank PL = Plants

State model:

$$\begin{bmatrix} X_{B\_SB,t} \\ X_{U\_SB,t} \\ X_{B\_PL,t} \\ X_{U\_PL,t} \end{bmatrix} = \begin{bmatrix} X_{B\_SB,t-1} \\ X_{U\_SB,t-1} \\ X_{B\_PL,t-1} \\ X_{U\_PL,t-1} \end{bmatrix} + \begin{bmatrix} \mu_{B\_SB} \\ \mu_{U\_SB} \\ \mu_{B\_PL} \\ \mu_{U\_PL} \end{bmatrix} + \begin{bmatrix} w_{B\_SB,t} \\ w_{U\_SB,t} \\ w_{B\_PL,t} \\ w_{U\_PL,t} \end{bmatrix}; \quad \mathbf{w}_t \sim MVN(\mathbf{0}, \mathbf{Q})$$

$$\mathbf{Q} = \begin{bmatrix} q_{B\_SB}^2 & q_{B\_SB,U\_SB} & q_{B\_SB,B\_PL} & q_{B\_SB,U\_PL} \\ q_{B\_SB,U\_SB} & q_{U\_SB}^2 & q_{U\_SB,B\_PL} & q_{U\_SB,U\_PL} \\ q_{B\_SB,B\_PL} & q_{U\_SB,B\_PL} & q_{B\_PL}^2 & q_{B\_PL,U\_PL} \\ q_{B\_SB,U\_PL} & q_{U\_SB,U\_PL} & q_{B\_PL,U\_PL} & q_{U\_PL}^2 \end{bmatrix}$$

Observation model:

$$\begin{bmatrix} Y_{B\_SB,plot\ 1,t} \\ \vdots \\ Y_{B\_SB,plot\ 15,t} \\ Y_{U\_SB,plot\ 1,t} \\ \vdots \\ Y_{U\_SB,plot\ 15,t} \\ Y_{B\_PL,plot\ 1,t} \\ \vdots \\ \vdots \\ Y_{U\_PL,plot\ 15,t} \end{bmatrix} = \begin{bmatrix} 1 & 0 & 0 & 0 \\ 0 & 1 & 0 & 0 \\ 0 & 0 & 1 & 0 \\ 0 & 0 & 0 & 1 \end{bmatrix} \begin{bmatrix} X_{B\_SB,t} \\ X_{U\_SB,t} \\ X_{B\_PL,t} \\ X_{U\_PL,t} \end{bmatrix} + \mathbf{A} + \begin{bmatrix} v_{B\_SB,t} \\ v_{U\_SB,t} \\ v_{B\_PL,t} \\ v_{U\_PL,t} \end{bmatrix}; \quad \mathbf{v}_t \sim MVN(\mathbf{0}, \mathbf{R})$$

$$\mathbf{R} = \begin{bmatrix} r_{B\_SB}^2 & 0 & 0 & 0 \\ 0 & r_{U\_SB}^2 & 0 & 0 \\ 0 & 0 & r_{B\_PL}^2 & 0 \\ 0 & 0 & 0 & r_{U\_PL}^2 \end{bmatrix}$$

Note: **Z** is actually a 60 × 4 (*n* × *m*) matrix whereby each row represents 15 repetitions of each entry. For example, the first row is repeated 15 times and relates the 15 plots of B_SB observations to the state $X_{B\_SB,t}$, the second row repeated 15 times relates the 15 plots of U_SB observations to the state $X_{U\_SB,t}$ and so on. The **A** matrix is a 60 × 1 column vector of estimates for the bias parameter for each observation, whereby the first observation for each state (i.e. the 1st, 16th, 31st, and 46th entries) equals 0.

Whole site model (*m* = 2)

SB = Seed bank PL = Plants

State model:

$$\begin{bmatrix} X_{SB,t} \\ X_{PL,t} \end{bmatrix} = \begin{bmatrix} X_{SB,t-1} \\ X_{PL,t-1} \end{bmatrix} + \begin{bmatrix} \mu_{SB,t} \\ \mu_{PL,t} \end{bmatrix} + \begin{bmatrix} w_{SB,t} \\ w_{PL,t} \end{bmatrix}; \quad \mathbf{w}_t \sim MVN(\mathbf{0}, \mathbf{Q})$$

$$\mathbf{Q} = \begin{bmatrix} q_{SB}^2 & q_{SB,PL} \\ q_{SB,PL} & q_{PL}^2 \end{bmatrix}$$

Observation model:

$$\begin{bmatrix} Y_{B\_SB,plot\ 1,t} \\ \vdots \\ Y_{B\_SB,plot\ 15,t} \\ Y_{U\_SB,plot\ 1,t} \\ \vdots \\ Y_{U\_SB,plot\ 15,t} \\ Y_{B\_PL,plot\ 1,t} \\ \vdots \\ \vdots \\ Y_{U\_PL,plot\ 15,t} \end{bmatrix} = \begin{bmatrix} 1 & 0 \\ 1 & 0 \\ 0 & 1 \\ 0 & 1 \end{bmatrix} \begin{bmatrix} X_{SB,t} \\ X_{PL,t} \end{bmatrix} + \mathbf{A} + \begin{bmatrix} v_{SB,t} \\ v_{PL,t} \end{bmatrix}; \quad \mathbf{v}_t \sim MVN(\mathbf{0}, \mathbf{R})$$

$$\mathbf{R} = \begin{bmatrix} r_{B\_SB}^2 & 0 & 0 & 0 \\ 0 & r_{U\_SB}^2 & 0 & 0 \\ 0 & 0 & r_{B\_PL}^2 & 0 \\ 0 & 0 & 0 & r_{U\_PL}^2 \end{bmatrix}$$

Note: **Z** is actually a 60 × 2 ($n \times m$) matrix whereby each row represents 15 repetitions of each entry. For example, the first two rows are both repeated 15 times and relate the 15 plots of B_SB observations and 15 plots of U_SB observations to the state $X_{SB,t}$. Similarly, rows 3 and 4 are both repeated 15 times and relate the 15 plots of B_PL observations and 15 plots of U_PL observations to the state $X_{PL,t}$. The **A** matrix is a 60 × 1 column vector of estimates for the bias parameter for each observation, whereby the first observation for each state (i.e the 1st and 31st entries) equals 0.

Unstructured model (*m* = 1)

State model:

$$X_{Pop,t} = X_{Pop,t-1} + \mu_{Pop,t} + w_{Pop,t}\ ; \quad w_{Pop,t} \sim N(0, Q)$$

Observation model:

$$\begin{bmatrix} Y_{B\_SB,plot\ 1,t} \\ Y_{B\_SB,plot\ 2,t} \\ \vdots \\ Y_{B\_SB,plot\ 15,t} \\ Y_{B\_PL,plot\ 1,t} \\ \vdots \\ Y_{U\_PL,plot\ 15,t} \end{bmatrix} = \begin{bmatrix} 1 \\ 1 \\ 1 \\ 1 \end{bmatrix} \begin{bmatrix} X_{Pop,t} \end{bmatrix} + \ \mathbf{A} + \begin{bmatrix} v_{SB,t} \\ v_{PL,t} \end{bmatrix}; \ \ \mathbf{v}_t \sim MVN(\mathbf{0}, \mathbf{R})$$

$$\mathbf{R} = \begin{bmatrix} r^2_{B\_SB} & 0 & 0 & 0 \\ 0 & r^2_{B\_PL} & 0 & 0 \\ 0 & 0 & r^2_{U\_SB} & 0 \\ 0 & 0 & 0 & r^2_{U\_PL} \end{bmatrix}$$

Note: **Z** is actually a 60 × 1 column vector whereby all observations relate to the single state $X_{pop,t}$. The **A** matrix is a 60 × 1 column vector of estimates for the bias parameter for each observation, whereby the first entry equals 0.

Regional models

Independent site model (*m* = 8)

MC = Main Camp FR = Field River CS = Carlo Shitty SS = South Site

B = Burnt U = Unburnt SB = Seed bank PL = Plant

State model:

$$\begin{bmatrix} X_{MC\_SB,t} \\ X_{MC\_PL,t} \\ X_{FR\_SB,t} \\ X_{FR\_PL,t} \\ X_{CS\_SB,t} \\ X_{CS\_PL,t} \\ X_{SS\_SB,t} \\ X_{SS\_PL,t} \end{bmatrix} = \begin{bmatrix} X_{MC\_SB,t-1} \\ X_{MC\_PL,t-1} \\ X_{FR\_SB,t-1} \\ X_{FR\_PL,t-1} \\ X_{CS\_SB,t-1} \\ X_{CS\_PL,t-1} \\ X_{SS\_SB,t-1} \\ X_{SS\_PL,t-1} \end{bmatrix} \begin{bmatrix} \mu_{MC\_SB} \\ \mu_{MC\_PL} \\ \mu_{FR\_SB} \\ \mu_{FR\_PL} \\ \mu_{CS\_SB} \\ \mu_{CS\_PL} \\ \mu_{SS\_SB} \\ \mu_{SS\_PL} \end{bmatrix} + \begin{bmatrix} w_{MC\_SB,t} \\ w_{MC\_PL,t} \\ w_{FR\_SB,t} \\ w_{FR\_PL,t} \\ w_{CS\_SB,t} \\ w_{CS\_PL,t} \\ w_{SS\_SB,t} \\ w_{SS\_PL,t} \end{bmatrix}; \quad \mathbf{w}_t \sim MVN(\mathbf{0}, \mathbf{Q})$$

$$\mathbf{Q} = \begin{bmatrix} q^2_{MC\_SB} & \cdots & q^2_{MC\_SB,SS\_PL} \\ \vdots & \ddots & \vdots \\ q^2_{MC\_SB,SS\_PL} & \cdots & q^2_{SS\_PL} \end{bmatrix}$$

Observation model:

$$\begin{bmatrix} Y_{MC\_B\_SB,plot\ 1,t} \\ \vdots \\ Y_{MC\_B\_SB,plot\ 15,t} \\ Y_{MC\_U\_SB,plot\ 1,t} \\ \vdots \\ Y_{MC\_U\_SB,plot\ 15,t} \\ Y_{MC\_B\_PL,plot\ 1,t} \\ \vdots \\ Y_{MC\_B\_PL,plot\ 15,t} \\ Y_{MC\_U\_PL,plot\ 1,t} \\ \vdots \\ Y_{MC\_U\_PL,plot\ 15,t} \\ Y_{FR\_B\_SB,plot\ 1,t} \\ \vdots \\ \vdots \\ Y_{SS\_U\_PL,plot\ 15,t} \end{bmatrix}$$

$$= \begin{bmatrix} 1 & 0 & 0 & 0 & 0 & 0 & 0 & 0 \\ 1 & 0 & 0 & 0 & 0 & 0 & 0 & 0 \\ 0 & 1 & 0 & 0 & 0 & 0 & 0 & 0 \\ 0 & 1 & 0 & 0 & 0 & 0 & 0 & 0 \\ 0 & 0 & 1 & 0 & 0 & 0 & 0 & 0 \\ 0 & 0 & 1 & 0 & 0 & 0 & 0 & 0 \\ 0 & 0 & 0 & 1 & 0 & 0 & 0 & 0 \\ 0 & 0 & 0 & 1 & 0 & 0 & 0 & 0 \\ 0 & 0 & 0 & 0 & 1 & 0 & 0 & 0 \\ 0 & 0 & 0 & 0 & 1 & 0 & 0 & 0 \\ 0 & 0 & 0 & 0 & 0 & 1 & 0 & 0 \\ 0 & 0 & 0 & 0 & 0 & 1 & 0 & 0 \\ 0 & 0 & 0 & 0 & 0 & 0 & 1 & 0 \\ 0 & 0 & 0 & 0 & 0 & 0 & 1 & 0 \\ 0 & 0 & 0 & 0 & 0 & 0 & 0 & 1 \\ 0 & 0 & 0 & 0 & 0 & 0 & 0 & 1 \end{bmatrix} \begin{bmatrix} X_{MC\_SB,t} \\ X_{MC\_PL,t} \\ X_{FR\_SB,t} \\ X_{FR\_PL,t} \\ X_{CS\_SB,t} \\ X_{CS\_PL,t} \\ X_{SS\_SB,t} \\ X_{SS\_PL,t} \end{bmatrix} + \mathbf{A}$$

$$+ \begin{bmatrix} v_{MC\_SB,t} \\ v_{MC\_PL,t} \\ v_{FR\_SB,t} \\ v_{FR\_PL,t} \\ v_{CS\_SB,t} \\ v_{CS\_PL,t} \\ v_{SS\_SB,t} \\ v_{SS\_PL,t} \end{bmatrix}; \mathbf{v}_t \sim MVN(\mathbf{0}, \mathbf{R})$$

$$\mathbf{R} = \begin{bmatrix} r^2_{MC\_SB} & \cdots & 0 \\ \vdots & \ddots & \vdots \\ 0 & \cdots & r^2_{SS\_PL} \end{bmatrix}$$

Note: **Z** is actually 240 × 8 (*n* × *m*) matrix whereby each row represents 15 repetitions of each entry. For example, the first two rows are both repeated 15 times and relate the 15 plots of MC_B_SB observations and 15 plots of MC_U_SB observations to the state $X_{MC\_SB,t}$, rows

3 and 4 are both repeated 15 times and relate the 15 plots of MC_B_PL observations and 15 plots of MC_U_PL observations to the state $X_{MC\_PL,t}$, and so on for Field River, Carlo Shitty and South Site. The **A** matrix is a 240 × 1 column vector of estimates for the bias parameter for each observation, whereby the first observation for each state equals 0.

Regional fire model (*m* = 4)

MC = Main Camp	FR = Field River	CS = Carlo Shitty	SS = South Site
B = Burnt	U = Unburnt	SB = Seed bank	PL = Plant

State model:

$$\begin{bmatrix} X_{B\_SB,t} \\ X_{U\_SB,t} \\ X_{B\_PL,t} \\ X_{U\_PL,t} \end{bmatrix} = \begin{bmatrix} X_{B\_SB,t-1} \\ X_{U\_SB,t-1} \\ X_{B\_PL,t-1} \\ X_{U\_PL,t-1} \end{bmatrix} + \begin{bmatrix} \mu_{B\_SB} \\ \mu_{U\_SB} \\ \mu_{B\_PL} \\ \mu_{U\_PL} \end{bmatrix} + \begin{bmatrix} w_{B\_SB,t} \\ w_{U\_SB,t} \\ w_{B\_PL,t} \\ w_{U\_PL,t} \end{bmatrix}; \quad \mathbf{w}_t \sim MVN(\mathbf{0}, \mathbf{Q})$$

$$\mathbf{Q} = \begin{bmatrix} q_{B\_SB}^2 & q_{B\_SB,U\_SB} & q_{B\_SB,B\_PL} & q_{B\_SB,U\_PL} \\ q_{B\_SB,U\_SB} & q_{U\_SB}^2 & q_{U\_SB,B\_PL} & q_{U\_SB,U\_PL} \\ q_{B\_SB,B\_PL} & q_{U\_SB,B\_PL} & q_{B\_PL}^2 & q_{B\_PL,U\_PL} \\ q_{B\_SB,U\_PL} & q_{U\_SB,U\_PL} & q_{B\_PL,U\_PL} & q_{U\_PL}^2 \end{bmatrix}$$

Observation model:

$$\begin{bmatrix} Y_{MC\_B\_SB,plot\ 1,t} \\ \vdots \\ Y_{MC\_B\_SB,plot\ 15,t} \\ Y_{MC\_U\_SB,plot\ 1,t} \\ \vdots \\ Y_{MC\_U\_SB,plot\ 15,t} \\ Y_{MC\_B\_PL,plot\ 1,t} \\ \vdots \\ Y_{MC\_B\_PL,plot\ 15,t} \\ Y_{MC\_U\_PL,plot\ 1,t} \\ \vdots \\ Y_{MC\_U\_PL,plot\ 15,t} \\ Y_{FR\_B\_SB,plot\ 1,t} \\ \vdots \\ \vdots \\ Y_{SS\_U\_PL,plot\ 15,t} \end{bmatrix} = \begin{bmatrix} 1 & 0 & 0 & 0 \\ 0 & 1 & 0 & 0 \\ 0 & 0 & 1 & 0 \\ 0 & 0 & 0 & 1 \\ 1 & 0 & 0 & 0 \\ 0 & 1 & 0 & 0 \\ 0 & 0 & 1 & 0 \\ 0 & 0 & 0 & 1 \\ 1 & 0 & 0 & 0 \\ 0 & 1 & 0 & 0 \\ 0 & 0 & 1 & 0 \\ 0 & 0 & 0 & 1 \\ 1 & 0 & 0 & 0 \\ 0 & 1 & 0 & 0 \\ 0 & 0 & 1 & 0 \\ 0 & 0 & 0 & 1 \end{bmatrix} \begin{bmatrix} X_{B\_SB,t} \\ X_{U\_SB,t} \\ X_{B\_PL,t} \\ X_{U\_PL,t} \end{bmatrix} + \mathbf{A} + \begin{bmatrix} v_{B\_SB,t} \\ v_{U\_SB,t} \\ v_{B\_PL,t} \\ v_{U\_PL,t} \end{bmatrix}; \mathbf{v}_t \sim MVN(\mathbf{0}, \mathbf{R})$$

$$\mathbf{R} = \begin{bmatrix} r_{MC\_SB}^2 & \cdots & 0 \\ \vdots & \ddots & \vdots \\ 0 & \cdots & r_{SS\_PL}^2 \end{bmatrix}$$

Note: **Z** is actually a 240 × 4 ($n \times m$) matrix in which the first consecutive string of 1's in the first column relates the 15 burnt plots in Main Camp of the seed bank to the state estimate for $X_{B\_SB,t}$, the second column relates the 15 burnt plots in Main Camp of the above ground plants to the state estimate for $X_{B\_PL,t}$, the third column relates the 15 unburnt plots in Main Camp of the seed bank to the state estimate for $X_{U\_SB,t}$ and the fourth column relates the 15 unburnt plots in Main Camp of the above ground plants to the state estimate for $X_{U\_PL,t}$ and so on for Field River, Carlo Shitty and South Site. The **A** matrix is a 240 × 1 column vector of estimates for the bias parameter for each observation, whereby the first observation for each state equals 0.

Overall region model (m = 2)

MC = Main Camp	FR = Field River	CS = Carlo Shitty	SS = South Site
B = Burnt	U = Unburnt	SB = Seed bank	PL = Plant

State model:

$$\begin{bmatrix} X_{SB,t} \\ X_{PL,t} \end{bmatrix} = \begin{bmatrix} X_{SB,t-1} \\ X_{PL,t-1} \end{bmatrix} + \begin{bmatrix} \mu_{SB} \\ \mu_{PL} \end{bmatrix} + \begin{bmatrix} w_{SB,t} \\ w_{PL,t} \end{bmatrix}; \quad \mathbf{w}_t \sim MVN(\mathbf{0}, \mathbf{Q})$$

Observation model:

$$\begin{bmatrix} Y_{MC\_B\_SB,plot\ 1,t} \\ \vdots \\ Y_{MC\_B\_SB,plot\ 15,t} \\ Y_{MC\_U\_SB,plot\ 1,t} \\ \vdots \\ Y_{MC\_U\_SB,plot\ 15,t} \\ Y_{MC\_B\_PL,plot\ 1,t} \\ \vdots \\ Y_{MC\_B\_PL,plot\ 15,t} \\ Y_{MC\_U\_PL,plot\ 1,t} \\ \vdots \\ Y_{MC\_U\_PL,plot\ 15,t} \\ Y_{FR\_B\_SB,plot\ 1,t} \\ \vdots \\ \vdots \\ Y_{SS\_U\_PL,plot\ 15,t} \end{bmatrix} = \begin{bmatrix} 1 & 0 \\ \vdots & \vdots \\ 0 & 1 \\ \vdots & \vdots \\ 1 & 0 \\ \vdots & \vdots \\ 0 & 1 \\ \vdots & \vdots \\ 1 & 0 \\ \vdots & \vdots \\ 0 & 1 \\ \vdots & \vdots \\ 1 & 0 \\ \vdots & \vdots \\ 0 & 1 \\ \vdots & \vdots \\ 0 & 1 \end{bmatrix} \begin{bmatrix} X_{SB,t} \\ X_{PL,t} \end{bmatrix} + \begin{bmatrix} v_{SB,t} \\ v_{PL,t} \end{bmatrix}; \quad \mathbf{v}_t \sim MVN(\mathbf{0}, \mathbf{R})$$

$$\mathbf{R} = \begin{bmatrix} r^2_{MC\_SB} & \cdots & 0 \\ \vdots & \ddots & \vdots \\ 0 & \cdots & r^2_{SS\_PL} \end{bmatrix}$$

Note: **Z** is a 240 × ($n \times m$) matrix in which the first consecutive string of 1's is 30 repetitions long and relates the 30 plots (combined burnt and unburnt) in Main Camp of the seed bank to the state estimate $X_{SB,t}$, the second column relates the 30 plots (combined burnt and unburnt) in Main Camp of the above ground plants to the state estimate $X_{PL,t}$, and so on for Field River, Carlo Shitty and South Site.

Jags script for Bayesian MARSS models

```
# ========================
# Set jags parameters
# ========================

# MCMC parameters
mcmcchains <- 3
mcmcthin <- 10
mcmcburn <- 5000
samples2Save <- 20000

# ================================
#     Local wildfire models
# ================================

# NOTE: Regional models follow the same structure, parameters and priors, but specification of the A
parameter and certain loops differ

# Set parameters
jags.params = c("x", "U","sigmaQ","sigmaR", "A", "B","Dsum")
jags.params.cov = c("x", "U","sigmaQ","sigmaR", "A", "B", "C", "Dsum")
jags.data = list("y","n.pop","n.t","n.states","z", "c")

jags.local <- function() {

  # PRIORS

  # Q prior from wishart distribution: dwish ~ (omega, degrees of freedom)
  tauQ[1:n.states, 1:n.states] ~ dwish(Omega, n.states);
  for (i in 1:n.states) {
    Omega[i,i] <- 1;
  }
  for (i in 1:(n.states-1)) {
    for (j in (i+1):n.states) {
      Omega[i,j] <- 0;
      Omega[j,i] <- 0;
    }
  }

  # MVN Process error
  sigmaQ[1:n.states, 1:n.states] <- inverse(tauQ[,]); # convert from precision to sd

  # MVN prior on initial state
  x[1:n.states,1] ~ dmnorm(x.mu[], x.sigma[,]);
  for (i in 1:n.states) {
    x.mu[i] ~ dunif(0,10)
  }

  for(i in 1:n.states) {
    x.sigma[i,i] <- 1;
  }
  for (i in 1:(n.states-1)) {
    for (j in (i+1):n.states) {
      x.sigma[i,j] <- 0;
      x.sigma[j,i] <- 0;
    }
  }

  # Normal prior for growth rate
```

```
for(i in 1:n.states) {
  U[i] ~ dnorm(0,1);
}

# Uniform prior on B
for (i in 1:n.states) {
  B[i] ~ dunif(0,1)
}

# Normal prior on C
for (i in 1:n.states) {
  C[i] ~ dnorm(0,1)
}

# PROCESS MODEL
for (t in 2:n.t) {
  for (i in 1:n.states) {
    predx[i,t] <- B[i]*x[i,t-1] + U[i] + C[i]*c[i,t];
  }
  x[1:n.states,t] ~ dmnorm(predx[1:n.states,t], tauQ[,])
}

# OBSERVATION MODEL

# Priors on bias parameter
for(i in 0:(n.states-1)) {
  A[i*(n.pop/n.states)+1] <- 0;
  for (j in 2:(n.pop/n.states)) {
    A[i*(n.pop/n.states)+j] ~ dnorm(0,1);
  }
}

# Observation error (diag, unique for each site and stage)
for(i in 0:3) {
  tauR[(i*15)+1] ~ dgamma(0.001,0.001);
  tauR[(i*15)+2] <- tauR[(i*15)+1];
  tauR[(i*15)+3] <- tauR[(i*15)+1];
  tauR[(i*15)+4] <- tauR[(i*15)+1];
  tauR[(i*15)+5] <- tauR[(i*15)+1];
  tauR[(i*15)+6] <- tauR[(i*15)+1];
  tauR[(i*15)+7] <- tauR[(i*15)+1];
  tauR[(i*15)+8] <- tauR[(i*15)+1];
  tauR[(i*15)+9] <- tauR[(i*15)+1];
  tauR[(i*15)+10] <- tauR[(i*15)+1];
  tauR[(i*15)+11] <- tauR[(i*15)+1];
  tauR[(i*15)+12] <- tauR[(i*15)+1];
  tauR[(i*15)+13] <- tauR[(i*15)+1];
  tauR[(i*15)+14] <- tauR[(i*15)+1];
  tauR[(i*15)+15] <- tauR[(i*15)+1];
}
for (i in 1:n.pop) {
  sigmaR[i] <- 1/sqrt(tauR[i]);
}

# Observation error model
for (i in 1:n.pop) {
  for (t in 1:n.t) {
    predy[i,t] <- inprod(z[i,], x[,t]) + A[i];

    # LOGNORMAL DISTRIBUTION
```

```
    y[i,t] ~ dnorm(predy[i,t], tauR[i])
    # NOTE: priors and jags parameters currently set for log-normal

    # POISSON DISTRIBUTION (WITH RANDOM EFFECTS)
    # log.lambda[i,t] ~ dnorm(predy[i,t], tauR[i]);
    # y[i,t] ~ dpois(exp(log.lambda[i,t]));

    # NEGATIVE BINOMIAL DISTRIBUTION
    # lambda.nb[i,t] <- exp(predy[i,t])
    # p[i,t] <- r[i,t]/(r[i,t]+lambda.nb[i,t])
    # y[i,t] ~ dnegbin(p[i,t],r[i,t])
    # r[i,t] ~ dunif(0,100)

    # For Posterior predictive loss
    # Generate replicated data
    y.rep[i,t] ~ dnorm(predy[i,t], tauR[i]);

    # Compute squared difference b/w observed and replicated data
    sqdiff[i,t] <- pow(y[i,t]-y.rep[i,t], 2);
   }
 }
 # For posterior predictive loss, sum squared differences across all years
 Dsum <- sum(sqdiff);
}
```

Appendix 3-4. State predictions and 95% credible intervals for MARSS-MCMC regional models. Points indicate census observations averaged over 15 plots at each site, model-predicted state estimates are given by the solid line, and their 95% credible intervals by the shaded areas. Seed bank trajectories are brown and above-ground plant trajectories are green.

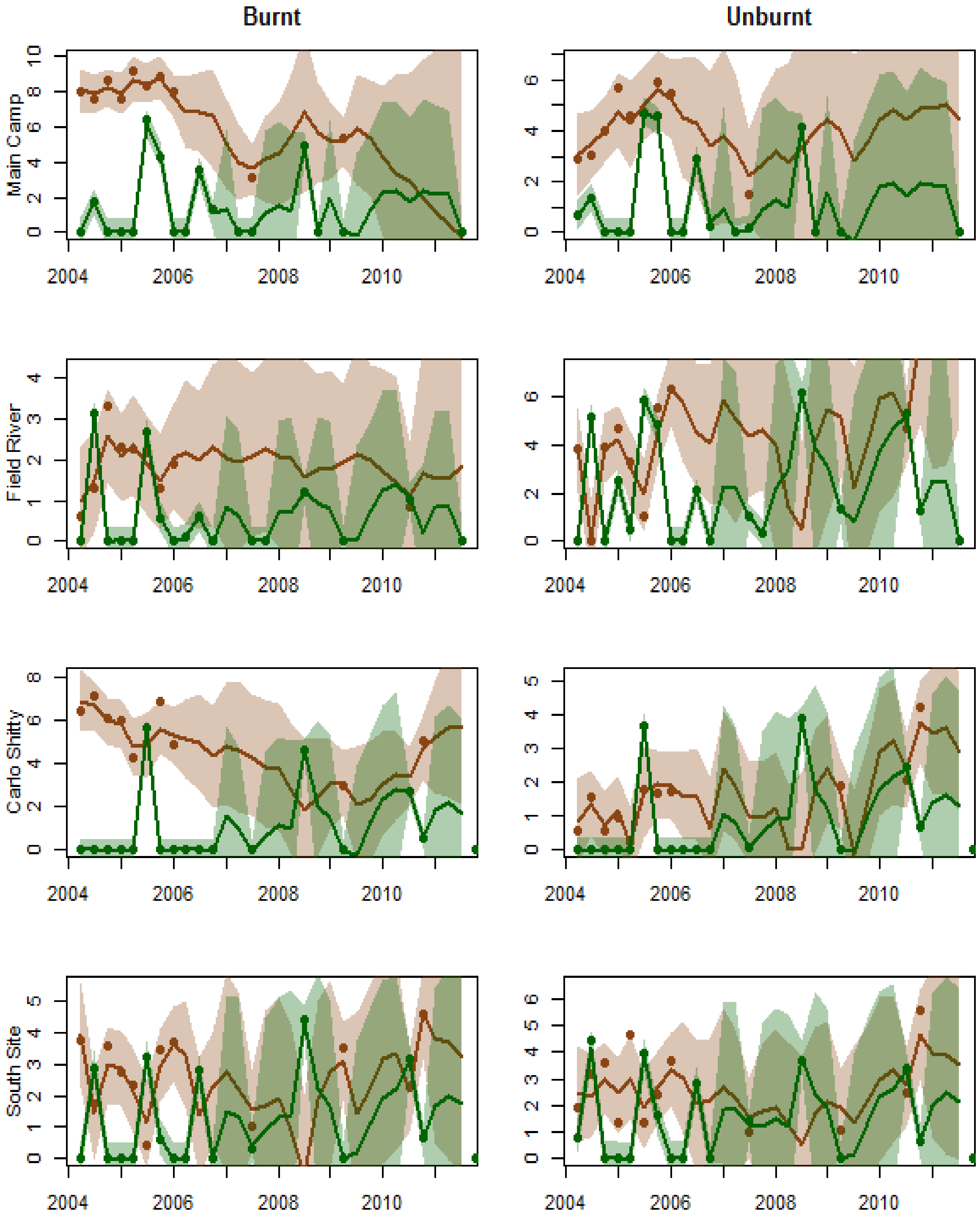

Appendix 4

Life form explains consistent temporal trends across species: the application of dynamic factor analysis

Appendix 4-1: Full species list for Main Camp, Field River and Carlo Shitty. Ticks indicate species that were present and included in dynamic factor analysis, crosses indicate species that were present but excluded from dynamic factor analysis, and blanks indicate species that were not present.

Species Name	Main Camp	Field River	Carlo Shitty
Abutilon otocarpum	✓	✓	✓
Acacia dictyophleba	✗	✓	
Acacia georginae	✗		
Acacia ligulata	✓	✓	✓
Acacia stenophylla		✗	✗
Adriana tormentosa	✗	✗	
Aristida contorta	✓	✓	✓
Atalaya hemiglauca		✗	
Blennodia canescens	✓	✗	✓
Boerhavia coccinea		✗	
Brunonia australis	✗	✓	✓
Calandrinia balonensis	✓	✓	✓
Calocephalus platycephalus	✓	✗	✓
Calotis erinacea	✗	✗	✓
Calotis hispidula	✓	✓	
Cleome viscosa	✗	✗	✗
Codonocarpus cotinifolius		✗	
Convolvulus erubescens	✗		✗
Dicrastylis costelloi	✓	✓	✓
Dodonaea viscosa	✗	✗	✗
Enneapogon polyphyllus	✗	✗	
Eragrostis dielsii	✗		
Eremophila ovata	✗		✗
Eriachne aristidea	✓	✓	✓
Eucalyptus pachyphylla			✗
Euphorbia drummondii	✓	✓	✓
Euphorbia tannensis	✓	✗	✓
Fimbristylis dichotoma	✗	✗	✗

Frankenia gracilis	✗	✗	✗
Goodenia cycloptera	✓	✓	✓
Grevillea juncifolia		✗	✗
Grevillea stenobotrya	✓	✓	✓
Grevillea striata	✗	✗	✓
Halganea cyanea		✓	
Haloragis gossei	✓	✓	✓
Helipterum floribundum	✓	✓	
Helipterum moschatum	✗		✗
Helipterum muelli	✗	✓	
Lechenaultia divaricata	✗	✗	
Lepidium phlebopetalum	✗	✓	✗
Maireana campanulata		✗	
Myriocephalus stuartii	✗	✗	
Newcastelia cephalantha	✗	✗	
Newcastelia spodiotricha	✓	✓	✗
Oldenlandia pterospora	✗	✓	✓
Othonna gregorii	✓	✓	✗
Paractaenum refractum	✓	✓	✓
Petalostylis cassioides	✗	✗	✗
Pimelea simplex	✗		
Portulaca pilosa	✗		✗
Psoralea eriantha	✗		
Pterocaulon sphacelatum	✗		
Ptilotus latifolius	✗	✗	✓
Salsola kali	✗	✗	✗
Scaevola depauperata	✓	✓	✓
Scaevola parvibarbata	✗		
Scaevola parviflora		✗	
Sclerolaena bicornis	✗	✗	
Sclerolaena eriacantha	✗	✗	✗
Sclerolaena muricata	✗	✗	✗
Senna pleurocarpa	✓	✓	✓
Setaria surgens	✗		✗
Sida fibulifera	✓	✓	✓
Sida trichopoda	✓	✓	✓
Solanum quadriloculatum	✗		
Spermacoce auriculata		✗	
Stylobasium spathulatum	✗		
Swainsona microphylla	✗	✓	✓
Swainsona phacoides	✗		
Tephrosia rosea	✓	✓	✓
Trachymene glaucifolia	✓	✓	✓
Tragus australianus	✗		
Trianthema pilosa	✗	✗	✗
Tribulus cistoides	✗		

Tribulus terrestris	✗		✗
Triodia basedowii	✓	✓	✓
Triraphis mollis	✗	✗	✗
Triumfetta winneckeana	✓	✗	✗
Velleia connata		✗	✗
Yakirra australiensis	✓	✓	✓
Zaleya galericulata		✗	
Zygochloa paradoxa		✗	✗
Zygophyllum simile	✗	✗	

Appendix 4-2: R functions used in Chapter 5 to manipulate data, conduct and produce plots for dynamic factor analysis, and construct presence/absence plots.

```
######################################
####  TYPO FIX
######################################

typo_fix = function(typos, true_values, string_distance = 1, ignore.case = FALSE) {
 require(stringdist)
 # Matrix with string distance from each typo to each true value
 if ( ignore.case == TRUE) {
  true_values_df = data.frame("True" = tolower(true_values))
  typo_stringdist = t(apply(true_values_df, 1, FUN = stringdist, tolower(typos)))
 } else {
  true_values_df = data.frame("True" = true_values)
  typo_stringdist = t(apply(true_values_df, 1, FUN = stringdist, typos))
 }

 #Vector holding replacement values and their locations
 typo_replacements = vector("character", length(typos))
 for (i in 1:length(true_values)) {
  typo_replacements[ which(typo_stringdist[i,] <= string_distance) ] = true_values[i]
 }

 to_fix = typo_replacements != ""
 typos[ to_fix ] = typo_replacements[ to_fix ]

 return(typos)
}

######################################
####  TRANSPOSE AND CLEAN DATA
######################################

t.clean = function(grid_name, dates_grid, dates_site) {
 # Remove NA's
 grid_name[ apply(grid_name, 2, is.na) ] = 0

 # Rename rownames and transpose
 rownames(grid_name) = grid_name[,1]
 grid_name = t(grid_name[sort(rownames(grid_name)),-1])

 rownames(grid_name) = dates_site
 # Keep only periods in which grid was censused
```

```
  if (length(dates_grid) != length(dates_site)) {
    grid_name = grid_name[ -c(which(rownames(grid_name) ==
setdiff(rownames(grid_name), as.numeric(dates_grid)))), ]
  }
  return(grid_name)
}

######################################
####  CONVERT DATES TO YEAR AND SEASON
######################################

year.season = function(grid) {
  month = as.numeric(rownames(grid)) - floor(as.numeric(rownames(grid)))
  season = numeric(nrow(grid))
  for (i in 1:nrow(grid)) {
    if (month[i] >= 2/12 & month[i] <= 4/12) {
      season[i] = 0.25
    } else if (month[i] >= 5/12 & month[i] <= 7/12) {
      season[i] = 0.5
    } else if (month[i] >= 8/12 & month[i] <= 10/12) {
      season[i] = 0.75
    } else {
      season[i] = 0
    }
  }
  rownames(grid) = floor(as.numeric(rownames(grid))) + season
  return(grid)
}

######################################
###  INSERT MISSING CENSUS DATES AS NA
######################################

insert.time = function(grid, start, end, NA.insert = TRUE) {
  grid = year.season(grid)
  full.ts = seq(start, end, by = 1/4)

  ts.missing = setdiff(full.ts, rownames(grid))
  ts.missing.matrix = matrix(0, ncol = ncol(grid), nrow = length(ts.missing))
  if (NA.insert) {
    ts.missing.matrix[,] = NA
  }
  rownames(ts.missing.matrix) = ts.missing
  colnames(ts.missing.matrix) = colnames(grid)
```

```
  full.ts = rbind(grid, ts.missing.matrix)
  full.ts = full.ts[sort(rownames(full.ts)), ]

  return(full.ts)
}

#####################################
###  STANDARDISE DATA
#####################################

z_score = function(data) {
  data.z = (data - mean(data, na.rm = TRUE)) / sd(data, na.rm = TRUE)
  return(data.z)
}

#####################################
###  PLOT PRESENCE/ABSENCE MATRICES
#####################################

abundance_matrix = function(grid_name, plot_type = c("pres_abs", "hellinger", "relative"),
                           sort_by = c("alpha", "presence", "life_form"), plot_title = "") {
  # grid_name   - dataset
  # plot_type   - presence/absence plot or heat map by hellinger abundance (relative to
community) or relative abundance to itself
  # sort_by     - sort species by alphabetical or by frequency of presence
  # plot_title  - paste(plot_title, c("Presence/absence", "Hellinger Abundances", "Relative
Abundances")

  # Calculate month: date - year
  month = as.numeric(rownames(grid_name)) - floor(as.numeric(rownames(grid_name)))
  season = character(nrow(grid_name))
  for (i in 1:nrow(grid_name)) {
    if (month[i] >= 2/12 & month[i] <= 4/12) {
      season[i] = "S2"
    } else if (month[i] >= 5/12 & month[i] <= 7/12) {
      season[i] = "S3"
    } else if (month[i] >= 8/12 & month[i] <= 10/12) {
      season[i] = "S4"
    } else {
      season[i] = "S1"
    }
  }
```

```
  # Presence absence data frame: 1 = present
  grid_pres = grid_name
  grid_pres[grid_pres >= 1] = 1
  rownames(grid_pres) = paste(floor(as.numeric(rownames(grid_name))), season)

  if (sort_by == "presence") {
    grid_name = grid_name[ , order(apply(grid_pres, 2, sum), decreasing = TRUE) ]
    grid_pres = grid_pres[ , order(apply(grid_pres, 2, sum), decreasing = TRUE) ]
  } else if (sort_by == "life_form") {
    life_forms = Species_class[match(colnames(grid_name), Species_class[,"Species"]), "Type"]
    grid_name = grid_name[ , order(life_forms)]
    grid_pres = grid_pres[ , order(life_forms)]
    colours  = c("black", "red", "pink", "green", "darkgreen", "gray", "blue", "orange", "cyan" , "darkgoldenrod")
    axis.colour = mapvalues(sort(life_forms), from = levels(Species_class[, "Type"]), to = colours)
  }

  # Complete time series of census dates
  full.ts = c(rep(2004:2012, each = 4), 2013, 2013)
  full.ts = paste(full.ts, rep(c("S1", "S2", "S3", "S4"), length = length(full.ts)))

  # Identify missing censuses
  ts.missing = setdiff(full.ts, rownames(grid_pres))
  ts.missing = grid_pres[1:length(ts.missing), ]
  ts.missing[,] = -1 # No census
  rownames(ts.missing) = setdiff(full.ts, rownames(grid_pres))

  # Complete time series matrix of -1's (no census), 0's (absence) and 1's (presence)
  full.ts = rbind(grid_pres, ts.missing)
  full.ts = full.ts[sort(rownames(full.ts)), ]


  ########################################
  # Presence/absence matrix plot
  if (plot_type == "pres_abs") {
    par(mar = c(4,10,1,1), font = 2)
    # 0 = No survey = black
    # 0.5 = Absence = white
    # 1 = Presence = red
    # Full.ts + 1 then divide by 2 to give appropriate numbers
    image(1:nrow(full.ts), 1:ncol(full.ts), (full.ts[,rev(colnames(full.ts))]+1)/2,
```

```
      col= c("black", "white","red"), xlab="Time", ylab="",
      axes=FALSE, zlim=c(0,1), main = paste(plot_title, "Presence/Absence"), lwd = 2)
  axis(side = 1, at=seq(1,nrow(full.ts),1), labels=rownames(full.ts),
     cex.axis=1.0)
  if (sort_by == "life_form") {
    Map(function(x,y,z)
      axis(side = 2, at=x, col.axis=y, labels=z, cex.axis = 0.8, las = 1),
      seq(1,ncol(full.ts),1),
      rev(as.character(axis.colour)),
      rev(colnames(full.ts)))
  } else {
    axis(side = 2, at=seq(1,ncol(full.ts),1), labels=rev(colnames(full.ts)), las= 1,
       cex.axis=0.8)
  }
  grid(nx=(dim(full.ts)[1]), ny=(dim(full.ts)[2]), col="black", lty="solid");
} else if (plot_type == "hellinger") {

  ########################################
  # Color scaled by hellinger abundance
  require(PCNM)
  grid_hel = decostand(grid_name, "hellinger")

  rownames(grid_hel) = paste(floor(as.numeric(rownames(grid_hel))), season)
  # Identify missing census and set to -1
  grid_hel = rbind(grid_hel, ts.missing)
  grid_hel = grid_hel[sort(rownames(grid_hel)), ]
  grid_hel[is.na(grid_hel)] = -1

  ColorRamp = c(rep("white", length = 50), rgb(rep(1, length = 50),
                                  seq(0.95, 0.05, length = 50),
                                  seq(0.95, 0.05, length = 50)))

  layout(matrix(data=c(1,2), nrow=1, ncol=2), widths=c(4,1),heights=c(1,1))
  par(mar = c(4,10,1,1), font = 2)
  # -1 = No survey = black
  # 0 = Absence = white
  # >0 = Presence, red
  image(1:nrow(grid_hel), 1:ncol(grid_hel), grid_hel[,rev(colnames(grid_hel))],
      col = c("black", ColorRamp), xlab="Time", ylab="",
      axes=FALSE, zlim=c(-1,1), main= paste(plot_title, "Hellinger Abundances"))
  axis(side = 1, at=seq(1,nrow(full.ts),1), labels=rownames(full.ts),
     cex.axis=1.0)
  if (sort_by == "life_form") {
    Map(function(x,y,z)
```

```
      axis(side = 2, at=x, col.axis=y, labels=z, cex.axis = 0.8, las = 1),
      seq(1,ncol(full.ts),1),
      rev(as.character(axis.colour)),
      rev(colnames(full.ts)))
   } else {
     axis(side = 2, at=seq(1,ncol(full.ts),1), labels=rev(colnames(full.ts)), las= 1,
        cex.axis=0.8)
   }
   grid(nx=(dim(full.ts)[1]), ny=(dim(full.ts)[2]), col="black", lty="solid")

   # Add legend for colour scaling
   par(mar = c(3,2.5,2.5,2))
   ColorLevels = seq(0, 1, length = length(ColorRamp)/2)
   image(1, ColorLevels,
        matrix(data=ColorLevels, ncol=length(ColorLevels),nrow=1),
        col=ColorRamp[51:100],xlab="",ylab="",xaxt="n", las = 1)
   par(mfrow = c(1,1))
 } else {

   ########################################
   # Color scaled by relative abundance

   grid_rel = apply(grid_name, 2, function(X) X/sum(X))

   rownames(grid_rel) = paste(floor(as.numeric(rownames(grid_rel))), season)
   # Identify missing census and set to -1
   grid_rel = rbind(grid_rel, ts.missing)
   grid_rel = grid_rel[sort(rownames(grid_rel)), ]
   grid_rel[is.na(grid_rel)] = -1

   ColorRamp = c(rep("white", length = 50), rgb(rep(1, length = 50),
                                   seq(0.95, 0.05, length = 50),
                                   seq(0.95, 0.05, length = 50)))

   layout(matrix(data=c(1,2), nrow=1, ncol=2), widths=c(4,1),heights=c(1,1))
   par(mar = c(4,10,1,1), font = 2)
   # -1 = No survey = black
   # 0 = Absence = white
   # >0 = Presence, red
   image(1:nrow(grid_rel), 1:ncol(grid_rel), grid_rel[,rev(colnames(grid_rel))],
        col = c("black", ColorRamp), xlab="Time", ylab="",
        axes=FALSE, zlim=c(-1,1), main= paste(plot_title, "Relative Abundances"))
   axis(side = 1, at=seq(1,nrow(full.ts),1), labels=rownames(full.ts),
       cex.axis=1.0)
```

```
  if (sort_by == "life_form") {
   Map(function(x,y,z)
    axis(side = 2, at=x, col.axis=y, labels=z, cex.axis = 0.8, las = 1),
    seq(1,ncol(full.ts),1),
    rev(as.character(axis.colour)),
    rev(colnames(full.ts)))
  } else {
   axis(side = 2, at=seq(1,ncol(full.ts),1), labels=rev(colnames(full.ts)), las= 1,
      cex.axis=0.8)
  }
  grid(nx=(dim(full.ts)[1]), ny=(dim(full.ts)[2]), col="black", lty="solid")

  # Add legend for colour scaling
  par(mar = c(3,2.5,2.5,2))
  ColorLevels = seq(0, 1, length = length(ColorRamp)/2)
  image(1, ColorLevels,
     matrix(data=ColorLevels, ncol=length(ColorLevels),nrow=1),
     col=ColorRamp[51:100],xlab="",ylab="",xaxt="n", las = 1)
  par(mfrow = c(1,1))
 }
}

#######################################
###  CONDUCT AND COMPARE DFA MODELS
#######################################

dfa_auto = function(time_series, states = 2, R = "diagonal and equal", covariates = NULL) {
 require(MARSS)
 dfa.model.data = data.frame()
 dfa.all = list()

 # Compute DFA's

 for (m in 1:states) {
  dfa.model = list(A = "zero", R = R, m = m)
  time_series.dfa = MARSS(t(time_series), model = dfa.model, z.score = TRUE, form =
"dfa",
              control = list(maxit = 50000, allow.degen = FALSE), covariates =
covariates)
  dfa.model.data = rbind(dfa.model.data,  data.frame(m = m, K =
time_series.dfa$num.params,
                            AICc = time_series.dfa$AICc))
  dfa.all[m] = list(time_series.dfa)
 }
```

```
  # Extract best model
  dfa.best = dfa.all[ dfa.model.data$AICc == min(dfa.model.data$AICc)][[1]]

  # Factor loadings
  dfa.z = coef(dfa.best, type = "matrix")$Z
  H.inv = varimax(dfa.z)$rotmat  # Inverse of rotation matrix H

  dfa.z.rot = dfa.z %*% H.inv
  # Adjusted common trends
  dfa.t.rot = solve(H.inv) %*% dfa.best$states

  # Identify which species belongs to which trends
  dfa.trends = matrix(FALSE, ncol(dfa.z.rot), nrow(dfa.z.rot))
  for (t in 1:nrow(dfa.t.rot)) {
    dfa.trends[t,] = abs(dfa.z.rot[,t]) >= 0.2
  }

  return(list(AICc = dfa.model.data, dfa.best = dfa.best, dfa.z.rot = dfa.z.rot, dfa.t.rot =
dfa.t.rot, dfa.trends = dfa.trends))
}

########################################
###  PLOT FACTOR LOADINGS
########################################

dfa_factor_plot = function(grid_name, z.rot, t.rot, species_trend, loading_threshold = 0.2,
splits = 1, Ann_per = FALSE, pos = TRUE, add.legend = FALSE, legend_pos = "topright") {
  # grid_name     - n x t matrix with species abundances over time
  # z.rot         - n x m matrix with n species and m trends
  # t.rot         - m x t matrix with m trends over t time steps
  # species_trend - logical matrix indicating which species belong to which trend
  # splits        - number of grids in matrix grid_name. grids must be symmetrical
  # Ann_per       - colour code by annual/perennial or life form
  # pos           - if factor loadings are majority negative, convert trends and loading to positive

  require(plyr)

  # Reverse sign is majority factor loadings are negative
  if (pos) {
    for (i in 1:ncol(z.rot)) {
      if (sum(z.rot[,i] > 0) < sum(z.rot[,i] < 0)) {
        z.rot[,i] = z.rot[,i] * -1
        t.rot[i,] = t.rot[i,] * -1
```

```
      }
    }
  }

  # Splits = 1 i.e. 1 grid
  if (splits == 1) {
    for (i in 1:ncol(z.rot)) {
      # Note: requires Species_Class data.frame
      # Colour coded by annual/perennial
      if (Ann_per) {
        life_forms = Species_class[match(colnames(grid_name[, species_trend[i,]]), Species_class[,"Species"]), "Ann...Per"]
        colours = c("black", "red", "purple", "blue")
        colour_code = as.character(mapvalues(life_forms, from = levels(life_forms), to = colours))
      } else {
        # Colour coded by life form
        life_forms = Species_class[match(colnames(grid_name[, species_trend[i,]]), Species_class[,"Species"]), "Type"]
        colours = c("black", "red", "green", "blue", "cyan", "orange", "yellow", "gray","darkgoldenrod","darkorchid")
        colour_code = as.character(mapvalues(life_forms, from = levels(life_forms), to = colours))
      }

      # Plot factor loadings
      plot(1:sum(species_trend[i,]), z.rot[species_trend[i,], i], pch = 16, ylim = c(-1.5, 1.5), col = colour_code,
           ylab = "", xlab = "", xaxt = "n", main = paste("Factor loading Trend", i)); abline(h = 0, lty = 2)
      # Add species labels
      text(1:sum(species_trend[i,]), 0, sapply(strsplit(colnames(grid_name[, species_trend[i,]]), " "), "[[", 1),
           cex = 1, srt = 90)

      # Add legend
      if (i == 1 & add.legend == TRUE) {
        legend(legend_pos, legend = levels(life_forms), col = colours, pch = 16, cex = 0.8)
      }
    }
  } else {
    # For multiple grids
    # Splits > 1
    # Identify how many unique species
```

```
    grid_split = ncol(grid_name)/splits

    # Divide dfa characteristics by grid into a list
    grid_name_list = grid_z_list = grid_trend_list = list(0)
    for (i in 1:splits) {
      grid_name_list[[i]] = grid_name[,(grid_split*(i-1)+1):(grid_split*i)]
      grid_z_list[[i]] = z.rot[ (grid_split*(i-1)+1):(grid_split*i), ]
      grid_trend_list[[i]] = species_trend[ , (grid_split*(i-1)+1):(grid_split*i)]
    }

    species_trend_length = matrix(0, ncol(z.rot), grid_split)
    species_trend_intersect = matrix(NA, ncol(z.rot), grid_split)

    # for ith trend
    for (i in 1:ncol(z.rot)) {
      # Identify species belonging to common trend from different grids
      species_trend_intersect.tmp = lapply(grid_trend_list, "[", i, ,drop = TRUE)
      species_trend_intersect.tmp = t(sapply(species_trend_intersect.tmp, rbind))
      species_trend_intersect[i,] = apply(species_trend_intersect.tmp,2,sum) > 0
      species_trend_length[i, species_trend_intersect[i,]] = 1

      # for jth grid
      for (j in 1:splits) {
        grid_name_J = grid_name_list[[j]]
        z.rot_J = grid_z_list[[j]]
        species_trend_J = grid_trend_list[[j]]

        # Colour coded by annual/perennial
        if (Ann_per) {
          # Note: requires Species_Class data.frame
          # Colour coding
          life_forms = Species_class[match(colnames(grid_name_J[,
species_trend_intersect[i,]]), Species_class[,"Species"]), "Ann...Per"]
          colours = c("black", "red", "purple", "blue")
          colour_code = as.character(mapvalues(life_forms, from = levels(life_forms), to =
colours))
        } else {
          # Colour coded by life form
          life_forms = Species_class[match(colnames(grid_name_J[,
species_trend_intersect[i,]]), Species_class[,"Species"]), "Type"]
          colours = c("black", "red", "green", "blue", "cyan", "orange", "yellow",
"gray","darkgoldenrod","darkorchid")
          colour_code = as.character(mapvalues(life_forms, from = levels(life_forms), to =
colours))
```

```
        }

        # Insert NA where species is not part of common trend for jth grid
        z.rot_J2 = z.rot_J[species_trend_intersect[i,], i]
        z.rot_J2[ abs(z.rot_J2) < loading_threshold ] = NA

        species_labels = z.rot_J2
        species_labels = sapply(strsplit(colnames(grid_name_J[, species_trend_intersect[i,]]), "
"), "[[", 1)

        if (j == 1) {
          # Alternate label for factor loading points
          # counter = round(z.rot_J2); counter[ is.na(counter) ] = 0

          plot(1:sum(species_trend_length[i,]), z.rot_J2, pch = 16, ylim = c(-1.5, 1.5), col =
colour_code,
               ylab = "", xlab = "", xaxt = "n", main = paste("Factor loading Trend", i)); abline(h =
0, lty = 2)
          text(1:sum(species_trend[i,]), z.rot_J2, paste(j), cex = 0.8, pos = 3)
          # Species labels
          text(1:sum(species_trend_length[i,]), 0, paste(species_labels),
               cex = 1, srt = 90)
        } else {
          # counter = counter + round(z.rot_J2)

          points(1:sum(species_trend_length[i,]), z.rot_J2, pch = 16, col = colour_code)
          text(1:sum(species_trend[i,]), z.rot_J2, paste(j), cex = 0.8, pos = 3)

        }

        # Add legend
        if (i == 1 & add.legend == TRUE) {
          legend(legend_pos, legend = levels(life_forms), col = colours, pch = 16, cex = 0.8)
        }
      }
    }
  }
}

######################################
###  CALCULATE STATE PREDICTIONS
######################################

dfa_pred = function(grid, z_rot, t_rot) {
```

```
  # Y[i,t] = Z[i,j] * X[j,t]

  # Y[i,t] = observation for ith species at time t
  # Z[i,j] = Factor loading for ith species and jth trend
  # X[j,t] = Value of jth common trend at time t

  state_predict = grid; state_predict[,] = 0

  # Calculate state predictions
  for (j in 1:ncol(grid)) {
    for (i in 1:nrow(t_rot)) {
      state_predict[,j] = state_predict[,j] + t_rot[i,] * z_rot[j,i]
    }
  }
  return(state_predict)
}

######################################
###  CALCULATE RELATIVE MSE
######################################

dfa_MSE = function(grid, state_predict) {
  # RelMSE = 1 - [ sum( (Z[i,t] - Z*[i,t])^2 ) / T ]

  # Z[i,t] = Standardised observations
  # Z*[i,t] = Predicted observations
  # T = time series length

  grid_standard = apply(grid,2, z_score)

  # Estimate MSE
  species_MSE = t((grid_standard - state_predict)^2)
  species_MSE = apply(species_MSE, 1, function(X) 1 - mean(X, na.rm = TRUE))
  species_MSE = round(data.frame(MSE = species_MSE), 3)

  return(species_MSE)
}
```

Appendix 4-3: Plots of presence/absence and relative frequency of species used in dynamic factor analysis for all grids sampled in Chapter 5 divided by life form. Grids that are burnt are indicated in the plot titles. Species in black are forbs, red are grasses, blue are shrubs and green are subshrubs. Red cells indicate presence, white indicates absence and gray indicates a missing value when a census was not conducted. Plots begin on next page.

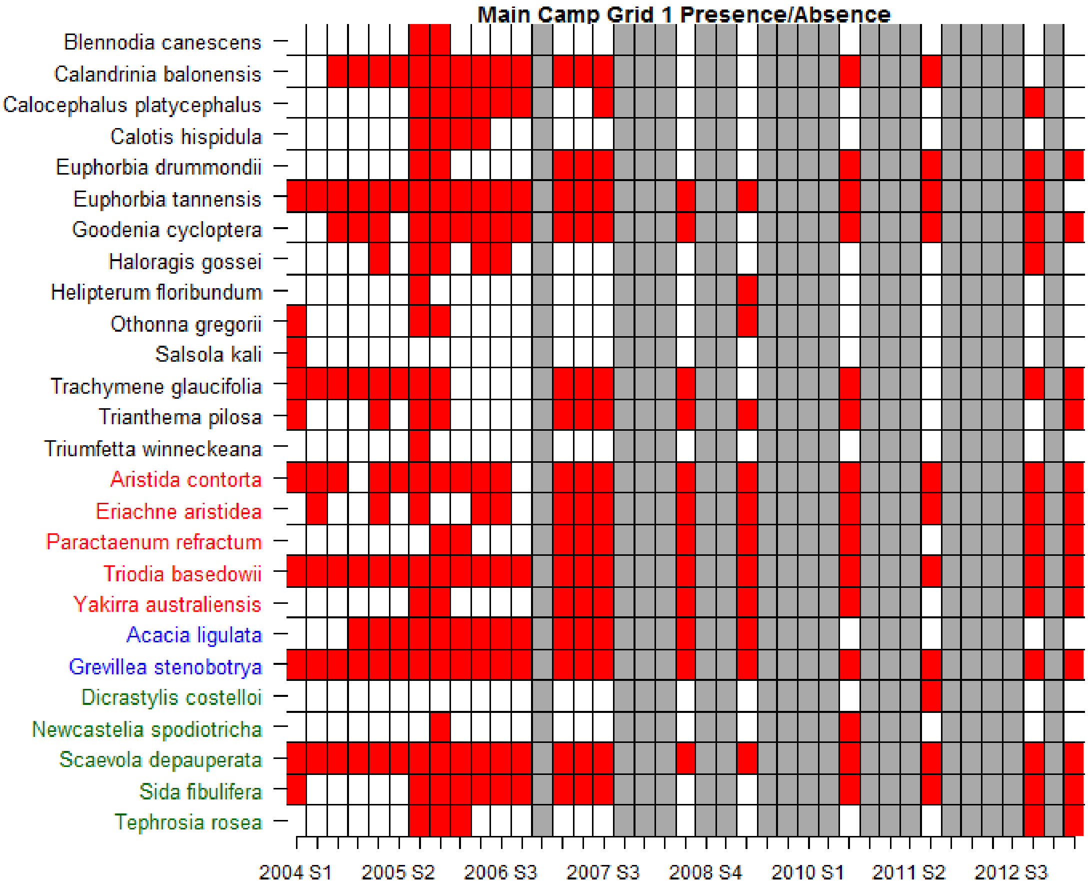
Main Camp Grid 1 Presence/Absence
Blennodia canescens
Calandrinia balonensis
Calocephalus platycephalus
Calotis hispidula
Euphorbia drummondii
Euphorbia tannensis
Goodenia cycloptera
Haloragis gossei
Helipterum floribundum
Othonna gregorii
Salsola kali
Trachymene glaucifolia
Trianthema pilosa
Triumfetta winneckeana
Aristida contorta
Eriachne aristidea
Paractaenum refractum
Triodia basedowii
Yakirra australiensis
Acacia ligulata
Grevillea stenobotrya
Dicrastylis costelloi
Newcastelia spodiotricha
Scaevola depauperata
Sida fibulifera
Tephrosia rosea
2004 S1
2005 S2
2006 S3
2007 S3
2008 S4
2010 S1
2011 S2
2012 S3

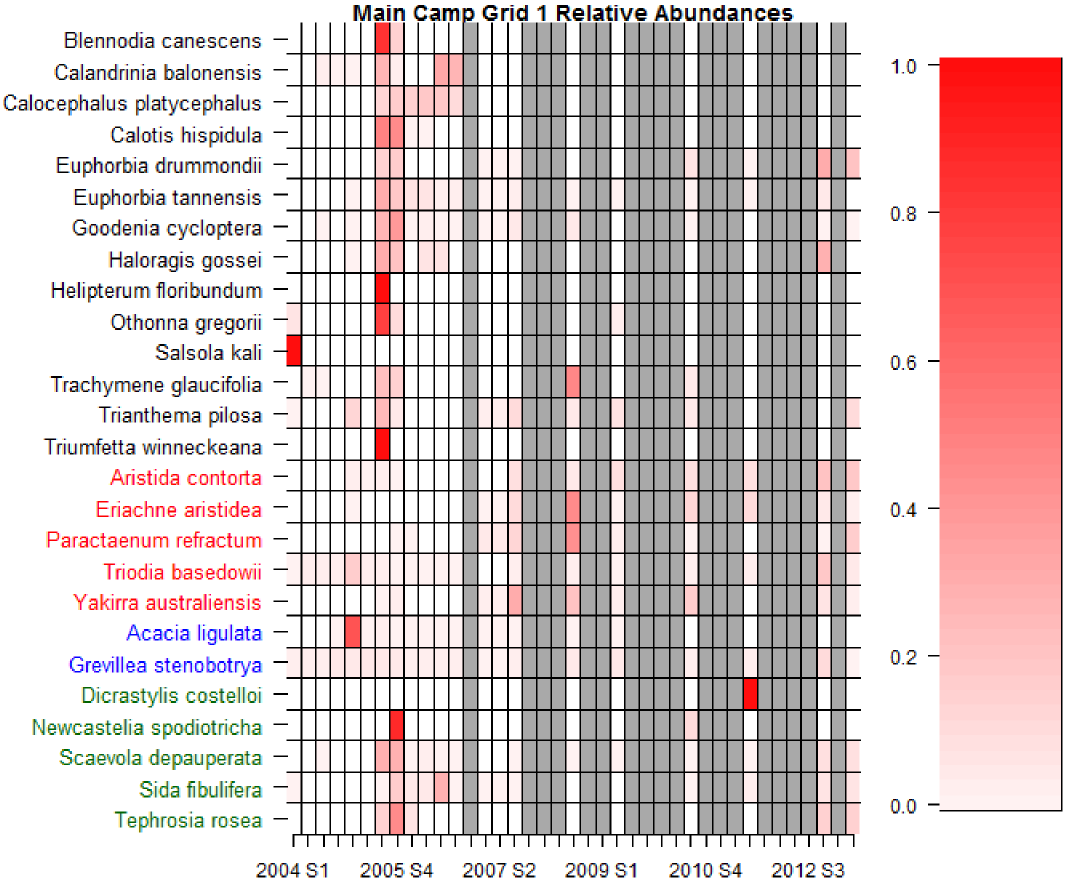
Main Camp Grid 1 Relative Abundances
Blennodia canescens
Calandrinia balonensis
Calocephalus platycephalus
Calotis hispidula
Euphorbia drummondii
Euphorbia tannensis
Goodenia cycloptera
Haloragis gossei
Helipterum floribundum
Othonna gregorii
Salsola kali
Trachymene glaucifolia
Trianthema pilosa
Triumfetta winneckeana
Aristida contorta
Eriachne aristidea
Paractaenum refractum
Triodia basedowii
Yakirra australiensis
Acacia ligulata
Grevillea stenobotrya
Dicrastylis costelloi
Newcastelia spodiotricha
Scaevola depauperata
Sida fibulifera
Tephrosia rosea
2004 S1
2005 S4
2007 S2
2009 S1
2010 S4
2012 S3
1.0
0.8
0.6
0.4
0.2
0.0

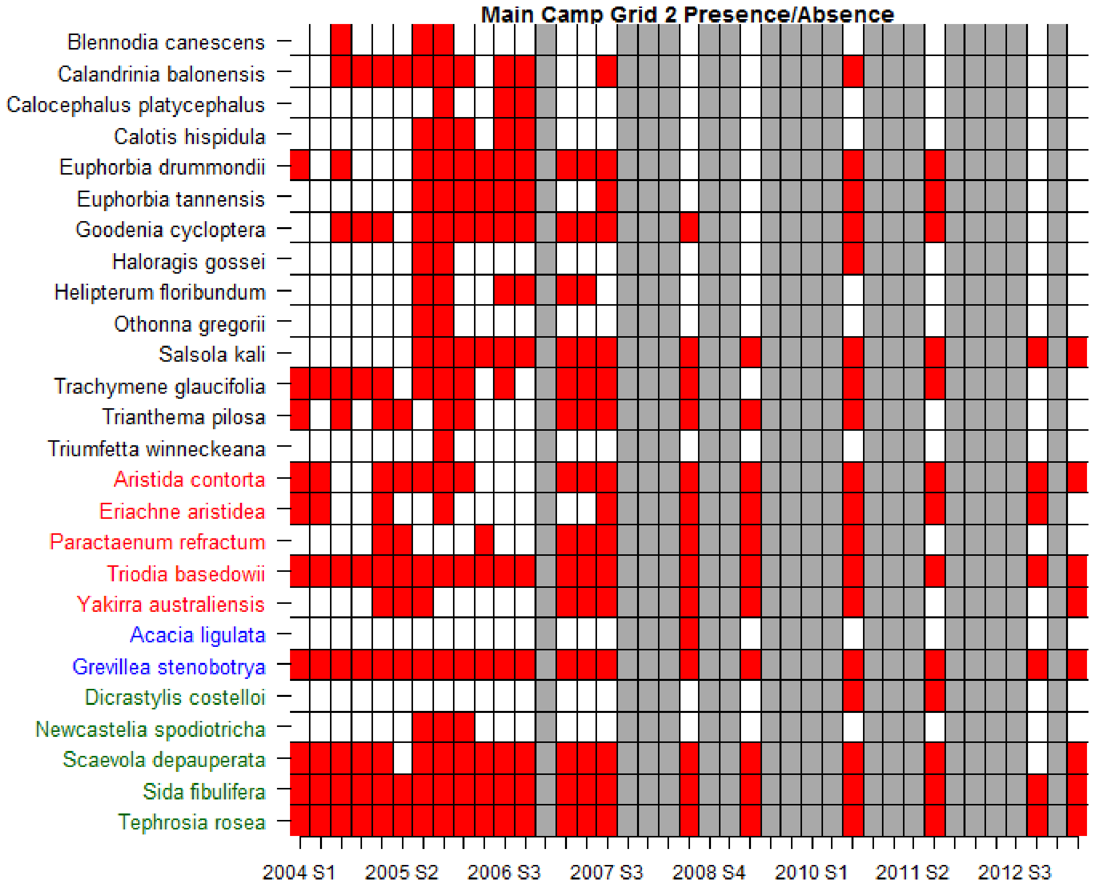
Main Camp Grid 2 Presence/Absence

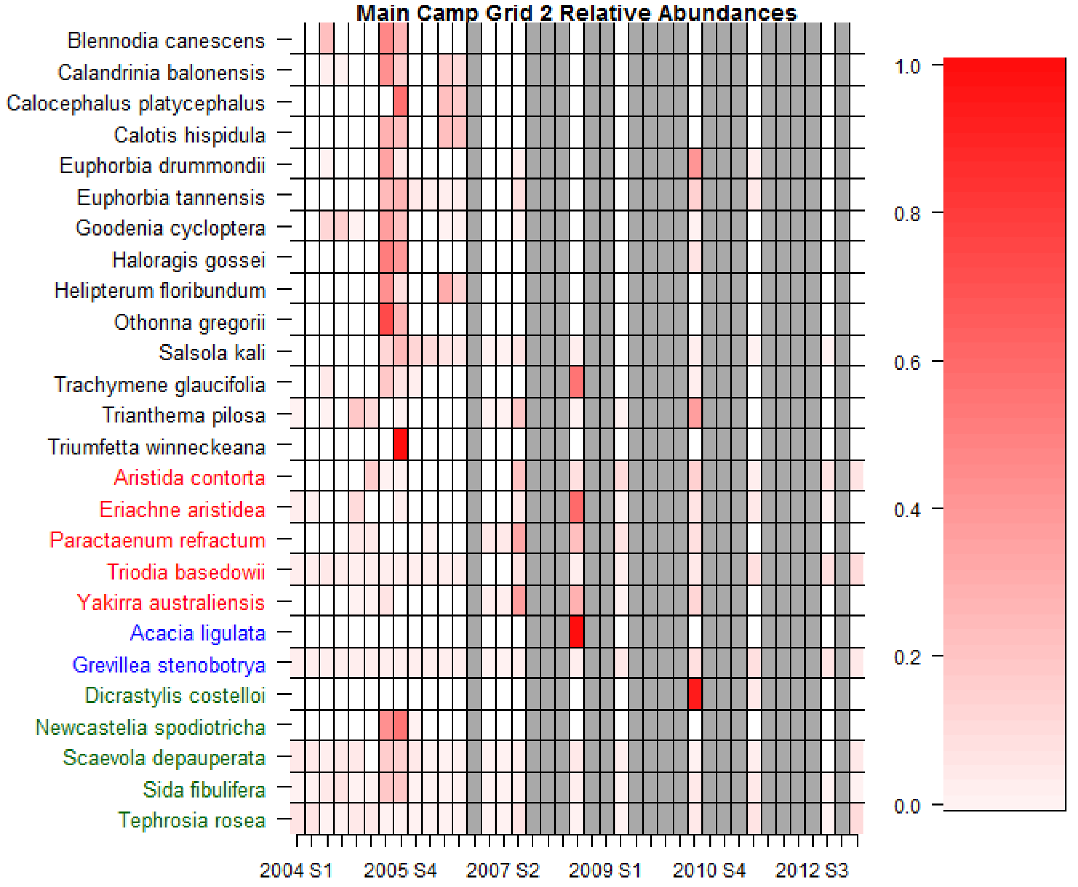
Main Camp Grid 2 Relative Abundances

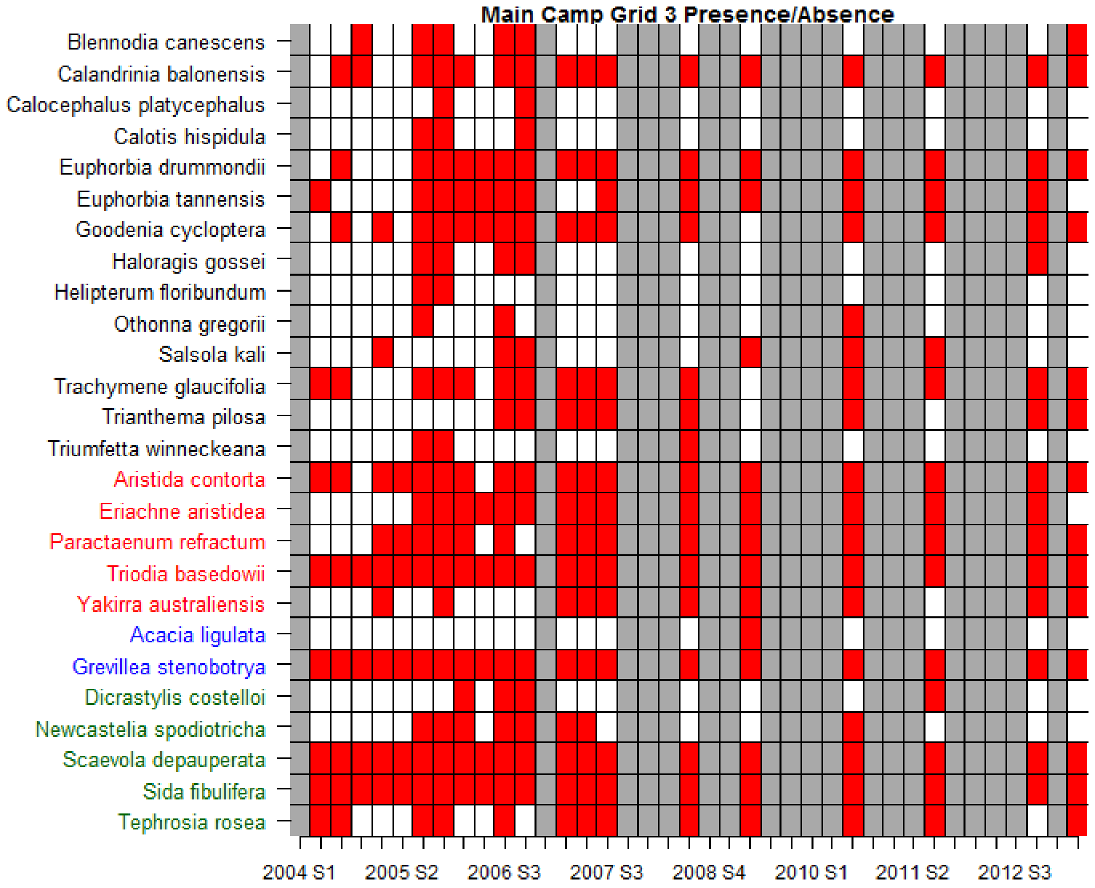
Main Camp Grid 3 Presence/Absence
Blennodia canescens
Calandrinia balonensis
Calocephalus platycephalus
Calotis hispidula
Euphorbia drummondii
Euphorbia tannensis
Goodenia cycloptera
Haloragis gossei
Helipterum floribundum
Othonna gregorii
Salsola kali
Trachymene glaucifolia
Trianthema pilosa
Triumfetta winneckeana
Aristida contorta
Eriachne aristidea
Paractaenum refractum
Triodia basedowii
Yakirra australiensis
Acacia ligulata
Grevillea stenobotrya
Dicrastylis costelloi
Newcastelia spodiotricha
Scaevola depauperata
Sida fibulifera
Tephrosia rosea
2004 S1
2005 S2
2006 S3
2007 S3
2008 S4
2010 S1
2011 S2
2012 S3

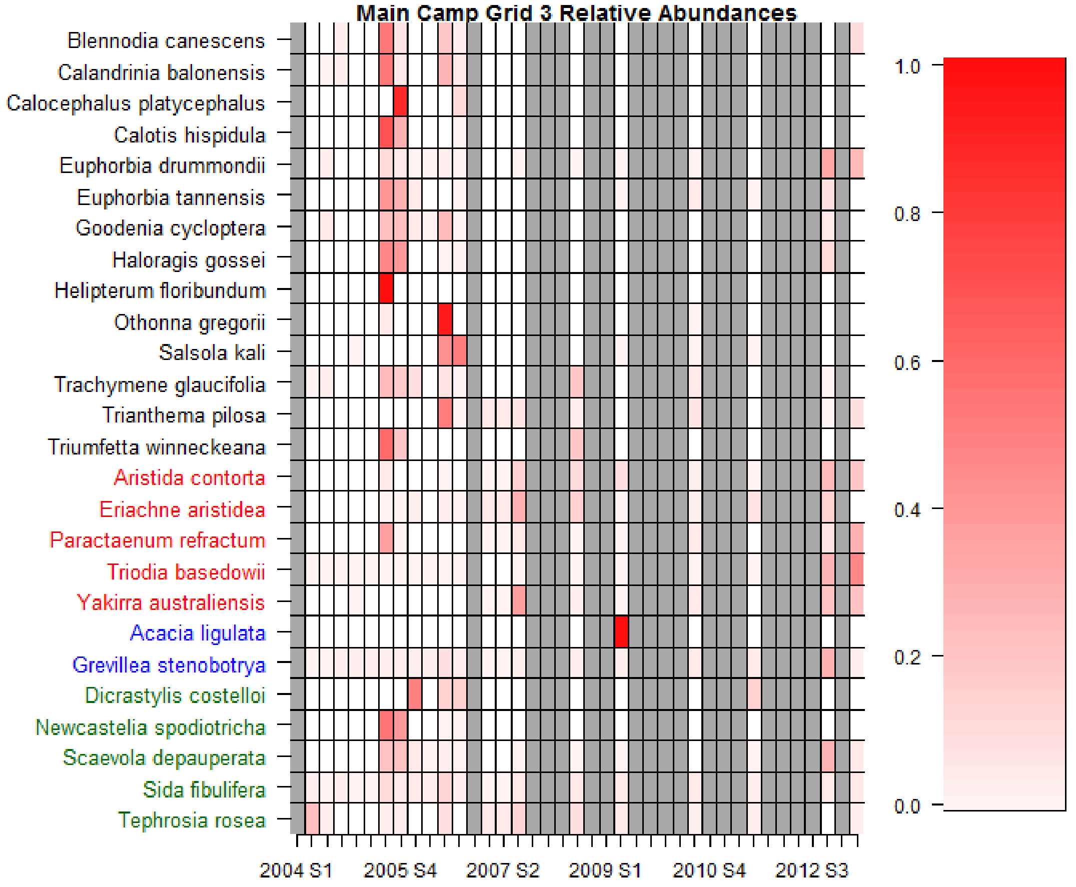
Main Camp Grid 3 Relative Abundances
Blennodia canescens
Calandrinia balonensis
Calocephalus platycephalus
Calotis hispidula
Euphorbia drummondii
Euphorbia tannensis
Goodenia cycloptera
Haloragis gossei
Helipterum floribundum
Othonna gregorii
Salsola kali
Trachymene glaucifolia
Trianthema pilosa
Triumfetta winneckeana
Aristida contorta
Eriachne aristidea
Paractaenum refractum
Triodia basedowii
Yakirra australiensis
Acacia ligulata
Grevillea stenobotrya
Dicrastylis costelloi
Newcastelia spodiotricha
Scaevola depauperata
Sida fibulifera
Tephrosia rosea
2004 S1
2005 S4
2007 S2
2009 S1
2010 S4
2012 S3
1.0
0.8
0.6
0.4
0.2
0.0

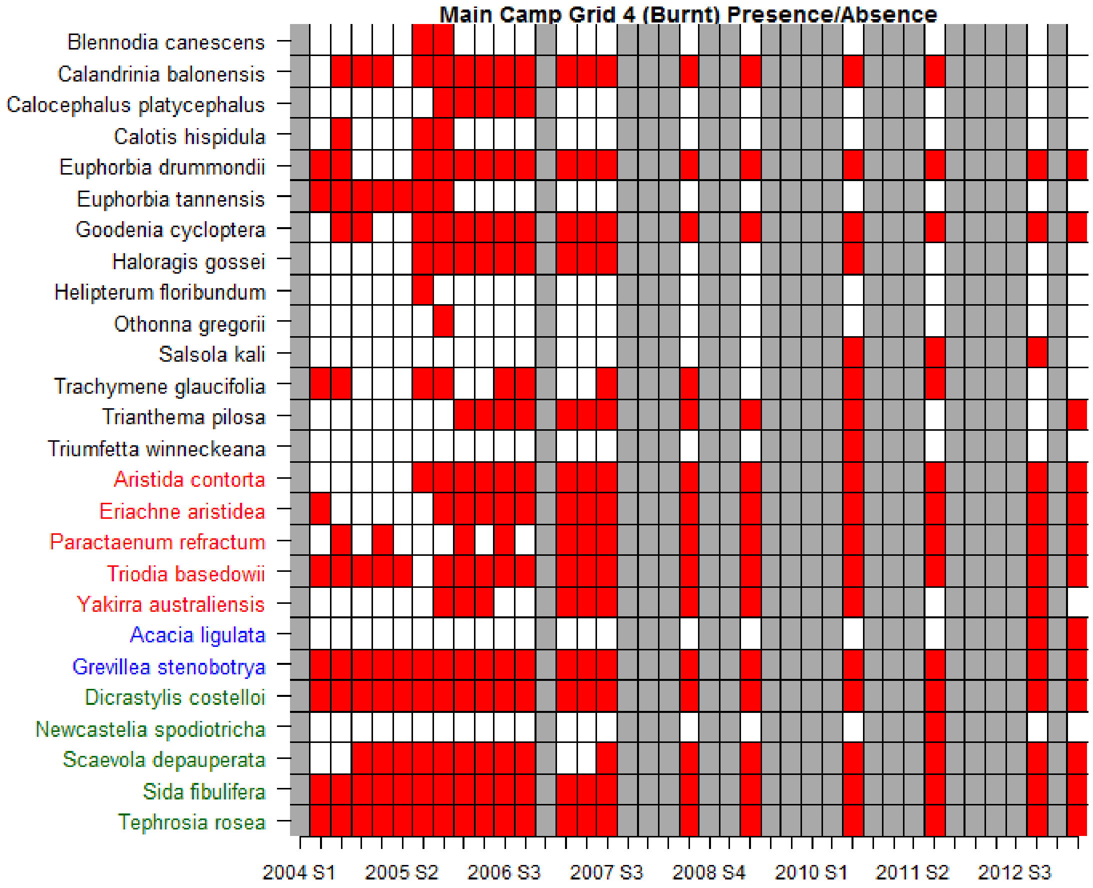
Main Camp Grid 4 (Burnt) Presence/Absence
Blennodia canescens
Calandrinia balonensis
Calocephalus platycephalus
Calotis hispidula
Euphorbia drummondii
Euphorbia tannensis
Goodenia cycloptera
Haloragis gossei
Helipterum floribundum
Othonna gregorii
Salsola kali
Trachymene glaucifolia
Trianthema pilosa
Triumfetta winneckeana
Aristida contorta
Eriachne aristidea
Paractaenum refractum
Triodia basedowii
Yakirra australiensis
Acacia ligulata
Grevillea stenobotrya
Dicrastylis costelloi
Newcastelia spodiotricha
Scaevola depauperata
Sida fibulifera
Tephrosia rosea
2004 S1
2005 S2
2006 S3
2007 S3
2008 S4
2010 S1
2011 S2
2012 S3

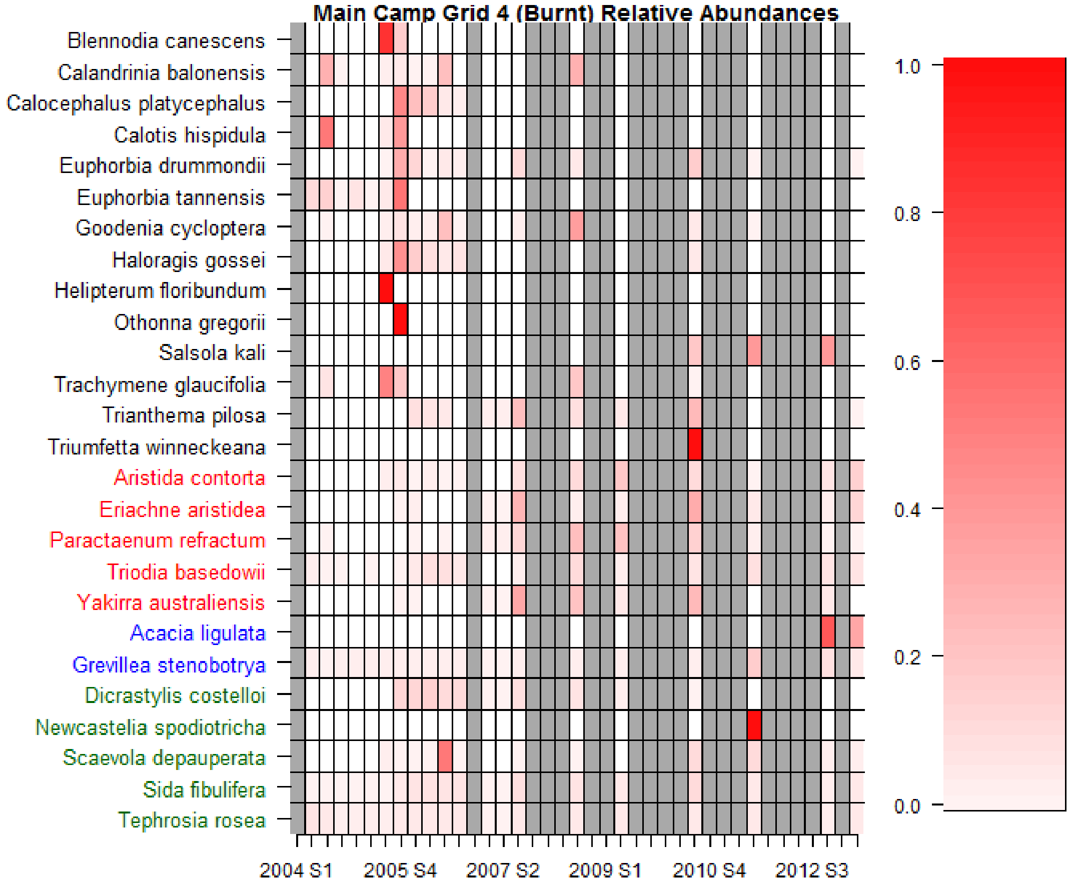
Main Camp Grid 4 (Burnt) Relative Abundances
Blennodia canescens
Calandrinia balonensis
Calocephalus platycephalus
Calotis hispidula
Euphorbia drummondii
Euphorbia tannensis
Goodenia cycloptera
Haloragis gossei
Helipterum floribundum
Othonna gregorii
Salsola kali
Trachymene glaucifolia
Trianthema pilosa
Triumfetta winneckeana
Aristida contorta
Eriachne aristidea
Paractaenum refractum
Triodia basedowii
Yakirra australiensis
Acacia ligulata
Grevillea stenobotrya
Dicrastylis costelloi
Newcastelia spodiotricha
Scaevola depauperata
Sida fibulifera
Tephrosia rosea
2004 S1
2005 S4
2007 S2
2009 S1
2010 S4
2012 S3
1.0
0.8
0.6
0.4
0.2
0.0

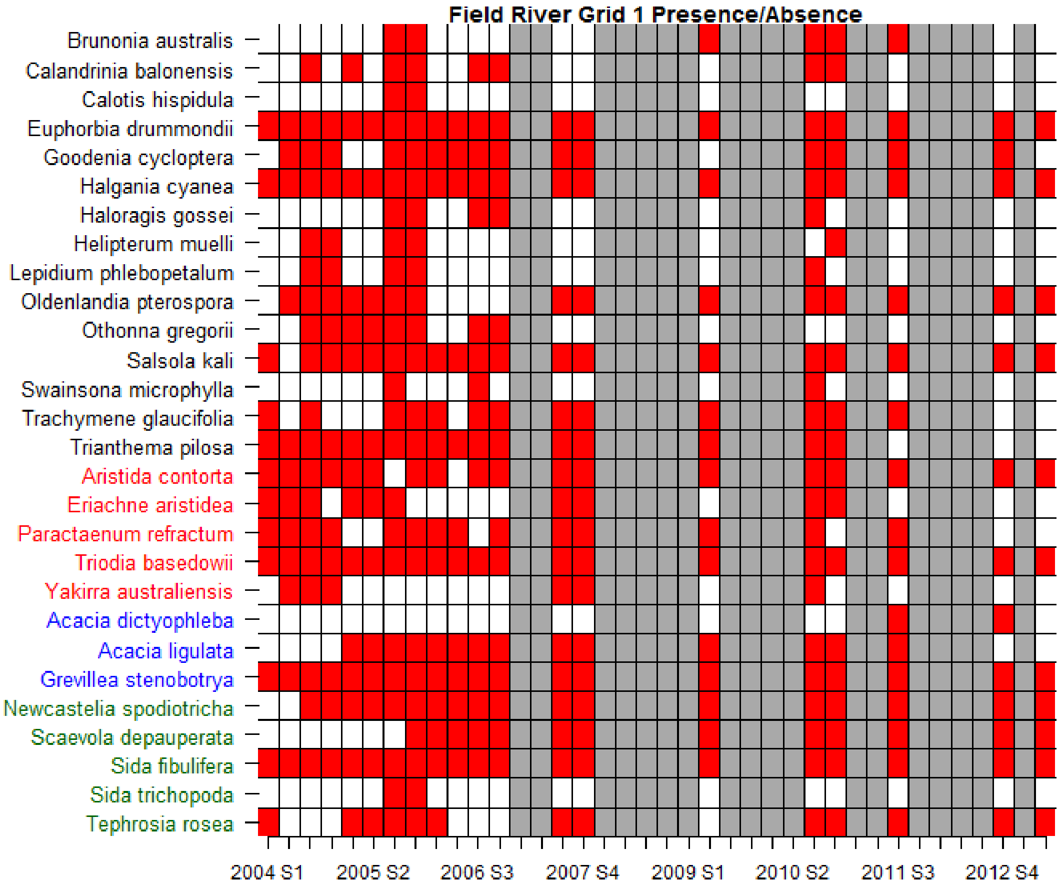
Field River Grid 1 Presence/Absence
Brunonia australis
Calandrinia balonensis
Calotis hispidula
Euphorbia drummondii
Goodenia cycloptera
Halgania cyanea
Haloragis gossei
Helipterum muelli
Lepidium phlebopetalum
Oldenlandia pterospora
Othonna gregorii
Salsola kali
Swainsona microphylla
Trachymene glaucifolia
Trianthema pilosa
Aristida contorta
Eriachne aristidea
Paractaenum refractum
Triodia basedowii
Yakirra australiensis
Acacia dictyophleba
Acacia ligulata
Grevillea stenobotrya
Newcastelia spodiotricha
Scaevola depauperata
Sida fibulifera
Sida trichopoda
Tephrosia rosea
2004 S1
2005 S2
2006 S3
2007 S4
2009 S1
2010 S2
2011 S3
2012 S4

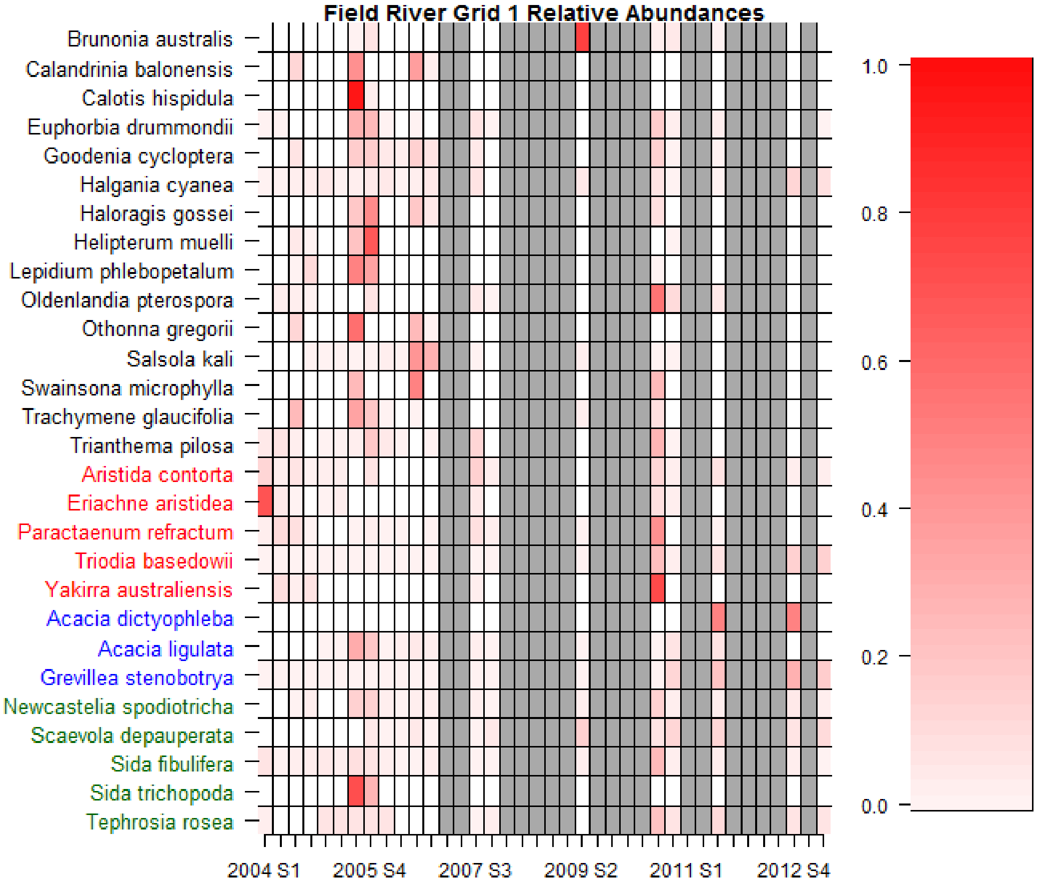
Field River Grid 1 Relative Abundances
Brunonia australis
Calandrinia balonensis
Calotis hispidula
Euphorbia drummondii
Goodenia cycloptera
Halgania cyanea
Haloragis gossei
Helipterum muelli
Lepidium phlebopetalum
Oldenlandia pterospora
Othonna gregorii
Salsola kali
Swainsona microphylla
Trachymene glaucifolia
Trianthema pilosa
Aristida contorta
Eriachne aristidea
Paractaenum refractum
Triodia basedowii
Yakirra australiensis
Acacia dictyophleba
Acacia ligulata
Grevillea stenobotrya
Newcastelia spodiotricha
Scaevola depauperata
Sida fibulifera
Sida trichopoda
Tephrosia rosea
2004 S1
2005 S4
2007 S3
2009 S2
2011 S1
2012 S4
1.0
0.8
0.6
0.4
0.2
0.0

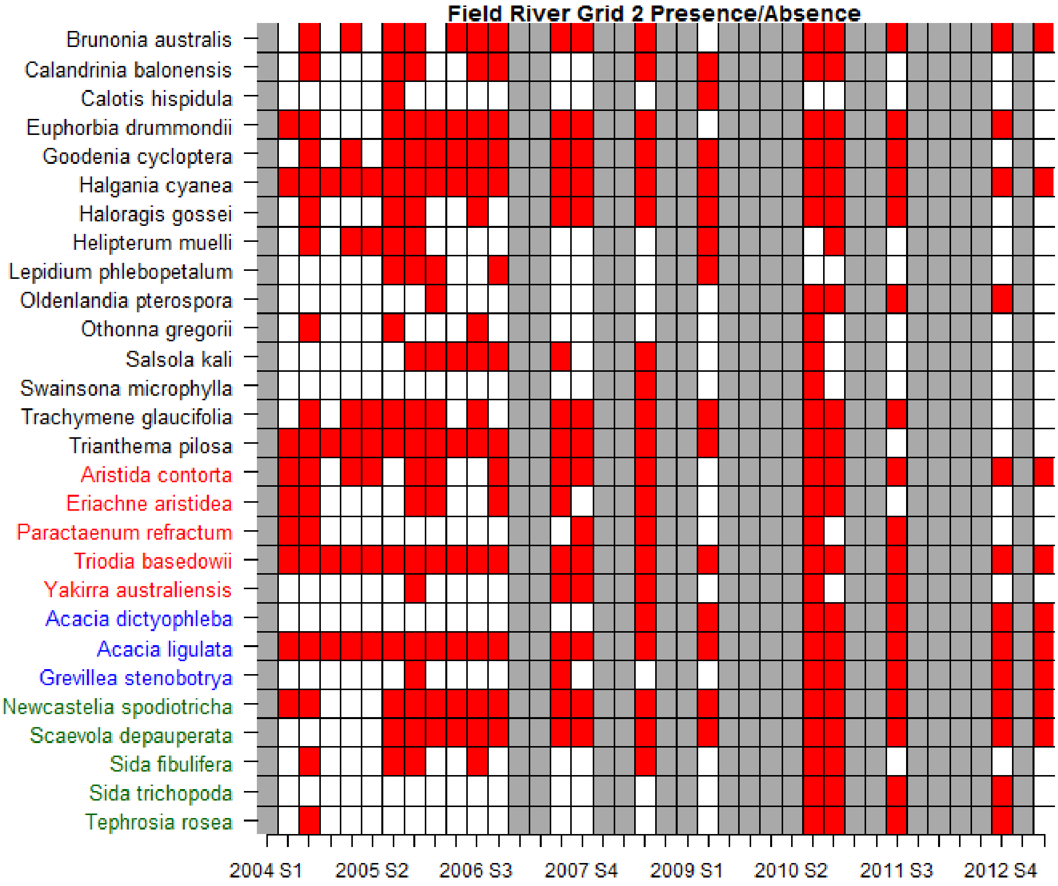
Field River Grid 2 Presence/Absence
Brunonia australis
Calandrinia balonensis
Calotis hispidula
Euphorbia drummondii
Goodenia cycloptera
Halgania cyanea
Haloragis gossei
Helipterum muelli
Lepidium phlebopetalum
Oldenlandia pterospora
Othonna gregorii
Salsola kali
Swainsona microphylla
Trachymene glaucifolia
Trianthema pilosa
Aristida contorta
Eriachne aristidea
Paractaenum refractum
Triodia basedowii
Yakirra australiensis
Acacia dictyophleba
Acacia ligulata
Grevillea stenobotrya
Newcastelia spodiotricha
Scaevola depauperata
Sida fibulifera
Sida trichopoda
Tephrosia rosea
2004 S1
2005 S2
2006 S3
2007 S4
2009 S1
2010 S2
2011 S3
2012 S4

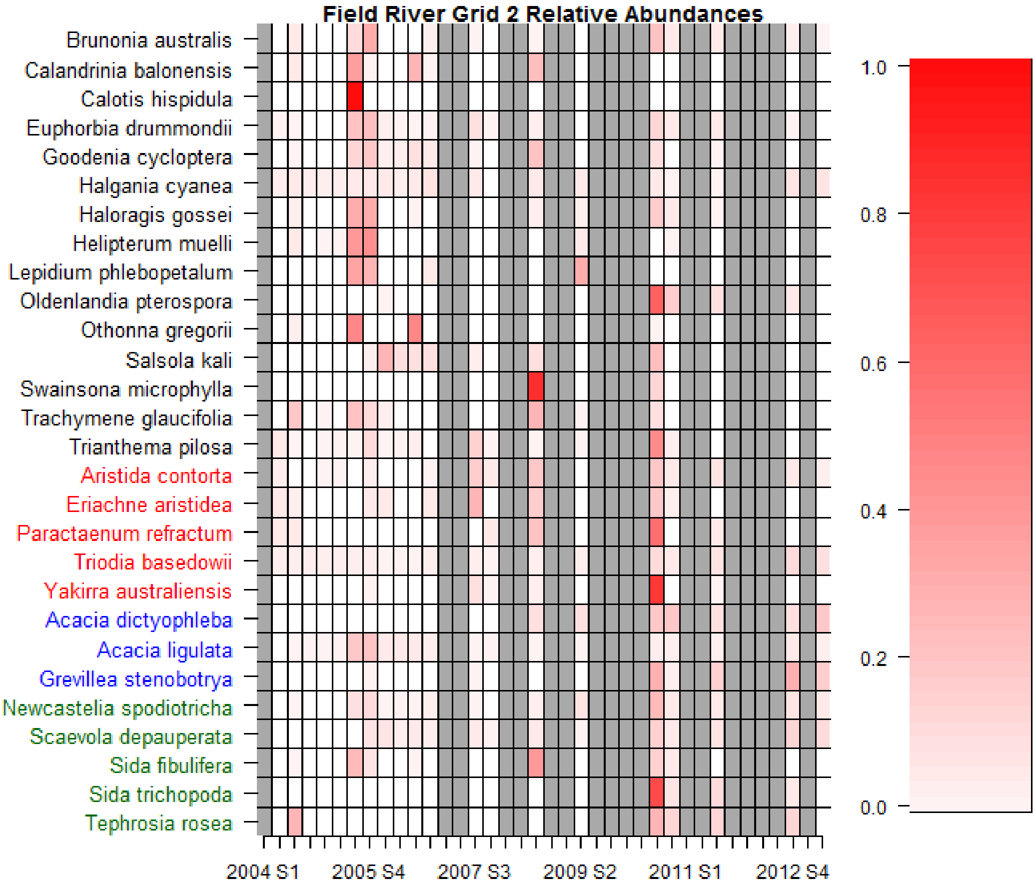
Field River Grid 2 Relative Abundances
Brunonia australis
Calandrinia balonensis
Calotis hispidula
Euphorbia drummondii
Goodenia cycloptera
Halgania cyanea
Haloragis gossei
Helipterum muelli
Lepidium phlebopetalum
Oldenlandia pterospora
Othonna gregorii
Salsola kali
Swainsona microphylla
Trachymene glaucifolia
Trianthema pilosa
Aristida contorta
Eriachne aristidea
Paractaenum refractum
Triodia basedowii
Yakirra australiensis
Acacia dictyophleba
Acacia ligulata
Grevillea stenobotrya
Newcastelia spodiotricha
Scaevola depauperata
Sida fibulifera
Sida trichopoda
Tephrosia rosea
2004 S1
2005 S4
2007 S3
2009 S2
2011 S1
2012 S4
1.0
0.8
0.6
0.4
0.2
0.0

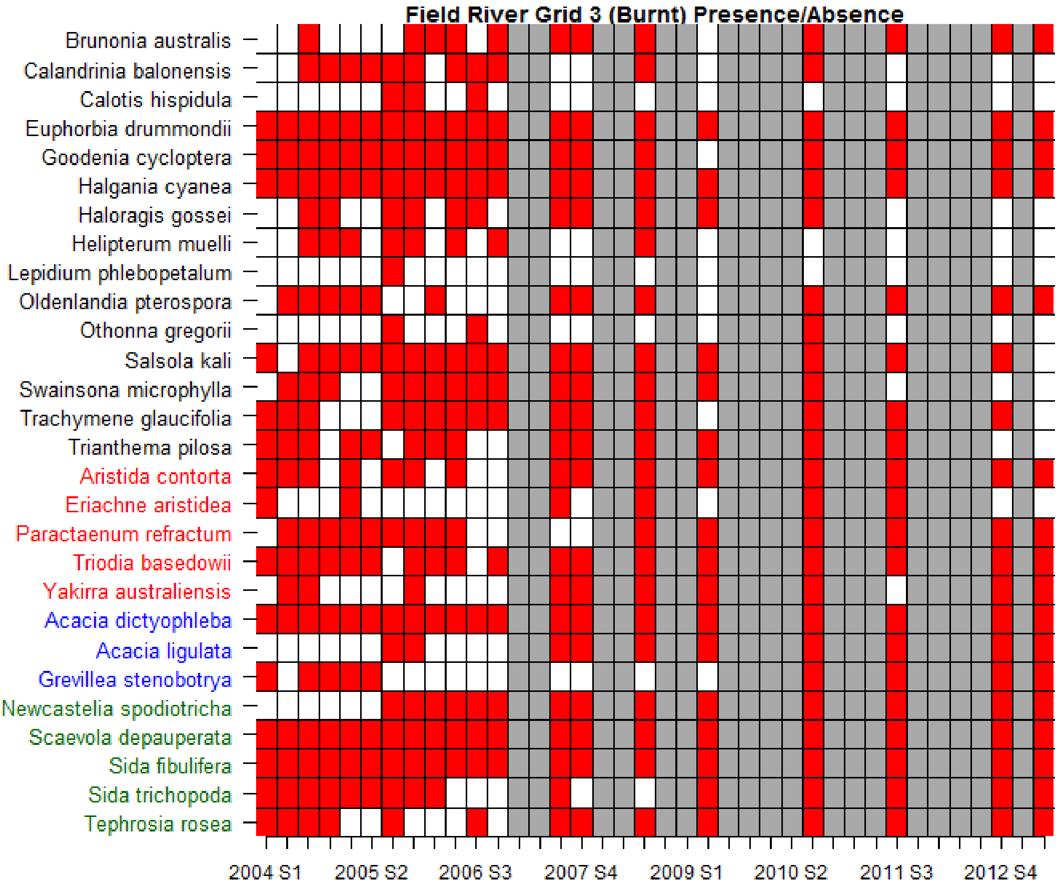
Field River Grid 3 (Burnt) Presence/Absence

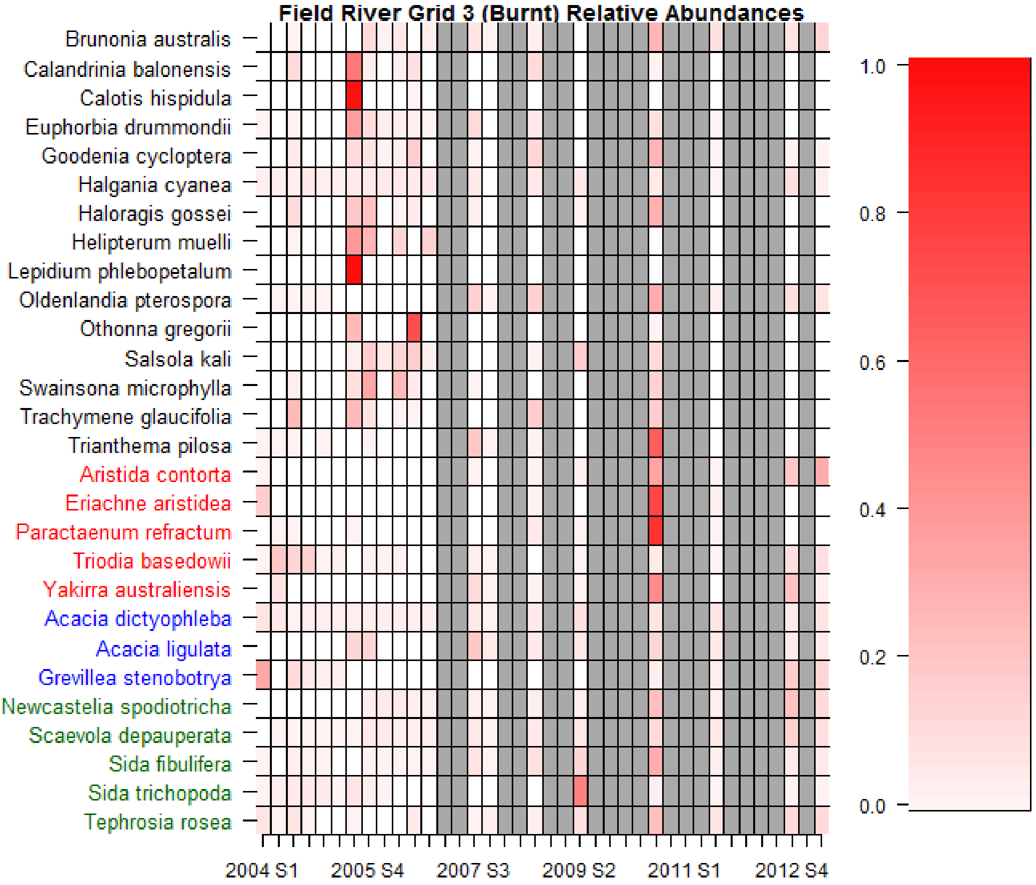
Field River Grid 3 (Burnt) Relative Abundances

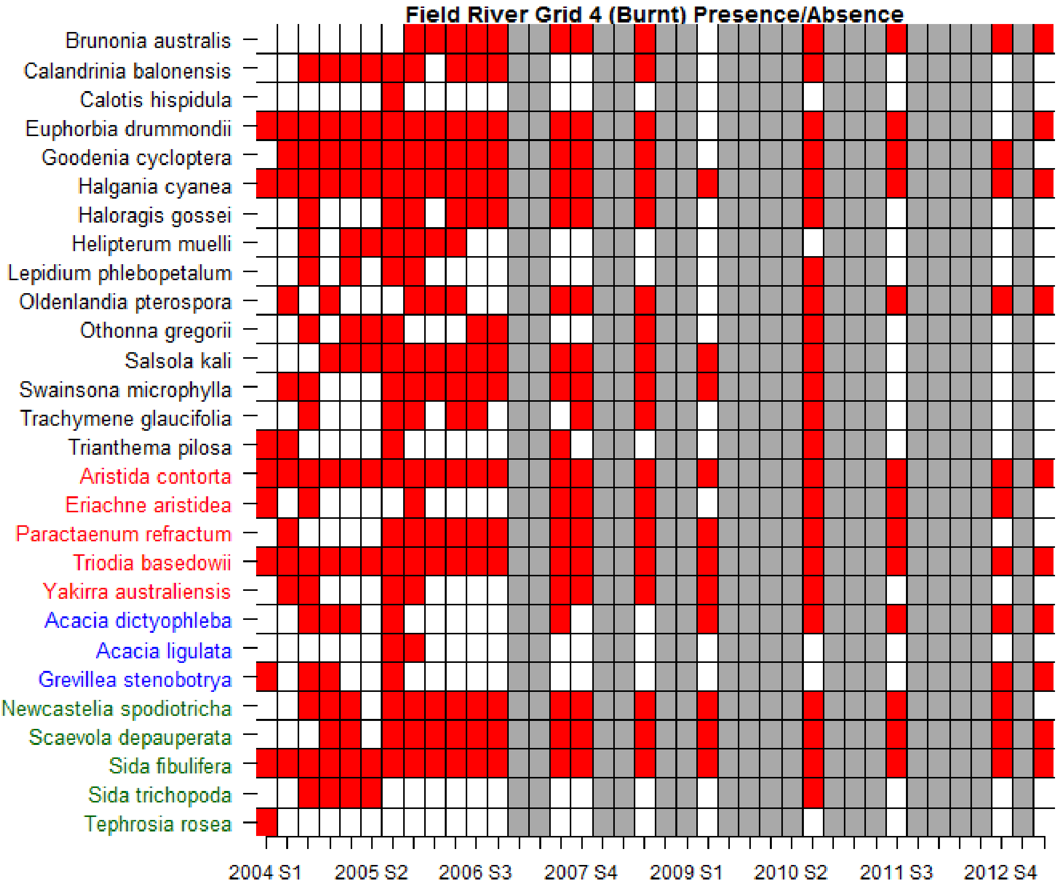
Field River Grid 4 (Burnt) Presence/Absence

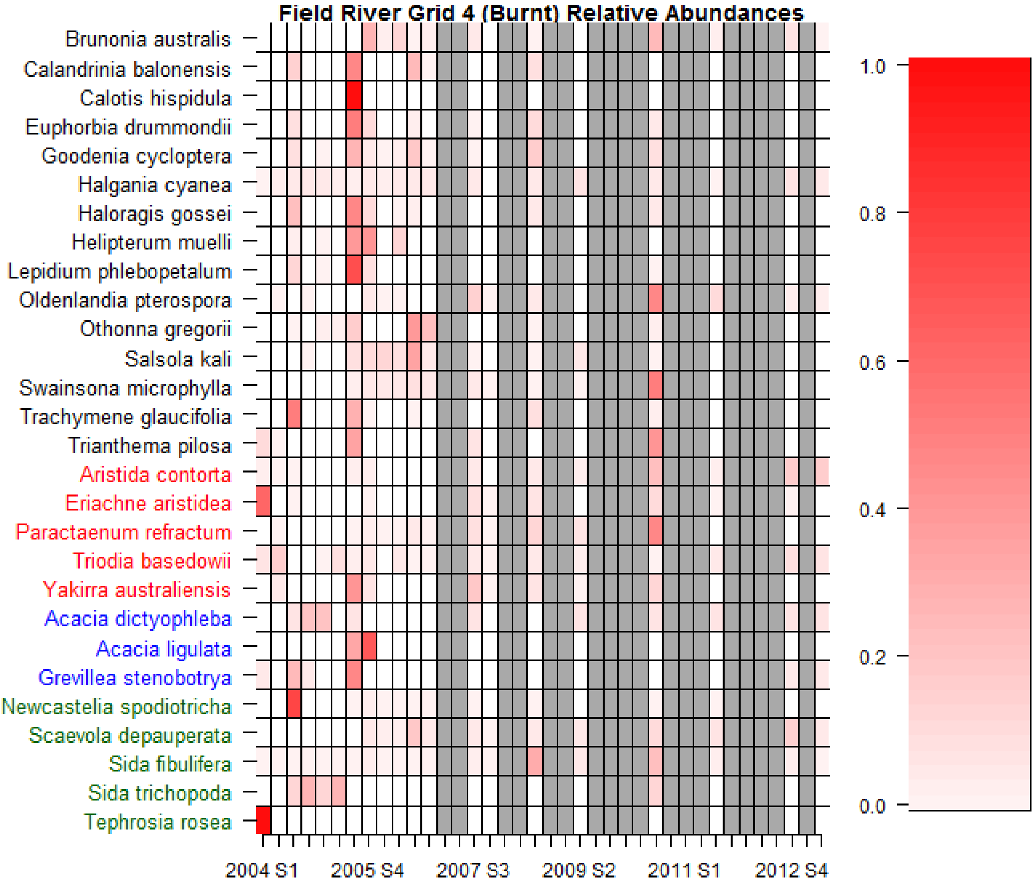
Field River Grid 4 (Burnt) Relative Abundances

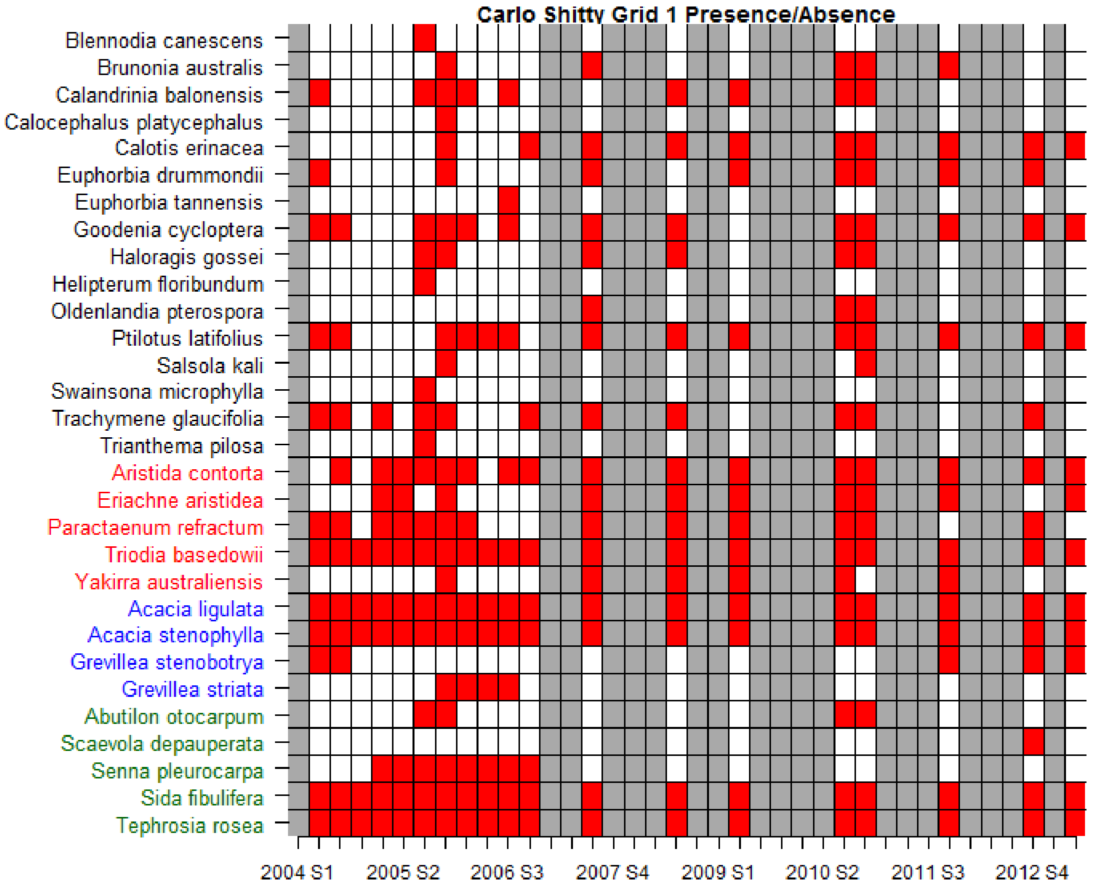
Carlo Shitty Grid 1 Presence/Absence
Blennodia canescens
Brunonia australis
Calandrinia balonensis
Calocephalus platycephalus
Calotis erinacea
Euphorbia drummondii
Euphorbia tannensis
Goodenia cycloptera
Haloragis gossei
Helipterum floribundum
Oldenlandia pterospora
Ptilotus latifolius
Salsola kali
Swainsona microphylla
Trachymene glaucifolia
Trianthema pilosa
Aristida contorta
Eriachne aristidea
Paractaenum refractum
Triodia basedowii
Yakirra australiensis
Acacia ligulata
Acacia stenophylla
Grevillea stenobotrya
Grevillea striata
Abutilon otocarpum
Scaevola depauperata
Senna pleurocarpa
Sida fibulifera
Tephrosia rosea
2004 S1
2005 S2
2006 S3
2007 S4
2009 S1
2010 S2
2011 S3
2012 S4

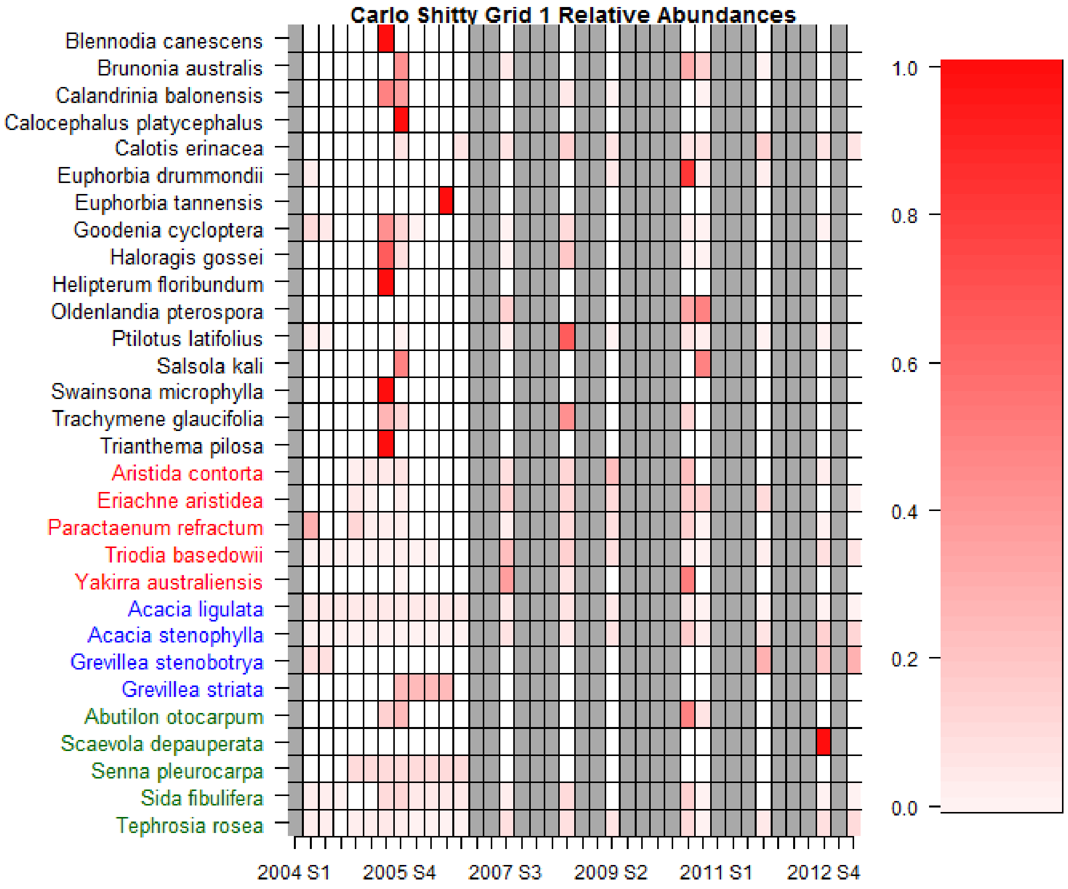
Carlo Shitty Grid 1 Relative Abundances
Blennodia canescens
Brunonia australis
Calandrinia balonensis
Calocephalus platycephalus
Calotis erinacea
Euphorbia drummondii
Euphorbia tannensis
Goodenia cycloptera
Haloragis gossei
Helipterum floribundum
Oldenlandia pterospora
Ptilotus latifolius
Salsola kali
Swainsona microphylla
Trachymene glaucifolia
Trianthema pilosa
Aristida contorta
Eriachne aristidea
Paractaenum refractum
Triodia basedowii
Yakirra australiensis
Acacia ligulata
Acacia stenophylla
Grevillea stenobotrya
Grevillea striata
Abutilon otocarpum
Scaevola depauperata
Senna pleurocarpa
Sida fibulifera
Tephrosia rosea
2004 S1
2005 S4
2007 S3
2009 S2
2011 S1
2012 S4
1.0
0.8
0.6
0.4
0.2
0.0

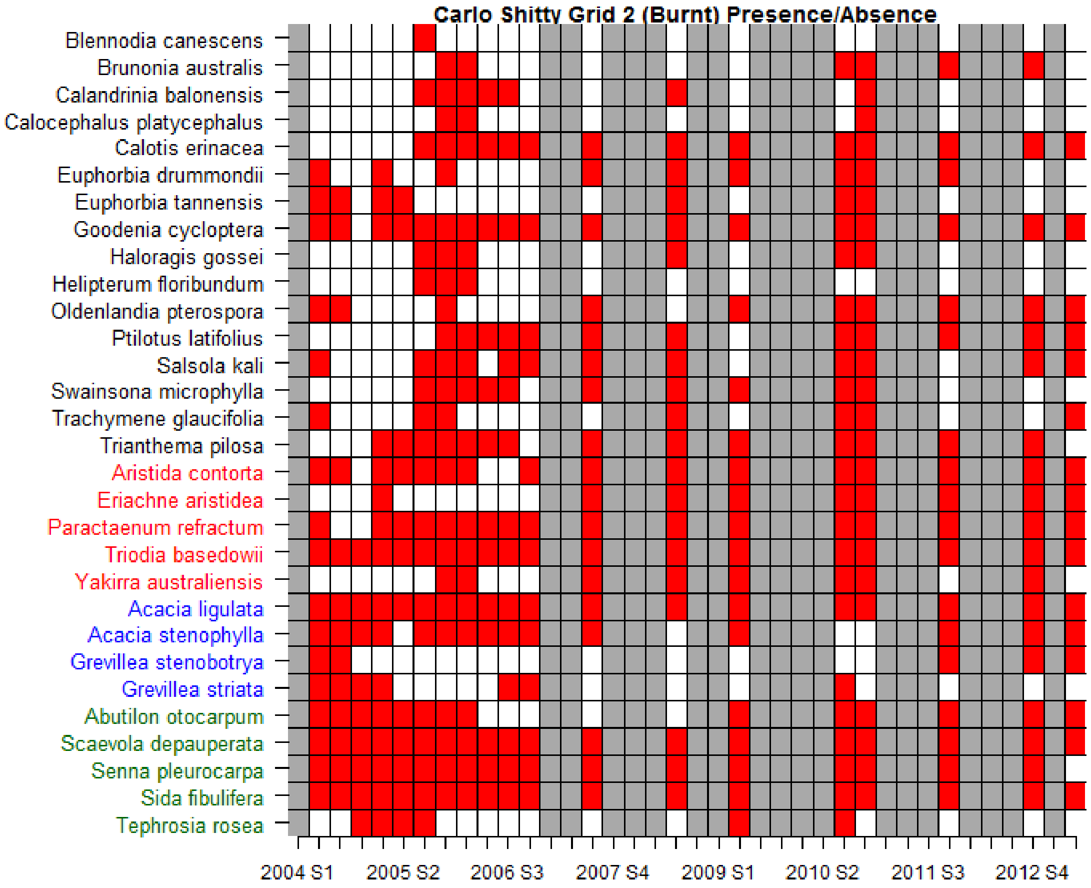
Carlo Shitty Grid 2 (Burnt) Presence/Absence
Blennodia canescens
Brunonia australis
Calandrinia balonensis
Calocephalus platycephalus
Calotis erinacea
Euphorbia drummondii
Euphorbia tannensis
Goodenia cycloptera
Haloragis gossei
Helipterum floribundum
Oldenlandia pterospora
Ptilotus latifolius
Salsola kali
Swainsona microphylla
Trachymene glaucifolia
Trianthema pilosa
Aristida contorta
Eriachne aristidea
Paractaenum refractum
Triodia basedowii
Yakirra australiensis
Acacia ligulata
Acacia stenophylla
Grevillea stenobotrya
Grevillea striata
Abutilon otocarpum
Scaevola depauperata
Senna pleurocarpa
Sida fibulifera
Tephrosia rosea
2004 S1
2005 S2
2006 S3
2007 S4
2009 S1
2010 S2
2011 S3
2012 S4

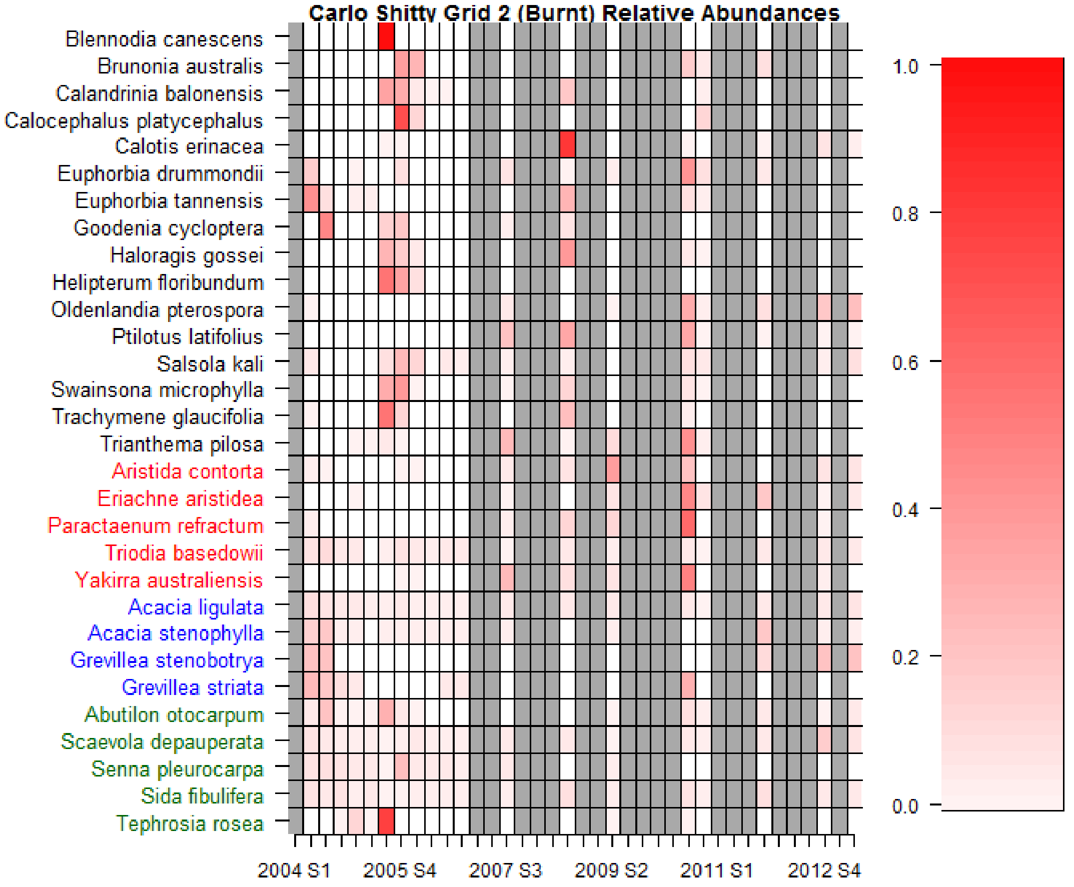
Carlo Shitty Grid 2 (Burnt) Relative Abundances
Blennodia canescens
Brunonia australis
Calandrinia balonensis
Calocephalus platycephalus
Calotis erinacea
Euphorbia drummondii
Euphorbia tannensis
Goodenia cycloptera
Haloragis gossei
Helipterum floribundum
Oldenlandia pterospora
Ptilotus latifolius
Salsola kali
Swainsona microphylla
Trachymene glaucifolia
Trianthema pilosa
Aristida contorta
Eriachne aristidea
Paractaenum refractum
Triodia basedowii
Yakirra australiensis
Acacia ligulata
Acacia stenophylla
Grevillea stenobotrya
Grevillea striata
Abutilon otocarpum
Scaevola depauperata
Senna pleurocarpa
Sida fibulifera
Tephrosia rosea
2004 S1
2005 S4
2007 S3
2009 S2
2011 S1
2012 S4
1.0
0.8
0.6
0.4
0.2
0.0

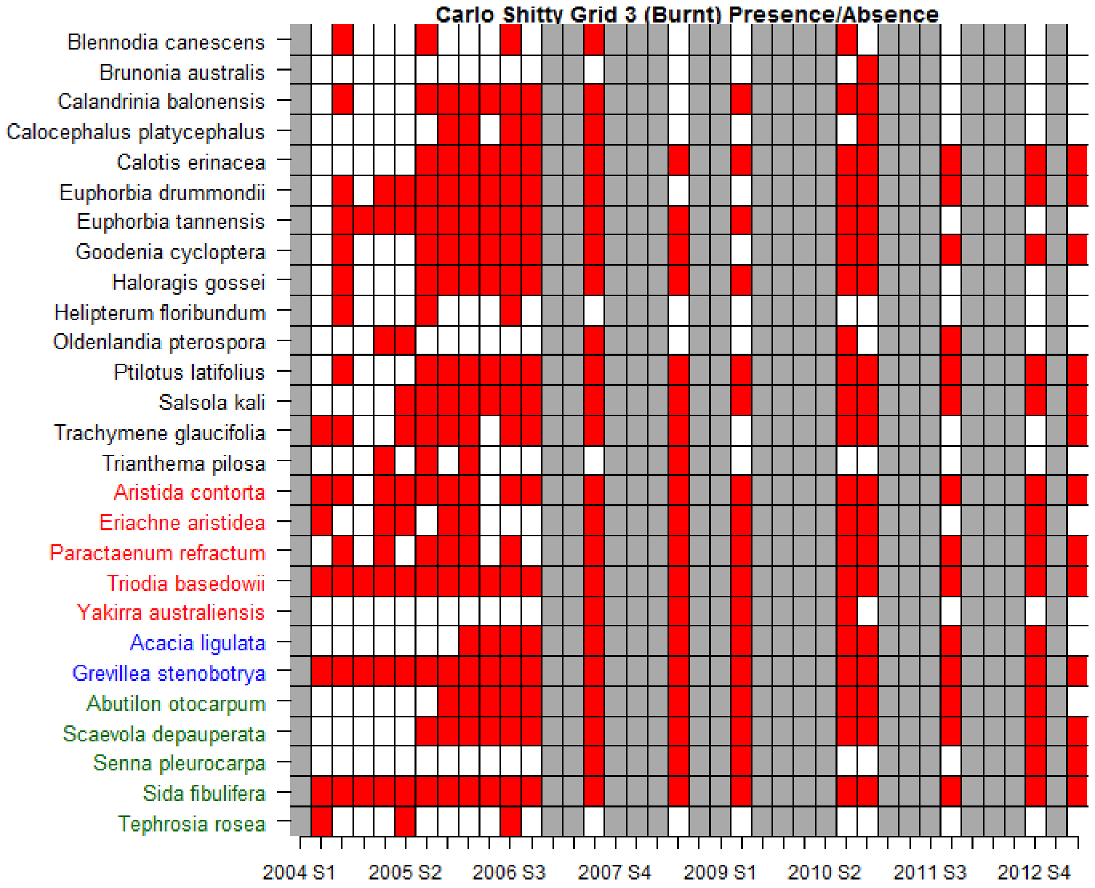
Carlo Shitty Grid 3 (Burnt) Presence/Absence
Blennodia canescens
Brunonia australis
Calandrinia balonensis
Calocephalus platycephalus
Calotis erinacea
Euphorbia drummondii
Euphorbia tannensis
Goodenia cycloptera
Haloragis gossei
Helipterum floribundum
Oldenlandia pterospora
Ptilotus latifolius
Salsola kali
Trachymene glaucifolia
Trianthema pilosa
Aristida contorta
Eriachne aristidea
Paractaenum refractum
Triodia basedowii
Yakirra australiensis
Acacia ligulata
Grevillea stenobotrya
Abutilon otocarpum
Scaevola depauperata
Senna pleurocarpa
Sida fibulifera
Tephrosia rosea
2004 S1
2005 S2
2006 S3
2007 S4
2009 S1
2010 S2
2011 S3
2012 S4

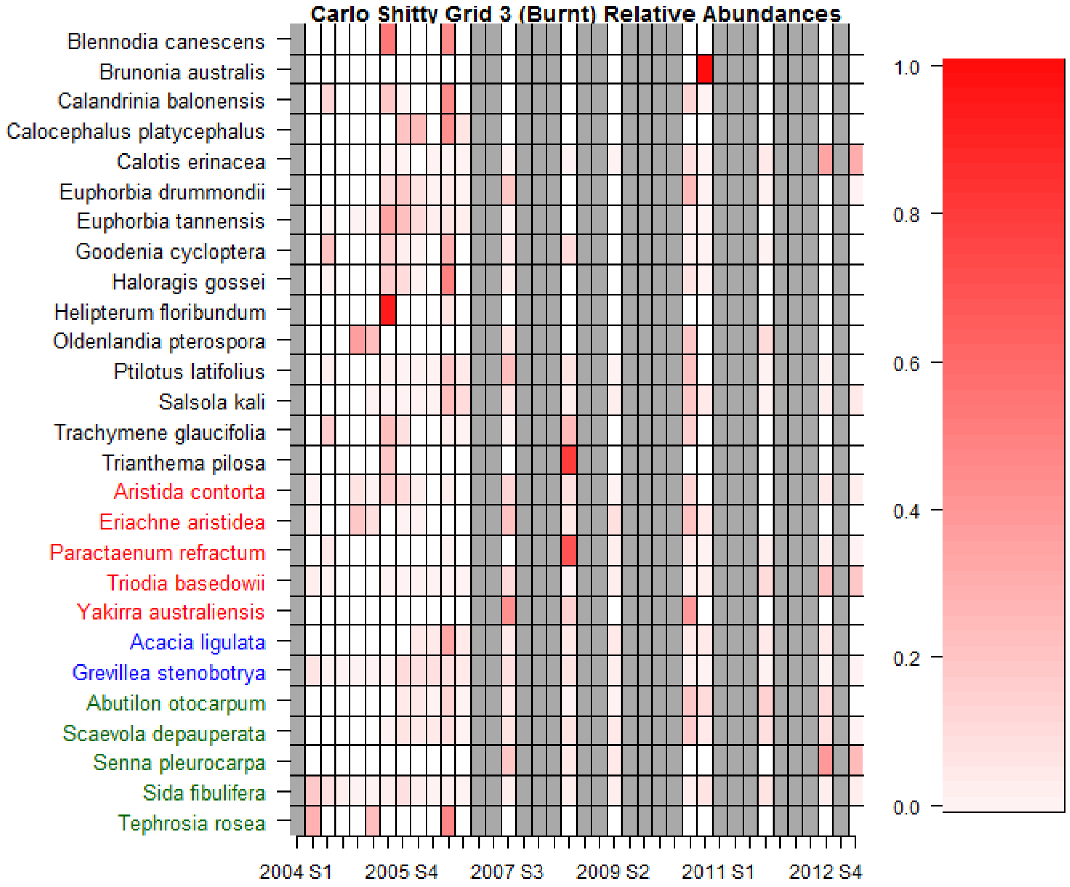
Carlo Shitty Grid 3 (Burnt) Relative Abundances
Blennodia canescens
Brunonia australis
Calandrinia balonensis
Calocephalus platycephalus
Calotis erinacea
Euphorbia drummondii
Euphorbia tannensis
Goodenia cycloptera
Haloragis gossei
Helipterum floribundum
Oldenlandia pterospora
Ptilotus latifolius
Salsola kali
Trachymene glaucifolia
Trianthema pilosa
Aristida contorta
Eriachne aristidea
Paractaenum refractum
Triodia basedowii
Yakirra australiensis
Acacia ligulata
Grevillea stenobotrya
Abutilon otocarpum
Scaevola depauperata
Senna pleurocarpa
Sida fibulifera
Tephrosia rosea
2004 S1
2005 S4
2007 S3
2009 S2
2011 S1
2012 S4
1.0
0.8
0.6
0.4
0.2
0.0

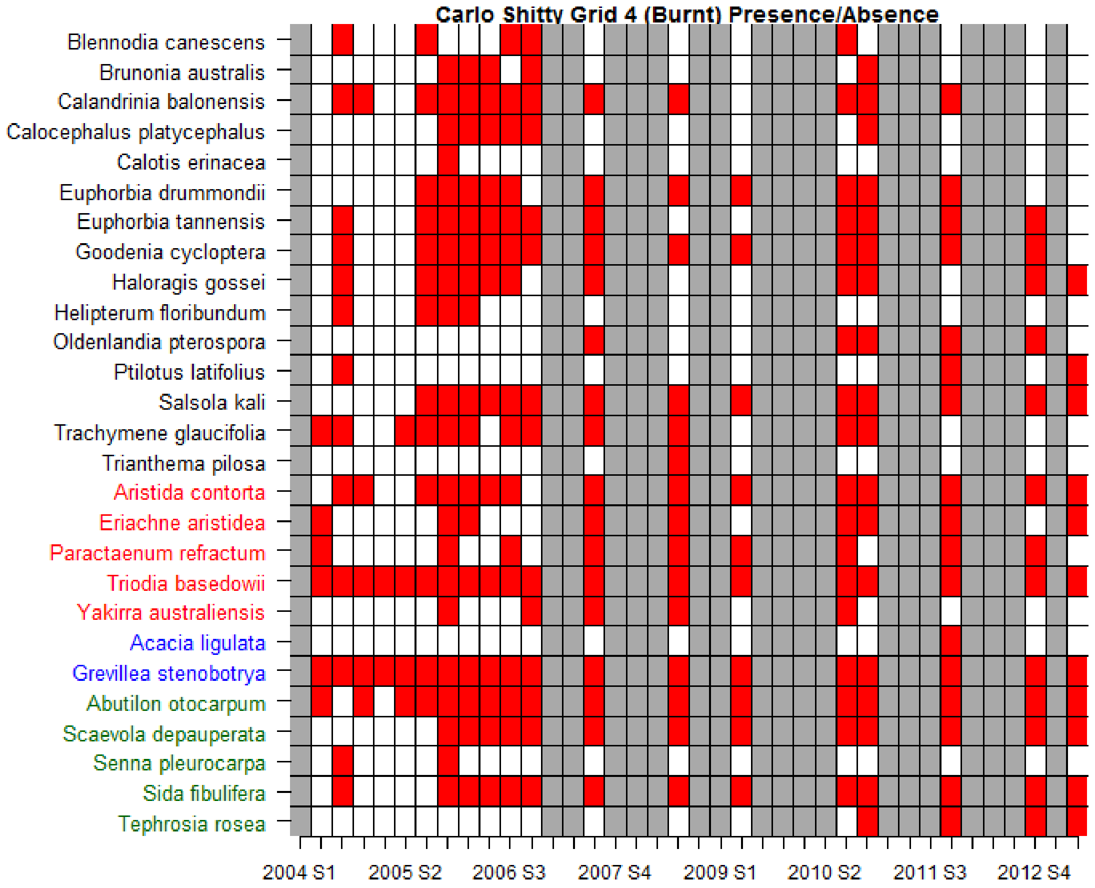
Carlo Shitty Grid 4 (Burnt) Presence/Absence
Blennodia canescens
Brunonia australis
Calandrinia balonensis
Calocephalus platycephalus
Calotis erinacea
Euphorbia drummondii
Euphorbia tannensis
Goodenia cycloptera
Haloragis gossei
Helipterum floribundum
Oldenlandia pterospora
Ptilotus latifolius
Salsola kali
Trachymene glaucifolia
Trianthema pilosa
Aristida contorta
Eriachne aristidea
Paractaenum refractum
Triodia basedowii
Yakirra australiensis
Acacia ligulata
Grevillea stenobotrya
Abutilon otocarpum
Scaevola depauperata
Senna pleurocarpa
Sida fibulifera
Tephrosia rosea
2004 S1
2005 S2
2006 S3
2007 S4
2009 S1
2010 S2
2011 S3
2012 S4

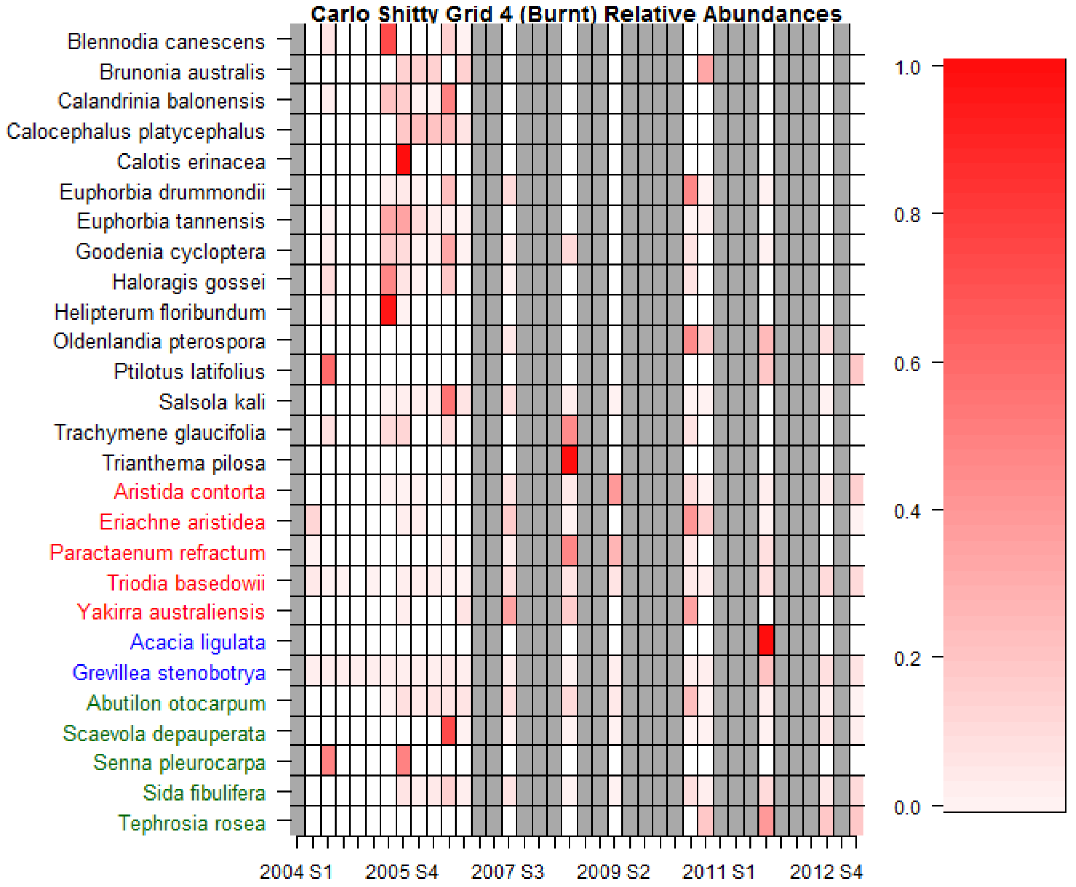
Carlo Shitty Grid 4 (Burnt) Relative Abundances
Blennodia canescens
Brunonia australis
Calandrinia balonensis
Calocephalus platycephalus
Calotis erinacea
Euphorbia drummondii
Euphorbia tannensis
Goodenia cycloptera
Haloragis gossei
Helipterum floribundum
Oldenlandia pterospora
Ptilotus latifolius
Salsola kali
Trachymene glaucifolia
Trianthema pilosa
Aristida contorta
Eriachne aristidea
Paractaenum refractum
Triodia basedowii
Yakirra australiensis
Acacia ligulata
Grevillea stenobotrya
Abutilon otocarpum
Scaevola depauperata
Senna pleurocarpa
Sida fibulifera
Tephrosia rosea
2004 S1
2005 S4
2007 S3
2009 S2
2011 S1
2012 S4
1.0
0.8
0.6
0.4
0.2
0.0

Appendix 4-4: State predictions for Carlo Shitty model with five common trends and no covariate

While AIC*c* scores indicated the model with five common trends with no covariate for Carlo Shitty was the best fit, we chose instead to report the results of the model with the covariate included as state predictions were incredibly poor under the former model. We plot the state predictions below, whereby points indicate standardised observations from the four grids, grey dashed lines indicate state predictions for each of the four grids and black solid lines indicate the mean state predictions across the four grids obtained from the no covariate five trend model.

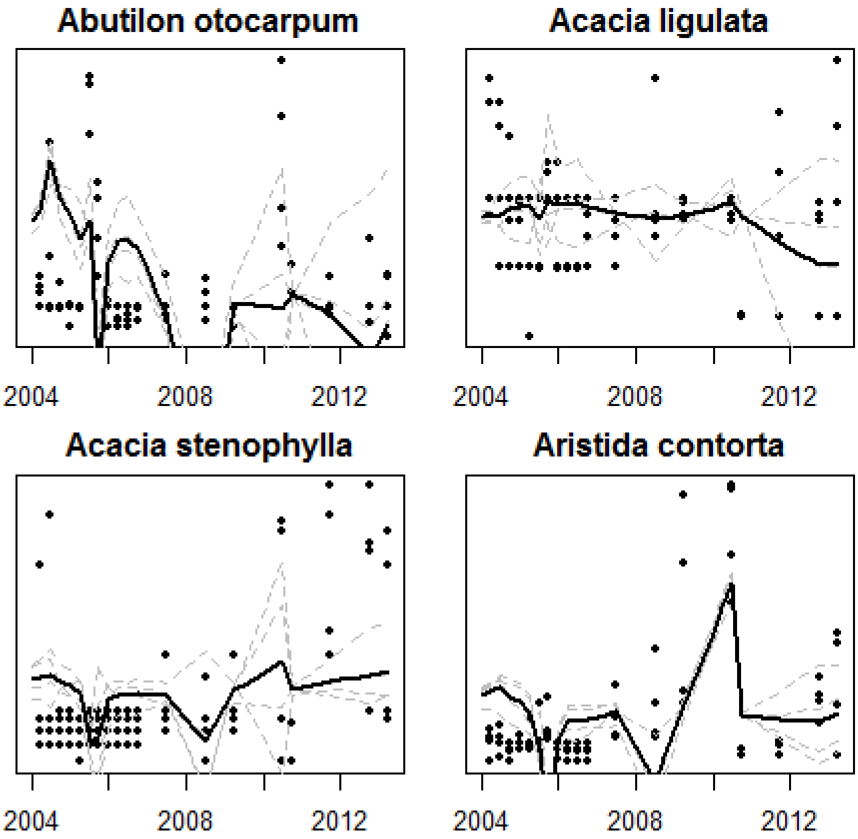

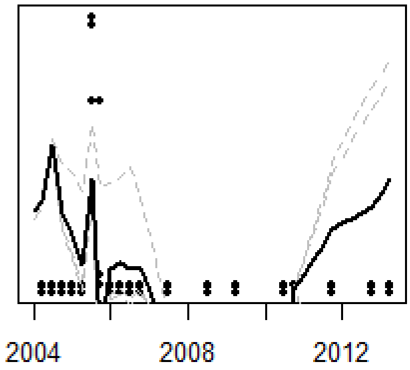

Blennodia canescens

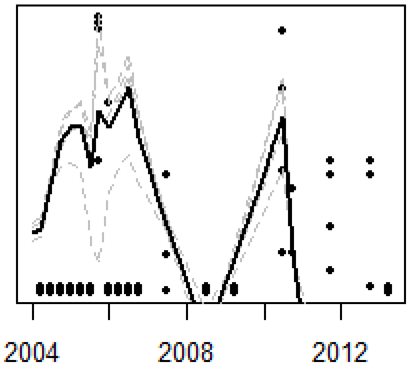

Brunonia australis

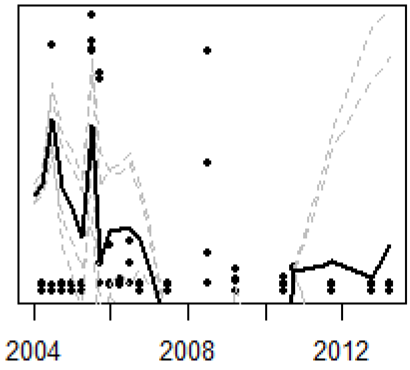

Calandrinia balonensis

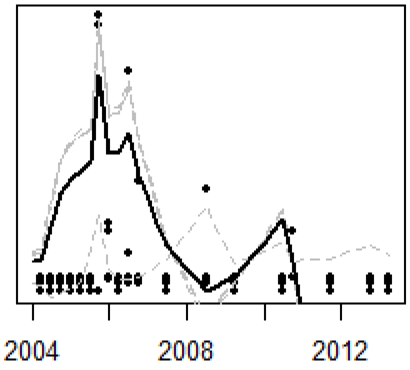

Calocephalus platycephalus

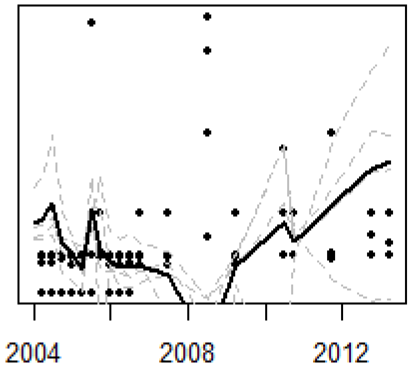

Calotis erinacea

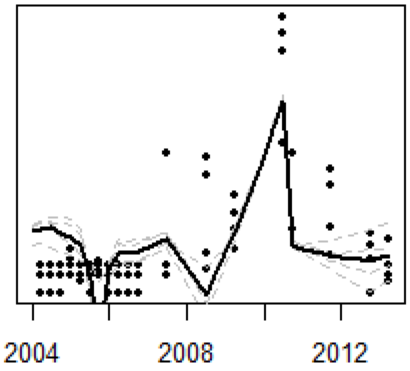

Eriachne aristidea

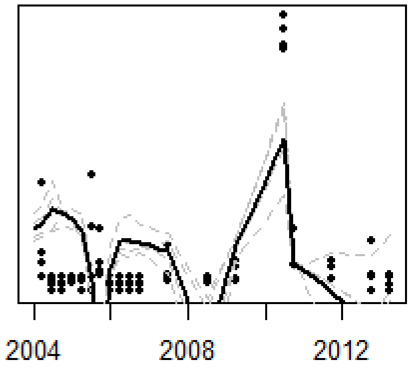

Euphorbia drummondii

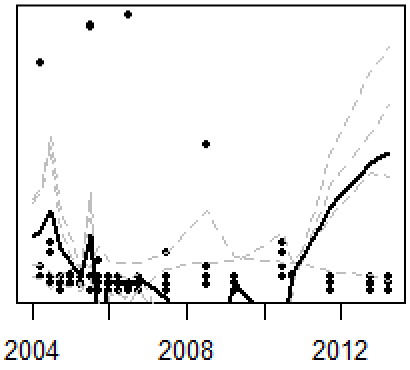

Euphorbia tannensis

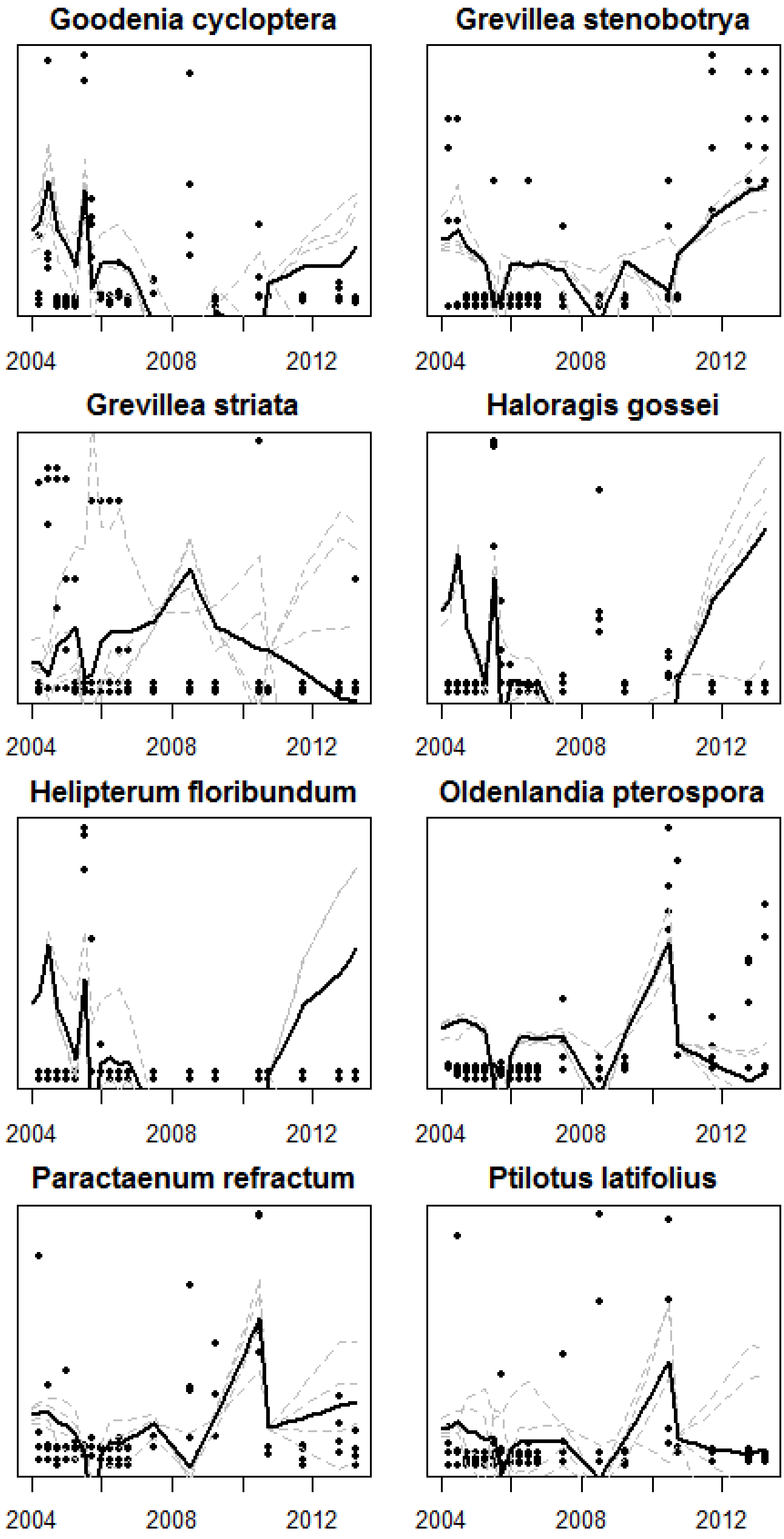
Goodenia cycloptera
Grevillea stenobotrya
Grevillea striata
Haloragis gossei
Helipterum floribundum
Oldenlandia pterospora
Paractaenum refractum
Ptilotus latifolius
2004
2008
2012

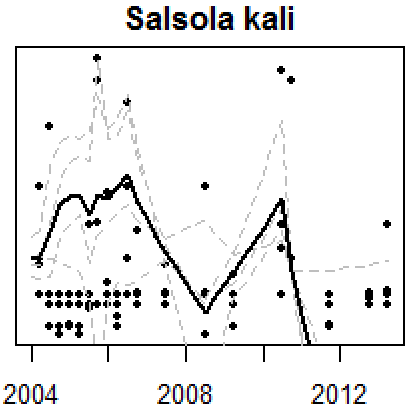
Salsola kali
2004
2008
2012

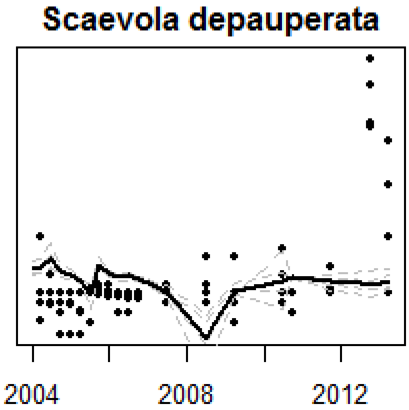
Scaevola depauperata
2004
2008
2012

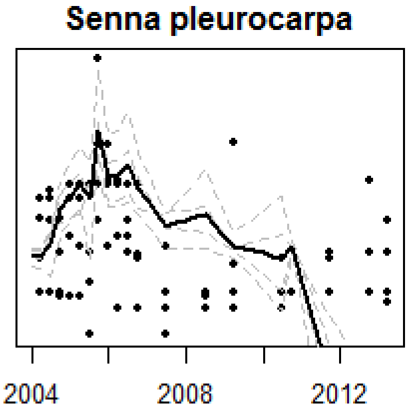
Senna pleurocarpa
2004
2008
2012

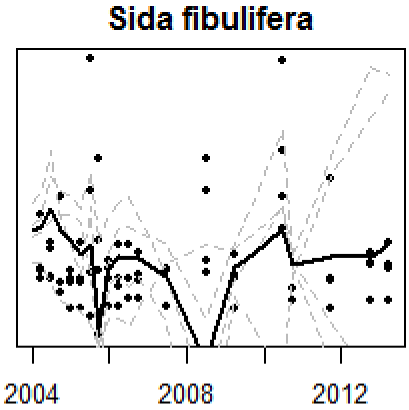
Sida fibulifera
2004
2008
2012

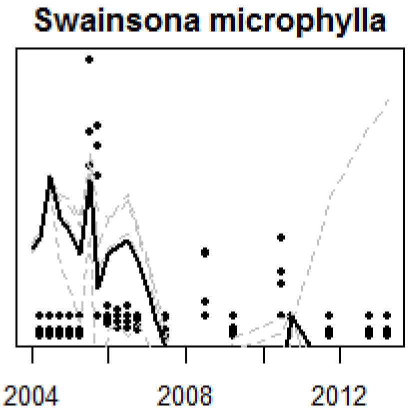
Swainsona microphylla
2004
2008
2012

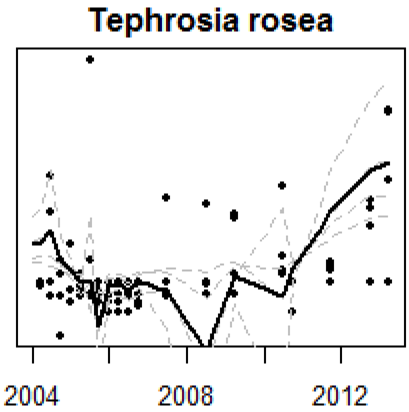
Tephrosia rosea
2004
2008
2012

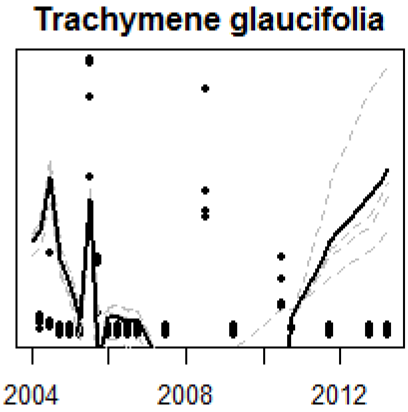
Trachymene glaucifolia
2004
2008
2012

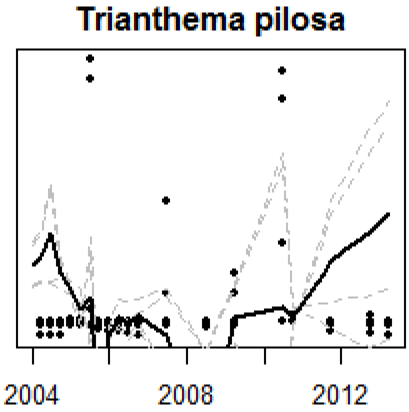
Trianthema pilosa
2004
2008
2012

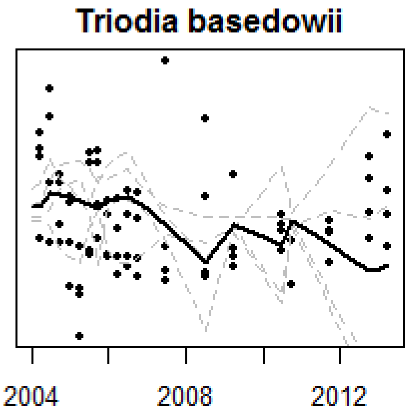
Triodia basedowii
2004
2008
2012

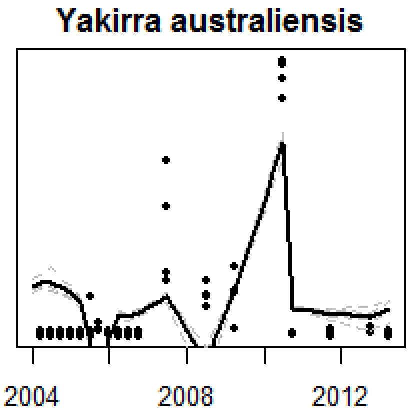
Yakirra australiensis
2004
2008
2012